# PERFORMANCE OF TACK COAT MATERIALS IN SASKATCHEWAN CLIMATE

A Thesis Submitted to the College of
Graduate and Postdoctoral Studies
In Partial Fulfillment of the Requirements
For the Degree of Master of Science
In the Department of Civil, Geological and Environmental Engineering
University of Saskatchewan
Saskatoon

**By**
**Laura Jane Stasiuk**

## PERMISSION TO USE

In presenting this thesis in partial fulfillment of the requirements for a Postgraduate degree from the University of Saskatchewan, I agree that the Libraries of this University may make it freely available for inspection. I further agree that permission for copying this thesis in any manner, in whole or in part, for scholarly purposes may be granted by the professor or professors who supervised the work presented in this thesis or, in their absence, by the Head of the Department or the Dean of the College through which my thesis work was done. It is understood that copying, publishing or using any portion of this thesis for financial gain is prohibited without my written permission. It is also understood that due recognition shall be given to me and to the University of Saskatchewan in any scholarly use of the material in my thesis.

Requests for permission to copy or to make other use of the material in this thesis, in whole or part, should be addressed to:

Head of the Department of Civil, Geological, and Environmental Engineering
University of Saskatchewan
Engineering Building
57 Campus Drive
Saskatoon, Saskatchewan S7N 5A9 Canada

OR

Dean
College of Graduate and Postdoctoral Studies
University of Saskatchewan
116 Thorvaldson Building, 110 Science Place
Saskatoon, Saskatchewan S7N 5C9 Canada

## ABSTRACT

Tack coat materials are used to provide sufficient bond between an existing asphalt concrete layer and a new asphalt concrete overlay or between two lifts of a new asphalt concrete layer. Tack coat materials are typically emulsified bituminous materials. Tack coat performance has not been extensively studied in the harsh climate of Saskatchewan. In practice, tack coat materials are often picked up on the tires of paving equipment, which leaves little tack coat material in the wheel paths where it is needed most. An ideal tack coat material should have a short curing time and a high bond strength to achieve better constructability and performance of the pavement structures. Improper installation of the tack coat material can lead to a poor bond and premature failure of the pavement structures.

The objective of this research is to evaluate the strength and performance of several tack coat materials in Saskatchewan climate. Findings from this research will be used by the Saskatchewan Ministry of Highways and Infrastructure to create a recommended tack coat material list and provide guidelines for construction best practices. Currently, most tack coat materials selected for road construction in Saskatchewan are the basic slow-setting emulsion, SS-1. The tack coat materials tested in this research include basic anionic emulsions: SS-1, SS-1h, MS-1, a cationic emulsion: CSS-1h, and three proprietary quick setting/non-tracking emulsions provided by industry partners. Tack coat performance was evaluated through a field study as well as a laboratory-testing program. Ten test sections were constructed in August 2017 on a two-way, two-lane rural highway near Blaine Lake, Saskatchewan.

At the time of test section construction, weather conditions, tack coat material curing properties, and application rate were measured. The proprietary products had faster setting and breaking times as well as less pickup of tack coat onto vehicle tires than all other products. All tested products had better setting and breaking times than SS-1. A correlation between tack coat breaking and setting times with temperature and humidity at the time of construction was observed. Two distress surveys were conducted post-construction in September 2017 and after one year in September 2018. The two distress surveys did not show early distresses or deformities in the road due to poor bonding between pavement layers.

Laboratory testing was conducted on the cores collected from the test sections to evaluate the interlayer shear strength using a Louisiana Interlayer Shear Strength Tester according to AASHTO TP 114. Cores collected after construction were separated into two groups: baseline cores and freeze-thaw conditioned cores. Baseline cores were tested to measure initial bond strength after construction. Conditioned cores were exposed to three levels of freeze-thaw cycling: 3, 9, and 15 freeze-thaw cycles. Each freeze-thaw cycle consisted of twelve hours of freezing at -25°C and twelve hours of thawing at 15°C. The baseline cores, one year cores, and laboratory conditioned cores were tested to evaluate the change in bond strength over time.

The laboratory-performance of tack coat materials was quantified based on interlayer shear strength (ISS), strain, k modulus, energy to peak stress, and the type of failure of core samples. Samples collected after one year showed higher ISS than baseline cores. Lab conditioned cores had higher ISS than baseline cores but lower ISS than year one cores. The increase in bond strength after one year and lab conditioning can be attributed to the continuous curing of tack coat materials.

The failure type of bond strength samples was classified into two types according to shape and location of the failure surface: Type A (clean failure at the tack coat surface) and Type B (failure partly in the mix). Failure Type B indicates that the tack coat material can successfully provide enough bond strength to make the two asphalt concrete lifts behave as one thick homogenous layer. Although TackMax™ and Colasphalt Tack had lower ISS values than SS-1 NB (50-50W) and SS-1 (30-70W), TackMax™ and Colasphalt Tack showed stronger type of failure (Type B). Therefore, failure mode should be considered when evaluating bond strength of cores in addition to ISS value.

The energy required to reach the peak shear stress is a comprehensive parameter that accounts for both the applied stress and the amount of deformation that the sample undergoes before reaching bond failure. Results show that the ranking of tack coat materials varies if the energy values are used as the ranking criterion instead of ISS values. Therefore, the energy required to reach peak shear stress is a significant parameter that should also be considered when evaluating tack coat materials. Overall, SS-1h, MS-1, CSS-1h, and the 3 proprietary products showed better performance than SS-1 emulsion according to the test results of the baseline and year one cores.

## ACKNOWLEDGEMENTS

I would like to acknowledge and thank my supervisor Dr. Haithem Soliman for his guidance and contributions to my research. I would like to thank the Saskatchewan Ministry of Highways and Infrastructure for their financial and material contribution to this project. Without the help of many people during the field component of this project, this research would not have been possible.

I would like to thank:

- Kelly Pederson, Manoj Jogi, Aziz Salifu, and Kamil Rogowski for their help during field work and coring
- The AMEC Foster Wheeler (now Wood) crew for the long days in the field coring and providing traffic control
- Michael McConell and Joshua Spanier for trimming the core samples
- The Gecan lab staff: Alex and Inderpal for their assistance during the first round of shear testing
- ACP Applied Products: Chris Dechkoff and Nathan Prosko for their assistance and input throughout the project
- Pounder Emulsions (now Husky Asphalt), McAsphalt Industries Ltd., and Colasphalt for their generous donation of product and input during construction
- HJR Asphalt LP and WSP for their contribution to the project
- Adam Hammerlindl for his assistance and willingness to help in the lab
- Hayden Reitenbach for his help with the environmental chamber
- My advisory committee members: Dr. Emmanuel Sacchi and Ania Anthony
- The University of Saskatchewan for providing funding through scholarships.

Special thanks to my support team: my parents Nancy and Ron, brother Dan, gramma Lou, and dog Charlie for all their support throughout the past few years.

## TABLE OF CONTENTS

## LIST OF TABLES

## LIST OF FIGURES

## LIST OF ABBREVIATIONS

| | |
|---|---|
| AADT | Annual Average Daily Traffic |
| AASHTO | American Association of State Highway and Transportation Officials |
| AC | Asphalt Concrete |
| ASTM | American Society for Testing and Materials |
| b.v. | By Volume |
| b.w. | By Weight |
| CV | Coefficient of Variation |
| DSR | Dynamic Shear Rheometer |
| ESAL | Equivalent Single Axle Load |
| FT | Freeze-Thaw |
| FHWA | Federal Highway Administration |
| IBT | Interface Bond Test |
| IRI | International Roughness Index |
| IWP | Inner Wheel Path |
| LISST | Louisiana Interlayer Shear Strength Tester |
| LTCQT | Louisiana Tack Coat Quality Tester |
| LTPP | Long Term Pavement Performance |
| NB | Northbound |
| NDT | Non-Destructive Testing |
| OFTT | Oregon Field Torque Tester |
| OWP | Outer Wheel Path |
| PVC | Polyvinyl Chloride |
| QA | Quality Assurance |
| QC | Quality Control |
| SB | Southbound |
| SK | Saskatchewan |
| s.f.s. | Saybolt Furol Seconds |
| TAADT | Truck Annual Average Daily Traffic |
| UPOD | UTEP Pull-Off Device |

# CHAPTER 1: INTRODUCTION

## 1.1 Background

There are 26,175 kilometres of highways in Saskatchewan, Canada. This includes 11,117 kilometres of asphalt concrete (AC) paved highways (Saskatchewan Ministry of Highways & Infrastructure, 2016). Maintaining this large network of roads is challenging due to limited budgets where the population of Saskatchewan is merely 1.16 million people (Statistics Canada, 2016). Ensuring the longevity of the road network is important in reducing spending and allowing the road maintenance budget to be used to its full potential. The use of proper road materials, procedures, and equipment during road construction and rehabilitation ensures meeting the target design life and optimizes the use of limited budgets.

Tack coat materials are used to provide sufficient bond between an existing AC layer and a new AC overlay or in-between two lifts of a new AC layer, as shown in Figure 1.1. Tack coat materials are typically emulsified bituminous materials but can also be cutback emulsions or hot paving cement. An ideal tack coat material has short break and set times to limit the inconvenience to the contractor and to the public which arise from long curing times. Short break and set times ensure achieving proper bond between AC layers without slowing down the construction process. In addition, short break and set times reduce pickup and tracking of emulsion residue on construction equipment and on traveling vehicles which occasionally end up traveling on a tacked road surface. A tack coat material "breaks" when its colour changes from brown to black as shown in Figure 1.2. The time for a tack coat material to break varies depending on the properties of the material, the dilution with water, and weather conditions during application setting of a tack coat material. A tack coat material "sets" when the emulsion residue is no longer picked up from the road surface. This can be determined by blotting the surface with a tissue on the emulsion, and by observing product transfer to vehicle tires. Minimal transfer of residue indicates that any water previously present in the material has evaporated and the bituminous residue is forming a homogeneous layer on the road surface. A tack coat material cures when its surface is no longer sticky.

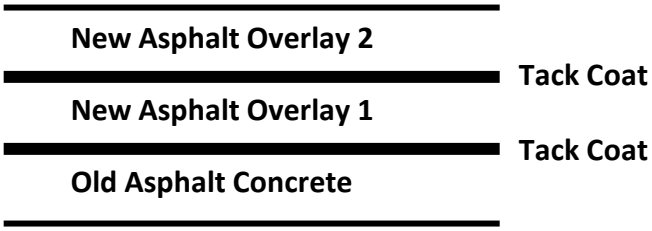


**Figure 1.1 Tack Coat Placement**


**Figure 1.2 Broken and Unbroken Tack Coat Emulsion**

Achieving proper bond strength between AC layers is critical to ensure that the bonded layers will act and resist stresses as one homogeneous system. If the bond is not adequate, layers of AC behave as multiple unbonded layers which will increase the stress levels within these layers and lead to cracking and premature failure, as demonstrated in Figure 1.3.

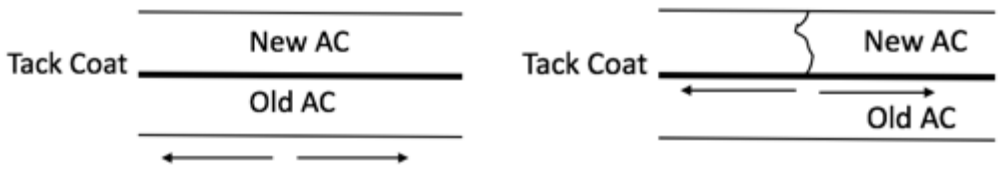


**Figure 1.3 Tack Coat Good Bond (A) and Tack Coat Poor Bond (B)**

## 1.2 Problem Statement

The performance of tack coat materials has not been studied extensively in cold climates similar to what is experienced in Western Canada. Transportation agencies limit the use of new tack coat materials due to the uncertainty of their performance. Currently, there are no performance-based specifications for tack coat selection and application of tack coat materials in cold regions. The procedures for diluting, applying, and curing a tack coat are not well defined or followed. Contractors often dilute tack coat materials heavily. Dilution allows for good coverage with very low application rates. This means there is less tracking and pickup but using low application rates could cause a poor bond between pavement layers (Asphalt Institute, 2016). These construction practices do not leave enough asphalt residue on the road for a good bond to form and contribute to early deterioration of pavement structures. This research aims to help optimize road construction and maintenance costs and prevent premature pavement failures related to poor selection and application practices of tack coat materials. This research provides laboratory and field testing data to support developing performance-based specifications for selection and application of tack coat materials.

## 1.3 Research Objectives

The goal of this research is to evaluate the performance of various emulsified bituminous asphalt products used as tack coat materials in Saskatchewan climate. Specifically, the research objectives are to:

1) Evaluate the performance of several tack coat materials in Saskatchewan climate to help Saskatchewan Ministry of Highway & Infrastructures expand their repertoire of tack coat materials.
2) Monitor the field performance of tack coat materials during construction and in the following year.
3) Compare the bond quality of tack coat materials using a Louisiana Interlayer Shear Strength Tester (LISST).
4) Compare field and lab performance of tack coat materials to develop parameters that can be used to establish performance-based specifications for selection of tack coat materials.
5) Compare the performance of materials subjected to simulated freeze-thaw cycling and real-world exposure.

## 1.4 Scope of Research

This research project is sponsored by the Saskatchewan Ministry of Highways and Infrastructure, Pounder Emulsions (Husky Asphalt), McAsphalt Industries Ltd., and Colasphalt. Monitoring of the field test sections will continue for 5 years (August 2017 ~ 2022). This thesis will document construction procedures for the field test sections, first year performance data, and laboratory conditioning of tack coat samples. This thesis will not include the results and analysis of the entire project but only for the first year (August 2017 – September 2018). The tack coat materials evaluated in this project were selected based on availability in Saskatchewan and in consultation with industry partners.

## 1.5 Thesis Layout

The organization of the thesis is as follows:

- Chapter 1: Introduction
  This chapter presents the background information, problem statement, objectives, and scope, and thesis organization.
- Chapter 2: Literature Review
  This chapter provides a literature review outlining the results and methodology of previous tack coat studies, asphalt emulsion theory, asphalt emulsion testing procedures, and freeze-thaw cycling studies.
- Chapter 3: Experimental Program
  This chapter outlines for methodology for the experimental program including the field study and laboratory testing.
- Chapter 4: Field Study Results and Analysis
  This chapter provides the results to the field study portion of the research.
- Chapter 5: Laboratory Test Results and Analysis
  This chapter provides the results and analysis to the laboratory testing portion of the research.
- Chapter 6: Summary, Conclusions, and Recommendations
  This chapter provides the concluding remarks from the research to date and recommendations for future work.

# CHAPTER 2: LITERATURE REVIEW

## 2.1 Introduction

This chapter introduces the background for asphalt emulsion theory and Quality Control (QC)/Quality Assurance (QA) testing procedures, and summarizes the current practices for application of tack coat materials and previous studies on optimizing their performance. A review of freeze-thaw cycling studies for pavement materials is also presented, a review of the climate in Saskatchewan, and quality control/assurance standardized testing for tack coat materials.

## 2.2 Asphalt Emulsion Theory

An asphalt emulsion or emulsified asphalt is an inflammable liquid that is created by blending asphalt and water with an emulsifier (also called a surfactant or a chemical stabilizer) such as soap, dust, or colloidal clays in a colloidal mill (Mohammad et al., 2012). Asphalt emulsions contain 55-75% asphalt by weight and 0.15-3% emulsifier. Emulsification is the process in which thermal energy is used to liquify the asphalt cement and mechanical energy is used to shear bitumen particles to disperse them into water. The process takes place at high temperatures up to 170°C. The emulsifier reduces the surface tension and allows the immiscible water and asphalt to transition together (Davidson, 1995). The emulsifier can bridge the water and oil phases together because the emulsifier molecule has two ends one of which is hydrophilic and is attracted to the more polar water phase, and the second which is lipophilic and is attracted to the less polar asphalt phase (James, 2006). The charge of an emulsion, anionic or cationic, is determined by the charge of the hydrophilic head of the emulsifier. Anionic emulsifiers contain negatively charged oxygen atoms and cationic emulsifier contain positively charged nitrogen atoms in their head (James, 2006).

Examples of emulsions include: mayonnaise, butter, homogenized milk, and cosmetic creams. In an emulsion, small droplets of one liquid are distributed in another. Many asphalt emulsions are of the type oil-in-water meaning that small oil droplets are dispersed in the abundance of water particles as shown in Figure 2.1. Asphalt emulsions are typically the oil-in-water type of emulsion. Asphalt emulsions can also be a more complex type of water-in-oil-in-water emulsion. Small droplets of water are inside oil particles which are in water as shown in Figure

2.2. Asphalt emulsions are considered to be macroemulsions because the particle size of bitumen droplets ranges from 0.1-20 micrometers (microns). The particle size and the distribution of sizes are important because they affect the parameters of the emulsion including viscosity and storage stability. Larger particles have a lower viscosity as do emulsions with a well-graded distribution of particle sizes (James, 2006). Because asphalt emulsions are largely made up of water, they have many of the same properties as water including: ability to freeze, ability to conduct electricity, and aptitude to mix with water but not mix with oil (Davidson, 1995).

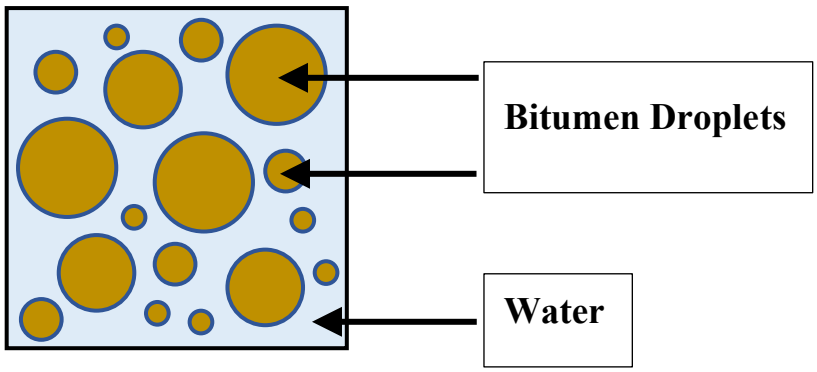


**Figure 2.1 Oil-In-Water Emulsion**

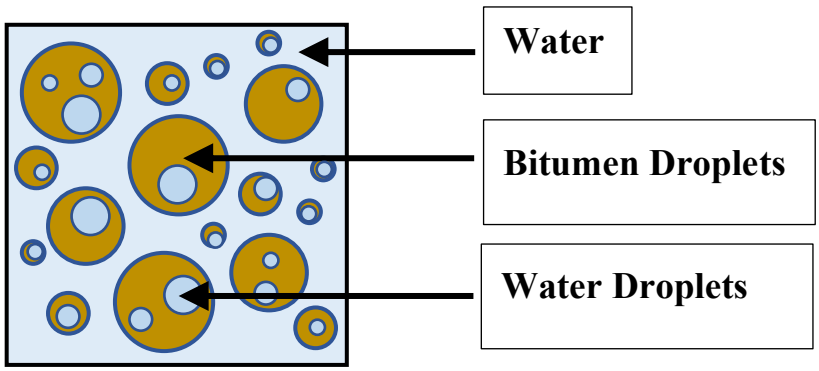


**Figure 2.2 Water-In-Oil-In-Water Emulsion**

Asphalt emulsions are unstable and the asphalt and water will separate from each other over a period of time which could be hours or years. Because asphalt particles are insoluble in water, the particles will eventually flocculate together and coalesce. The charged particles typically repel each other because they have the same charge (negative for anionic emulsions and positive for cationic emulsions), but these particles can overcome the repulsion and flocculate together if

they have enough energy to do so. At the flocculation stage, particles can be separated by dilution, addition of emulsifier, or by agitation. As the particles latch (flocculate) together, water is expelled leading to full coalescence where the particles merge together. Flocculation and coalescence will continue until the asphalt emulsion is no longer blended and asphalt and water have separated. The coalescence cannot be reversed through the remediation measures listed above to reverse flocculation. Factors that accelerate coalescence include gravity, evaporation, and extreme temperatures causing freezing. Emulsions with lower viscosity coalesce faster than high viscosity emulsions (James, 2006).

Coalescence in storage and prior to application of the product onto the road is not good but after the product has been placed, coalescence is ideal and is part of the curing process (James, 2006). When coalescence occurs, the asphalt "breaks", and a continuous film is formed on the road. The speed of the coalescence is affected by many factors including: the emulsion recipe and the quantities of asphalt, water, and surfactant; the particle size of the dispersed asphalt; the type of surfactant used; the chemicals, salts, and other content in the water; the temperature at which the emulsion is stored at and placed at; the humidity and air temperature at the time of placement; and the size and type of the aggregate used. An aggregate with small particles has a higher surface area and leads to faster breaks than an aggregate with large particles and lower surface area (Davidson, 1995).

Emulsions are named based on their properties including: charge, setting speed, hardness of residue, viscosity, and additives such as polymer or latex etc. The emulsion CSS-1h will be used as an example below. The letters before the hyphen are the prefix, and the letters and numbers after the hyphen are the suffix.

Anionic emulsions are the most commonly used emulsions; the emulsion is assumed to be anionic unless it begins with a "C" indicating that it is a cationic emulsion (as in CSS-1h). Anionic emulsions have a negative charge and cationic emulsions have a positive charge. The charge of the emulsion is based on the charge of the surfactant used. The second two letters indicate how fast the emulsion sets. "SS" indicates that it is a slow-setting emulsion (as in CSS-1h), "QS" for quick-setting emulsion which sets faster than SS but slower than "MS" which represents medium-setting emulsions, and "RS" for rapid-setting emulsions.

"HF" is another prefix which indicates that the emulsion has a "high float". A high float emulsion is more gel-like and has higher resistance to flow or creep. The name high float is derived from the float test which is performed in the lab to measure this gelling property (O'Connor, 1982).

The suffix number after the hyphen indicates the viscosity of the emulsion. "1" is for low viscosity emulsions (as in CSS-1h) and "2" is for high viscosity emulsions. The absence of a letter behind the number indicates that the emulsion residue hardness is normal. "h" implies that the product has a hard residue (as in CSS-1h), and "s" implies the product has a soft residue. Additional suffix can follow including "P" representing a polymer modified emulsion, or "LM" (or "L") indicating a latex modified emulsion (James, 2006).

Some products which follow this nomenclature include: RS-1, RS-2, HFRS-2, MS-1, MS-2, MS-2h, HFMS-1, HFMS-2, HFMS-2h, HFMS-2s, SS-1, SS-1h, QS-1h, CRS-1, CRS-2, CRS-2P, CRS-2L, CMS-2, CMS-2h, CSS-1, CSS-1h, and CQS-1h (ASTM D977, ASTM D2397). Products that do not follow this naming scheme including emulsified asphalt prime (EAP) products, and proprietary products. Products will sometimes have a suffix indicating the penetration value in dmm (decimillimetre = 0.1mm) of the residue (ex. 100, 150, 300, etc.). The procedure for determining the penetration value of the residue is further explained in Section 2.3.8 and in ASTM D5/D5M.

Asphalt emulsions have numerous applications including use as a tack coat, slurry seal, dust control, chip seal, and microsurfacing. Only some of the emulsions mentioned above are suitable to be used as tack coats, specifically SS, MS, and RS products.

### 2.3 Asphalt Emulsion Testing Procedures

Asphalt emulsion products are tested according to ASTM standards. Tests are either performed on the emulsion or on the residue of the emulsion. ASTM D977 and ASTM D2377 list the test methods and specification requirements necessary for each type of emulsion. Each test listed in these standards will be briefly summarized below. The desirable limits for the properties of emulsion products is discussed in Chapter 3.2.

### 2.3.1 Viscosity

Viscosity is an important property of emulsions because it determines the efficacy (sprayability and workability) of the product (ASTM D7226). Viscosity is the measure of the resistance of a fluid to flow. The product needs to have low enough viscosity that it can be sprayed by the distributor onto the road but have high enough viscosity that the emulsion stays in place and does not run due to the cross-sectional grade on the road (ASTM D7496). Viscosity can be determined by a Saybolt Furol viscometer, a rotational paddle viscometer, or by Zahn-cup.

**Viscosity-Test Method ASTM D7496 Standard Test Method for Viscosity of Emulsified Asphalt by Saybolt Furol Viscometer & ASTM D88 Standard Test Method for Saybolt Viscosity**

Viscosity can be determined by means of a Saybolt Furol viscometer. Emulsions are conditioned to 25°C or 50°C depending on the product. The emulsion is screened through an 850µm sieve prior to testing. The emulsion is poured into the preheated Saybolt Furol viscometer. The cork from the viscometer is removed and emulsion flows out the bottom into a 60mL flask. The time it takes for the 60mL flask to be filled is recorded. This time is the viscosity in Saybolt Furol seconds (s.f.s.).

**Viscosity-Test Method ASTM D7226 Standard Test Method for Determining the Viscosity of Emulsified Asphalts Using a Rotational Paddle Viscometer**

Viscosity can be determined by means of a rotational paddle viscometer. The emulsion is screened through an 850µm sieve prior to testing. Emulsion is placed into the paddle viscometer and heated until a desired temperature of either 25°C or 50°C is reached. When the temperature is reached, the paddle will begin rotating at 100rpm. An apparent viscosity reading is outputted in units of centipoises (1mPa·s, millipascal-second).

**Viscosity-Test Method ASTM D4212 Standard Test Method for Viscosity by Dip-Type Viscosity Cups**

Zahn cups are primarily used to measure the viscosities of Newtonian or near-Newtonian fluids. A Newtonian fluid is one whose viscosity is independent of shear stress. Emulsion viscosity can be determined using a Zahn cup but may not be as accurate as using the above methods. The emulsion is heated to 25°C (when using number 2 Zahn cup) or 50°C (when using number 3

Zahn cup) depending on the thickness of the product. The emulsion is placed in a can and heated in a hot bath to the desired temperature. The Zahn cup is immersed into the container holding the emulsion. The emulsion flows from a hole in the bottom of the cup and the time it takes for the cup to be emptied is recorded. A correlation factor is then applied to determine the viscosity in Saybolt Furol Seconds (s.f.s.).

### 2.3.2 Storage Stability and Settlement-Test Method ASTM D6930 Standard Test Method for Settlement and Storage Stability of Emulsified Asphalts

The storage stability test is used to determine if an emulsion can remain uniform in dispersion while being stored. This is significant to determine how long an emulsion can remain stored before settlement. An emulsion sample is placed into a cylinder and stoppered at the top. The sample is left undisturbed for 24 hours for the stability test and for 5 days for the settlement test. After the undisturbed period, a sample is syphoned from the top of the sample and from the bottom sample. These two samples are heated until only the residue is left. The difference in residual content in the bottom sample and the top sample is computed and reported as the storage stability in % and the settlement in %. A high storage stability is desirable to ensure that products maintain uniformity for application.

### 2.3.3 Demulsibility-Test Method ASTM D6936 Standard Test Method for Determining Demulsibility of Emulsified Asphalt

A demulsibility test is performed to determine the chemical breaking present in rapid-setting emulsions and medium-setting emulsions and classify them as such. Depending on the emulsion charge, a titrant of 0.80% Dioctyl Sodium Sulfosuccinate Solution is used for cationic emulsions and a titrant of 0.10N or 0.02N $CaCl_2$ solution is used for anionic emulsions. This titrant is loaded into a burette at a desired amount. The titrant is slowly released into a can containing emulsion and stirred. After the titrant amount is released into the can, the contents of the can are poured over a sieve to be retained. The can is rinsed and poured over the sieve many times until all unreacted emulsion is rinsed through the sieve. The can, sieve and stir rod are then placed on a hot plate until all water has evaporated off. The weight of the test residue is compared to the weight of the residue obtained from distillation to calculate the demulsibility which gives the percentage of emulsion that reacted with the titrant.

### 2.3.4 Coating Ability and Water Resistance—Test Method ASTM D244 Standard Test Methods and Practices for Emulsified Asphalts-Practice for Determining Field Coating of Emulsified Asphalts & Emulsified Asphalt/Job Aggregate Coating Practice

The coating test determines if the emulsion is able to coat an aggregate, remain on the aggregate through mixing, and remain on the aggregate through a washing cycle. Aggregate is mixed with emulsion by hand for a given length of time – 5 seconds to 120 seconds in the field or 5 minutes in the lab. The ability of the emulsion to coat the aggregate is observed. The coated aggregate is then repeatedly rinsed with water to see the resistibility of the emulsion is observed. The results of the test are rated fair, good, or poor.

### 2.3.5 Cement Mixing-Test Method ASTM D6935 Standard Test Method for Determining Cement Mixing of Emulsified Asphalt

The cement mixing test determines the ability of an emulsion to mix with cement. Cement is a fine material with high surface area. The ability for emulsion to mix with cement may predict its ability to mix with clay and be used for soil stabilization (Davidson, 1995). The results of this test measure the amount of emulsion that breaks when mixed with clay. Diluted emulsion is mixed with cement and the rinsed over a sieve to weigh the large particles resulting from the emulsion breaking.

### 2.3.6 Sieve Test-Test Method D6933 Standard Test Method for Oversized Particles in Emulsified Asphalts (Sieve Test)

This test quantifies the homogeneity of the emulsion and the amount of solid asphalt particles in an emulsion. This test is important because it can help identify problems in the emulsion which may affect the application of the product including blocked spray nozzles and its performance. Particles retained in the sieve are caused by the coalescence of asphalt particles that are supposed to be dispersed. The particles may coalesce because of temperature, storage condition, age, cleanliness of the tank and storage equipment, and handing of the material. The test may be performed at room temperature or at 50°C depending on the viscosity of the emulsion. Approximately 1L of emulsion is poured over an 850μm sieve. The sieve is rinsed to eliminate excess emulsion, but the sieve retains the large pieces. The sieve is heated in a can until the water has evaporated off. The percentage of emulsion retained on the sieve is computed. A very low value for emulsion retained on the sieve is desired.

### 2.3.7 Residue

The residue of an emulsion is the asphalt content of the emulsion. The residue of the emulsion can be determined by distillation, evaporation, or by moisture analyzer.

**Residue by Distillation—Test Method ASTM D6997 Standard Test Method for Distillation of Emulsified Asphalt**

Residue by distillation is performed to calculate the asphalt content in the emulsion as well as determine the water volume and oil volume of the sample. Residue obtained from the test is often subjected to further testing. Emulsion is heated to 260°C in a still for approximately one hour. In Figure 2.3 below, a test setup including the still, ring burner, thermometer, and graduated cylinder is shown. The ring burner is positioned approximately 150mm from the bottom of the still until the emulsion reaches a temperature of 215°C. The ring burner is then moved to the bottom of the still for the remainder of the test. Water and oil are collected from the test in a graduated cylinder and measured. The still is taken off the burner and weighed to calculate the residue. The residue is then poured into molds for further testing.

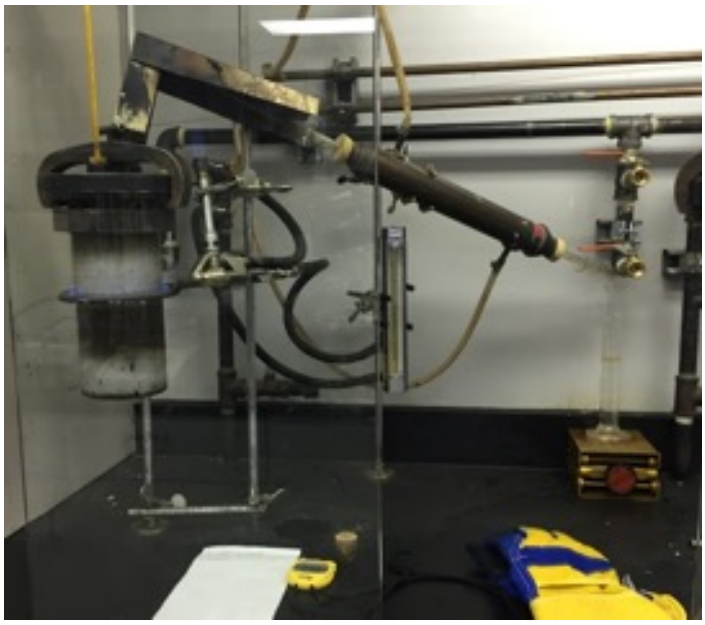

**Figure 2.3 Residue by Distillation Test Setup**

**Residue by Evaporation-Test Method ASTM D6934 Standard Test Method for Residue by Evaporation of Emulsified Asphalt**

Residue by evaporation is performed by heating a sample of emulsion in an open beaker to 163°C to determine the residual content. Residue by evaporation is not as accurate as residue by distillation and often yields residue that gives lower penetration and ductility values than residue by distillation. Residue by evaporation can be used for emulsions to pass specifications but cannot be used to reject. If emulsions do not meet specifications, the tests should be performed again using residue by distillation method instead.

**Residue by Moisture Analyzer-Test Method ASTM D7404: Standard Test Method for Determination of Emulsified Asphalt Residue by Moisture Analyzer**

This method can be used to determine the residue content of an asphalt emulsion in 50s to 140s. A small sample size of 1mL to 3mL is taken and heated in a moisture analyzer up to a maximum of 163°C. The residue results are outputted. This method of determining residue should not replace residue by distillation and is only used for reference.

### 2.3.8 Penetration-Test Method ASTM D5/D5M Standard Test Method for Penetration of Bituminous Materials

This test is performed on the residue of the asphalt emulsion to measure hardness. After the asphalt emulsion has been distilled (see distillation process above), the residue is poured from the still into a can and left to cool underneath a beaker for an hour and a half. This can is then moved into a 25°C bath for another hour and a half. The emulsion residue is then tested using a penetrometer. A needle with a standard mass and length is released and allowed to penetrate the emulsion for 5 seconds. The depth of penetration is read off of the device in tenths of a mm (decimilimeters). This is performed several times and the average of the penetration is taken.

### 2.3.9 Ductility-Test Method ASTM D113 Standard Test Method for Ductility of Asphalt

This test is performed on the residue of the emulsion to measure the ductility. The reported value is the distance in which the residue can be stretched prior to rupturing at a rate of 5cm/minute at 25°C.

### 2.3.10 Solubility-Test Method ASTM D2042 Standard Test Method for Solubility of Asphalt Materials in Trichloroethylene

This test is performed on the residue of the emulsion to determine its solubility in trichloroethylene. According to ASTM D2042: "The portion that is soluble in trichloroethylene represents the active cementing constituents. The residue is dissolved in trichloroethylene and filtered through a glass fiber pad. The insoluble material is washed, dried, and weighed. This test method covers the determination of the degree of solubility in trichloroethylene of asphalt materials having little or no mineral matter."

### 2.3.11 Float Test-Test Method ASTM D139 Standard Test Method for Float Test for Bituminous Materials and ASTM D244 Standard Test Methods and Practices for Emulsified Asphalts

This test is performed on high float emulsions and measures the resistance to flow. Once an emulsion has been distilled, the residue from the distillation is poured into the float collar at 260°C. This rests for 30 minutes. The thimble is then attached to a float saucer placed into a cold bath at 5°C for 30 minutes. Then the thimble is screwed into a float saucer and placed in a 60°C bath. If the saucer stays afloat for 20 minutes, the emulsion passes the float test.

### 2.3.12 Kinematic Viscosity-Test Method ASTM D2170/D2170M Standard Test Method for Kinematic Viscosity of Asphalts (Bitumens)

This test is performed on the residue of the emulsion to determine its kinematic viscosity. Kinematic viscosity is the ratio of the liquid's viscosity to its density. It quantifies a liquid's resistance to flow under gravity alone with no other contributing forces. Kinematic viscosities are expressed in units of $mm^2/s$. A variety of viscometers can be used to determine the kinematic viscosity of residue. The viscometer is selected based on the assumed range in which the kinematic viscosity will be. Viscometers are different in capillary shape. The viscometer is placed into a 60°C bath and conditioned to bath temperature. Residue is poured into the viscometer and conditioned to 60°C. The flow of the residue is started through suction and then gravity allows the emulsion to continue flowing through the viscometer. The efflux time for the residue to travel to a marked line is recorded and a calibration constant is applied to calculate the kinematic viscosity.

### 2.3.13 Apparent Viscosity-Test Method ASTM D4957 Standard Test Method for Apparent Viscosity of Asphalt Emulsion Residues and Non-Newtonian Asphalts by Vacuum Capillary Viscometer

This test is performed on the residue. The test is similar to the kinematic viscosity test in that it uses a viscometer conditioned in a 60°C bath, the residue flows through the capillary tube, and the efflux time is recorded. The viscometer in this test is straight and open ended which differs from the kinematic viscosity test. The viscosity is sucked by vacuum through the tube. The efflux time is multiplied by a calibration constant to determine the apparent viscosity in the unit of poise, P which equals 0.1Pa·s.

### 2.3.14 Density-Test Method ASTM D6937 Standard Test Method for Determining Density of Emulsified Asphalt

This test is performed to determine the density or weight in grams/litre of an emulsion. The weight of the empty cup is known. Emulsion is put into the cup at 25°C or 50°C and the lid is closed over top. Excess emulsion is squeezed out the top of the cup through a hole. The cup is wiped clean of excess emulsion and the weight of the filled cup is recorded. By calculation, the density can be found.

### 2.3.15 Identifying Cationics-Test Method ASTM D7402 Standard Practice for Identifying Cationic Emulsified Asphalts

This test is performed to determine whether an emulsion has a positive or negative charge which may be important for compatibility with an aggregate of a certain charge. A particle charge tester is used to determine the charge of the emulsion. The cathode and anode (electrodes) are immersed in the emulsion and connected to direct current. The accumulation of asphalt deposit is observed on the electrodes. If an emulsion is cationic, there will be considerable amount of deposit on the cathode (negative electrode).

### 2.3.16 DSR Testing-Test Method ASTM D7175 Standard Test Method for Determining the Rheological Properties of Asphalt Binder Using a Dynamic Shear Rheometer

A dynamic shear rheometer (DSR) is used to test the rheological properties (linear viscoelastic properties) including the dynamic shear modulus (complex shear modulus, G*) and phase angle, δ. The G* indicates the stiffness of the asphalt binder or the resistance of the asphalt binder to

deform under repeated loading. The δ is the delay between the applied shear stress and the shear strain. A high δ value indicates a more viscous material (Pavement Interactive, 2019).

### 2.4 Current Tack Coat Application and Previous Studies

Asphalt emulsions are often diluted with water on site before application. A diluted emulsion has additional water added to it that is not present at the time of manufacturing. A dilution of 50% emulsion, 50% water is common. The tack coat application rate is the rate in which the diluted tack coat is applied to the road. The residual application rate is the resulting rate after water has evaporated and the emulsion is set. It is important to know the residual content of the asphalt emulsion and adjust the application rate accordingly to achieve proper residual rate on the road. The asphalt residual content is typically between 57-70% of the undiluted asphalt emulsion (FHWA, 2016).

The height of the spray bar and nozzle spacing of the distributor can be adjusted so that the nozzles can achieve an overlap. A double or triple overlap is desired to ensure that the entire surface of the road is coated thoroughly with the tack coat material. A double/triple overlap means that the pattern of spray results in each part of the road is being coated by the product from two or three nozzles. Figure 2.4 shows the different types of overlap based on spray bar height.

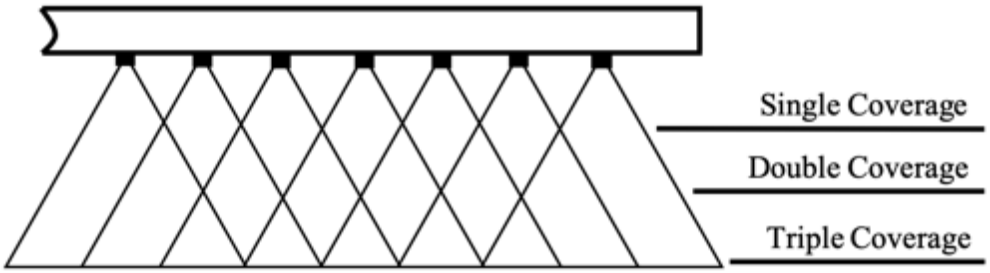


**Figure 2.4 Nozzle Height Overlap**

Tack coat material application procedures are not well defined or followed by many transportation agencies. Some construction practices allow construction trucks to drive on the tack coat layer before it is set, which does not leave enough tack coat material in the wheel paths to form a strong bond between the AC layers. Poor bonding between AC layers contributes to early deterioration of pavements and can cause premature cracking, delamination, and potholes

(Romanoschi, 1999). Other factors contributing to poor bonding include weather conditions during construction, and type of asphalt bitumen and surface texture of the underlying layer (Rahman et al., 2017 & Salinas et al., 2013).

The surface texture and cleanliness of the underlying layer are known to have an effect on the bond strength between AC layers. Several studies evaluated the effect of surface preparation, aging, and characteristics of pavement structure on bond strength between AC layers. These studies showed varying results for the effect of these factors. Destrée and De Visscher (2017) concluded that there was no significant difference between the bond strength of cores exposed to varying levels of pressure washing prior to tack coat application on a milled surface. In terms of surface roughness of the underlying AC layer, results of bond strength test were inconsistent. Mohammad et al. (2010) found that roughness of the underlying AC layer had an effect on bond strength. A milled AC layer yielded the highest bond strength followed by an existing unmilled layer and then a new AC lift. Das et al. (2017) contradicts the results of the above study and found that the highest bond strength is achieved by milled AC layer, followed by a new AC lift, and then an existing unmilled layer. In terms of the effect of age on the strength of the bond between layers, Raab et al. (2015) found that the interlayer shear bond increases with aging as long as the traffic loading remains lower than the design life of the pavement structure. A rate of increase in strength of 1% per month for up to 10 years is predicted (Raab et al., 2015). Using finite element (FE) analysis, Mohammad et al. (2011) found that the interface bond characteristics of a thick AC layer is less affected by tack coat type and application rate than a thinner AC layer (Mohammad et al., 2011).

Tack coat materials typically cost between 1 and 2% of the total pavement construction cost (Asphalt Institute, 2014). If the bond is weak, the resulting rehabilitation costs can amount to 30% to 100% of total pavement cost (Asphalt Institute, 2014). Ensuring that an adequate bond is formed between pavement layers will maximize the agency paving budgets and taxpayer investment into road infrastructure. Due to construction challenges, fast curing and non-tracking emulsions are recently considered as better candidates for tack coat materials. Using a fast curing tack coat material minimizes construction delay, reduces pickup and tracking of emulsion residue on construction equipment, and ensures achieving proper bond between AC layers.

A worldwide survey was conducted on construction practices and quality assurance method for tack coat materials (Mohammad et al., 2012). According to this worldwide survey, 26% of the surveyed agencies allow construction trucks to drive on unbroken emulsion. Furthermore 70% of the surveyed agencies allow construction trucks on broken emulsion before it has set. Out of the 53 surveyed agencies, 74% of the agencies allow paving to begin immediately after the tack coat material breaks, whereas 26% do not allow paving until the tack coat emulsion sets. Of the surveyed agencies, 92% stated that they do not test to measure the bond strength at the interface between AC layers. Based on the above statistics, there is clearly a need for fast breaking and setting tack coat materials and better construction practices and monitoring (Mohammad et al., 2012).

Despite the multitude of studies on tack coat performance in the literature, the choice of tack coat product, application rate, and application procedures are mostly based on empirical judgement (Mohammad et al., 2009). Several studies reviewed the bond strength and application procedures of tack coat materials including a recent comprehensive study performed by the Transportation Research Board (TRB) summarized in a technical publication titled NCHRP 712: Optimization of Tack Coat for HMA Placement (Mohammad et al., 2012). This study explores multiple aspects of tack coat procedures including application rates, effects of poor construction practices, development of an in-situ tack coat quality test, and the development of the lab test, AASHTO TP 114 (Mohammad et al., 2012). However, these studies did not take into account the extreme weather conditions experienced in the Canadian Prairies.

Selecting the optimum residual application rate is critical to ensure proper bonding. Excess application of tack coat material results in shear slippage at the interface between two AC layers (Mohammad et al., 2009). Young Seo et al. (2017) evaluated the tackiness and rheological properties of trackless emulsions using the DSR. This study recommends a tackiness test for evaluating stickiness and tracking resistance of emulsions. A trackless emulsion with low stickiness and adhesive failure is ideal for use as a tack coat material (Young Seo et al., 2017).

There are many methods for measuring the bond between AC layers. The NCHRP 712 report identified twenty testing methods used by agencies for tack coat bonds including both laboratory and in-situ tests (Mohammad et al, 2012). Most of these tests measure shear stress or tensile

strength. Some of these tests include the Leutner Shear Test, Florida Direct Shear Test, and the Switzerland Pull Off Test (Mohammad et al., 2012). The Louisiana Interlayer Shear Strength Tester (LISST) was developed and then adopted by AASHTO as standard TP 114-15 to be used as the standard test for tack coat materials. The LISST is a direct shear device that can be used in conjunction with a universal testing machine to test the interlayer shear strength (ISS) of core samples by applying vertical shearing force at the interface between two AC layers. The LISST device is made up of a reaction frame, which remains stationary throughout the test, and a moving shearing frame. A cylindrical core sample is placed into the device and load is applied to the shearing frame. As the load increases, the core sample shears at the interface (Mohammad et al., 2012). The advantages of the LISST are that it has a nearly frictionless linear bearing to maintain vertical travel and that it fits in any universal testing machine (AASHTO, 2015).

Two of the most common field tests to measure tensile strength are the A-Tacker Test and the UTEP Pull-Off Device (UPOD). These devices are operated manually and therefore do not have uniform loading which causes unreliable results. The A-Tacker device was improved with the creation of the Louisiana Tack Coat Quality Tester (LTCQT) as a reliable field test for tack coat material. The LTCQT provided repeatable results with a coefficient of variation less than 11% (Mohammad et al., 2009).

Mahmoud et al. (2017) developed a field test for tack coat materials called the Oregon Field Torque Tester (OFTT). This in-situ bond strength tester offers a cheaper and less destructive method of testing for interlayer shear strength. The OFTT requires smaller core samples than previously mentioned methods. Cores are 2.5 inches in diameter and are not taken at full depth. The OFFT devices measures peak torque in the field. Peak torque was correlated with interlayer shear strength results obtained in the lab from AASHTO TP 114. Field results from the OFTT were highly correlated with the shear strength results of core samples tested with the LISST in the lab. An $R^2$ value of 0.972 was observed for the average of all samples in each section for both field and laboratory settings (Mahmoud et al., 2017).

The studies below by Mohammad et al. (2002) and Das et al. (2017) have compared the strength of various tack coat products. These results are only partly useful as some of these products are not used in Saskatchewan. Mohammad et al. (2002) evaluated the shear strength of several tack

coat products using a simple shear test. Results from the shear strength test showed that CRS-2P had the highest interface shear strength compared to SS-1, CSS-1, SS-1h, and two performance-graded asphalt cements (PG 64-22 and PG 76-22M). At its optimum application rate of 0.09L/$m^2$, CRS-2P had 83% of the shear strength of a single asphalt layer indicating that there is weakness in between asphalt layers even with a strong tack bond (Mohammad et al., 2002). Das et al. (2017) found that non-tracking, rapid setting emulsions have a higher ISS than the typical SS-1 and SS-1h emulsions due to stiffer asphalt cements used in non-tracking products (Das et al., 2017).

Hakimzadeh et al. (2012) used an interface bond test (IBT), a laboratory tension test, to evaluate the bond between AC layers for laboratory compacted cores. This study recommended evaluating tack coat materials in both shear and tensile test modes. Two tack coat materials, SS-1hp and a trackless emulsion, were tested in both tension and shear modes. Results of tension tests indicated that a higher tack coat amount is required to create a satisfactory adhesive bond when compared to shear testing. In shear testing, the trackless emulsion had a higher shear strength than the slow setting SS-1hp. Laboratory compacted core specimens had higher shear strength when the tack coat was immediately overlayed compared to cores with a two hour delay between tack placement and overlay (Hakimzadeh, 2012).

Bae et al. (2010) tested tack coat materials for ISS using a LISST device at temperatures between -10°C and 60°C. This study found that interlayer shear strength of tack coat materials increases with the decrease in test temperature (Bae et al., 2010). These results indicate that the bond between AC layers have a stronger bond in the winter months and a weaker bond during warm temperatures.

### 2.5 Effect of Freeze-Thaw Cycling on AC Materials

There have been many studies focused on the effect of moisture and freeze and thaw cycling on AC materials. These studies have not focused on the effect of cold climate on the bond between AC layers, but on the effect on other properties of the AC including viscoelastic, mechanical, and thermovolumetric properties. AC is a thermoplastic material with viscoelastic characteristics, and its behavior varies with temperature (Doré & Zubeck, 2009). For this reason, AC used in

climates with high temperature variations needs to be studied to understand its performance at different conditions.

The longevity and durability of pavements in cold climates is significantly affected by freeze-thaw cycling (Gubler et al., 2005). AC deteriorates with freeze-thaw cycling and exposure to moisture. AC is a porous medium that contains asphalt binder, aggregate, and air voids within the mixture. The air voids are dispersed within the mixture in a complex structure which allows water to find a flow path within the mixture. Permeability of the AC pores is an important parameter and has a direct relation to the longevity of pavements. Moisture in the voids of the AC mixtures in combination with temperature change leads to premature failure (Goh & You, 2012). The pressure inside the saturated pores is dynamic due to vehicle loading. (Kutay & Aydilek, 2007). Moisture travelling through AC is a function of: aggregate gradation, layer thickness, binder creep, void size and distribution. Water in AC is not evenly distributed and rarely entirely fills the voids (Huining et al., 2018).

Freeze-thaw cycling in pavement occurs when water inside the voids freezes or thaws with the change in temperature below and above freezing temperature. AC mixtures are damaged due to the expansion and contraction of water as it changes in phase from liquid to solid, which causes adhesion and cohesion loss within the AC mixtures (Goh & You, 2012). The factors affecting adhesion and cohesion loss include: traffic loading, aggregate gradation, weather conditions, quality of construction, compatibility of the cement and aggregate, water absorption on the aggregate-cement interfaces (McCann & Sebaaly, 2003). A study by Yi et al. (2014) found that by subjecting AC samples to freeze-thaw cycling and testing uniaxial compression, a loss of cohesion in the asphalt binder is the main method of failure in freeze-thaw cycling and the reason for the loss in strength within the samples. AC samples had more elastic-plastic properties after freeze-thaw cycling (Yi et al., 2014).

AC pavements are affected by the mechanical loading of traffic, specifically heavy truck traffic, and environmental factors including temperature, moisture, and freeze-thaw cycling. Freeze-thaw cycling of AC samples may lead to thermal cyclic damage due to the nonuniformity of the temperature within the sample. The surface of an AC sample heats and cools faster than the interior of the sample, which causes differences between expansion and contractions within the

sample (Badeli et al., 2018). Microdamage accumulates instead of cracking when the expansion of water combined with vehicular traffic causes compressive stresses lower than the tensile strength of the AC (Si et al., 2014). With many freeze-thaw (FT) cycles, the compressive stress will exceed the tensile strength and macrodamage including cracks and other distresses will occur (Feng et al., 2010). The effect of temperature fluctuations, including daily and seasonal fluctuations, on fatigue damage is large. Up to 98% of fatigue damage is caused by these fluctuations including 96% due to seasonal fluctuations and 2% due to daily fluctuations (Tarefder, 2013). The contraction of the asphalt binder during freezing is restricted by the aggregate (Teguedi et al., 2017). There are two types of cracking that result from thermal changes: thermal fatigue cracking, and low temperature transverse cracking. Cracks develop in the pavement when the thermal tensile stresses exceed the tensile strength of the pavement. Low temperature transverse cracks are caused by shrinkage due to cold temperatures. Thermal fatigue cracking is caused by ageing asphalt and a large number of cyclical loads (Qiao et al., 2013).

The permeability of asphalt mixes is affected by freeze-thaw cycling. The more freeze thaw cycling, the easier it is for water to flow through an AC mix. During freeze-thaw cycling, voids expand and new voids form. AC mixes that are open graded mixes are more susceptible to damage through freeze-thaw cycling than well graded (dense) mixes (Xu et al., 2016). Ozgan & Serin (2013) found that laboratory compacted AC samples experienced a void change of 39.4% after 24 FT cycles, one day in length (Özgan & Serin, 2013). Although it is well known that water freezes at 0°C, this may not be the case for water trapped in the pores of the asphalt. The size of the void determines the temperature required for freezing. A larger void requires a colder temperature for water to freeze than a smaller void. When water freezes it expands 9%. An AC mix with lower density (a larger percentage of voids) achieves steady state temperature faster than a denser AC mix (a smaller percentage of voids) because of its lower specific heat capacity and thermal conductivity (Hassn et al., 2016).

Many studies found the properties of AC degrade with increased exposure to FT cycling. An image processing study found that samples subjected to eight freeze-thaw cycles per day for 38 days showed more cracking and moisture damage after each freeze-thaw cycle (Goh & You, 2012).

Another study found that the splitting strength of asphalt decreases with freeze-thaw cycling (Feng et al. 2009). A study using up to twenty freeze thaw cycles and a 4-point bending test on AC beams found that stiffness decreases with increased freeze-thaw cycling (Barlas, 2013). A study by Gilmore et al. (1985) found that the tensile strength of AC significantly decreased after exposure to 11 FT cycles each one day in length (Gilmore et al., 1985). A sensitivity analysis was performed to see what effects temperature, precipitation, windspeed, percent sunshine, ground water level, and seasonal temperature variation had on longitudinal cracking, fatigue cracking, rutting, and IRI. The study found that both an increase in average annual temperature and seasonal temperature variation are the biggest factors leading to fatigue cracking, rutting, and longitudinal cracking. Temperature and moisture both decrease the longevity of pavement as they affect the stiffness of the binder (Qiao et al., 2013).

There were a plethora of different FT cycle techniques, durations, and temperatures in the literature. Most studies involved conditioning and testing samples prepared and compacted within a laboratory setting. Some studies involving conditioning samples by vacuum saturation prior to freeze-thaw cycling. Because there are no studies researching the effect of freeze-thaw cycling on tack coat materials or bond between pavement layers, it was difficult to choose a test to follow as a guideline. A summary table of some of these methods used in previous studies involving FT cycling related to pavement materials is shown below in Table 2.1.

**Table 2.1 Freeze-Thaw Cycle Patterns**

| Prior Conditioning | Freeze Temp | Thaw Temp | Cycle Pattern | Sample Info | Additional Notes | Standard | Reference |
|---|---|---|---|---|---|---|---|
| Dry and Vacuum Saturated | -18°C | 6°C | 150 and 300 cycles | Cores from a Lab Compacted Slab. 150mm height, 74mm diameter | Temperature increase and decrease at 4.5°C/min, temperature sustained for 1.5 hours. | ASTM C666 | Badeli et al., 2018 |
| Vacuum Saturated | -18°C in air | 25°C in water | 0, 5, 10, 15, 20, 25, 30 cycles | Cylindrical samples compacted in the lab | Freezing for 16 hours and thawing for 12 hours. | - | Xu et al., 2016 |
| Vacuum Saturated | 18°C in air | 60°C in water | N/A | Cylindrical samples compacted in the lab. 120mm in height, 100mm in diameter. | Freezing for 15 (or 16) hours. Thawing for 24 hours. | ASTM D4867 | Hamzah et al., 2017 |
| N/A | -5°C | 30°C | 150 cycles | Cylindrical samples compacted in the lab. 50mm in height, 100mm in diameter. | Freezing for 16 hours. Thawing for 8 hours. | ASTM C1645 | Islam & Tarefder, 2016 |
| N/A | N/A | N/A | 6, 12, 18, 24 days of FT cycling | Laboratory compacted samples | Each FT cycle was one day in length | - | Özgan & Serin, 2013 |

| | | | | | | | |
|---|---|---|---|---|---|---|---|
| Humidity added, 15% at freeze, 40% at thaw | -5°C | 30°C | 20 FT cycles | Laboratory compacted cylindrical samples with 63.5mm in height and 100mm diameter, also BBR samples, and beam samples | Freezing for 16 hours. Thawing for 8 hours | ASTM C1645 | Barlas, 2013 |
| N/A | -18°C | 60°C | 0, 2, 4, 6, 8, 10 FT cycles | Cylindrical samples compacted in the lab. 100mm in height, 100mm in diameter. | Freezing for 16 hours. Thawing for 24 hours. | - | Yi et al, 2014 |
| Vacuum Saturated | -11°C | 20°C | 3 cycles | Cylindrical samples compacted in the lab. 90mm in height, 80mm in diameter. | Freezing for 3 hours. Thawing for 1 hour. | - | Teguedi et al., 2017 |
| Dry and Saturated | -18°C | 10°C | 1,2, 7, 20, 30 cycles | Cylindrical samples cored from lab compacted slab. 80mm in diameter, 120mm in height. | Freezing for 11.5 hours. Thawing for 11.5 hours. Rate of change 56°C/h. | - | Lamothe et al., 2015 |
| Saturated in a 60°C bath for 14 days | -18°C | 25°C | 3 and 10 cycles | Cylindrical samples compacted in the lab. 150mm in height, 75mm in diameter. | Freezing 24 hours. Thawing 24 hours. | - | Lachance-Tremblay et al., 2018 |
| Vacuum Saturated | N/A | 60°C | Up to 11 cycles | N/A | Freezing 24 hours. Thawing 24 hours. | - | Gilmore et al., 1985 |

| | | | | | | | |
|---|---|---|---|---|---|---|---|
| Vacuum Saturated | -18°C in air | 60°C in water | 1 and 3 cycles | Lab prepared | Freezing for 16 hours. Thawing for 24 hours. | ASTM D4867 | Hamzah et al., 2014 |
| Saturated | -18°C | 60°C | 1 and 3 cycles | Laboratory compacted. 4 inch in diameter | Freezing for 16 hours. Thawing for 24 hours. | AASHTO T283 | Porras et al., 2014 |
| Saturated | -25°C | 25°C | 14 cycles | Laboratory compacted. 100mm in height, 100mm in diameter. | Freezing for 12 hours. Thawing for 12 hours. | - | Ma et al., 2015 |
| Saturated in a 60°C bath for 14 days | -18°C | 25°C | 3 and 10 cycles | Cylindrical samples compacted in the lab. 150mm in height, 75mm in diameter. | Freezing 24 hours. Thawing 24 hours. | - | Lachance-Tremblay et al., 2017 |
| Vacuum Saturated | -10°C | 10°C | 7 cycles | Laboratory compacted. 90mm in height, 80mm in diameter. | Increase and decrease rate of 20°C per hour. Maintained for 11 hours. | - | Maudit et al., 2010 |
| Saturated | -18°C | 60°C | 1, 3, 6, 9, 12, 15, 18, 21 cycles | Laboratory compacted cylindrical cores | Freezing for 16 hours. Thawing for 24 hours and 2 hours at 25°C. | AASHTO T283 | Hajj et al., 2011 |
| Saturated | -18°C | 60°C | 13 cycles | Laboratory compacted slabs | Freezing for 16 hours. Thawing for 8 hours. | - | Obaidat et al., 2005 |

| | | | | | | | |
|---|---|---|---|---|---|---|---|
| Water Flow Over Surface | -17.8°C | 4.4°C | 7 cycles | Laboratory compacted cylindrical cores. 100mm in diameter | Each cycle was 24 hours with freezing maintained for 8 hours and thawing for 4 hours. | - | Amini & Tehrani, 2014 |
| N/A | -18°C | 60°C | 1, 2, 5, 10, 15 cycles | Laboratory compacted cylindrical cores. | Each cycle was 24 hours. 16 hours freezing, 8 hours thawing. | - | Tang et al., 2013 |
| N/A | -24°C | 24°C | 2 cycles | Laboratory compacted samples | 24 hours of freezing, 24 hours of thawing. | ASTM D560 | Attia & Abdelrahman, 2010 |
| Saturated | -25°C | 25°C | Up to 14 cycles | Laboratory compacted samples 102mm in diameter. 64mm in height. | Freezing 12 hours. Thawing 12 hours | - | Si et al., 2014 |
| N/A | -17.8°C in air | 4.4°C in water | 300 cycles | Laboratory compacted samples 183mmx50mmx70mm | One cycle was 3 hours. | ASTM C666 | Goh & You, 2012 |
| N/A | -5°C | 30°C | 5, 10, 15, 20 cycles | Laboratory compacted samples. 100mm in diameter, 64mm in height. | Freezing for 16 hours, thawing for 8 hours. | ASTM C1645 | Tarefder, et al., 2018 |
| N/A | -20°C | 60°C in water | 2, 4, 6, 8 cycles | Laboratory compacted | Freezing for 8 hours, thawing for 4 hours | - | Feng et al., 2009 |

| | | | | | | | |
|---|---|---|---|---|---|---|---|
| N/A | -18°C in air and water | 25°C | 5, 10, 15, 20, 25, 30 cycles | Laboratory compacted to a height of 63.5mm | Freezing for 16 hours, thawing for 12 hours | - | Xu et al., 2015 |
| Vacuum Saturated | -20°C | 60°C in water | 2, 4, 6, 8 cycles | Laboratory compacted. 63.5mm in height, 100mm in diameter | Freezing for 8 hours, thawing for 4 hours | - | Badeli et al., 2018 |

Note: Data that is not available has been marked as N/A.

## 2.6 Climatic Conditions in Saskatchewan

The climate in southern Saskatchewan is considered to be warm summer humid continental (Dfb) climate according to the Koppen Climate Classification. In this climate classification there are large seasonal differences in temperature including warm to hot summers and cold winters. Precipitation is spread throughout the year. The coldest month must have a mean temperature below -3°C and there must be four months whose mean temperatures are above 10°C. The warmest month must have a mean temperature less than 22°C (Arnfield, 2009). Table 2.2 shows the average daily mean temperature for each month for the first year after construction of field test sections for this project. The nearest Government of Canada weather station to Blaine Lake, SK is the Saskatoon International Airport Station. This station was used to retrieve ambient temperature information from the date of construction of field test sections on August 22, 2017 to August 21, 2018, one year post construction. Note that this station is 75km south of the test site meaning that there could be differences in temperature. Ideally pavement temperature data would be available too, but air temperature is the only data available. Blaine Lake will likely have slightly cooler temperatures than Saskatoon because it in more northerly. As required by the Koppen Climate Classification for Dfb category, the coldest month, February has a mean temperature of -18.1°C which is less than -3°C. The Dfb category requires 4 months to have a mean temperature above 10°C and there are 5 months: May, June, July, August, and September. The warmest month is required to have a mean temperature less than 22°C, and the warmest months July and August have a mean of 18.7°C.

**Table 2.2 Average Daily Mean Temperature by Month for Saskatoon**

| Month | Average Daily Mean Temperature (°C) |
|---|---|
| January | -12.9 |
| February | -18.1 |
| March | -8.6 |
| April | -0.7 |
| May | 14.4 |
| June | 17.3 |
| July | 18.7 |
| August | 18.7 |
| September | 12.8 |
| October | 5.0 |
| November | -9.8 |
| December | -12.3 |

The maximum, minimum, and mean daily temperatures are summarized by frequency in 5°C bins as shown in Figure 2.5, Figure 2.6, and Figure 2.7. The most frequent 5°C bin for the maximum temperature is 25°C to 30°C. The second most frequent 5°C bin for maximum temperature is tied between 20°C to 25°C, and -10°C to -5°C. The most frequent 5°C bin for minimum daily temperature is 5°C to 10°C. The second most frequent 5°C bin for minimum daily temperature is tied between 0°C to 5°C and 10°C to 15°C. The most frequent 5°C bin for mean daily temperature is 15°C to 20°C. The second most frequent 5°C bin is -10°C to -5°C.

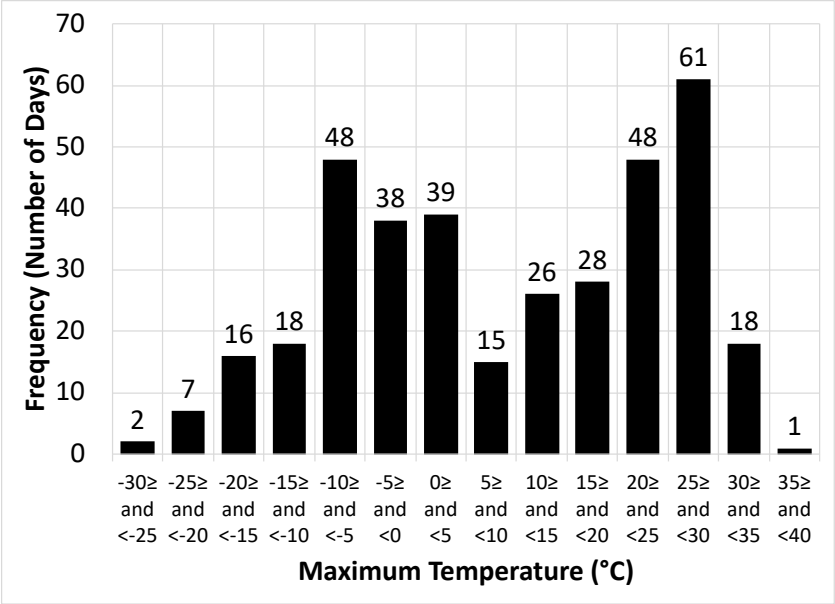


**Figure 2.5 Maximum Daily Temperature**

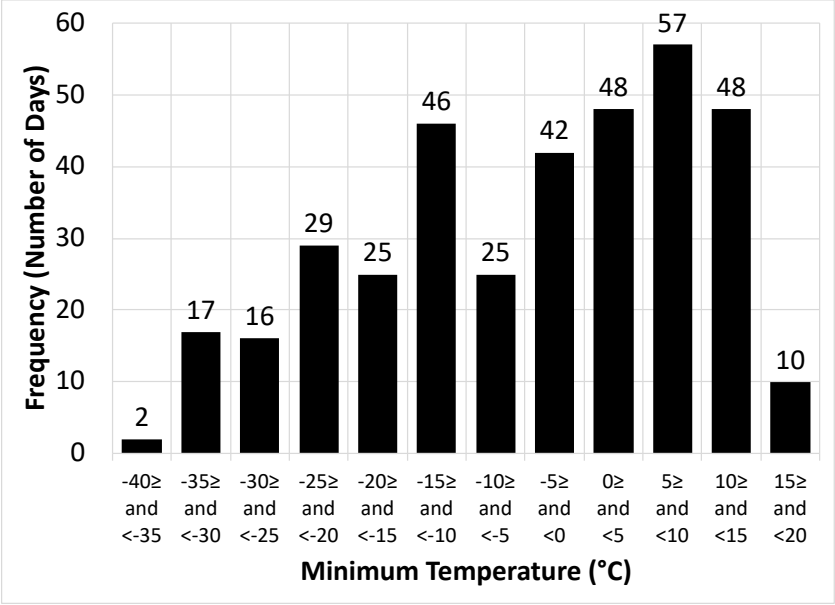


**Figure 2.6 Minimum Daily Temperature**

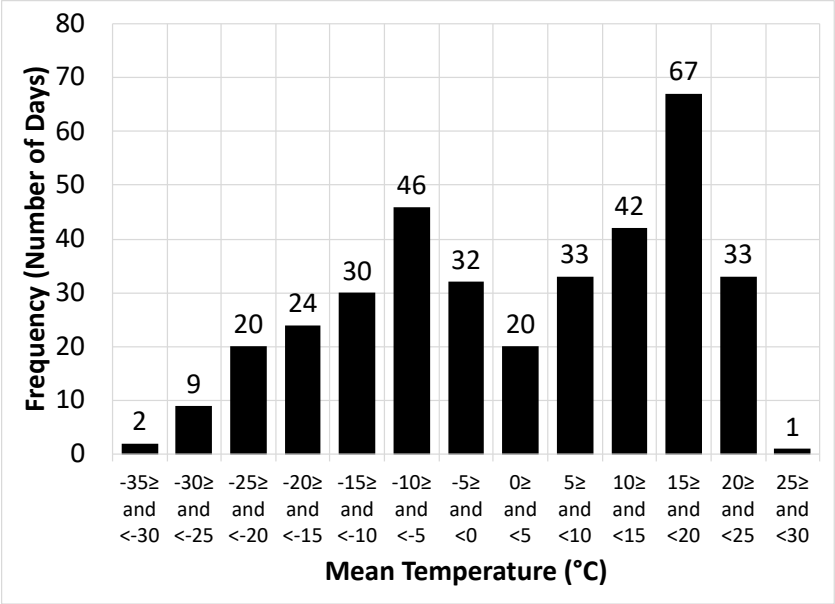


**Figure 2.7 Mean Daily Temperature**

A summary of the weather data during the year between August 21, 2017 and August 21, 2018 is shown in Table 2.3. There were 292 days that either stayed above 0°C or stayed below 0°C meaning there was no freeze or thaw. There were 73 days which fluctuated between positive and negative temperatures meaning there was freezing or thawing. The maximum temperature experienced was 38.2°C and the minimum temperature was -36.5°C meaning that there is a 75°C range in temperature. There was precipitation on 123 days, approximately 1/3 of all days in the year. Figure 2.8 shows the daily minimum, maximum, and mean ambient temperatures for the year.

**Table 2.3 Weather Data Summary**

| Condition | No. of Days |
|---|---|
| Days without freeze or thaw | 292 |
| Days with freeze or thaw | 73 |
| Days min temp is less than 0°C. | 202 |
| Days min temp is greater than or equal to 0°C. | 163 |
| Days max temp is less than 0°C. | 129 |
| Days max temp is greater than or equal to 0°C. | 236 |
| Total precipitation days | 123 |
| Max Temperature (°C) | 38.2 |
| Min Temperature (°C) | -36.5 |
| Min Mean Temperature (°C) | -31.7 |
| Max Mean Temperature (°C) | 25.9 |

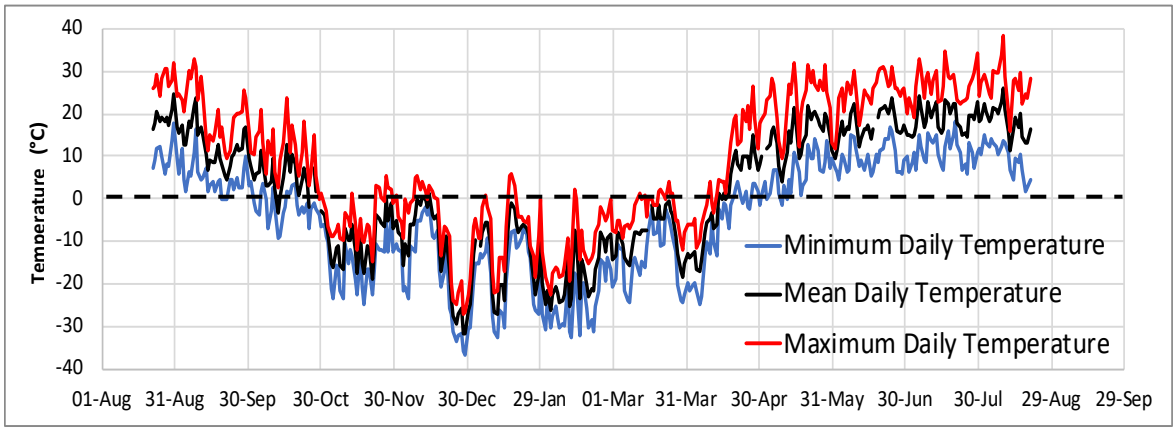


**Figure 2.8 Daily Minimum, Maximum, and Mean Air (Ambient) Temperatures**

Historical climatic data from the Long-Term Pavement Performance (LTPP) program shows the trends created from temperature data taken between 1942 and 2012 (LTPP, 2019). The average number of FT cycles in a year between 1942 and 2012 is 79. The FT cycles per year are shown in Figure 2.9. The maximum and minimum temperatures recorded every year between 1942 and 2012 are shown in Figure 2.10. The average minimum temperature recorded for each year is -38°C and the average maximum temperature is 34°C. These statistics show that 2017-2018 was a typical year in Saskatchewan with 73 FT cycles and a maximum and minimum temperatures of 38°C and -37°C, respectively.

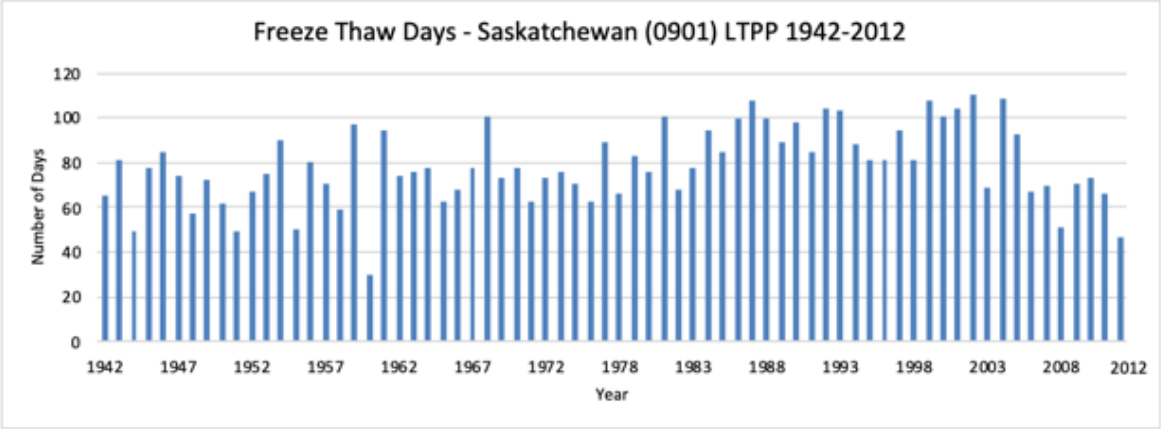


**Figure 2.9 Freeze-Thaw Days per Year**

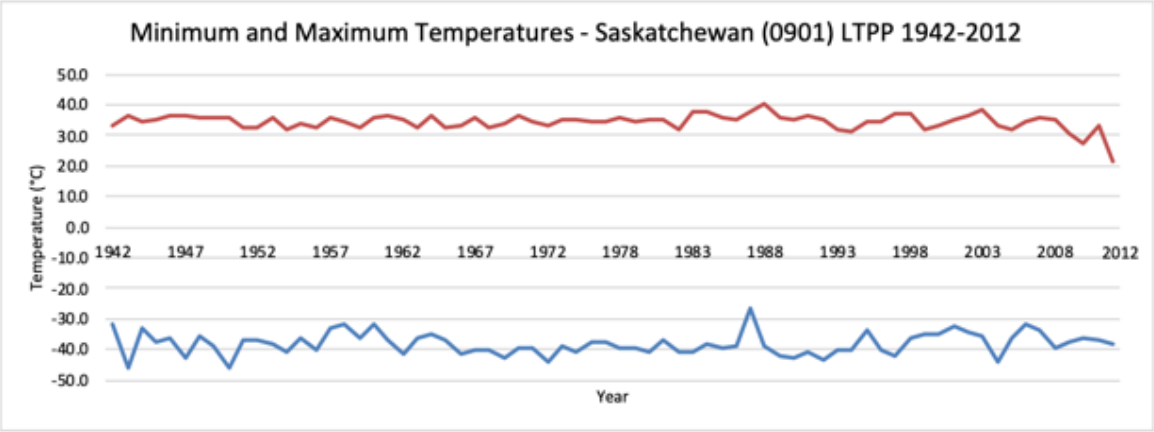


**Figure 2.10 Minimum and Maximum Temperatures from Each Year**

# CHAPTER 3: EXPERIMENTAL PROGRAM

## 3.1 Introduction

This research project is comprised of a field study and a laboratory testing program. The field study evaluated the constructability and performance of tack coat materials in normal field conditions. Construction and environmental data were recorded at the time of installation of tack coat materials. A post-construction distress survey was completed to document early distresses related to the construction process. A second distress survey was completed in Summer 2018 approximately one year after construction. In addition to distress surveys, core samples were collected after construction to evaluate the initial bond strength. Additional core samples were collected in Summer 2018 to assess the changes in bond due to traffic loading and environmental conditions.

The laboratory testing program focuses on testing the bond strength of the tack coat materials using the core samples collected from the field test sections. Bond strength tests were conducted according to AASHTO TP 114: Determining the Interlayer Shear Strength (ISS) of Asphalt Pavement Layers. Part of the post-construction core samples were conditioned in the lab under accelerated freeze-thaw cycling to simulate field conditions in cold regions. A flowchart showing the experimental program layout is shown in Figure 3.1.

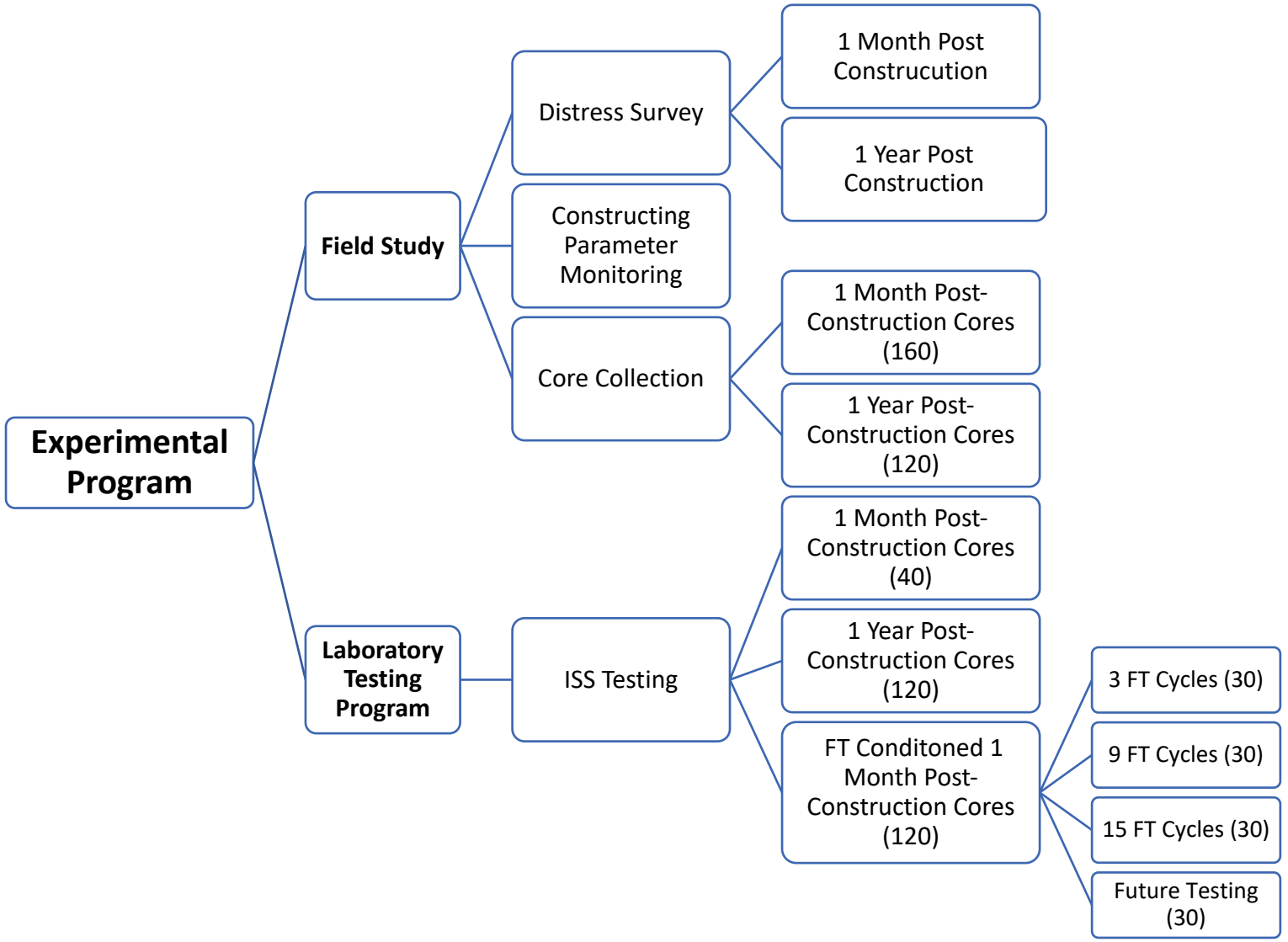


**Figure 3.1 Experimental Program Flowchart**

### 3.2 Materials

Seven tack coat materials provided by industry partners were evaluated in this study. Three slow setting emulsions were provided: SS-1, SS-1h, and a cationic SS-1h (CSS-1h). An anionic medium setting emulsion, MS-1, was also tested. The slow setting anionic emulsion SS-1 was tested in three sections and SS-1h was tested in two sections. SS-1 was used as the control material for comparison because it is the typical material used in all Saskatchewan Highways projects. Three fast breaking/quick setting proprietary products were also provided by the industry partners: TackMax$^{TM}$, Colasphalt Tack, and Clean Bond.

According to the manufacturer datasheet, Colasphalt Tack is fast breaking, stable enough to store for longer than traditional fast breaking emulsions, compatible with standard distributors, and equal in bonding to typically used emulsified tack coats (Colasphalt, 2018).

According to the manufacturer datasheet, Clean Bond is a cationic or anionic slow setting asphalt emulsion that allows for faster curing than traditional tack coats with a non-tracking, non-tacky finish. It is designed for stability during application and allows for quick curing times in the field. It can be applied diluted or non-diluted (McAsphalt Industries Limited, 2017).

The manufacturer data sheets were provided with the typical property specification for each product. The tests performed on these products includes the following ASTM Standard tests:

- ASTM D6937: Standard Test Method for Determining Density of Emulsified Asphalt
- ASTM D6997: Standard Test Method for Distillation of Emulsified Asphalt
- ASTM D7496: Standard Test Method for Viscosity of Emulsified Asphalt by Saybolt Furol Viscometer
- ASTM D6933: Standard Test Method for Oversized Particles in Emulsified Asphalts (Sieve Test)
- ASTM D6930: Standard Test Method for Settlement and Storage Stability of Emulsified Asphalts
- ASTM D6935: Standard Test Method for Determining Cement Mixing of Emulsified Asphalt
- ASTM D7402: Standard Practice for Identifying Cationic Emulsified Asphalts

- ASTM D6936: Standard Test Method for Determining Demulsibility of Emulsified Asphalt
- ASTM D244: Standard Test Methods and Practices for Emulsified Asphalts
- ASTM D5: Standard Test Method for Penetration of Bituminous Materials
- ASTM D113: Standard Test Method for Ductility of Asphalt Materials
- ASTM D2042: Standard Test Method for Solubility of Asphalt Materials in Trichloroethylene

For each product, the specification range and typical values for each property is listed in Table 3.1.

## Table 3.1 Specifications According to Manufacturer Data Sheets

| | | Product | | | | | | | | | | | | | | | | | | | | |
|---|---|---|---|---|---|---|---|---|---|---|---|---|---|---|---|---|---|---|---|---|---|---|
| | | SS-1 | | | SS-1H | | | MS-1 | | | CSS-1H | | | TackMax | | | Colasphalt Tack | | | Clean Bond | | |
| | | Acceptable Range | | | Acceptable Range | | | Acceptable Range | | | Acceptable Range | | | Acceptable Range | | | Acceptable Range | | | Acceptable Range | | |
| **Property** | **Test Standard** | **Min** | **Max** | **Typica** | **Min** | **Max** | **Typica** | **Min** | **Max** | **Typica** | **Min** | **Max** | **Typical** | **Min** | **Max** | **Typica** | **Min** | **Max** | **Typical** | **Min** | **Max** | **Typical** |
| **Tests on Emulsion** | | | | | | | | | | | | | | | | | | | | | | |
| Specific Gravity (Density) at 15.6°C, kg/L | ASTM D6937 | - | - | 1.015 | - | - | 1.022 | - | - | 1.006 | - | - | 1.020 | - | - | 1.015 | - | - | 1.010 | N/A | | |
| Residue by Distillation, % by mass | ASTM D6997 | 55 | - | 60 | 55 | - | 60 | 55 | - | 60 | 57 | - | 60 | 55 | - | 58 | 57 | - | 60 | 55 | - | 60.5 |
| Viscosity at 25°C, S.F.S. | ASTM 7496-D88 | 20 | 100 | 25 | 20 | 60 | 30 | 20 | 100 | 30 | 20 | 100 | 22 | 20 | 100 | 40 | 20 | 100 | 21.21 | 20 | - | 28 |
| Oversized Particles (Sieve), % by mass | ASTM D6933 | - | 0.100 | <0.001 | - | 0.100 | 0.003 | - | 0.1 | <0.001 | - | 0.3 | <0.3 | - | 0.100 | <0.001 | - | 0.10 | 0.03 | - | 0.1 | 0.02 |
| Settlement (24 hours), % by mass | ASTM D6930 | - | 1.5 | 0.4 | - | 1.5 | 0.4 | - | 1.5 | 0.2 | - | 1.0 | 0.5 | - | 1.5 | 0.4 | - | 1.0 | 0.3 | N/A | | |
| Cement Mixing Test, % by mass | ASTM D6935 | N/A | | | - | 2.0 | 1.0 | N/A | | | N/A | | | - | 2.0 | 1.0 | N/A | | | N/A | | |
| Particle Charge Test | ASTM D7402 | N/A | | | N/A | | | N/A | | | | Positive | Positive | N/A | | | | | Positive | Positive or Negative | | |
| Demulsibility (50mL, 0.10N CaCl2), % by mass | ASTM D6936 | N/A | | | N/A | | | 60 | - | 95 | N/A | | | N/A | | | N/A | | | N/A | | |
| Coating Ability and Water Resistance | ASTM D244 | Pass | | Pass | N/A | | | N/A | | | N/A | | | N/A | | | N/A | | | N/A | | |
| | | | | | | | | | | | | | | | | | | | | | | |
| **Tests on Residue** | | | | | | | | | | | | | | | | | | | | | | |
| Penetration at 25°C (100g, 5s), dmm | ASTM D5 | 100 | 200 | 145 | 40 | 100 | 65 | 100 | 200 | 140 | 40 | 125 | 100 | 40 | 90 | 55 | 100 | 250 | 126 | 20 | 55 | 35 |
| Ductility at 25°C (5cm/min), cm | ASTM D113 | 60 | - | >60 | 60 | - | >60 | 60 | - | >60 | 40 | - | >40 | N/A | | | 60 | - | >60 | N/A | | |
| Solubility in Trichloroethylene, % by mass | ASTM D2042 | 97.5 | - | >97.5 | 97.5 | - | >97.5 | 97.5 | - | >97.5 | 97.5 | - | >97.5 | 97.5 | - | >97.5 | 97.5 | - | 99.99 | N/A | | |
| Ash Content, % | | N/A | | | N/A | | | N/A | | | N/A | | | N/A | | | N/A | | | - | 1.0 | 0.15 |

A comparison of the typical values for viscosity, residue, and penetration of each product is shown in Figure 3.2, Figure 3.3, and Figure 3.4. Viscosity values ranged from 21 to 40 s.f.s. The product with the lowest viscosity is Colasphalt Tack and the highest is TackMax™. Penetration values range between 35 and 145 dmm. SS-1, MS-1, and Colasphalt Tack have high penetration values; SS-1h, TackMax™, and Clean Bond have low penetration values; and CSS-1h has a penetration value in the middle. The residue by distillation values for all products are all comparable and range between 58% and 60.5% by mass.

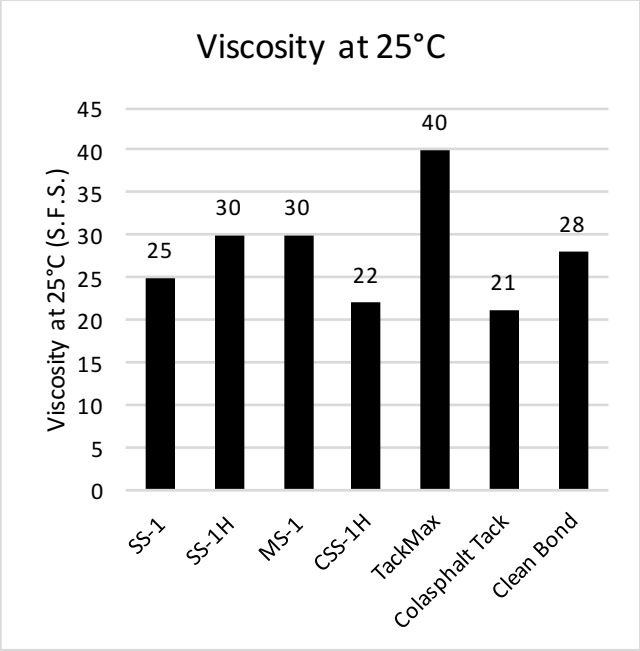


**Figure 3.2 Typical Viscosities for Tack Coat Materials at 25°C**

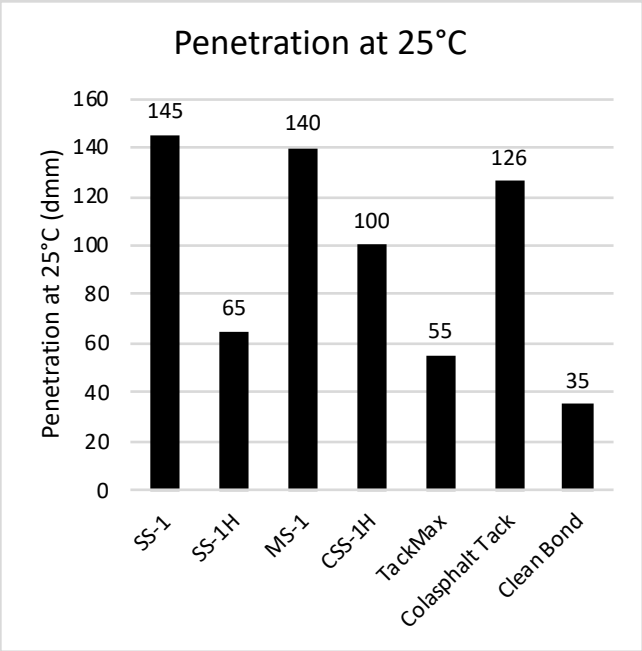


**Figure 3.3 Typical Penetrations for Tack Coat Materials at 25°C**

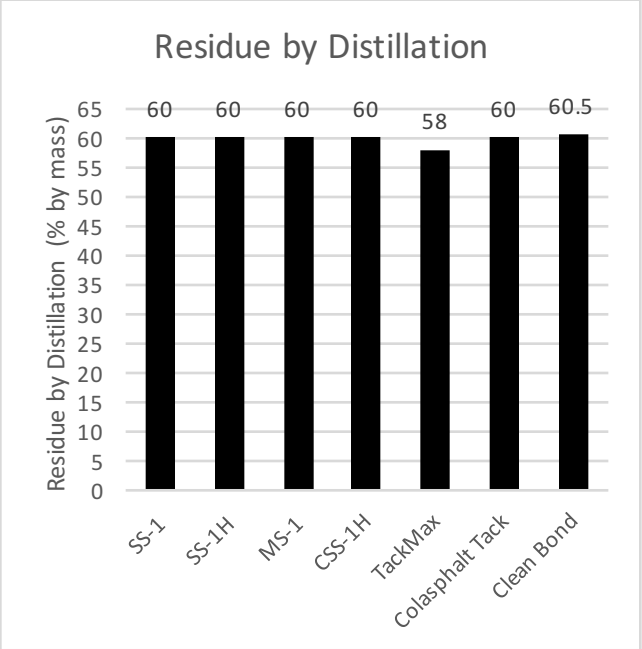


**Figure 3.4 Residue by Distillation**

Properties of the undiluted tack coat materials prior to loading the materials into totes and shipping to the construction site can be found in Table 3.2. Tests performed on the tack coat materials prior to the trial include:

- ASTM D6997: Standard Test Method for Distillation of Emulsified Asphalt
- ASTM D5: Standard Test Method for Penetration of Bituminous Materials
- ASTM D7496: Standard Test Method for Viscosity of Emulsified Asphalt by Saybolt Furol Viscometer
- ASTM D6933: Standard Test Method for Oversized Particles in Emulsified Asphalts (Sieve Test)
- ASTM D6930: Standard Test Method for Settlement and Storage Stability of Emulsified Asphalts
- ASTM D113: Standard Test Method for Ductility of Asphalt Materials

Note that the residue values for SS-1, SS-1h, CSS-1h, and Clean Bond shown in Table 3.2 are slightly higher than the typical values but still in the acceptable range found in the manufacturer data sheets in Table 3.1. The other parameters all fit within the specified limits according to the manufacturer data sheets.

**Table 3.2 Laboratory Properties of Tack Coat Materials Prior to Trial**

| Product | SS-1 | SS-1h | MS-1 | CSS-1h | TackMax™ | Colasphalt Tack | Clean Bond |
|---|---|---|---|---|---|---|---|
| **Residue by Distillation (% b.m.) - ASTM D6997** | 60.1 | 61.3 | 59.5 | 61 | 55.6 | 58.9 | 61.4 |
| **Oil Portion of Distillate (% b.v.) - ASTM 6997** | 0.5 | 0.5 | 0.8 | 1.0 | 0.5 | 2 | 0.5 |
| **Penetration (dmm) - ASTM D5** | 130 | 69 | 151 | 95 | 70 | 135 | 46 |
| **Saybolt Furol Viscosity (s.f.s.) - ASTM D7496** | | | | | | 66.1 | |
| **Oversized Particles on 850-µm wire cloth (% b.m.) - ASTM D6933** | | | | | | 0.0 | 0.03 |
| **Storage Stability (%) - ASTM D6930** | | | | | | 0.9 | |
| **Ductility (cm) - ASTM D113** | | | | | | 70+ | |

### 3.2.1 Emulsified Asphalt Lab Quality Control Tests

During construction, two samples of each product were taken from the distributor at the time of application. These samples were sent to two industry partner labs (Gecan lab and Husky Asphalt (Pounder Emulsions lab) for quality control testing. Tests included:

- ASTM D6997: Standard Test Method for Distillation of Emulsified Asphalt
- ASTM D7496: Standard Test Method for Viscosity of Emulsified Asphalt by Saybolt Furol Viscometer
- ASTM D5: Standard Test Method for Penetration of Bituminous Materials

- ASTM 7404: Standard test Method for Determination of Emulsified Aspahlt Residue by Moisture Analyzer
- ASTM D6933: Standard Test Method for Oversized Particles in Emulsified Asphalts (Sieve Test)
- ASTM D7175: Standard Test Method for Determining the Rheological Properties of Asphalt Binder Using a Dynamic Shear Rheometer

Note that these products are tested after dilution. Results may differ from test results prior to the trial due to dilution, contamination inside the totes, contamination within the distributor, and separation in the distributor. Table 3.3 shows a comparison of results from Pounder Emulsion's lab and Gecan's lab. The viscosity and residue values for all products are below their specified minimums in the manufacturer data sheets. The penetration values for SS-1, SS-1h for Section 9, TackMax™, and Clean Bond are higher than permitted. The results for the sieve test for oversized particles for SS-1 in Sections 1 and 6, SS-1h, MS-1, and TackMax™ are all higher than the permitted 0.1% mentioned in the manufacturer data sheets.

## Table 3.3 Comparison of Lab Properties of Products Once Diluted and Put into Totes

| | | | Product | | | | | | | | | | | | | | | | | | | |
|---|---|---|---|---|---|---|---|---|---|---|---|---|---|---|---|---|---|---|---|---|---|---|
| | | | SS-1 | | SS-1 | | SS-1 | | SS-1H | | SS-1H | | MS-1 | | CSS-1H | | TackMax | | Colasphalt | | Clean Bond | |
| | | Lab | P | G | P | G | P | G | P | G | P | G | P | G | P | G | P | G | P | G | P | G |
| | | Dilution | 50-50W | | 50-50W | | 30-70W | | 50-50W | | 50-50W | | 70-30W | | 50-50W | | - | | - | | - | |
| **Property** | **Test Standard** | **Section** | 1 | | 6 | | 5 | | 2 | | 9 | | 4 | | 7 | | 3 | | 8 | | 10 | |
| Viscosity at 25°C, S.F.S. | ASTM D7496 | | 6.4 | 8.59 | 8.6 | 8.48 | 8.6 | 8.06 | 8.6 | 8.92 | 12.6 | 9.12 | 9.9 | 8.22 | 15.6 | 8.78 | 11.7 | 7.98 | 9.1 | 11.03 | 15.7 | 12.32 |
| Residue by Distillation, % by mass | ASTM D6997 | | 31.15 | 28.6 | 30 | 28.33 | 19.6 | 13.86 | 29.7 | 29.49 | 26.7 | 28.06 | 39.3 | 38.36 | 26.5 | 30.1 | 50.4 | 49.72 | 56.2 | 55.95 | 52.6 | 52.2 |
| Total Distillate, % by volume | ASTM D6997 | | 69.5 | | 66.5 | | 80.3 | | 70.5 | | 76 | | 61.5 | | 65.5 | | 49 | | 40.5 | | 45.5 | |
| Oil Portion of Distillate, % by volume | ASTM D6997 | | 2 | 3.5 | 0.5 | 1 | 0.5 | 1 | 1.0 | 3 | 9.5 | 13 | 2 | 4 | 3 | 1.5 | 1.5 | 2.5 | 1.5 | 1.5 | 3 | 4 |
| Penetration at 25°C (100 g, 5s), dmm | ASTM D5 | | >250 | 450 | 116 | 153 | 110 | 125 | 84 | 116 | 211 | 180 | 124 | 174 | 105 | 135 | 124 | 141 | 139 | 169 | 59 | 94 |
| Moisture Analyzing Balance, % Residue | ASTM D7404 | | 29.7 | 27.15 | 29 | 30.3 | 20.4 | 19.9 | 29.9 | 29.3 | 27 | 24.15 | 38.4 | 38.6 | 26.8 | 29.8 | 51.3 | 38.6 | 55.7 | 56.15 | 52 | 52 |
| Oversized Particles (Sieve), % by mass | ASTM D6933 | | | 6.18 | | 0.04 | | 0.31 | | 1.79 | | 0 | | 0.23 | | 0.09 | | 2.18 | | 0 | | 0.1 |

Note: Lab P indicates results from Pounder Emulsion's lab and Lab G indicates results from Gecan's lab.

The results from the DSR including comparison of G*/sin(δ), phase angle, and complex shear modulus are shown in Table 3.4, Table 3.5, and Table 3.6. Additional plots comparing the manufacturer specification values, properties of the tack coat materials after manufacturing, and the properties of the tack coats samples off of the distributor can be found in Appendix A.

**Table 3.4 Comparison of DSR Results from Pounder (P) and Gecan (G) Labs**

| | | Lab ID | P | G | P | G | P | G |
|---|---|---|---|---|---|---|---|---|
| | | Test Temp | 52°C | 52°C | 58°C | 58°C | 64°C | 64°C |
| Product | Dilution | Section Number | G*/sin (δ) (kPa) | | | | | |
| SS-1 | 50-50W | 1 | 0.956 | 0.71 | | 0.35 | | 0.19 |
| SS-1H | 50-50W | 2 | 6.18 | 4.55 | 2.69 | 2 | 1.23 | 0.93 |
| TackMax | - | 3 | 4.04 | 3.52 | 1.83 | 1.62 | 0.868 | 0.78 |
| MS-1 | 70-30W | 4 | 3.32 | 2.74 | 1.61 | 1.31 | 0.827 | 0.67 |
| SS-1 | 30-70W | 5 | 3.77 | 3.57 | 1.68 | 1.6 | 0.787 | 0.76 |
| SS-1 | 50-50W | 6 | 3.47 | 3.14 | 1.55 | 1.41 | 0.73 | 0.66 |
| CSS-1H | 50-50W | 7 | 4.11 | 3.6 | 1.85 | 1.63 | 0.879 | 0.78 |
| Colasphalt Tack | - | 8 | 2.65 | 2.54 | 1.20 | 1.16 | 0.575 | 0.55 |
| SS-1H | 50-50W | 9 | 3.62 | 2.09 | 1.62 | 0.97 | 0.767 | 0.476 |
| Clean Bond | - | 10 | 9.21 | 8.22 | 3.97 | 3.55 | 1.79 | 1.61 |

**Table 3.5 Comparison of Phase Angles from Pounder (P) and Gecan (G) Labs**

| | | Lab ID | P | G | P | G | P | G |
|---|---|---|---|---|---|---|---|---|
| | | Test Temp | 52°C | 52°C | 58°C | 58°C | 64°C | 64°C |
| Product | Dilution | Section Number | Phase Angle, δ | | | | | |
| SS-1 | 50-50W | 1 | 85.8 | 87.1 | | 88.2 | | 88.9 |
| SS-1H | 50-50W | 2 | 81.9 | 83.2 | 84.3 | 85.4 | 86.3 | 87.1 |
| TackMax | - | 3 | 82.8 | 83.2 | 85 | 85.2 | 86.8 | 87 |
| MS-1 | 70-30W | 4 | 80.3 | 81.5 | 81.6 | 83.1 | 82.1 | 84.1 |
| SS-1 | 30-70W | 5 | 83 | 83 | 85.3 | 85.3 | 87.1 | 87.1 |
| SS-1 | 50-50W | 6 | 83.3 | 83.7 | 85.5 | 86 | 87.3 | 87.9 |
| CSS-1H | 50-50W | 7 | 84 | 84.1 | 85.6 | 85.8 | 87 | 87.2 |
| Colasphalt Tack | - | 8 | 85 | 85 | 86.7 | 86.7 | 88 | 88.2 |
| SS-1H | 50-50W | 9 | 84.3 | 85.6 | 86.2 | 87.3 | 87.7 | 88.5 |
| Clean Bond | - | 10 | 81.0 | 81.6 | 83.3 | 83.9 | 85.3 | 85.8 |

**Table 3.6 Comparison of G* Values from Pounder (P) and Gecan (G) Labs**

| | | Lab ID | P | G | P | G | P | G |
|---|---|---|---|---|---|---|---|---|
| | | Test Temp | 52°C | 52°C | 58°C | 58°C | 64°C | 64°C |
| Product | Dilution | Section Number | G* (kPa) | | | | | |
| SS-1 | 50-50W | 1 | 0.95 | 0.714 | | 0.354 | | 0.185 |
| SS-1H | 50-50W | 2 | 6.12 | 4.52 | 2.68 | 1.99 | 1.23 | 0.925 |
| TackMax | - | 3 | 4.01 | 3.49 | 1.82 | 1.62 | 0.87 | 0.778 |
| MS-1 | 70-30W | 4 | 3.27 | 2.71 | 1.59 | 1.3 | 0.82 | 0.657 |
| SS-1 | 30-70W | 5 | 3.74 | 3.54 | 1.67 | 1.6 | 0.79 | 0.756 |
| SS-1 | 50-50W | 6 | 3.45 | 3.12 | 1.55 | 1.4 | 0.73 | 0.663 |
| CSS-1H | 50-50W | 7 | 4.09 | 3.58 | 1.84 | 1.63 | 0.88 | 0.78 |
| Colasphalt Tack | - | 8 | 2.64 | 2.53 | 1.20 | 1.16 | 0.57 | 0.554 |
| SS-1H | 50-50W | 9 | 3.60 | 2.08 | 1.62 | 0.971 | 0.77 | 0.476 |
| Clean Bond | - | 10 | 9.10 | 8.13 | 3.94 | 3.53 | 1.78 | 1.61 |

### 3.3 Field Study Location and History

Highway 12 is a North-South two-lane rural highway in Saskatchewan which is approximately 135 kilometres long. It begins in Saskatoon and terminates in Shell Lake. Highway 12 services many communities including the city of Martensville, the town of Hepburn, Big Shell Lake, Memorial Lake, and many acreages and farms. Highway 12 is a major corridor for North-South traffic involved in the industries of aggregate production, agriculture, and tourism (Saskatchewan Ministry of Highways and Infrastructure, 2017).

Resurfacing of this highway was underway and a portion of the highway was allocated to the tack coat field study. The resurfacing project involved milling 30mm of the old asphalt surface and laying two lifts of AC, each 50 mm in thickness. The test sections for the study were set up just south of Blaine Lake, Saskatchewan. Figure 3.5 and Figure 3.6 show the location of Blaine Lake within Saskatchewan and Canada. The total length of the sections was a 1.1km stretch between stations 24.9 and 26.0. Figure 3.7 shows a map of the construction area. This area of the highway is on moraine plane and the soil consists of stratified surficial deposits (Saskatchewan Ministry of Highways & Infrastructure, 2017). The test section was setup once the bottom lift of AC was completed. Therefore, this study focuses on evaluating the bond strength between the two new layers of AC. Construction of the test sections and field work took place on August 22 and 23, 2017.

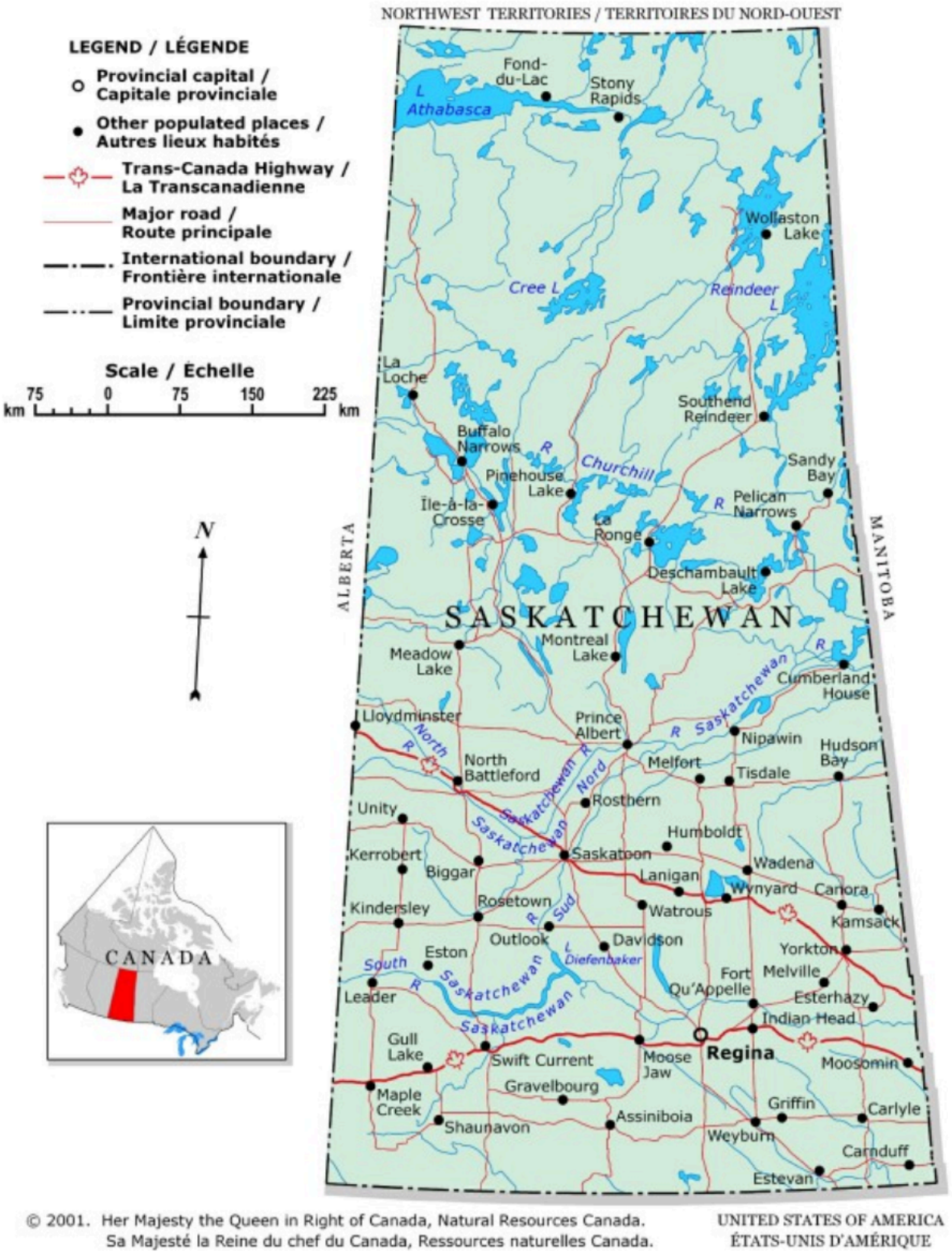


**Figure 3.5 Map of Saskatchewan (Natural Resources Canada, 2001)**

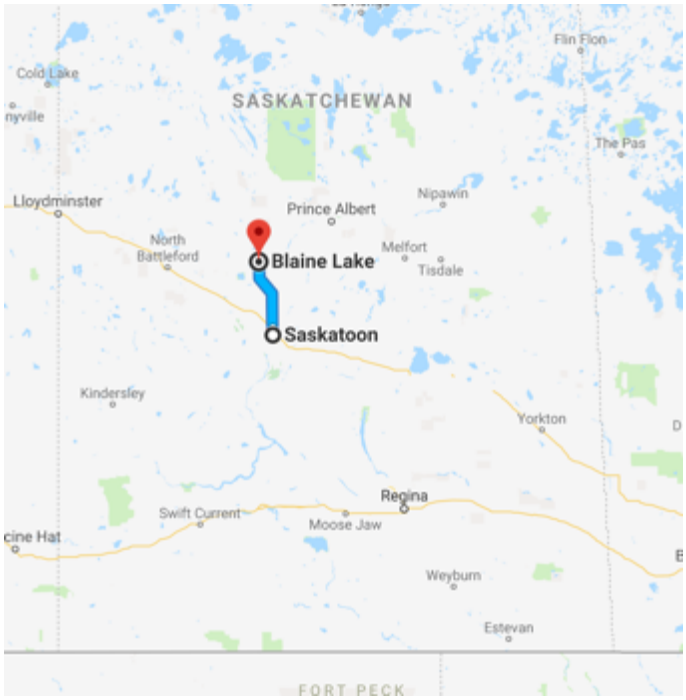


**Figure 3.6 Location of Blaine Lake Relative to Saskatoon (Google Maps, 2018)**

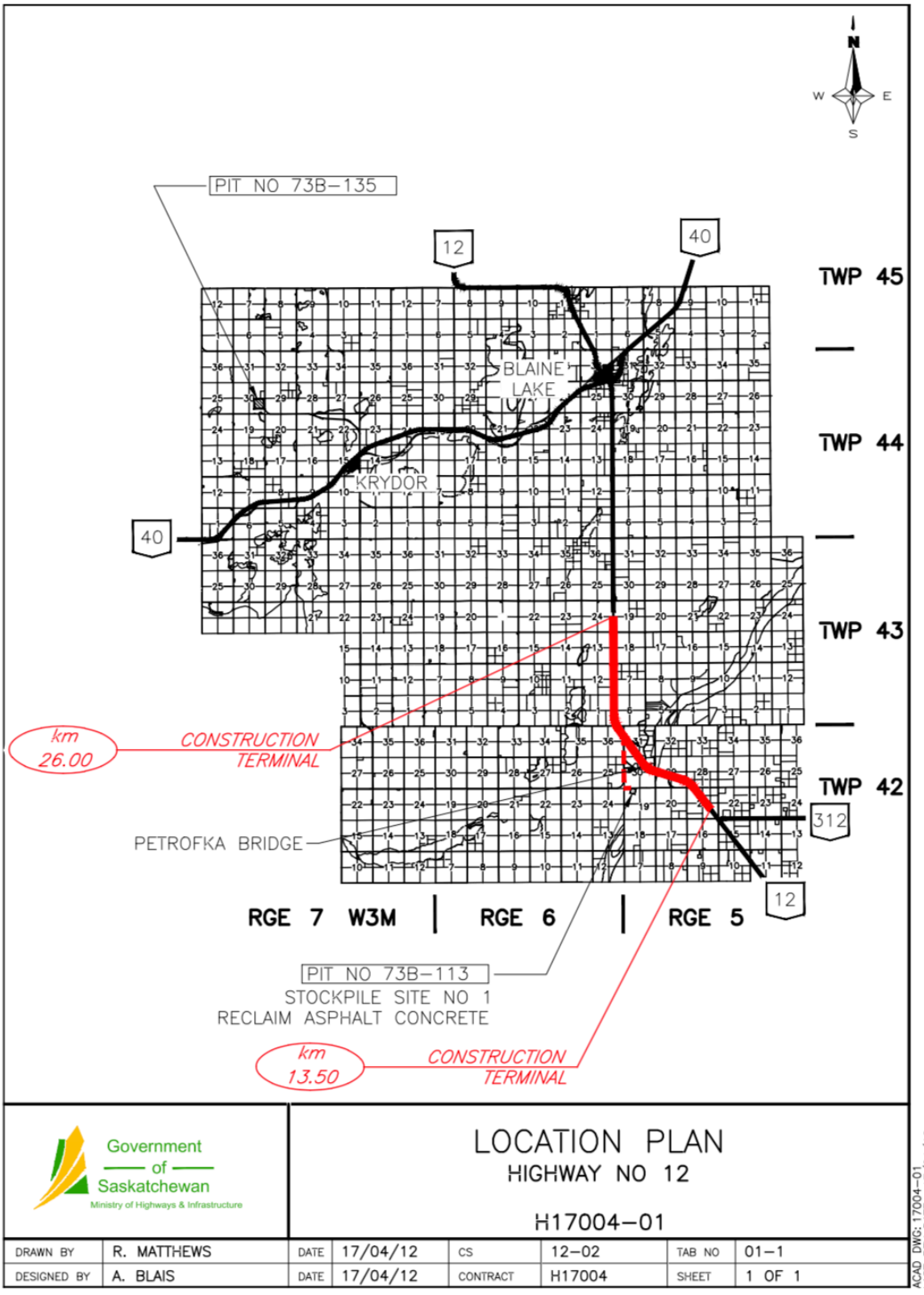


**Figure 3.7 Construction Area Map (Ministry of Highways & Infrastructure, 2017)**

A brief history of the construction of this Highway 12 segment is as follows:

- The subgrade was originally constructed in 1962.
- In 1979 it was upgraded to a sealed granular surface.
- In 1990 it was upgraded again including the addition of more base aggregate and 80 mm of AC.
- Since 1990 there has not been a full rehabilitation project, but various surface treatments and patching has occurred (Saskatchewan Ministry of Highways & Infrastructure, 2017).

Based on previous construction logs, the thicknesses of the layers are as follows: base layer of 252mm and subbase thickness of 226mm, for a total of 478mm of granular material, and 80mm of asphalt; this is shown in Figure 3.8 In 2017, bore holes were drilled to test for the thickness of the layers and were found as follows: total granular material of 340mm, and total asphalt thickness of 95mm (Saskatchewan Ministry of Highways & Infrastructure, 2017).

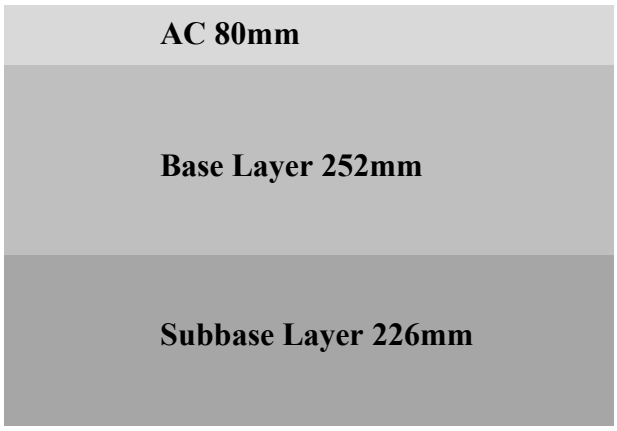


**Figure 3.8 Layer Thicknesses Based on Construction Logs**

The cross-section of Highway 12 consists of 3.7m wide lanes with 2.5% cross slope. The reason for the rehabilitation project is due to the poor condition of the road including rutting.

The traffic on Highway 12 in the study location has been recorded and is as follows:

- The 2015 Annual Average Daily Traffic (AADT) is 1940.
- The Truck Annual Average Daily Traffic (TAADT) is 330 which is 17% of total traffic.

- There is an annual grain haul in the South direction of approximately 32,300 Equivalent Single Axle Loads (ESALs).
- The design AADT is 2037 vehicles per day because it is adjusted due to growth forecasting (Saskatchewan Ministry of Highways & Infrastructure, 2017).

### 3.3.1 Test Sections Setup

The 1.1km stretch of Highway 12 dedicated to the project was divided into 10 approximately equal sections, 5 in the south bound lane and 5 in the north bound lane. Figure 3.9 shows the layout of the test sections, the product applied in each section, and product-water mixing proportions.

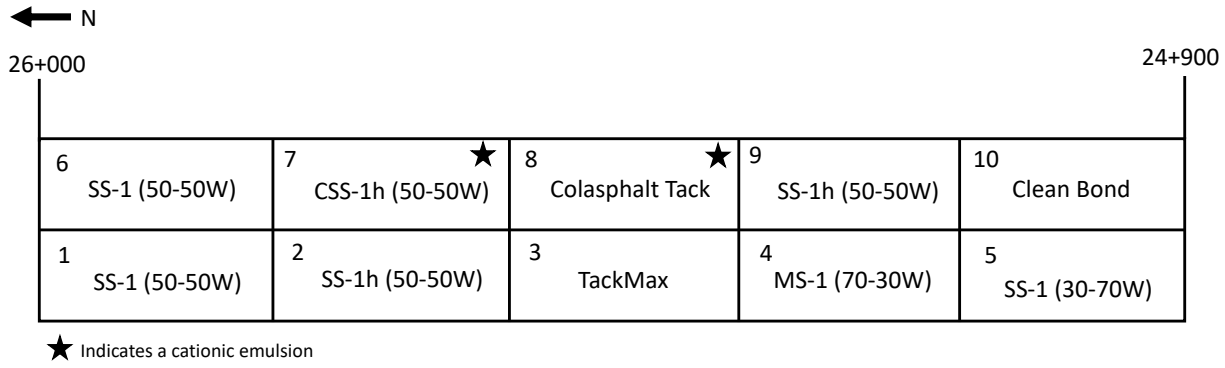


**Figure 3.9 Test Sections and Products Layout**

Prior to construction, a plan was created to best collect the information needed. Ten test sections were constructed within a 1.1km section of Highway 12. Five sections were constructed in the northbound lane and five sections were constructed in the southbound lane. Within each test section, further sections were created to ensure all parameters were measured accurately. Each test section was approximately 225m in length and was further divided into specific testing areas. These areas are calibration/application rate testing area, pick up and tracking testing area, non-destructive testing (NDT) area, and two coring areas. Figure 3.10 shows the different areas within each test section. Specific measurements for each test sections can be found in Appendix B.

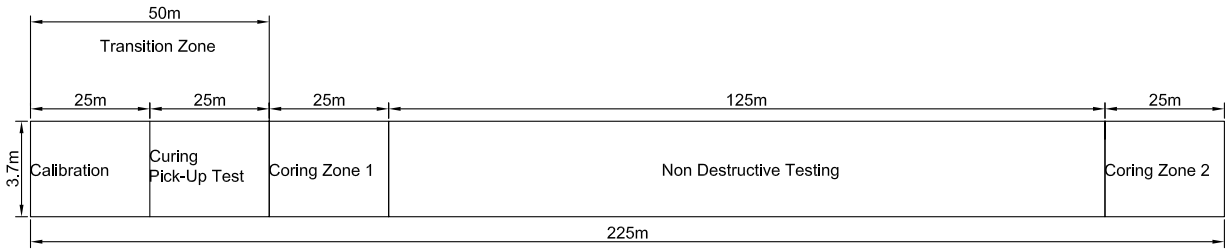


**Figure 3.10 Test Section Schematic**

The first area was the calibration/application rate testing area. This 25m segment was used to calibrate the distributor application rate by means of a patch test. This patch test was a modified version of ASTM D2995. The patch test was performed to ensure the distributor was applying a consistent application rate as desired. Eleven absorbent square patches 0.53m in width were placed on the road. The distributor sprayed this 25m section and stopped. Patches were weighed and the actual application rate was determined. Adjustments were made to the distributor on-board rate control computer, if necessary. The setup of the patches is shown in Figure 3.11. Five patches are laid out along the width of the spray bar. Six more pads are placed in the wheel paths, three in the inner wheel path and three in the outer wheel path.

The application rate from the patch test was calculated by:

$$\text{Application Rate } \left[\frac{L}{m^2}\right] = \frac{\text{Mass of patch after spray [kg]-Mass of patch before spray [kg]}}{\text{Specific Gravity of Oil x Area of Patch [m}^2\text{]}}$$

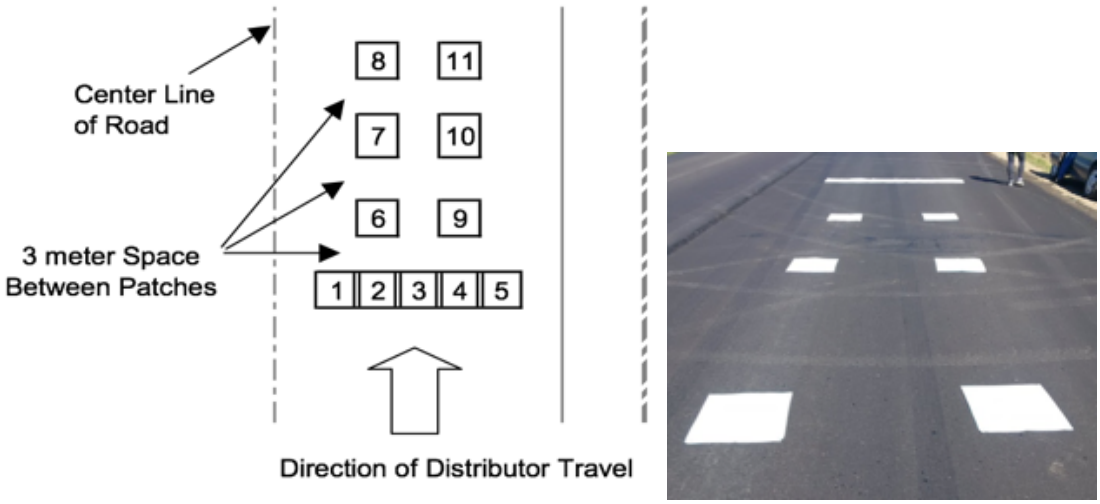


**Figure 3.11 Layout of Patch Test (WSP, 2017)**

The recorded construction information was target application rate, actual application rate from patch test, and average application rate from the distributor data. A comparison of the application rates is shown below in Figure 3.12. A more detailed comparison of the application rates according to wheel path location is shown in Appendix A. Once the calibration of the distributor was finalized, the remaining 200 metres were sprayed.

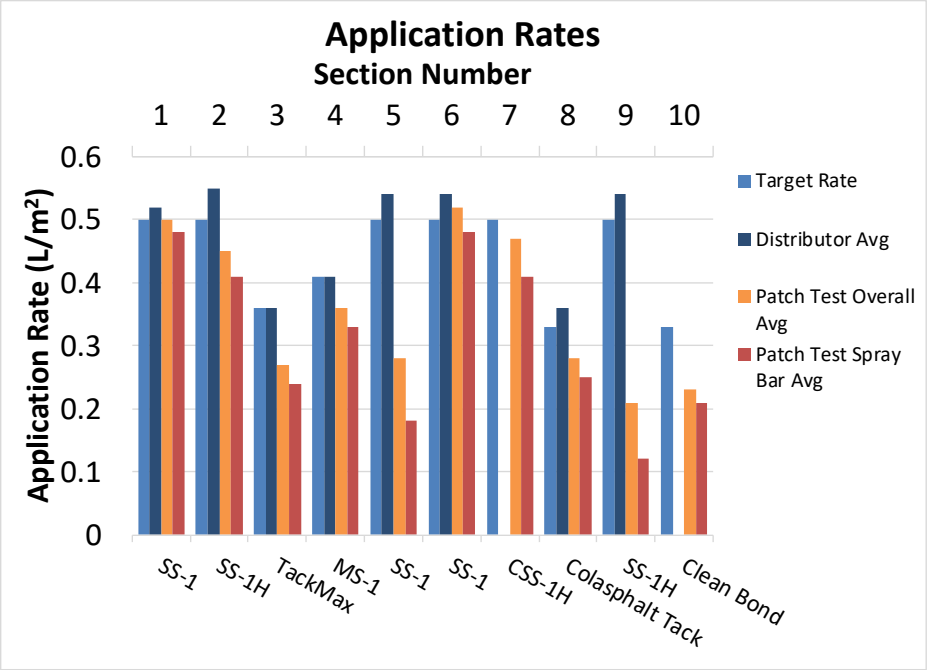


**Figure 3.12 Application Rates**

The second testing area focused on pick-up and tracking of tack coat emulsion on truck tires. This 25m zone was used to evaluate the breaking and setting times as well as the severity of pickup/tracking on truck tires. Once the product had set, a truck was driven over the section and the material was given a visual rating of none, low, medium, or high according to its pick-up/tracking by truck tires. The third area is the non-destructive testing area. This 125m area was used to perform the distress survey post construction and one year after construction. The last areas are the two coring areas. Each coring area will be used to extract 32 cores over 5 years.

Additional photos from construction can be found in Appendix C.

### 3.3.2 Coring Plan

Cores were collected from the inner and outer wheel paths (IWP & OWP), and the centre of each lane. Since the tack coat trial project will take five years to complete, a detailed coring plan for five years was created. The OWP, centre, and IWP cores were collected at distances of 0.9m, 1.8m, and 2.7m respectively, from the outside edge of the lane as per the Saskatchewan Ministry of Highways procedures. During the first coring period on September 11 & 12, 2017 eight cores were collected from each area as shown as the red circles in Figure 3.13 below. Since there are two coring areas per section, a total of 16 cores were obtained from each section. On September 10 & 11, 2018 a second set of cores was collected. The remaining 18 cores will be taken from the road following the winters of years 2019, 2020, and 2021.

Table 3.7 and Table 3.8 show a breakdown of the cores collected post-construction and one year later. These cores are depicted as the blue circles in Figure 3.13 below. A detailed coring map for each of the ten test sections can be found in Appendix D.

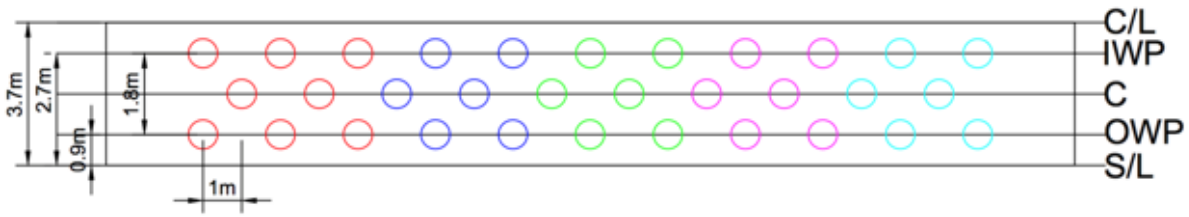


| | | |
|---|---|---|
| 3 Weeks Post Construction | Period 1 | 16 Cores |
| Summer 2018 | Period 2 | 12 Cores |
| Summer 2019 | Period 3 | 12 Cores |
| Summer 2020 | Period 4 | 12 Cores |
| Summer 2021 | Period 5 | 12 Cores |
| Total | | 64 Cores |

**Figure 3.13 Core Plan for a Single Zone**

**Table 3.7 Core Breakdown for Post Construction (Period 1)**

| | Zone 1 | | | Zone 2 | | | | | | |
|---|---|---|---|---|---|---|---|---|---|---|
| Core Location | IWP | OWP | Centre | IWP | OWP | Centre | Total IWP | Total OWP | Total Centre | **Overall Total** |
| No. of Cores | 3 | 3 | 2 | 3 | 3 | 2 | 6 | 6 | 4 | 16 |

Figure 3.14 shows the road following coring and the eight four-inch cores collected from a coring area. Core holes were filled with a cold mix asphalt. Cores were drilled using a coring drill mounted on the back of a pickup truck. Following extraction, each core was labelled based on test section number (1-10), coring zone number (1 or 2), and location in the road (IWP, centre, or OWP. Cores were carefully wrapped in bubble wrap to prevent damage during transport and while in storage as shown in Figure 3.15. Although careful steps were taken to avoid damage to the core, a few cores were cracked and were excluded from testing. Cores were stored at room temperature.


**Figure 3.14 Core Extraction**

**Figure 3.15 Bubble Wrapped Cores**

The subsequent coring periods in Summer of 2018, 2019, 2020, and 2021 follow the same coring scheme. As shown in Figure 3.13, fewer cores will be collected during these periods as no cores will be required for accelerated conditioning in the lab prior to bond strength testing. Arrows will be drawn on the cores in periods 2-5 to ensure the bond strength of the tack coat is tested in the direction of traffic flow. Table 3.8 shows the breakdown of the cores collected in periods 2-5. Period 2 coring followed this scheme for a total of 12 cores from each section including 6 cores from each zone. As shown in Figure 3.16, arrows were painted on the road prior to coring to indicate the traffic direction. This set of cores was placed into tight fitting PVC pipes prior to being stored in the coolers with bubble wrapped was placed between them to ensure that they did not shift during transportation as shown in Figure 3.17. Cores were transferred to boxes and stored at room temperature in the laboratory.

**Table 3.8 Core Breakdown for Periods 2-5**

| | Zone 1 | | | Zone 2 | | | | | | |
|---|---|---|---|---|---|---|---|---|---|---|
| Core Location | IWP | OWP | Centre | IWP | OWP | Centre | Total IWP | Total OWP | Total Centre | **Overall Total** |
| No. of Cores | 2 | 2 | 2 | 2 | 2 | 2 | 4 | 4 | 4 | 12 |

**Figure 3.16 Period 2 Core Marking**

**Figure 3.17 Core Transportation Setup**

### 3.3.3 Distress Surveys

Distress surveys are performed to document any defects or deterioration on the road and assess the cause of these flaws to consider in future preservation and rehabilitation plans. The types of distresses that could be identified during distress surveys according to the Saskatchewan Ministry of Highway & Infrastructures Pavement Distress Legend include the following:

- Coarse aggregate loss

- Raveling
- Flushing
- Polishing of aggregate
- Potholes
- Rippling corrugations
- Shoving
- Wheel track rutting
- Distortion
- Snow plow damage (Saskatchewan Ministry of Highways & Infrastructure, 1995).

Furthermore, types of cracking could be identified including:

- Wheel track – single and multiple
- Wheel track – alligator
- Centreline – single and multiple
- Centreline – alligator
- Pavement edge – single and multiple
- Pavement edge – alligator
- Transverse – half and full and multiple
- Transverse – alligator
- Meander
- Mid-lane longitudinal
- Random and map cracking (Saskatchewan Ministry of Highways & Infrastructure, 1995).

A post-construction distress survey was performed on September 11$^{th}$ and 12$^{th}$, 2017, approximately three weeks after construction, in the non-destructive testing (NDT) zone for each of the ten test sections. The distress survey form was provided by the Ministry of Highways & Infrastructure. A template of this form can be found in Appendix E. A second distress survey was performed in the Summer of 2018 on September 10$^{th}$.

### 3.3.4 Construction Parameters Monitoring

The distributor used to apply the tack coat materials was a 2015 BearCat Computer Rate Controlled Distributor, as shown in Figure 3.18. The precision on the distributor was 0.1L/m$^2$. The nozzles were set at a height of 15-20 cm from the road surface, with a nozzle angle of 30 degrees, which allowed for a triple overlap to be achieved. The distributor computer was set to spray a constant application rate independent of the speed of the distributor. The application rate in the distributor computer was adjusted based on the dilution percentage of the tack coat materials to aim for the same residual application rate for all products. The distributor was flushed clean between anionic and cationic products to ensure that there was no contamination.

**Figure 3.18 Tack Coat Distributor Truck**

Construction took place over two consecutive days (5 test sections/day) to minimize differences in weather conditions. However, there were still differences in weather conditions including temperature and humidity. Sections constructed in the morning were exposed to colder and more humid conditions than sections constructed later in the afternoon. The paving crew paved over the tack coat materials late in the afternoon of each day. Tack coat materials placed earlier in the day had more time to break and set than products placed later in the day. Although traffic control was in place, a few passenger vehicles managed to drive on the tack coat materials before setting was complete.

Temperatures during construction were between 11°C and 24°C. Humidity was between 39% and 85%. While the construction took place, parameters related to materials, weather, and construction process were recorded. The sheets used to record parameters during construction can be found in Appendix F. The recorded information about the tack coat materials were percent of dilution, tack coat application temperature (at the sprayer nozzle), break time, set time, and pick-up/tracking rating. The recorded weather information parameters were: air temperature, wind speed, pavement temperature, humidity, and weather condition. Weather data was taken from the Weather Network website for the location of Blaine Lake. The tracking/pickup test was performed on six of the ten test sections. The four sections that were not tested were two test sections of SS-1h (Sections 2 and 9, both 50-50W) and two test sections of SS-1 (Section 5 30-70W and Section 6 50-50W). These products took too long to break and set and these times could not be fully monitored before paving on top of products.

### 3.4 Laboratory Testing Program

The laboratory testing program complements the field study program. The laboratory testing program analyzes the bond strength and performance of the core samples taken from the field using the LISST. The first set of 40 cores were tested according to AASHTO TP 114 to evaluate the initial bond strength of the tack coat materials. These bond strength results are considered the baseline for subsequent core bond strength results. The remaining 80 cores were lab conditioned to simulate free-thaw cycling prior to testing for bond strength. The 120 cores taken one year post construction in September 2018 were tested for bond strength.

Prior to testing, the tack coat surface was identified and marked on each core by examining the aggregate orientation. Once the tack coat had been identified on each core, 50mm was measured below the tack coat surface and marked as the cut line. The tack coat marking and cut line are noted on the core in Figure 3.19. A wet masonry saw was used to trim the cores to a length of 50mm below the tack coat surface as specified in AASHTO TP 114. An image of the masonry saw setup is shown in Figure 3.20. The top lift above the tack coat varied in thickness between 35mm and 50mm. The thickness of layers above and below the tack coat surface was required to be 50±5mm according to the AASHTO TP 114 standard. Most samples met this requirement. Prior to beginning the test, each sample was weighed, and the diameter and height of each layer

were measured.  Any flaws in the condition of the core were noted.  Cracked cores were excluded from the testing program.


**Figure 3.19 Core with Tack Coat Surface and Cut Line Marked**

**Figure 3.20 Wet Masonry Saw**

A 44.5kN capacity Karol Warner load frame was used to test the initial 40 core samples. A 50kN Humboldt Master Loader 5030 was used for the remaining cores. The loading machine provided a uniform vertical loading rate of 2.54 mm/minute (0.1 inches/minute) according to AASHTO TP 114 test standard. A testing temperature of 25°C was used. The direction of traffic was not marked on the cores collected after construction because both lifts were of new construction and the effect of traffic loading is considered negligible at this stage. In the cores collected after one year of construction, the direction of traffic was indicated on the cores so that shear force was applied in the direction of traffic. The top overlay was placed on the shearing side of the LISST device. The tack coat surface was centered between the frame gap.

As the test was running, measurements of displacement and load were recorded every second. The test was run past the peak load until the load-displacement graph began to stabilize. Figure 3.21 shows a sketch for test setup which includes a movable and non-movable frame, the applied load, and the asphalt sample. Figure 3.22 shows the actual test setup with a core sample placed and ready for testing.

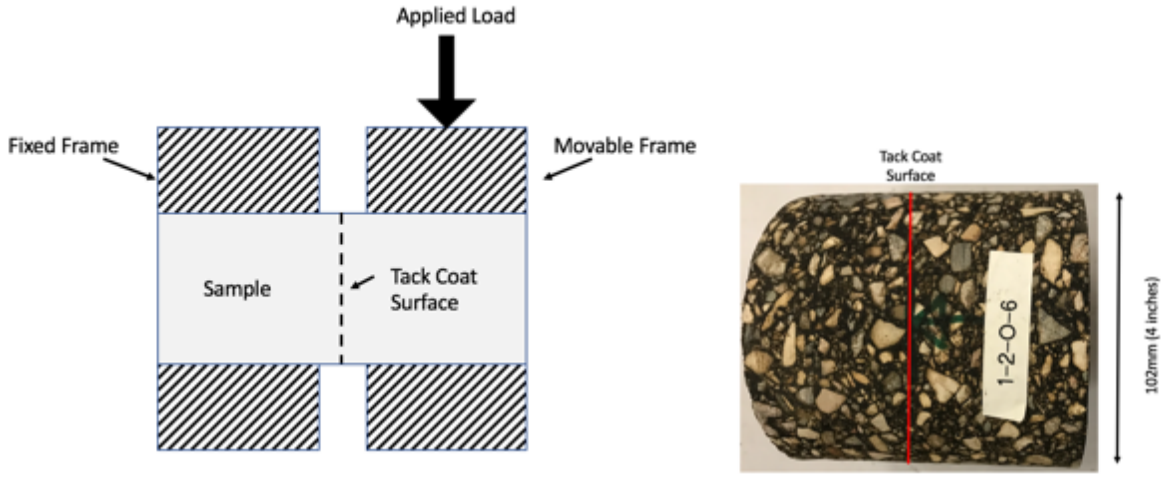


**Figure 3.21 Simplified Sketch of Shear Strength Test**

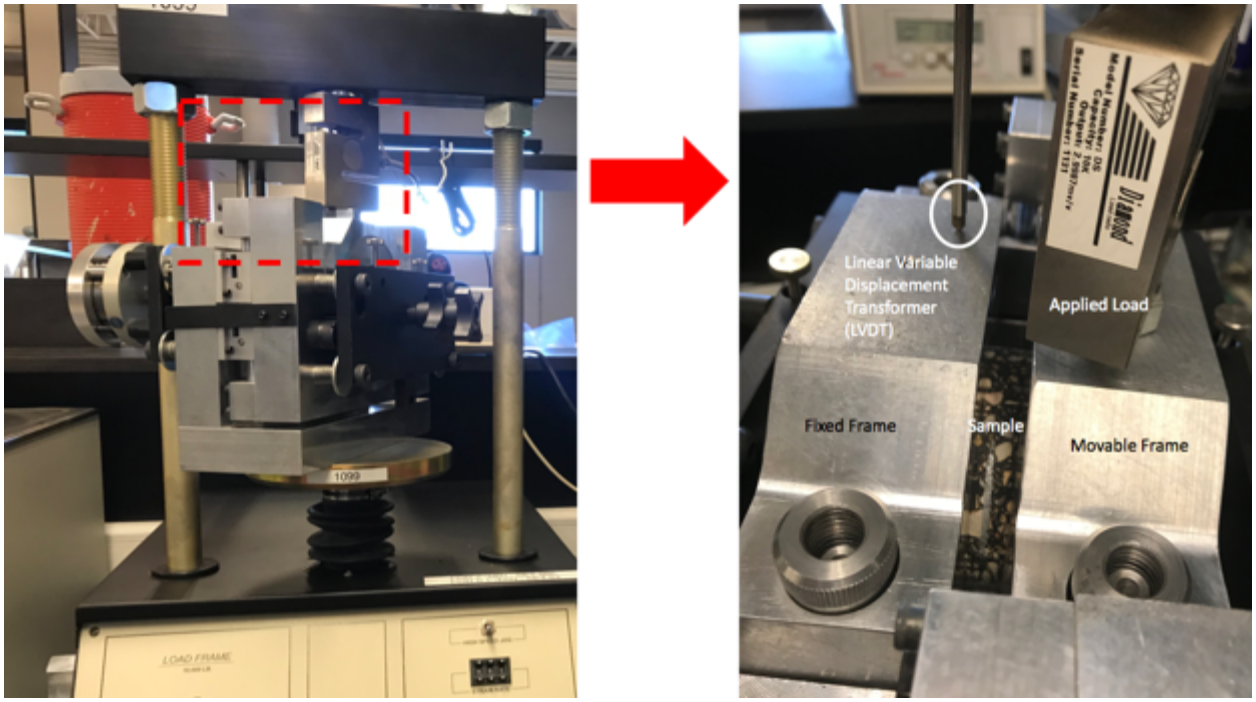


**Figure 3.22 Test Setup**

The output from the LISST was the displacement and load curve with readings every second. The core sample failure shape was documented.

### 3.5 Environmental Conditioning

The Conviron environmental chamber is a cold chamber capable of reaching temperatures in the range of -40°C to 20°C. A Nortec NHMC 030 Steam Humidifier is able to generate steam which is pumped into the chamber through a pipe. The temperature in the chamber was monitored by three thermocouples placed near the walls on two sides of the chamber and above the door. The temperature inside the centre of a core was monitored by a thermocouple installed in a dummy sample. The computer connected to the chamber recorded the temperature and humidity data by a National Instruments data acquisition system. The chamber is capable of fluctuating between two temperature and two humidity setpoints. Photos of the test set up are shown below in Figure 3.23 and Figure 3.24.

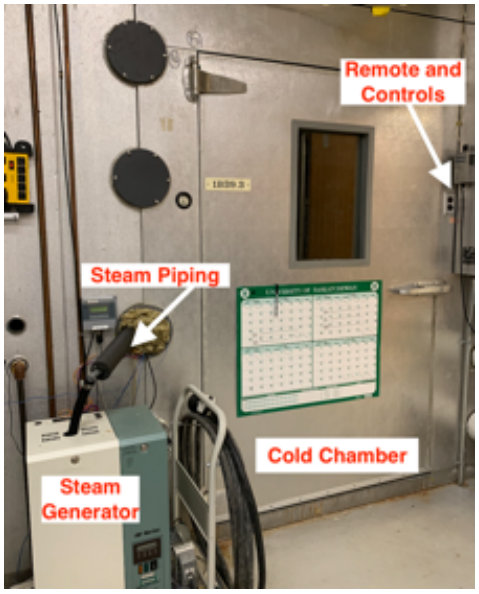


**Figure 3.23 Exterior of the Environmental Chamber**


**Figure 3.24 Interior Schematic of the Environmental Chamber**

A portion of the cores collected after construction were subjected to accelerated conditioning through freeze-thaw cycling. Cores were placed in the environmental chamber and subjected to three freeze-thaw conditioning levels: 3, 9, and 15 cycles. At each conditioning level, three cores from each of the test sections were taken out from the chamber and tested. There is no standardized method for FT conditioning of tack coat materials. A FT pattern was developed and was intended to be conservative and aimed to minimize the damage caused to AC mixture from extreme temperature fluctuations. If the AC mixture sustained too much FT damage, failure will occur within the AC mixture instead of the tack coat material. One FT cycle consisted of freezing the cores at -25°C for 12 hours followed by thawing the cores at 15°C for 12 hours. Humidity was maintained between 50-60% relative humidity.

It took approximately one hour for the chamber to reach the desired freeze and thaw temperatures and approximately two hours for the centre of the core sample to reach desired temperatures. Figure 3.25 shows the freeze-thaw cycle pattern based on the measured temperature at the centre of a dummy AC core sample.

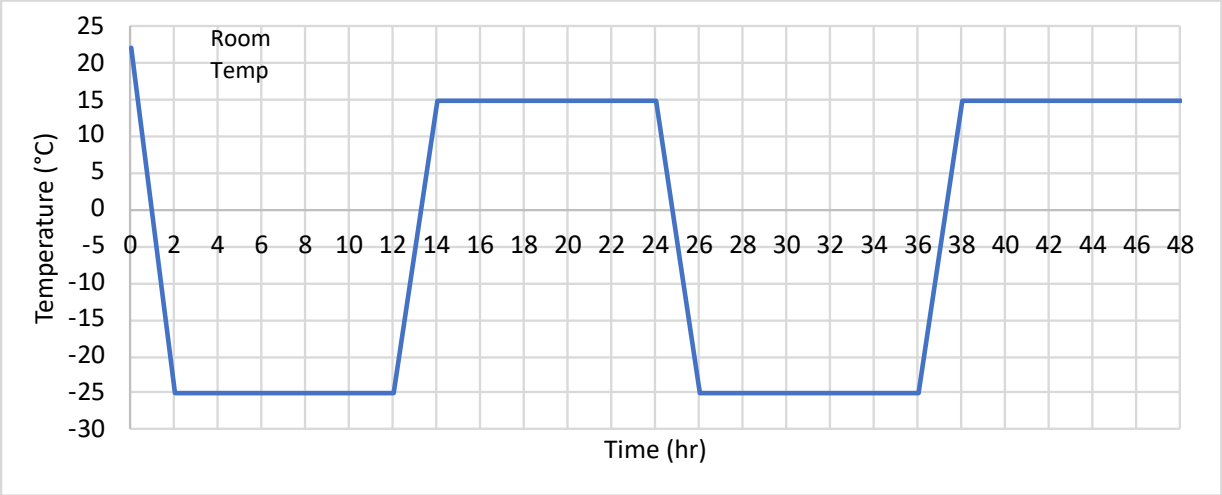


**Figure 3.25 FT Cycle Pattern Based on the Measured Temperatures Inside the Sample**

# CHAPTER 4: FIELD STUDY RESULTS AND ANALYSIS

## 4.1 Introduction

This chapter presents the results of the field study including the distress survey results for the survey post-construction and the survey one year later. It also presents the results of the construction parameter survey including the break and set times and pick up test results.

## 4.2 Distress Survey Results

The first distress survey performed 3 weeks after construction on September 11th and 12th, 2017 showed no early distresses or construction defects to report. The second distress survey was performed one year later on September 10th, 2018. The survey showed minor distresses in the road including: coarse aggregate loss, raveling, and transverse cracking. Table 4.1 summarizes the distresses observed in the survey, their locations, and severity. Note that these types of distresses are considered to be minimal and typical and do not indicate any poor performance from any of the tack coat materials. Appendix G contains pictures of each distress from the survey.

**Table 4.1 Distress Survey Summary**

| Section # | Product | Location | Distress | Severity |
|---|---|---|---|---|
| 1 | SS-1 (50-50W) | 25+926.6 to 25+896.6 | Coarse Aggregate Loss | Very Slight, <5% |
| | | 25+838.1 | Full Transverse Crack | Very Slight, Crack Width <5mm |
| | | 25+792.6 | Full Transverse Crack | Very Slight, Crack Width <5mm |
| 2 | SS-1h (50-50W) | 25+637.35 | Full Transverse Crack | Very Slight, Crack Width <5mm |
| | | 25+640.35 to 25+610.35 | Coarse Aggregate Loss | Very Slight, <5% |
| | | 25+604.85 | Full Transverse Crack | Very Slight, Crack Width <5mm |
| 3 | TackMax™ | 25+458.4 to 25+452.9 | Raveling | Very Slight, <5% |
| | | 25+442.9 to 25+412.9 | Coarse Aggregate Loss | Very Slight, <5% |
| | | 25+409.9 | Full Transverse Crack | Very Slight, Crack Width <5mm |

| | | | | |
|---|---|---|---|---|
| 4 | MS-1 (70-30W) | 25+146.1 | Full Transverse Crack | Very Slight, Crack Width <5mm |
| | | 25+152.1 to 25+182.1 | Coarse Aggregate Loss | Very Slight, <5% |
| | | 25+242.1 to 25+212.1 | Coarse Aggregate Loss | Very Slight, <5% |
| | | 25+215.1 | Full Transverse Crack | Very Slight, Crack Width <5mm |
| 5 | SS-1 (30-70W) | 24+922.05 to 25+022 | Coarse Aggregate Loss | Very Slight, <5% |
| 6 | SS-1 (50-50W) | 25+926.6 to 25+836.6 | Coarse Aggregate Loss | Very Slight, <5% |
| | | 25+905.6 to 25+899.6 | Raveling | Very Slight, <5% |
| | | 25+861.6 | Full Transverse Crack | Very Slight, Crack Width <5mm |
| | | 25+837.1 | Full Transverse Crack | Very Slight, Crack Width <5mm |
| | | 25+811.6 | Full Transverse Crack | Very Slight, Crack Width <5mm |
| 7 | CSS-1h (50-50W) | 25+700.35 to 25+640.35 | Coarse Aggregate Loss | Very Slight, <5% |
| | | 25+651.85 | Half Transverse Crack | Very Slight, Crack Width <5mm |
| | | 25+610.35 to 25+580.35 | Coarse Aggregate Loss | Very Slight, <5% |
| | | 25+550.85 | Full Transverse Crack | Very Slight, Crack Width <5mm |
| 8 | Colasphalt Tack | 25+472.9 to 25+348.25 | Coarse Aggregate Loss | Very Slight, <5% |
| | | 25+420.9 | Full Transverse Crack | Very Slight, Crack Width <5mm |
| 9 | SS-1h (50-50W) | 25+221.66 to 25+122.1 | Coarse Aggregate Loss | Very Slight, <5% |
| | | 25+172.16 | Half Transverse Crack | Very Slight, Crack Width <5mm |
| | | 25+126.16 | Full Transverse Crack | Very Slight, Crack Width <5mm |
| 10 | Clean Bond | 25+022 to 24+922.05 | Coarse Aggregate Loss | Very Slight, <5% |

### 4.3 Construction Parameters

Table 4.2 shows the results of the pick-up/tracking test, the breaking and setting times, and weather information during construction. The products that did not have the pickup test are labelled with N/A in the pickup column. These results show reduced tracking for proprietary products, which have faster breaking and setting times than slow setting tack coat materials. The slower setting emulsions CSS-1h and MS-1 broke and set faster than SS-1. These early results indicate that using any of the tested products instead of SS-1 can be beneficial, where break and set were achieved before placing the second AC lift. Supplier proprietary products were the fastest to break and set and proved superior in tracking and pick-up performance.

**Table 4.2 Weather Parameters with Break and Set Times**

| Product | Dilution | Section | Pickup | Break Time (min) | Set Time (min) | Pavement Temperature (°C) | Air Temperature (°C) | Humidity (%) | Emulsion Application Temp (°C) | Wind Speed (km/h) | Wind Gust (km/h) | Weather Condition |
|---|---|---|---|---|---|---|---|---|---|---|---|---|
| SS-1 | 50-50W | 1 | None | 79 | 134 | 19.5 | 16 | 64 | 26.3 | 9 | | Partly Cloudy |
| SS-1H | 50-50W | 2 | N/A | N/A | N/A | 31 | 18 | 50 | 30.1 | 8 | 12 | |
| TackMax | - | 3 | None | 10 | 120 | 37 | 20 | 47 | 32 | 9 | 14 | Partly Cloudy |
| MS-1 | 70-30W | 4 | Medium | 20 | 49 | 41.7 | 22 | 44 | 32.3 | 10 | 15 | Sunny |
| SS-1 | 30-70W | 5 | N/A | N/A | N/A | 37 | 22 | 48 | 40 | 2 | 3 | Sunny |
| SS-1 | 50-50W | 6 | N/A | 360 | N/A | 23.6 | 11 | 85 | 31 | 11 | 16 | Sunny |
| CSS-1H | 50-50W | 7 | None | 30 | 68 | 33.1 | 17 | 65 | 36.3 | 10 | 16 | Sunny |
| Colasphalt Tack | - | 8 | None | 5 | 14 | 41.2 | 22 | 49 | 40.8 | 17 | 25 | Sunny |
| SS-1H | 50-50W | 9 | N/A | N/A | N/A | 40.4 | 24 | 39 | 42.2 | 18 | | Sunny |
| Clean Bond | - | 10 | None | 3 | 10 | 35.3 | 24 | 43 | 49.7 | 17 | 26 | Sunny |

*N/A indicates that the product did not break or set prior to being paved over therefore a pickup test could not be performed.

The weather conditions from at the time of construction including air temperature, pavement temperature, application temperature, humidity, wind speed, and wind gust are plotted and shown in Figure 4.1 and Figure 4.2.

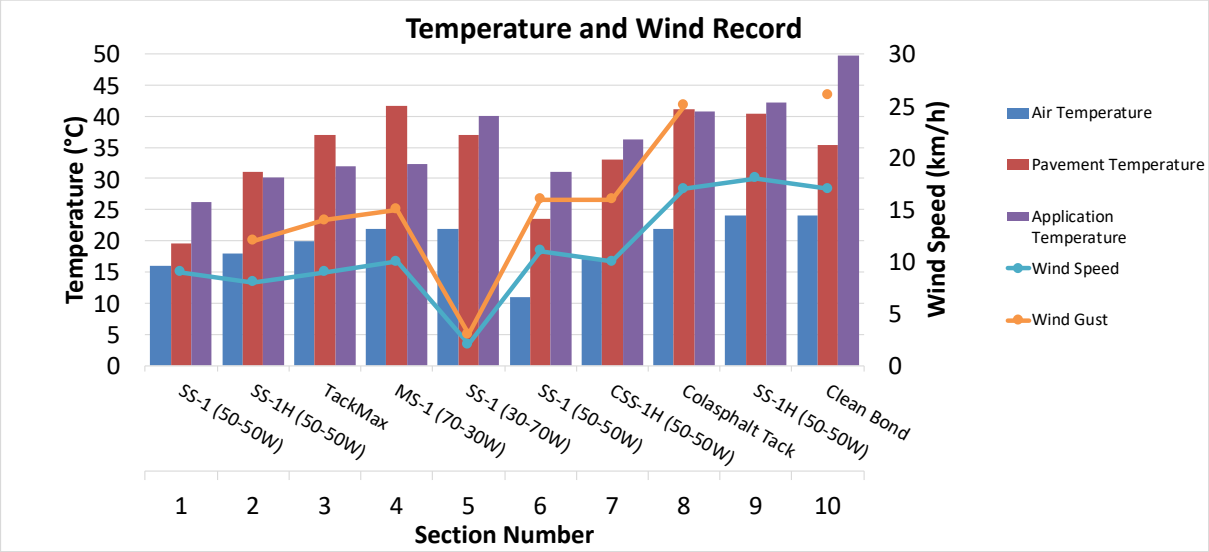


**Figure 4.1 Temperature and Wind Record**

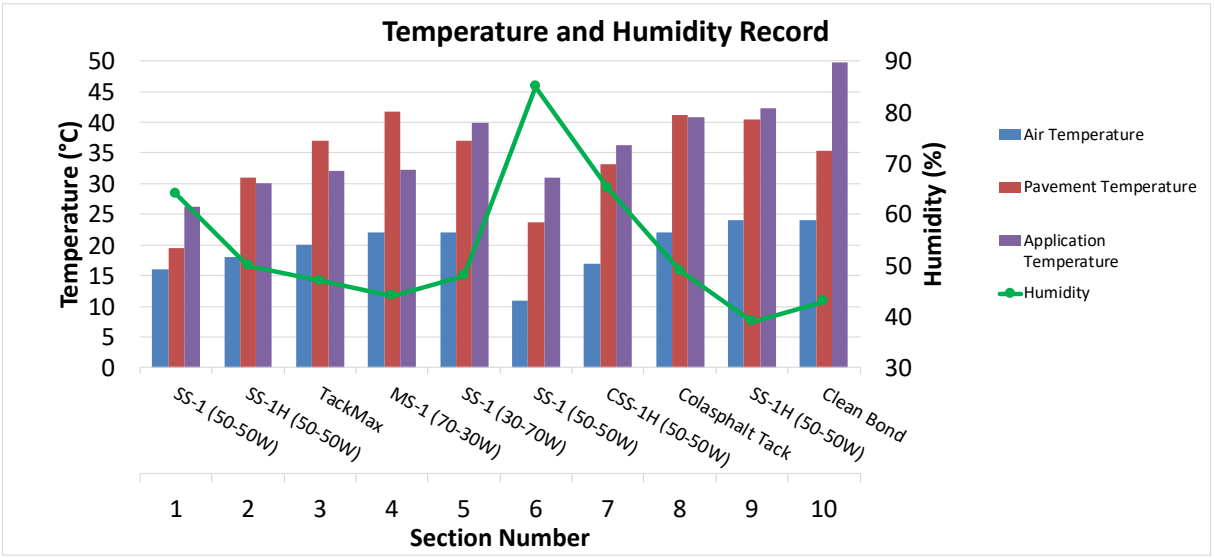


**Figure 4.2 Temperature and Humidity Record**

The break and set times of the tested products were plotted with temperature readings to see if any trends can be observed. From Figure 4.3, it can be noted that break and set times showed some correlation to pavement temperature, air temperature, and application temperature. As

application temperature, air temperature, and pavement temperature increase, the break and set times decrease. This indicates that temperature has an effect on these parameters. In addition, Figure 4.4 shows the correlation between humidity and break and set times. Figure 4.4 shows that lower humidity correlates to faster breaking and setting times. A lower humidity level accelerates the evaporation rate of water from the tack coat materials. Figure 4.5 shows the wind speed plotted with break and set times. No observed correlation between wind speed and break and set times. However, a higher wind speed can accelerate breaking and setting of tack coat materials.

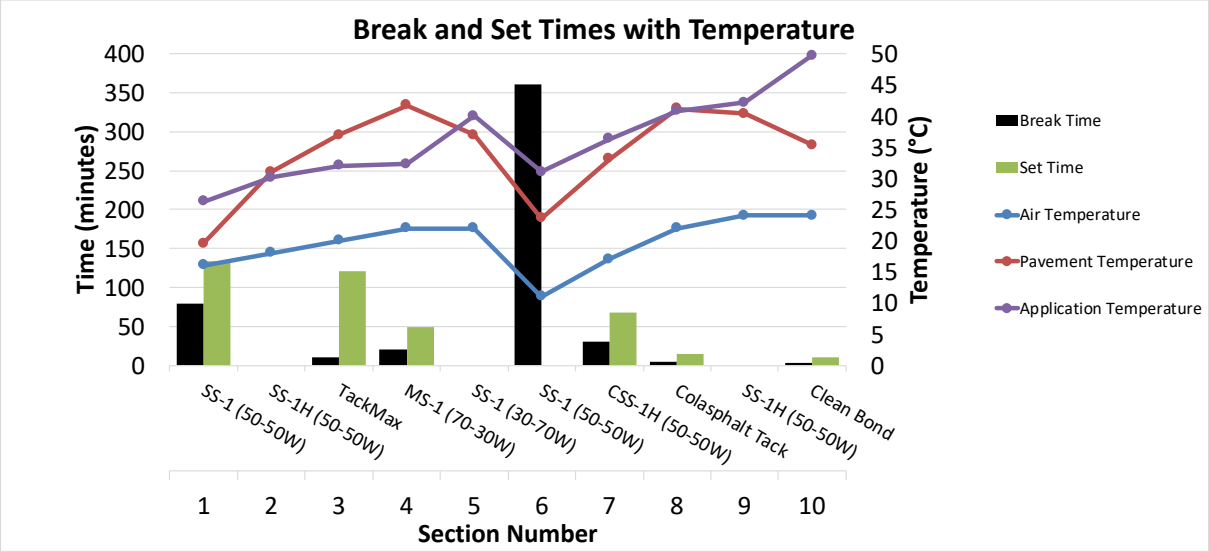


**Figure 4.3 Break and Set Times with Temperature**

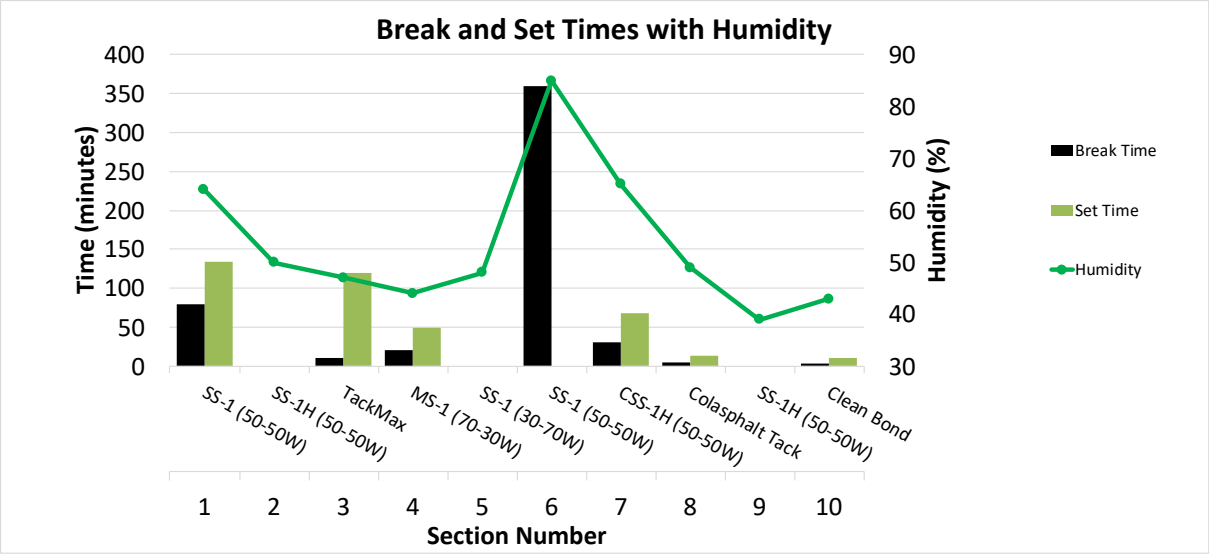


**Figure 4.4 Break and Set Times with Humidity**

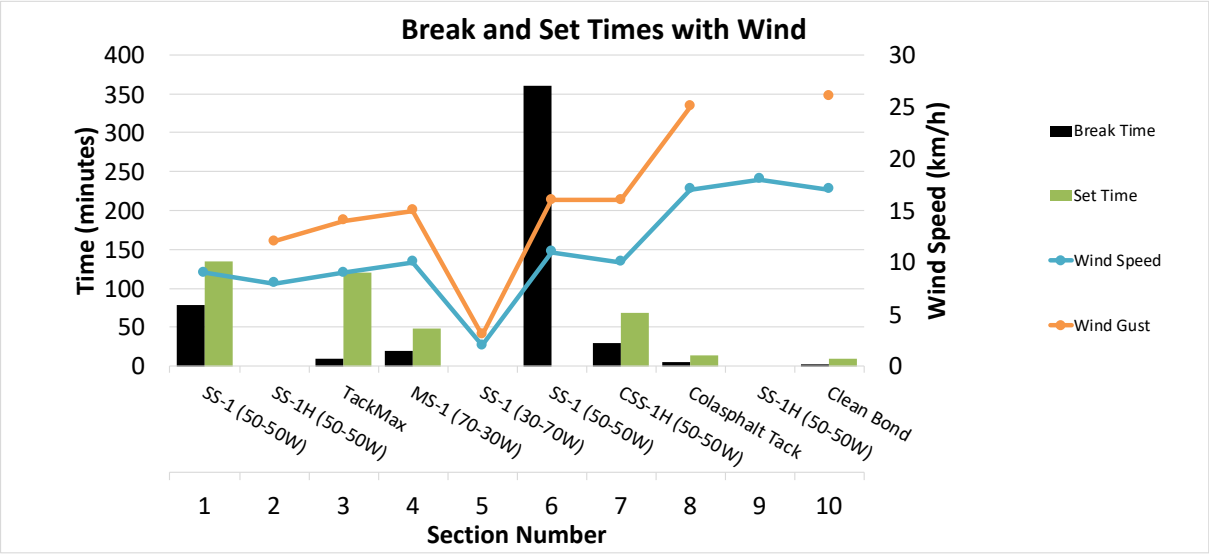


**Figure 4.5 Break and Set Times with Wind Speed**

### 4.4 Limitations of the Field Study

Although precautionary measures were established to reduce the differences in factors that could affect the test results, there were still variations due to factors associated with construction process. The factors that may have affected the results of the field study are discussed below.

- The selection of construction dates was done in consultation with the contractor to fit within the actual project schedule. Construction of the ten test sections was completed

over two consecutive days to minimize the impact of weather condition variability but these variations still would have had an impact on the results. There were differences in humidity and temperature between tack coat placements for the ten test sections. Test sections installed earlier in the day were exposed to more humid and colder conditions than were experienced by test sections constructed later in the day.

- Test sections constructed in the morning had more time to break and set prior to being paved over than test sections installed in the afternoon.
- The length of time the cores were in storage has an effect on the bond strength because of the continuous curing of the tack coat material. The baseline cores were stored from September 2017 to April 2018. The year one cores were stored from September 2018 to January 2019. The FT conditioned cores were stored from September 2017 to February 2019 when they were placed into FT cycling and then stored after their removal from the chamber for a few days prior to testing. The continuous curing of the tack coat material is due to length of time, air temperature, and humidity the core samples are exposed to. Core samples were stored at room temperature.
- The core samples were collected at a distance between 20-200m from where the calibration of the distributor took place meaning that the application rate on the coring test area may differ from the computed rate in the calibration zone.
- The distributor was emptied between anionic emulsions but washed out between anionic and cationic emulsions. Anionic emulsions may have different properties due to contamination within the distributor.
- The road was relatively clean because the tack coat was placed between two new lifts of AC. This being said, there was still exposure of the bottom lift to vehicular traffic before the tack coat had been placed meaning there could be dust or other debris between the bottom lift and the tack coat material.
- Core samples could have different amounts of tack coats due to their position on the road. Cores in the outer wheel paths may have more tack coat due to the cross slope of the road.
- Core samples in the NB and SB directions have been exposed to different loading conditions due to different patterns in vehicular traffic.

- Some tack coat material had been partially tracked onto the tires of few vehicles driving through the construction zone. Although properly marked, some drivers chose to drive onto fresh products. Incidents like these simulate actual construction conditions.

# CHAPTER 5: LABORATORY TEST RESULTS AND ANALYSIS

## 5.1 Introduction

This chapter presents the results and analysis of the bond strength tests. The bond strength tests include the ISS results for baseline cores, one year cores, and accelerated FT cycled cores. Additional parameters including failure mode, energy values, strain values, and the interlayer tangential modulus values are quantified and analyzed.

## 5.2 Analysis Procedure

From the output data, stress-displacement graph, interlayer shear strength, strain at bond failure, energy to peak stress, and interlayer tangential modulus could be determined. Visual representation of these values is shown in Figure 5.1.

The interlayer shear strength (ISS) in kPa strength was determined by:

$$ISS = \frac{P_{ult}}{A}$$

where:

$P_{ult}$ is the ultimate load recorded during the test, kN

A is the cross-sectional area of the core, $m^2$.

The energy to reach peak shear stress in $J/m^2$ were computed by finding the area under the stress-displacement curve. The energy to reach peak shear stress accounts for both the applied stress and the amount of deformation that the sample undergoes before reaching bond failure. Therefore, the energy required to reach peak shear stress is a significant parameter that shall be considered when evaluating tack coat materials.

The strain at bond failure as a percentage of initial diameter was determined by:

$$Strain\ (\%) = \frac{d}{D} \times 100$$

where:

d is the displacement at maximum load, mm

D is the diameter of the sample, mm.

The interlayer tangential modulus, k, represents the slope of the stress-displacement curve. It is in units of N/mm$^3$ was determined by:

$$k = \frac{ISS}{d} \times 10^{-3}$$

where:

ISS is the interlayer shear strength in kPa

d is the displacement at maximum load, mm.

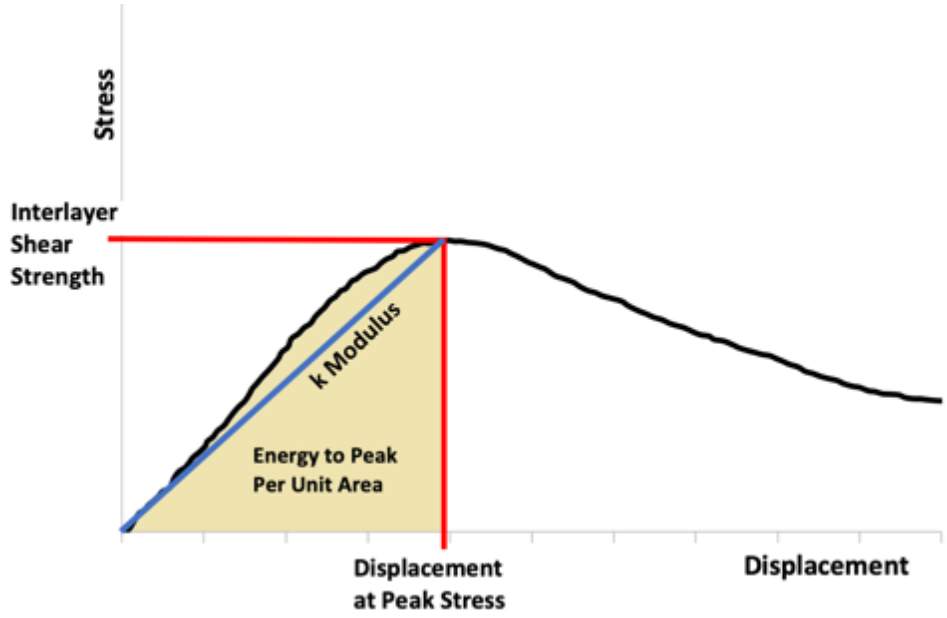


**Figure 5.1 Parameter Definitions**

When comparing the differences between data sets a % Change value was computed. The % Change value indicates how much the results have changed from the baseline core data. A positive value indicates that the data is higher than the baseline data and a negative value indicates that the data is lower than the baseline data.

$$\%\ Change = \frac{New\ Value - Baseline\ Value}{Baseline\ Value} \times 100$$

The coefficient of variation (CV) was calculated to show the dispersion of the data set and is a ratio between the standard deviation and the mean of the data set:

$$CV\ (\%) = \frac{Standard\ Deviation}{Mean} \times 100$$

The mode of failure for the bond strength samples were classified into two types according to shape and location of the failure surface (Figure 5.2 and Figure 5.3):

- Type A: clean failure at the tack coat surface
- Type B: failure partly or completely within the mix

Type A indicates that the tack coat surface is the weakest plane (location) within the sample. Type B indicates that the tack coat material can provide enough bond strength to make the two AC lifts behave as one thick homogenous layer.

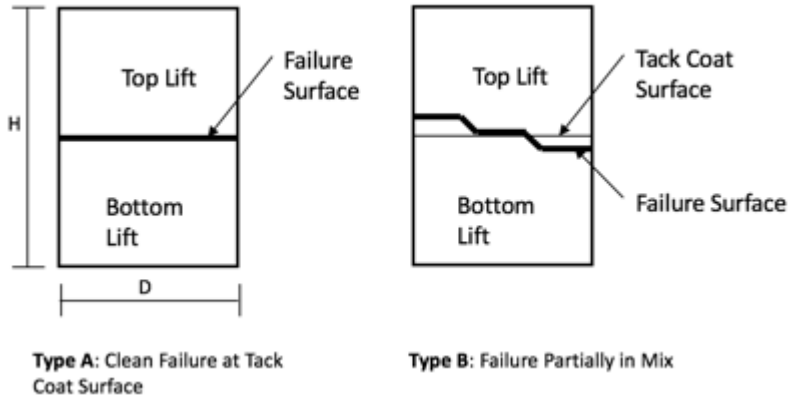


**Figure 5.2 Failure Types**

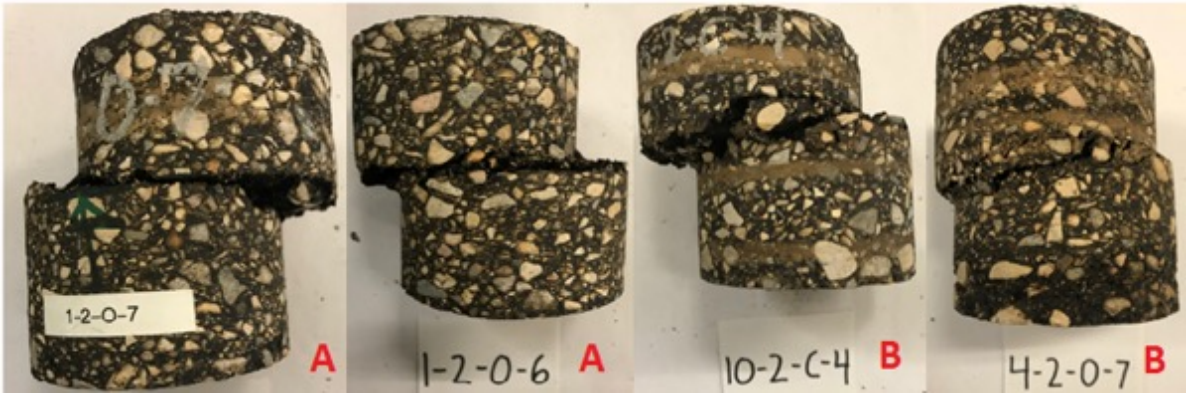


**Figure 5.3 Images of Type A: Clean Failure at the Tack Coat Surface and Type B: Failure Partially in the Mix**

### 5.3 Outlier Identification

A core sample was identified as an outlier if the ISS value was 25% greater or smaller than the average ISS of the remaining cores for the same test section. For the one year cores, core sample outliers were compared by section and by location and outliers were identified as such. Once identified, outliers were excluded from the remainder of the analysis and were not included in further calculations.

### 5.4 Limitations of the Laboratory Testing Program

There are sources of error that could have contributed to variation within the data set including the following factors.

- The placement of the core sample within the LISST device can vary with the operator.
- The FT cycled cores could have experienced different temperature and humidity conditions based on their location in the chamber and proximity to the humidifier and refrigeration unit as well as the difference in sizes of the core samples. Core samples that are shorter in height will freeze faster than cores with a larger height meaning that the duration of freezing and thawing is dependent on core height and varies within the core sample set.
- Some core samples did not have a top lift of 50mm which is required by AASHTO TP 114-15. The differences in the top lift height may have had an effect on bond strength results.
- The tack coat materials used in this research were contributed by material suppliers. All classification tests for tack coat materials were completed by the material suppliers, where the required equipment is not available at the university.

### 5.5 Bond Strength of Baseline Cores

Of the sixteen cores sampled from each test section in September 2017, four were tested for post construction bond strength, three cores from the outer wheel path and one core from the centre. A total of 40 cores, four from each of the ten tested sections were tested using a LISST device and a loading frame. The procedure for bond strength tests followed the AASHTO TP 114 Standard: Determining the Interlayer Shear Strength (ISS) of Asphalt Pavement Layers.

Figure 5.4 to Figure 5.12 show the stress-displacement curves for the tested cores from each test section. The ISS for all tested samples ranged from 219.2kPa to 500.2kPa. SS-1 was installed in three test sections; two of them had a dilution 50-50W but in opposite traffic directions (Sections 1 and 6) and one section with dilution 30-70W (Section 5). The stress-displacement curves for SS-1 are shown in Figure 5.4 to Figure 5.6.

For SS-1 with dilution 50-50W (Figure 5.4 and Figure 5.5), the ISS values ranged from 219.2kPa to 348.1kPa and the displacement at bond failure ranged from 1.94mm to 2.84mm. For SS-1 with dilution 30-70W (Figure 5.6), the ISS values ranged from 317.2kPa to 326.9kPa and the displacement at bond failure ranged from 1.65mm to 2.55mm. SS-1 with dilution 30-70W showed less variably in the ISS values that SS-1 with dilution 50-50W.

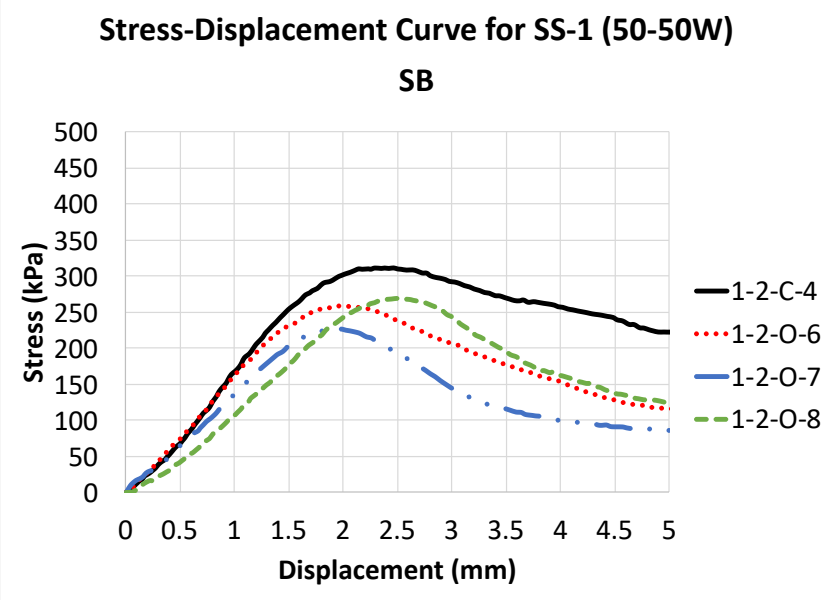


**Figure 5.4 Stress-Displacement Curve for SS-1 (50-50W) SB Baseline Cores – Section 1**

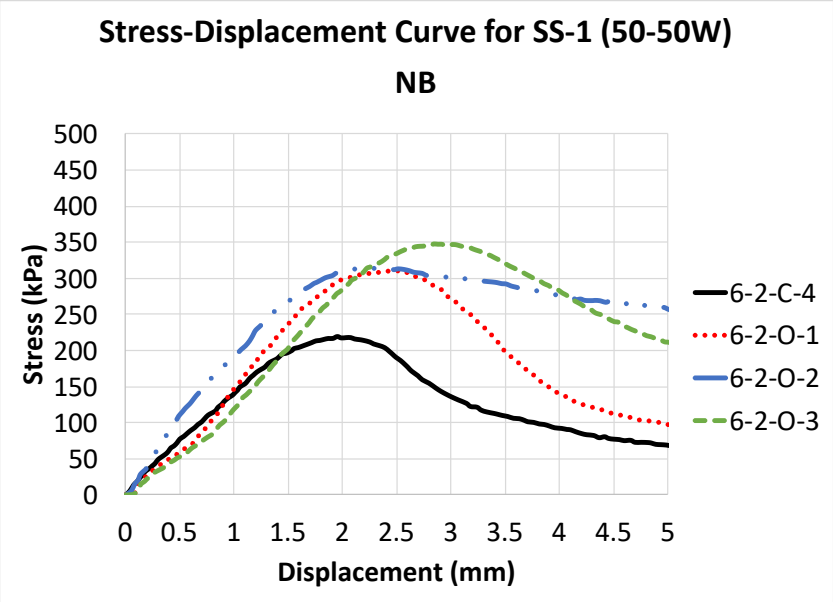


**Figure 5.5 Stress-Displacement Curve for SS-1 (50-50W) NB Baseline Cores – Section 6**

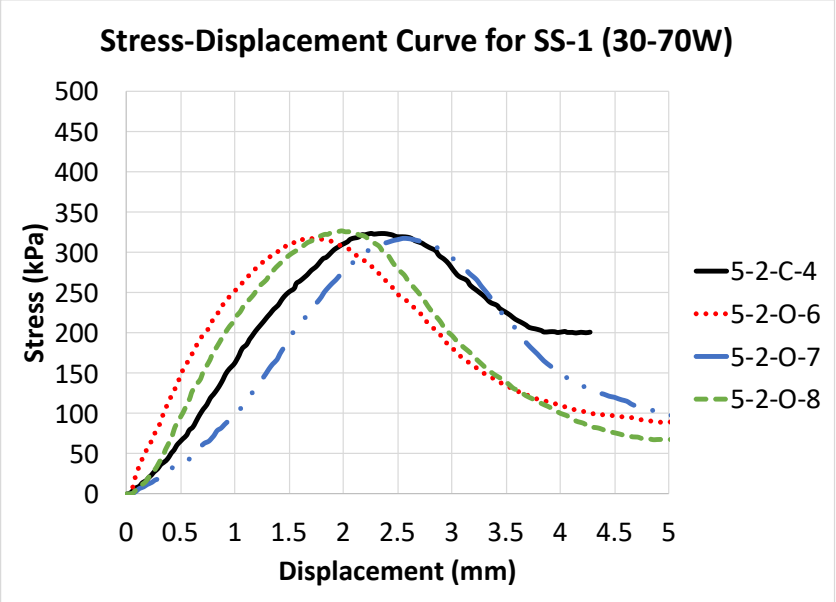


**Figure 5.6 Stress-Displacement Curve for SS-1 (30-70W) Baseline Cores – Section 5**

SS-1h was installed in two test sections (Section 2 and Section 9). Both sections had a dilution of 50-50W but opposite traffic directions. Figure 5.7 and Figure 5.8 shows the stress-displacement curves for SS-1h. For Figure 5.7 (Section 2), the ISS values ranged from 325.0kPa to 360.8kPa and the displacement at bond failure ranged from 1.81mm to 2.47mm. For Figure

5.8 (Section 9), the ISS values ranged from 275.5kPa to 388.5kPa and the displacement at bond failure ranged from 1.48mm to 3.05mm. Section 9 (Figure 5.8) showed higher variability in both ISS values and the displacement at bond failure.

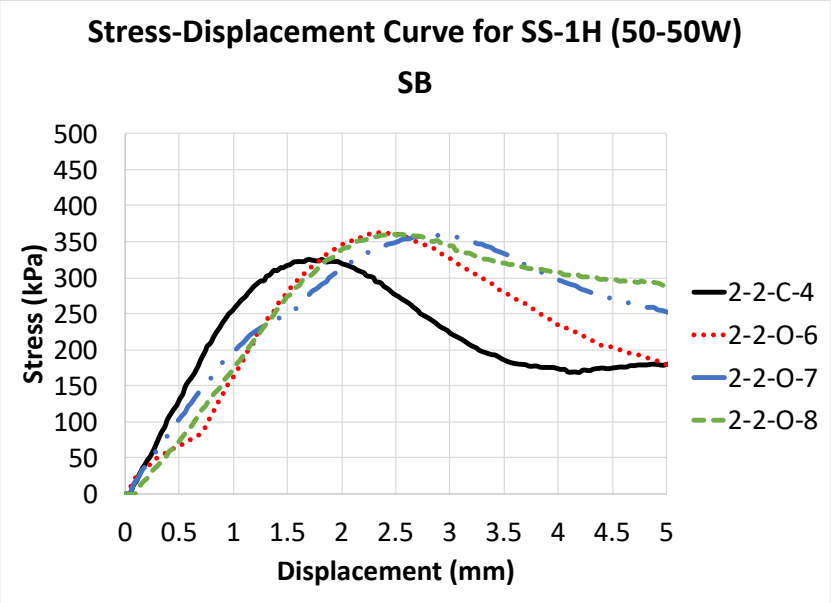


**Figure 5.7 Stress-Displacement Curve for SS-1h (50-50W) SB Baseline Cores – Section 2**

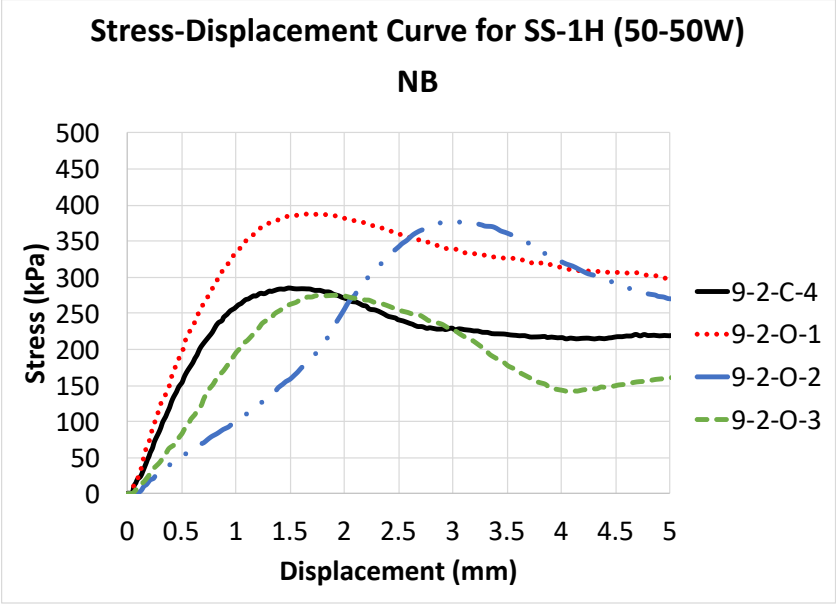


**Figure 5.8 Stress-Displacement Curve for SS-1h (50-50W) NB Baseline Cores – Section 9**

MS-1 was installed in Section 4 with a dilution of 70-30W. Figure 5.9 shows the stress-displacement curves for MS-1. The ISS values ranged from 284.9kPa to 500.7kPa and the displacement at bond failure ranged from 1.86mm to 2.54mm. Although the ISS values varied greatly, the displacement at peak stress had low variability.

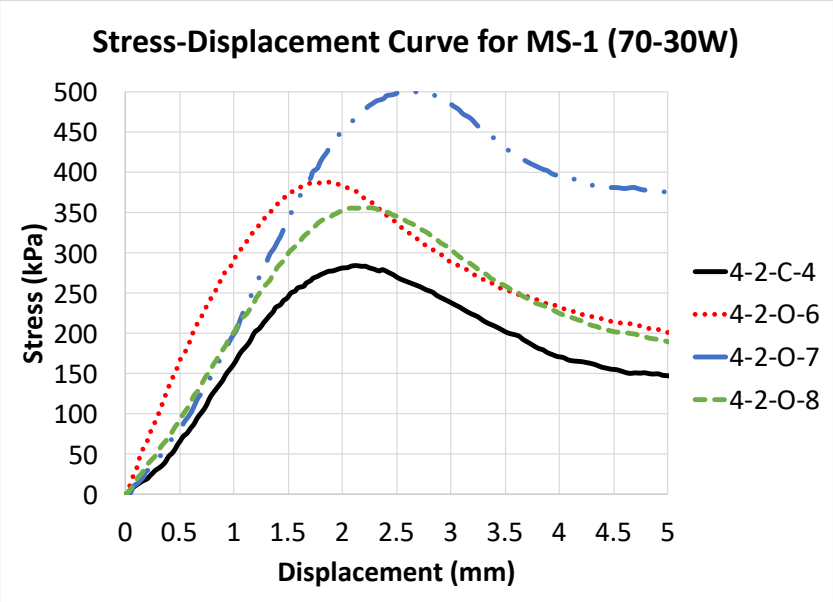


**Figure 5.9 Stress-Displacement Curve for MS-1 (70-30W) Baseline Cores – Section 4**

CSS-1h was installed in Section 7 with a dilution of 50-50W. Figure 5.10 shows the stress-displacement curves for CSS-1h. The ISS values ranged from 323.4kPa to 384.8kPa. The displacement at bond failure ranged from 2.36mm to 3.91mm. The shape of the stress-displacement curves was consistent for all cores except core 7-2-O-2.

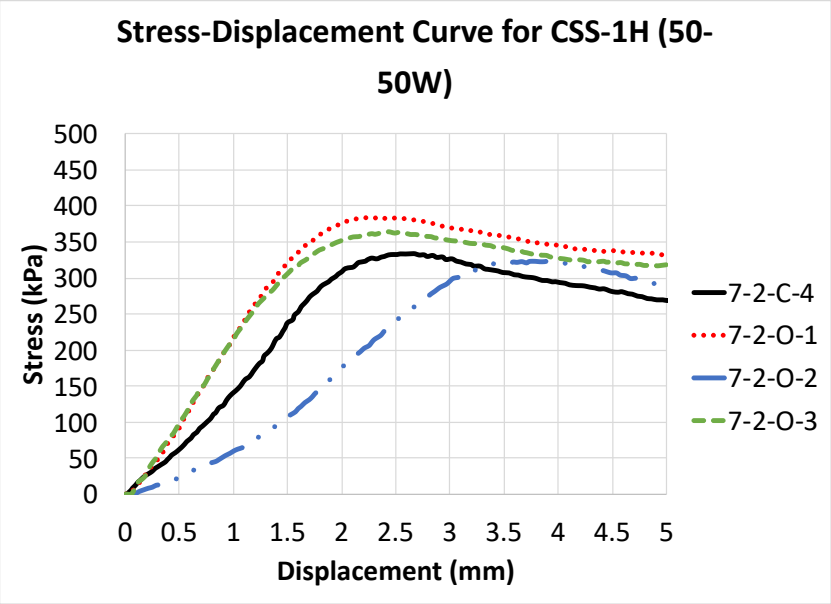


**Figure 5.10 Stress-Displacement Curve for CSS-1h (50-50W) NB Baseline Cores – Section 7**

The proprietary products: TackMax™, Clean Bond, and Colasphalt Tack were installed with no dilution in Sections 3, 10, and 8, respectively. For TackMax™, the ISS values ranged from 306.4kPa to 402.0kPa and the displacement at bond failure ranged from 1.72mm to 2.32mm as shown in Figure 5.11. For Clean Bond, the ISS values ranged from 252.6kPa to 413.2kPa and the displacement at bond failure ranged from 1.95mm to 2.90mm as shown in Figure 5.12. For Colasphalt Tack, the ISS values ranged from 232.2kPa to 331.9kPa and the displacement at bond failure ranged from 2.50mm to 2.73mm as shown in Figure 5.13. Colasphalt Tack had the most consistent shape of stress-displacement curves among all the tested products.

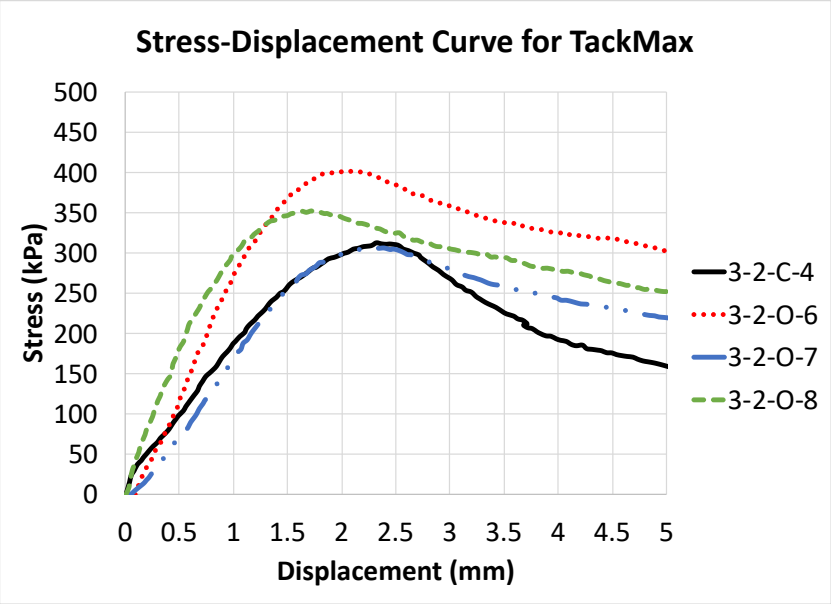


**Figure 5.11 Stress-Displacement Curve for TackMax™ Baseline Cores – Section 3**

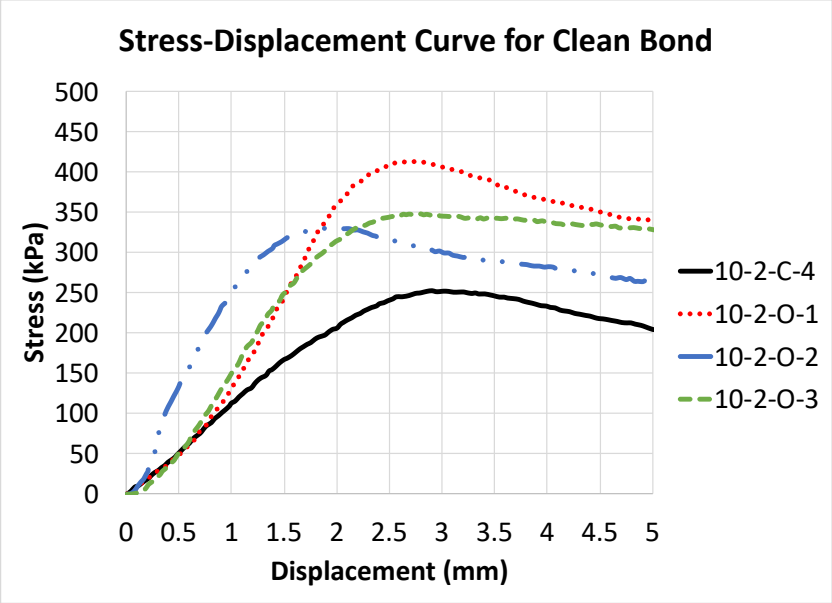


**Figure 5.12 Stress-Displacement Curve for Clean Bond Baseline Cores – Section 10**

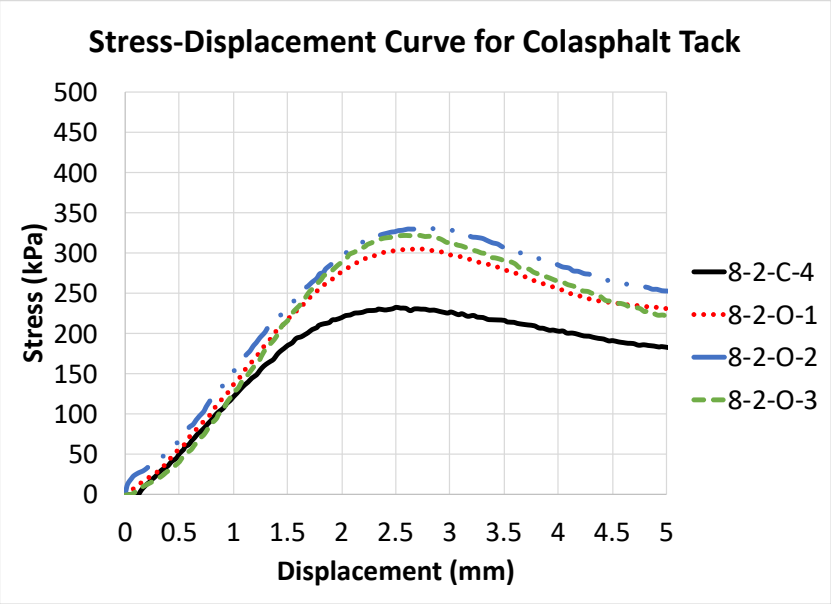


**Figure 5.13 Stress-Displacement Curve for Colasphalt Tack Baseline Cores – Section 8**

For all tested products, outliers were identified and removed from the bond strength testing data. For each test section (four core samples), an outlier was identified when the ISS value for a sample was lower or higher than the average of the remaining three samples by more than 25%. According to this procedure, five samples were identified as outliers and were excluded from the data analysis (3-2-O-6, 4-2-O-7, 6-2-C-4, 8-2-C-4, and 10-2-C-4). For the analysis of the baseline cores, lab conditioned cores, and year one cores, data will be shown presented in table form. To view the data in bar chart format, refer to Appendix H.

Table 5.1 shows the average ISS for each section. Clean Bond had the highest average ISS value of 364.3kPa; while SS-1 SB had the lowest average ISS value of 267.0kPa. The products with the highest average ISS were Clean Bond, SS-1h SB, and CSS-1h. The products with the lowest average ISS were SS-1 SB, TackMax™, and CSS-1h. The coefficient of variation (CV) for the average ISS value ranged from 1.2% for TackMax™ to 17.9% for SS-1h NB. TackMax™ and SS-1 (30-70W) had the most consistent test results for average ISS with coefficient of variances of 1.2% and 1.5% respectively. Most products had ISS values within the mid 300kPa range with the exception of SS-1 SB which was the lowest. Although the average ISS values after construction for all products, except SS-1 SB, varied in a narrow range, this does not indicate that all products will have a similar long-term performance.

**Table 5.1 Interlayer Shear Strength for Baseline Cores**

| Section | Material | Average ISS (kPa) | CV (%) |
|---|---|---|---|
| 1 | SS-1 (50-50W) SB | 267.0 | 13.3 |
| 6 | SS-1 (50-50W) NB | 324.1 | 6.4 |
| 5 | SS-1 (30-70W) | 321.1 | 1.5 |
| 2 | SS-1h (50-50W) SB | 351.9 | 5.1 |
| 9 | SS-1h (50-50) NB | 331.4 | 17.9 |
| 4 | MS-1 (70-30W) | 343.2 | 15.4 |
| 7 | CSS-1h (50-50W) | 351.8 | 8.0 |
| 3 | TackMax™ | 310.6 | 1.2 |
| 10 | Clean Bond | 364.3 | 11.9 |
| 8 | Colasphalt Tack | 319.7 | 4.2 |

Table 5.2 shows the average strain at peak stress. The average strain at peak stress ranged from 2.15% for SS-1h NB to 3.00% for CSS-1h. The products with the highest average strain values were CSS-1h, Colasphalt Tack, and SS-1 NB. The products with the lowest strain values were SS-1h NB, MS-1, and SS-1 (30-70W). Colapshalt Tack had the most consistent test results for average strain with a coefficient of variance of 2.9%. Note that Colasphalt Tack also had a low coefficient of variance for its ISS as well of 4.2%. Overall, the CV values are larger for strain values than they were for the ISS values.

**Table 5.2 Average Strain at Bond Failure for Baseline Cores**

| Section | Material | Average Strain at Bond Failure (%) | CV (%) |
|---|---|---|---|
| 1 | SS-1 (50-50W) SB | 2.36 | 13.0 |
| 6 | SS-1 (50-50W) NB | 2.70 | 11.9 |
| 5 | SS-1 (30-70W) | 2.23 | 18.3 |
| 2 | SS-1h (50-50W) SB | 2.54 | 18.2 |
| 9 | SS-1h (50-50) NB | 2.15 | 34.2 |
| 4 | MS-1 (70-30W) | 2.18 | 8.6 |
| 7 | CSS-1h (50-50W) | 3.00 | 25.7 |
| 3 | TackMax™ | 2.24 | 15.7 |
| 10 | Clean Bond | 2.63 | 19.0 |
| 8 | Colasphalt Tack | 2.83 | 2.9 |

Table 5.3 shows the failure type for all tack coat materials. All tack coat materials experienced a failure Type B (failure in the mix) except the three test sections with SS-1 which experienced failure Type A (failure at the tack coat surface). The type of failure data indicates that all tack coat materials except SS-1 were successfully bonded to make the top and bottom AC lifts behave as one thick homogenous layer. Although TackMax™ and Colasphalt Tack had lower ISS values than SS-1 NB (50-50W) and SS-1 (30-70W), TackMax™ and Colasphalt Tack showed stronger type of failure.

**Table 5.3 Failure Type for Baseline Cores**

| Material | Failure Type |
|---|---|
| SS-1 (50-50W) SB | A |
| SS-1 (50-50W) NB | A |
| SS-1 (30-70W) | A |
| SS-1h (50-50W) SB | B |
| SS-1h (50-50) NB | B |
| MS-1 (70-30W) | B |
| CSS-1h (50-50W) | B |
| TackMax™ | B |
| Clean Bond | B |
| Colasphalt Tack | B |

The interlayer tangential modulus (slope to peak) for each section is shown in Table 5.4. The interlayer tangential modulus values range from 0.119 N/mm$^3$ for Colasphalt Tack to 0.172 N/mm$^3$ for SS-1h NB. The products with the highest k modulus were SS-1h NB, MS-1, and TackMax™. The products with the lowest k modulus were Colasphalt Tack, SS-1 SB, and SS-1 NB. The coefficient of variance values were higher for the interlayer tangential modulus than for the ISS and strain values. This may indicate that these measures are not as reliable. Coefficient of variance values range from 5.0% for Colasphalt Tack to 27.1% for SS-1h NB and CSS-1h. Note that products with higher k moduli have higher coefficients of variance as well.

**Table 5.4 Interlayer Tangential Modulus for Baseline Cores**

| Section | Material | k Modulus ($N/mm^3$) | CV (%) |
|---|---|---|---|
| 1 | SS-1 (50-50W) SB | 0.121 | 8.2 |
| 6 | SS-1 (50-50W) NB | 0.129 | 5.8 |
| 5 | SS-1 (30-70W) | 0.156 | 18.7 |
| 2 | SS-1h (50-50W) SB | 0.152 | 14.7 |
| 9 | SS-1h (50-50W) NB | 0.172 | 27.1 |
| 4 | MS-1 (70-30W) | 0.169 | 22.4 |
| 7 | CSS-1h (50-50W) | 0.131 | 27.1 |
| 3 | TackMax™ | 0.159 | 25.5 |
| 10 | Clean Bond | 0.149 | 15.2 |
| 8 | Colasphalt Tack | 0.119 | 5.0 |

Table 5.5 shows the average energy required to reach the peak shear stress per unit area of the tack coat surface. CSS-1h, Clean Bond, and SS-1h SB had the highest average energy to reach peak shear stress; while SS-1 SB, SS-1 (30-70W), and SS-1h NB had the lowest average energy to reach peak shear stress. The CV values were higher for the average energy to peak shear stress than for the ISS and strain values but similar to the CV range for the interlayer tangential modulus. Coefficient of variance values range from 6.7% for TackMax™ to 32.3% for SS-1h NB.

**Table 5.5 Average Energy to Reach Peak Stress for Baseline Cores**

| Section | Material | Energy to Peak ($J/m^2$) | CV (%) |
|---|---|---|---|
| 1 | SS-1 (50-50W) SB | 1108 | 26.7 |
| 6 | SS-1 (50-50W) NB | 1521 | 11.4 |
| 5 | SS-1 (30-70W) | 1220 | 8.3 |
| 2 | SS-1h (50-50W) SB | 1616 | 22.8 |
| 9 | SS-1h (50-50W) NB | 1311 | 32.3 |
| 4 | MS-1 (70-30W) | 1370 | 15.3 |
| 7 | CSS-1h (50-50W) | 1837 | 11.6 |
| 3 | TackMax™ | 1360 | 6.7 |
| 10 | Clean Bond | 1699 | 17.7 |
| 8 | Colasphalt Tack | 1588 | 9.1 |

### 5.6 Bond Strength of Lab Conditioned Cores

Of the sixteen cores sampled from each test section in September 2017, nine were conditioned through FT cycling prior to having their bond strength tested; three cores at 3 FT cycle, three cores at 9 FT cycles, and three cores at 15 FT cycles. The placement of the core in the centre or wheel paths was not taken into consideration because this would have a negligible effect on the cores because they were collected shortly after construction. A total of 90 cores, nine from each of the ten tested sections were tested using a LISST device and a loading frame after conditioning at either 3, 9, or 15 FT cycles. Outliers for this group of cores were identified by section and by length of FT cycle conditioning. Only one outlier was identified in the 3 FT cycle group (7-1-C-4). No outliers were identified for the cores exposed to 9 FT cycles. One outlier was identified for the cores exposed to 15 FT cycles (1-2-C-5) and one core was damaged and not tested (6-2-I-6). Figure 5.14 to Figure 5.23 show the stress-displacement curves for the tested cores from each test section. The ISS for all tested samples ranged from 208.4kPa to 422.6kPa.

The stress-displacement curves for SS-1 for lab conditioned cores are shown in Figure 5.14 to Figure 5.16. For SS-1 with dilution 50-50W (Figure 5.14 and Figure 5.15), the ISS values ranged from 220.0kPa to 409.5kPa and the displacement at bond failure ranged from 2.34mm to

4.45mm. For SS-1 with dilution 30-70W (Figure 5.16), the ISS values ranged from 296.1kPa to 385.1kPa and the displacement at bond failure ranged from 2.24mm to 3.68mm.

The shear strength, displacement, and k modulus do not appear to be affected by the number of FT cycles. For SS-1 SB, the highest shear strength is achieved by a sample that has been exposed to 9 FT cycles and the lowest is achieved in a sample that has received 15 FT cycles. For SS-1 NB, the highest and lowest shear strengths are achieved by a sample that has received 3 FT cycles. For SS-1 (30-70W), the highest and lowest shear strengths are achieved by a sample that has received 15 FT cycles. SS-1 (30-70W) had a smaller variability in displacement than the other SS-1 sections as well as a smaller range in k modulus values.

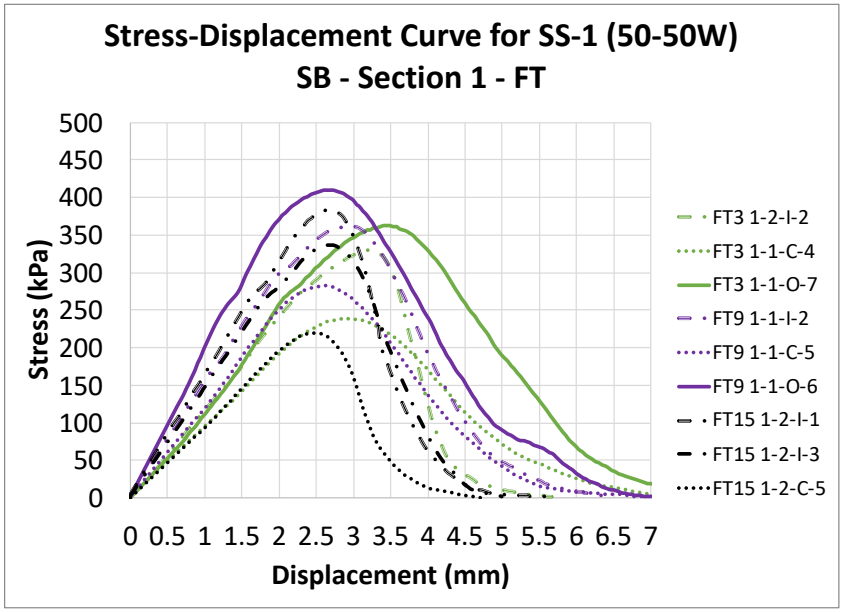


**Figure 5.14 Stress-Displacement Curve for SS-1 (50-50W) SB Lab Conditioned Cores – Section 1**

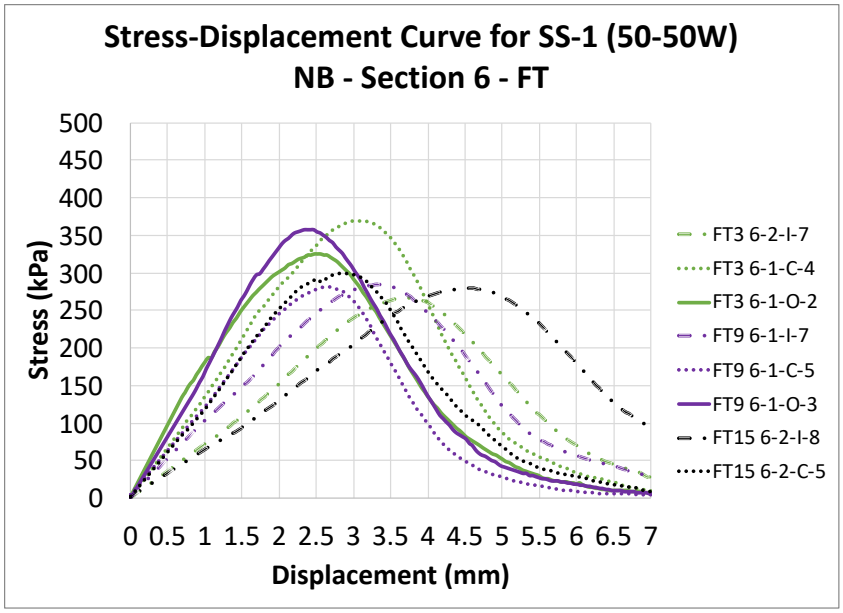


**Figure 5.15 Stress-Displacement Curve for SS-1 (50-50W) NB Lab Conditioned Cores – Section 6**

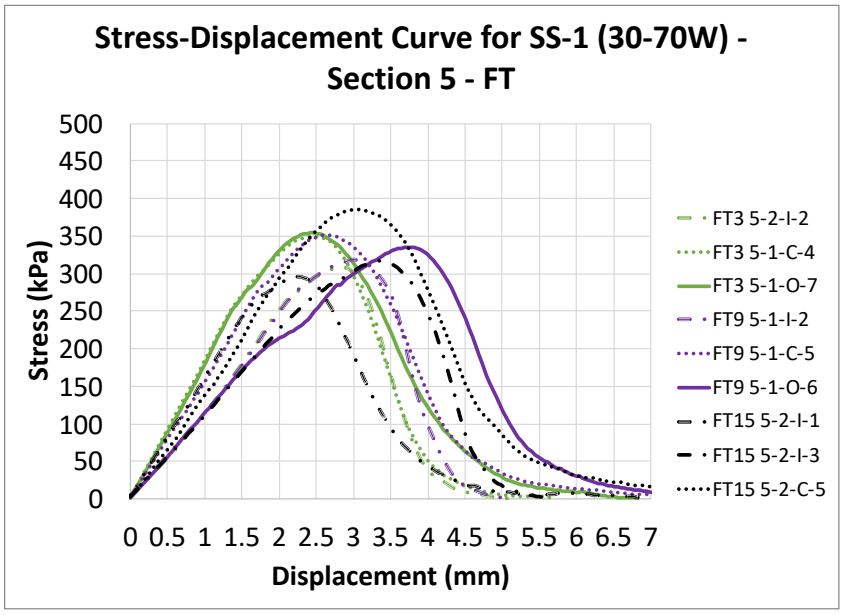


**Figure 5.16 Stress-Displacement Curve for SS-1 (30-70W) Lab Conditioned Cores – Section 5**

Figure 5.17 (Section 2) and Figure 5.18 (Section 9) shows the stress-displacement curves for SS-1h. For Figure 5.17 (Section 2), the ISS values ranged from 290.9kPa to 380.8kPa and the displacement at bond failure ranged from 2.55mm to 3.49mm. For Figure 5.18 (Section 9), the

ISS values ranged from 307.3kPa to 409.1kPa and the displacement at bond failure ranged from 2.55mm to 3.91mm. Both sections of SS-1h has much less variability in plot-shape including displacements, k modulus values, and ISS than SS-1 for the lab conditioned cores. For SS-1h SB, the highest ISS is achieved by a sample that has had 15 FT cycles, and the lowest ISS is achieved from a sample that has received 3 FT cycles. For SS-1h NB, the highest and lowest ISS is achieved by samples that have been through 3 FT cycles.

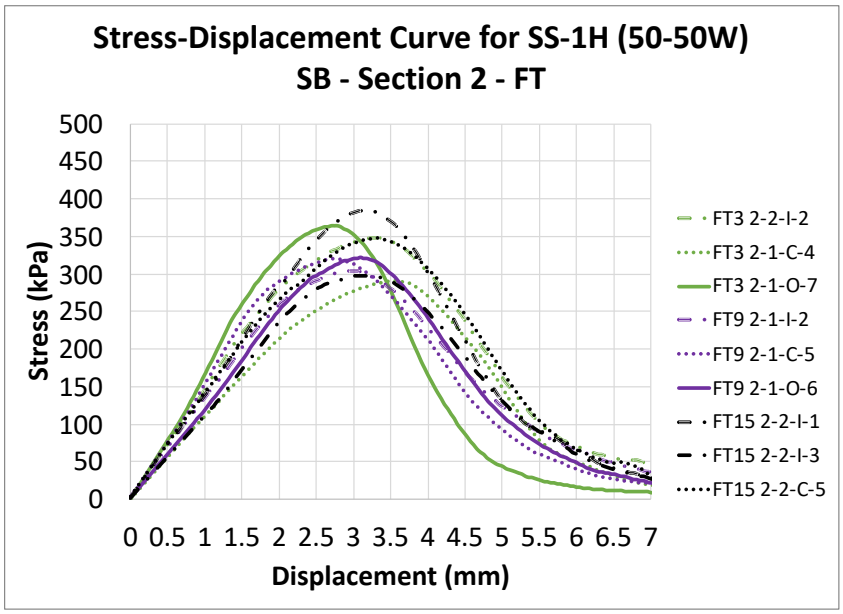


**Figure 5.17 Stress-Displacement Curve for SS-1h (50-50W) SB Lab Conditioned Cores – Section 2**

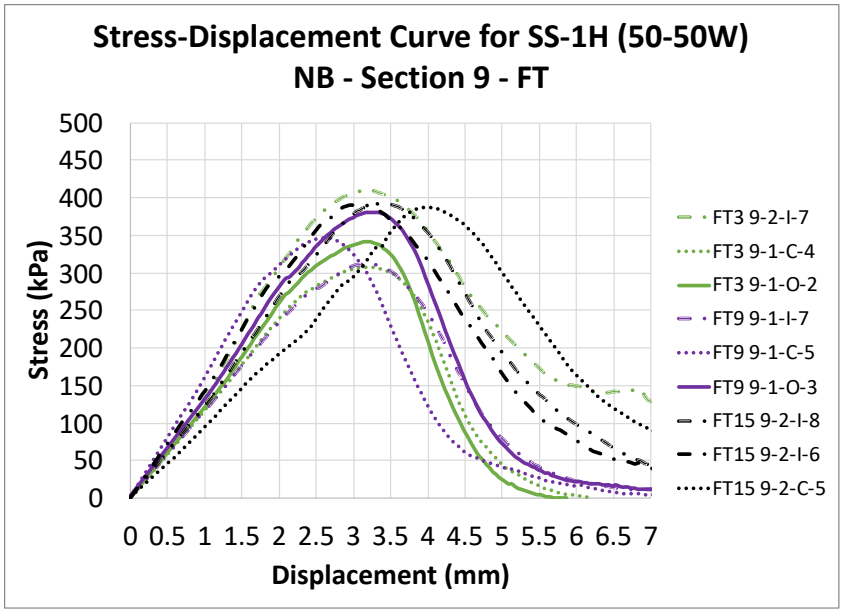


**Figure 5.18 Stress-Displacement Curve for SS-1h (50-50W) NB Lab Conditioned Cores – Section 9**

Figure 5.19 (Section 4) shows the stress-displacement curves for MS-1. The ISS values ranged from 302.1kPa to 422.6kPa and the displacement at bond failure ranged from 2.48mm to 3.58mm. For MS-1 the highest ISS is achieved by a sample that has had 9 FT cycles, and the lowest ISS is achieved from a sample that has received 3 FT cycles. Two of the three samples exposed to 3 FT cycles had lower k modulus values than the other samples which had low variability.

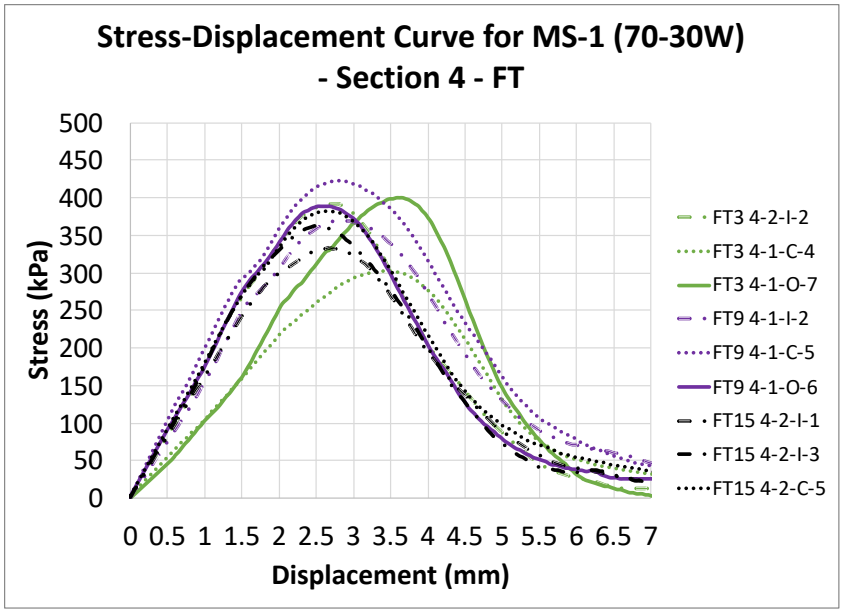


**Figure 5.19 Stress-Displacement Curve for MS-1 (70-30W) Lab Conditioned Cores – Section 4**

Figure 5.20 (Section 7) shows the stress-displacement curves for CSS-1h. The ISS values ranged from 208.4kPa to 400.6kPa and the displacement at bond failure ranged from 2.59mm to 3.34mm. Although there is a large range for the ISS values, there is consistency which the ISS with the exception of the one low value which was found to be an outlier. For CSS-1h the highest ISS is achieved by a sample that has had 15 FT cycles, and the lowest ISS is achieved from a sample that has received 3 FT cycles. Excluding the outlier, the k modulus values for CSS-1h had low variability, as do the displacement values, and the ISS values.

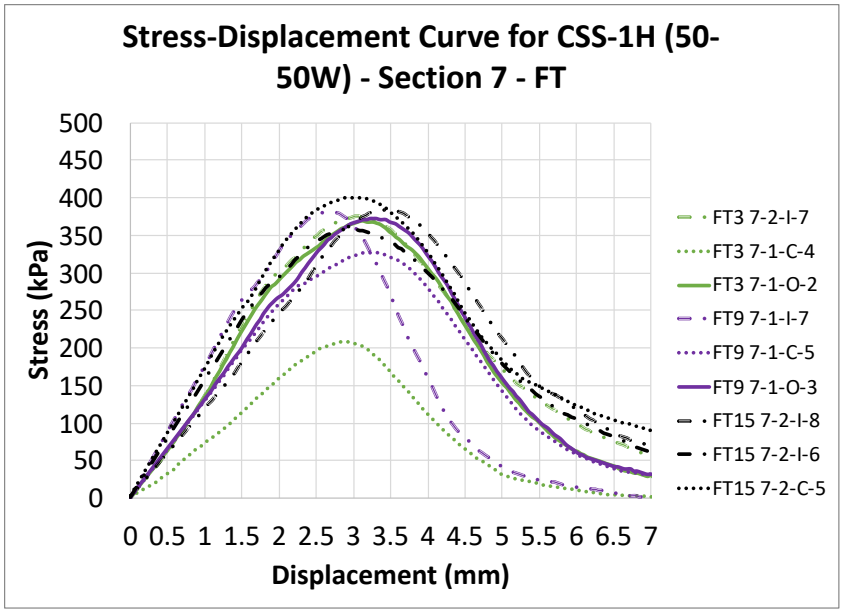


**Figure 5.20 Stress-Displacement Curve for CSS-1h (50-50W) Lab Conditioned Cores – Section 7**

Figure 5.21 (Section 3) shows the stress-displacement curves for TackMax™. The ISS values ranged from 253.6kPa to 401.4kPa and the displacement at bond failure ranged from 2.36mm to 3.40mm. For TackMax™ there is large variation for the ISS values. The highest ISS is achieved by a sample that has been subjected to 9 FT cycles, and the lowest ISS is achieved from a sample that has received 15 FT cycles.

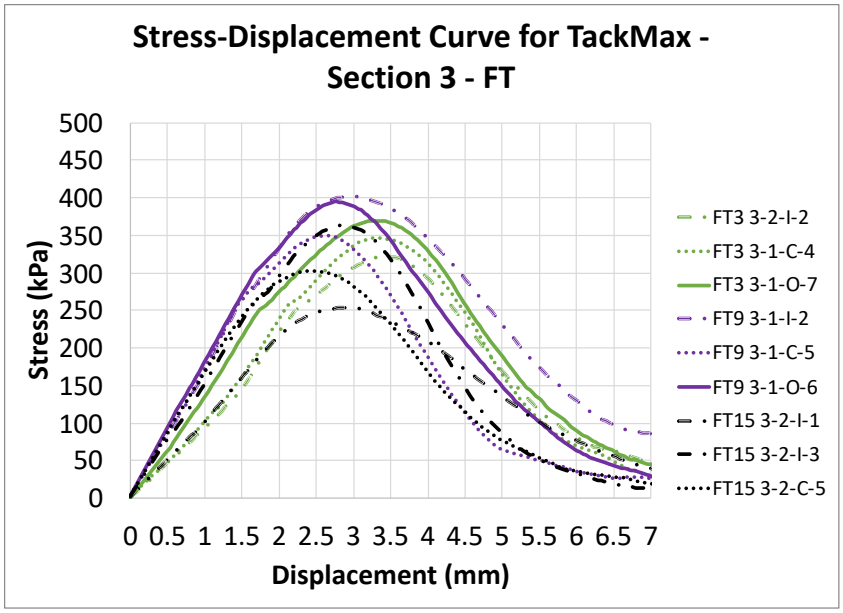


**Figure 5.21 Stress-Displacement Curve for TackMax™ Lab Conditioned Cores – Section 3**

Figure 5.22 (Section 10) shows the stress-displacement curves for Clean Bond. The ISS values ranged from 306.5kPa to 407.8kPa and the displacement at bond failure ranged from 2.13mm to 3.34mm. Clean Bond has a large variation in k modulus values. The highest ISS is achieved by a sample that has been subjected to 9 FT cycles, and the lowest ISS is achieved from a sample that has received 3 FT cycles.

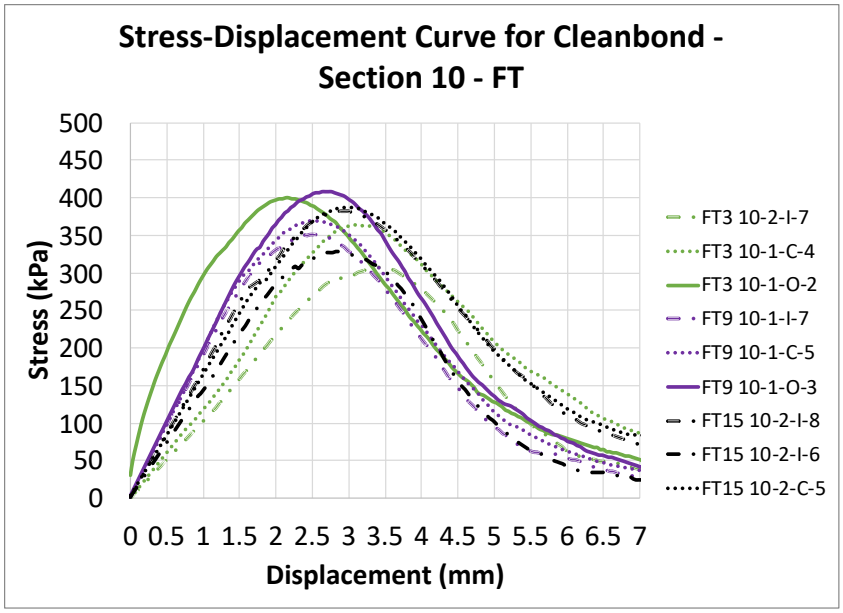


**Figure 5.22 Stress-Displacement Curve for Clean Bond Lab Conditioned Cores – Section 10**

Figure 5.23 (Section 8) shows the stress-displacement curves for Colasphalt Tack. The ISS values ranged from 285.8kPa to 414.6kPa and the displacement at bond failure ranged from 2.40mm to 3.65mm. The highest and lowest ISS is achieved by samples that has been subjected to 15 FT cycles.

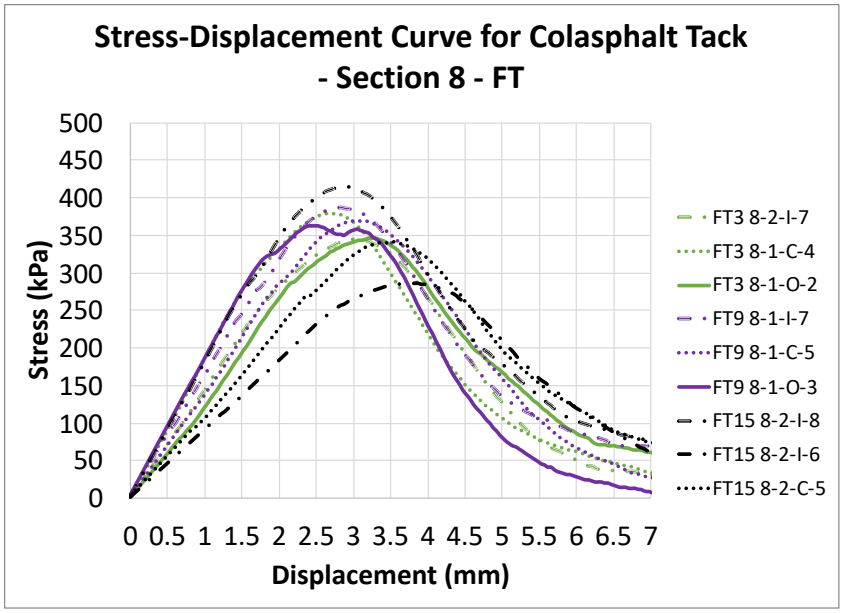


**Figure 5.23 Stress-Displacement Curve for Colasphalt Tack Lab Conditioned Cores – Section 8**

Table 5.6 and Figure 5.24 show the average ISS for each section and for each cycle pattern as well as the CV and % change from the baseline core ISS value. Overall, the FT cycled cores had an increase in the strength of the interface bond as shown by positive % change values for this data set. The range of % change values is from -11% to 32% from the original baseline core ISS values. The increase in bond after FT cycling can be due to continuous curing of tack coat materials. The number of freeze thaw cycles does not show a large impact on the strength of the interface; there is not a large or consistent difference in the ISS values between the core samples subjected to 3 FT cycles compared to the samples subjected to 15 FT cycles. It is interesting to note that the samples exposed to 9 FT cycles has the greatest % change for 6 of the 10 sections. FT cycling was done without saturation of cores because this would have been too aggressive and could have resulted in failure within the AC mix which would have made it impossible to test the core samples in shear strength testing. When looking at the 15 FT cycled cores, the three products with the highest ISS values are SS-1h NB, CSS-1h, and Clean Bond. The three products with the lowest ISS values are SS-1 NB, TackMax$^{TM}$, and SS-1 SB.

**Table 5.6 Interlayer Shear Strength for Lab Conditioned Cores**

| | | 3 FT Cycles | | | 9 FT Cycles | | | 15 FT Cycles | | |
|---|---|---|---|---|---|---|---|---|---|---|
| **Section** | **Material** | **Avg ISS (kPa)** | **CV (%)** | **% Change** | **Avg ISS (kPa)** | **CV (%)** | **% Change** | **Avg ISS (kPa)** | **CV (%)** | **% Change** |
| 1 | SS-1 (50-50W) SB | 310.5 | 20.6 | 16 | 351.7 | 18.1 | 32 | 309.1 | 14.2 | 16 |
| 6 | SS-1 (50-50W) NB | 320.5 | 16.2 | -1 | 307.5 | 14.1 | -5 | 289.2 | 4.6 | -11 |
| 5 | SS-1 (30-70W) | 337.6 | 7.3 | 5 | 334.5 | 4.8 | 4 | 332.5 | 14.0 | 4 |
| 2 | SS-1h (50-50W) SB | 334.1 | 11.5 | -5 | 314.8 | 3.1 | -11 | 343.9 | 12.8 | -2 |
| 9 | SS-1h (50-50W) NB | 352.4 | 14.7 | 6 | 346.3 | 9.8 | 5 | 389.8 | 0.7 | 18 |
| 4 | MS-1 (70-30W) | 364.0 | 14.8 | 6 | 393.7 | 6.8 | 15 | 359.7 | 6.7 | 5 |
| 7 | CSS-1h (50-50W) | 372.6 | 1.3 | 6 | 360.2 | 8.0 | 2 | 380.7 | 5.7 | 8 |
| 3 | TackMax™ | 346.1 | 6.7 | 11 | 382.0 | 7.4 | 23 | 306.9 | 18.0 | -1 |
| 10 | Clean Bond | 356.5 | 13.2 | -2 | 375.5 | 7.8 | 3 | 365.4 | 9.0 | 0 |
| 8 | Colasphalt Tack | 356.8 | 5.4 | 12 | 380. 8 | 3.8 | 19 | 347.4 | 18.6 | 9 |

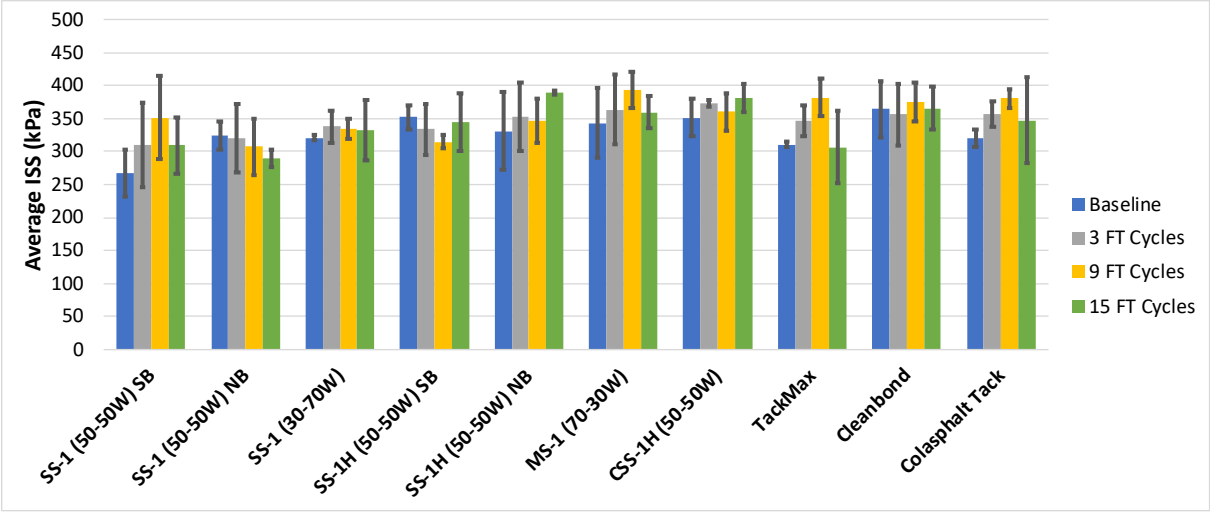


**Figure 5.24 Average Interlayer Shear Strength for Lab Conditioned Cores**

Table 5.7 and Figure 5.25 show the average strain at bond failure for each section and for each cycle pattern as well as the CV and % change from the baseline core strain value. Overall, the FT cycling increased the ability of the AC samples to deform as shown by the positive % change in strain value. This is a result of the increased displacement (higher deformation) of the samples prior to failure compared to the baseline cores. The range of % change values is much larger for the strain values than it is for the ISS values. The range of % change in strain is from 0% to 66% from the original baseline core strain values. The number of freeze thaw cycles does not show a large impact on the strain at bond failure values; there is not a large or consistent difference in the strain values between the core samples subjected to 3 FT cycles compared to the samples subjected to 15 FT cycles. When looking at the 15 FT cycled cores, the three products with the highest strain values are SS-1 NB, SS-1h NB, and Colasphalt Tack. The three products with the lowest strain values are MS-1, SS-1 SB, and TackMax™.

**Table 5.7 Average Strain at Bond Failure for Lab Conditioned Cores**

| | | 3 FT Cycles | | | 9 FT Cycles | | | 15 FT Cycles | | |
|---|---|---|---|---|---|---|---|---|---|---|
| **Section** | **Material** | **Strain at Peak (%)** | **CV (%)** | **% Change** | **Strain at Peak (%)** | **CV (%)** | **% Change** | **Strain at Peak (%)** | **CV (%)** | **% Change** |
| 1 | SS-1 (50-50W) SB | 3.3 | 8.9 | 42 | 2.9 | 6.8 | 22 | 2.8 | 1.8 | 20 |
| 6 | SS-1 (50-50W) NB | 3.2 | 19.2 | 19 | 2.9 | 17.5 | 7 | 3.8 | 32.3 | 42 |
| 5 | SS-1 (30-70W) | 2.7 | 8.8 | 21 | 3.3 | 17.6 | 47 | 3.0 | 19.3 | 35 |
| 2 | SS-1h (50-50W) SB | 3.3 | 12.7 | 32 | 3.1 | 6.4 | 22 | 3.4 | 4.6 | 32 |
| 9 | SS-1h (50-50W) NB | 3.3 | 0.9 | 53 | 3.1 | 11.9 | 45 | 3.6 | 14.4 | 66 |
| 4 | MS-1 (70-30W) | 3.4 | 15.3 | 54 | 2.8 | 4.7 | 29 | 2.7 | 4.0 | 25 |
| 7 | CSS-1h (50-50W) | 3.2 | 2.1 | 8 | 3.2 | 11.6 | 5 | 3.2 | 9.3 | 7 |
| 3 | TackMax™ | 3.5 | 3.1 | 56 | 2.9 | 5.4 | 31 | 2.8 | 9.6 | 27 |
| 10 | Clean Bond | 3.0 | 22.1 | 14 | 2.6 | 5.5 | 0 | 3.0 | 1.3 | 14 |
| 8 | Colasphalt Tack | 3.1 | 9.9 | 9 | 2.9 | 10.7 | 2 | 3.5 | 13.2 | 23 |

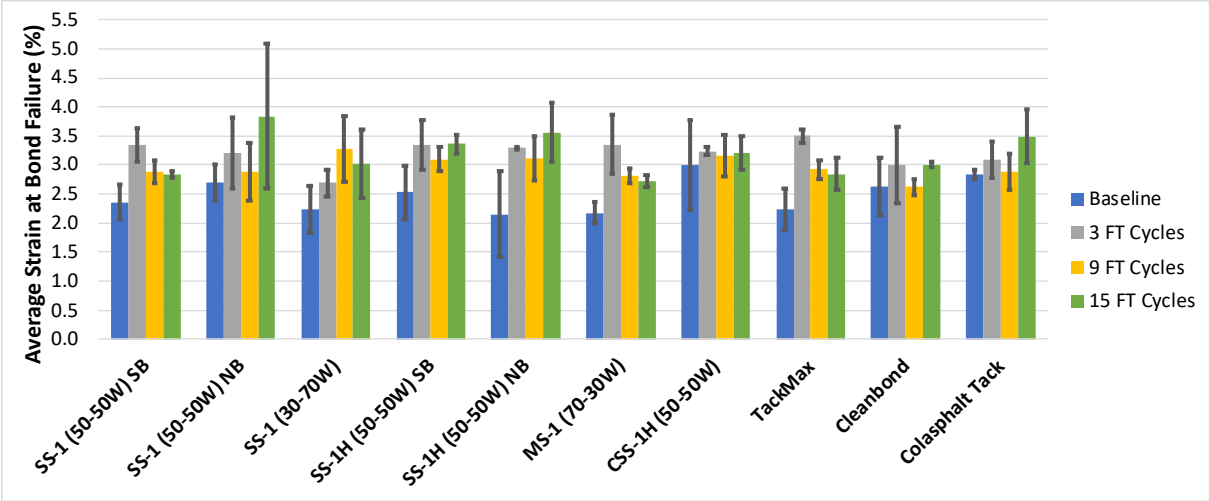


**Figure 5.25 Average Strain at Bond Failure for Lab Conditioned Cores**

Table 5.8 shows the type of failure for all tack coat materials for the lab conditioned cores. The most consistent products in terms of failure type after FT cycling were SS-1 (30-70W), SS-1h SB, MS-1, TackMax™, Clean Bond, and Colasphalt Tack. These products, with the exception of SS-1, experienced failure within the mix (Type B failure) before conditioning as well as after 3, 9, and 15 FT cycles. This shows that these products performed well and were able to bond the layers adequately even after exposure to FT cycling. SS-1 (30-70W) had failure at the tack coat surface (Type A failure) for the baseline cores as well as the cores conditioned with 3, 9, and 15 FT cycles. The other products including SS-1 NB, SS-1h NB, and CSS-1h experienced a mixture of failure Type A and Type B indicating that FT cycling may have had an effect on the strength of the bond between layers.

**Table 5.8 Failure Type for Lab Conditioned Cores**

| Section | Material | Baseline | 3 FT Cycles | 9 FT Cycles | 15 FT Cycles |
|---|---|---|---|---|---|
| 1 | SS-1 (50-50W) SB | A | A | A/B | A |
| 6 | SS-1 (50-50W) NB | A | B | A/B | B |
| 5 | SS-1 (30-70W) | A | A | A | A |
| 2 | SS-1h (50-50W) SB | B | B | B | B |
| 9 | SS-1h (50-50W) NB | B | A | A | B |
| 4 | MS-1 (70-30W) | B | B | B | B |
| 7 | CSS-1h (50-50W) | B | B | A/B | B |
| 3 | TackMax™ | B | B | B | B |
| 10 | Clean Bond | B | B | B | B |
| 8 | Colasphalt Tack | B | B | B | B |

Most materials showed decrease in tangential modulus with FT cycling as shown in Table 5.9 and Figure 5.26. This decrease in tangential modulus is due to increase in the ISS. The range for the % change values is from -34% to 3% with the majority of the % change values being negative. The strain values for the 3 FT cycled samples do not differ significantly from the samples exposed to 15 FT cycles. When looking at the 15 FT cycled cores, the three products with the highest k modulus values are MS-1 NB, SS-1 SB, and Clean Bond. The three products with the lowest k modulus values are SS-1 NB, Colasphalt Tack, and SS-1h SB.

**Table 5.9 Interlayer Tangential Modulus for Lab Conditioned Cores**

| | | 3 FT Cycles | | | 9 FT Cycles | | | 15 FT Cycles | | |
|---|---|---|---|---|---|---|---|---|---|---|
| **Section** | **Material** | **k Modulus ($N/mm^3$)** | **CV (%)** | **% Change** | **k Modulus ($N/mm^3$)** | **CV (%)** | **% Change** | **k Modulus ($N/mm^3$)** | **CV (%)** | **% Change** |
| 1 | SS-1 (50-50W) SB | 0.098 | 12.9 | -19 | 0.131 | 18.5 | 9 | 0.136 | 9.0 | 13 |
| 6 | SS-1 (50-50W) NB | 0.110 | 29.1 | -15 | 0.116 | 29.3 | -10 | 0.085 | 36.9 | -34 |
| 5 | SS-1 (30-70W) | 0.134 | 15.6 | -14 | 0.111 | 20.3 | -29 | 0.119 | 17.2 | -24 |
| 2 | SS-1h (50-50W) SB | 0.109 | 23.7 | -28 | 0.108 | 7.5 | -28 | 0.109 | 9.6 | -28 |
| 9 | SS-1h (50-50W) NB | 0.113 | 14.4 | -34 | 0.119 | 15.1 | -31 | 0.117 | 14.4 | -32 |
| 4 | MS-1 (70-30W) | 0.117 | 24.7 | -31 | 0.148 | 7.6 | -12 | 0.140 | 9.3 | -17 |
| 7 | CSS-1h (50-50W) | 0.122 | 3.0 | -7 | 0.122 | 18.0 | -6 | 0.126 | 9.5 | -3 |
| 3 | TackMax™ | 0.106 | 9.6 | -33 | 0.139 | 2.8 | -12 | 0.116 | 18.4 | -27 |
| 10 | Clean Bond | 0.132 | 37.4 | -11 | 0.151 | 2.5 | 1 | 0.128 | 7.9 | -14 |
| 8 | Colasphalt Tack | 0.123 | 15.6 | 3 | 0.138 | 9.5 | 16 | 0.108 | 33.1 | -10 |

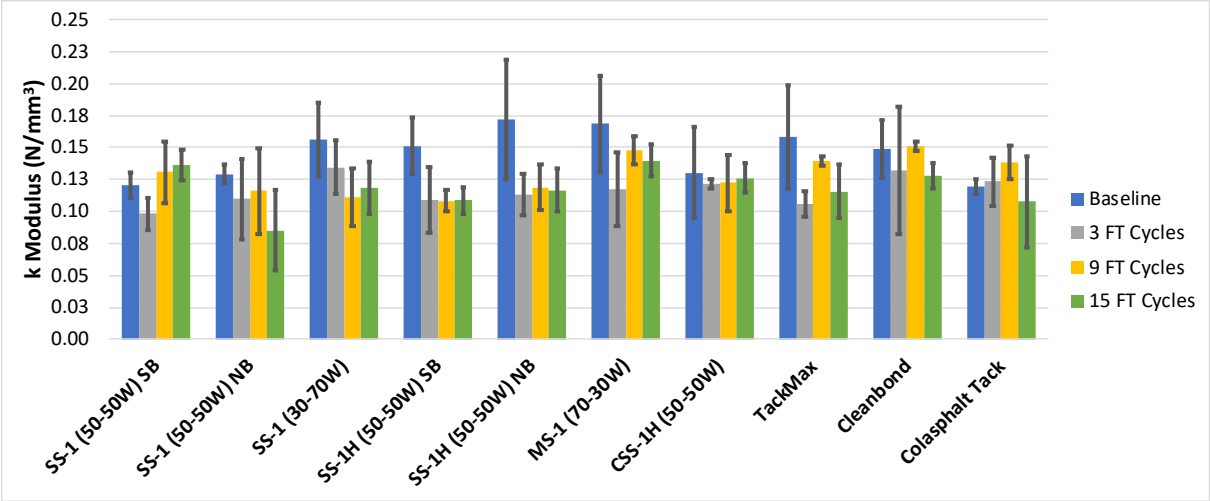


**Figure 5.26 Average Interlayer Tangential Modulus for Lab Conditioned Cores**

Most materials showed increase in average energy to peak stress with FT cycling as shown in Table 5.10 and Figure 5.27. This increase in energy to peak stress is due to the change in shape of the stress-displacement curve. Due to the increase in strain and decrease in k modulus resulting from the increase in displacement, the area under the stress strain curve before reaching peak stress is larger. This means that it takes more energy to achieve bond failure. The range for the % change values are from -1% to 70% with all values being positive except one. There is no observed pattern between the samples exposed to 3, 9, and 15 FT cycles. When looking at the 15 FT cycled cores, the three products with the highest average energy to peak stress SS-1h NB, CSS-1h, and Colasphalt Tack. The three products with the lowest average energy to peak stress TackMax™, SS-1 (30-70W), and SS-1 SB.

**Table 5.10 Average Energy to Peak Stress for Lab Conditioned Cores**

| | | 3 FT Cycles | | | 9 FT Cycles | | | 15 FT Cycles | | |
|---|---|---|---|---|---|---|---|---|---|---|
| **Section** | **Material** | **Average Energy to Peak ($J/m^2$)** | **CV (%)** | **% Change** | **Average Energy to Peak ($J/m^2$)** | **CV (%)** | **% Change** | **Average Energy to Peak ($J/m^2$)** | **CV (%)** | **% Change** |
| 1 | SS-1 (50-50W) SB | 1762 | 27.6 | 59 | 1764 | 22.1 | 59 | 1741 | 11.3 | 57 |
| 6 | SS-1 (50-50W) NB | 1726 | 11.5 | 13 | 1505 | 12.5 | -1 | 1813 | 23.8 | 19 |
| 5 | SS-1 (30-70W) | 1568 | 3.0 | 29 | 1862 | 17.9 | 53 | 1736 | 23.8 | 42 |
| 2 | SS-1h (50-50W) SB | 1999 | 8.3 | 24 | 1748 | 3.9 | 8 | 2021 | 17.2 | 25 |
| 9 | SS-1h (50-50W) NB | 1982 | 13.1 | 51 | 1862 | 14.1 | 42 | 2230 | 8.9 | 70 |
| 4 | MS-1 (70-30W) | 2038 | 15.8 | 49 | 1941 | 11.5 | 42 | 1747 | 4.4 | 28 |
| 7 | CSS-1h (50-50W) | 2095 | 0.8 | 14 | 1970 | 9.0 | 7 | 2095 | 6.6 | 14 |
| 3 | TackMax™ | 1986 | 7.7 | 46 | 1993 | 11.6 | 46 | 1537 | 21.8 | 13 |
| 10 | Clean Bond | 1908 | 2.7 | 12 | 1808 | 13.0 | 6 | 1977 | 9.2 | 16 |
| 8 | Colasphalt Tack | 1945 | 4.3 | 23 | 1905 | 10.8 | 20 | 2073 | 7.3 | 31 |

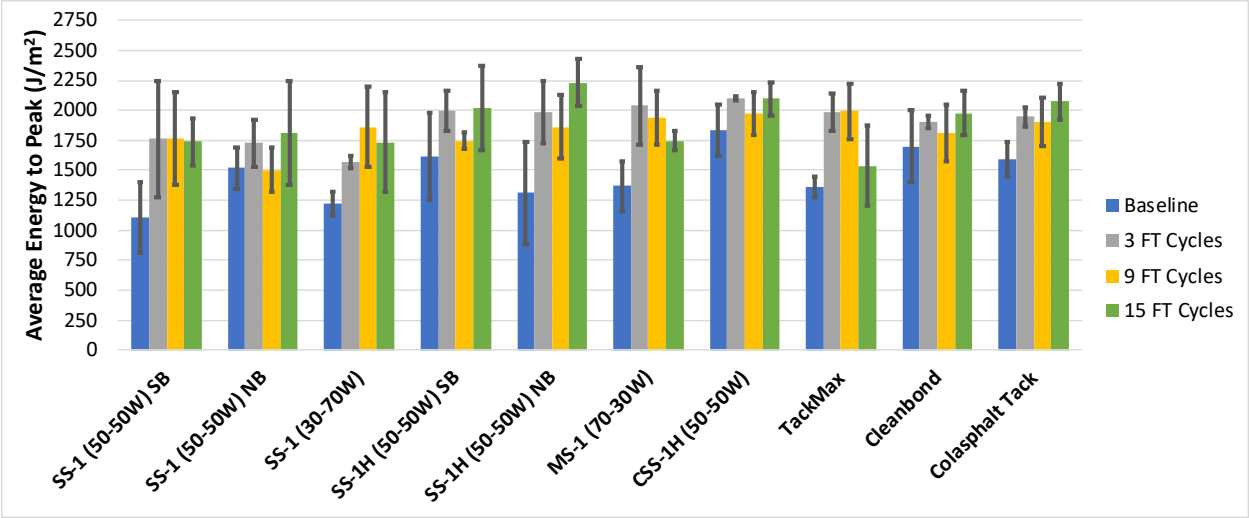


**Figure 5.27 Average Energy to Peak Stress Per Unit Area for Lab Conditioned Cores**

### 5.7 Bond Strength of One Year Post Construction Cores

Twelve cores were sampled from each test section in September 2018 for a total of 120 cores. Four cores were collected from the outer wheel path, four from the inner wheel path and four cores from the centre. Because these cores were exposed to vehicular traffic for one year, the positioning of the core (IWP, OWP, and centre) is treated with significance during the analysis.

Outliers for this group of cores were identified by section and by wheel path location. For example, in Section 1, all cores in the outer wheel path were compared to each other to see if their ISS was 25% greater or smaller than the average ISS of the remaining outer wheel path cores in Section 1. Only one outlier was identified in the one year post construction cores (8-2-O-1) and one core was not tested because it was damaged (4-2-C-4). Figure 5.28 to Figure 5.37 show the stress-displacement curves for the tested cores from each test section for the cores collected after one year. The ISS for all tested samples ranged from 261.9kPa to 493.8kPa.

The stress-displacement curves for SS-1 for one year cores are shown in Figure 5.28 to Figure 5.30. For SS-1 with dilution 50-50W (Figure 5.28 and Figure 5.29), the ISS values ranged from 331.2kPa to 449.1kPa and the displacement at bond failure ranged from 2.21mm to 4.27mm. For SS-1 with dilution 30-70W (Figure 5.30), the ISS values ranged from 341.9kPa to 493.8kPa and the displacement at bond failure ranged from 2.28mm to 3.24mm.

The shear strength, displacement, and k modulus do not appear to be affected by the placement of the core in the inner wheel path, centre of the lane, or outer wheel path. For SS-1 SB (Section 1), the highest shear strength is achieved by a sample that was extracted from the inner wheel path and the lowest is achieved in a sample that was extracted from the outer wheel path. For SS-1 NB (Section 6), the highest shear strength is achieved by a sample that was extracted from the centre of the lane and the lowest is achieved in a sample that was extracted from the outer wheel path. For SS-1 (30-70W) (Section 5), the highest shear strength is achieved by a sample that was extracted from the inner wheel path and the lowest is achieved in a sample that was extracted from the outer wheel path. All three SS-1 sections had the minimum ISS from a core sample taken from the outer wheel path. SS-1 SB and SS-1 (30-70W) have a lower variation in k modulus than SS-1 NB.

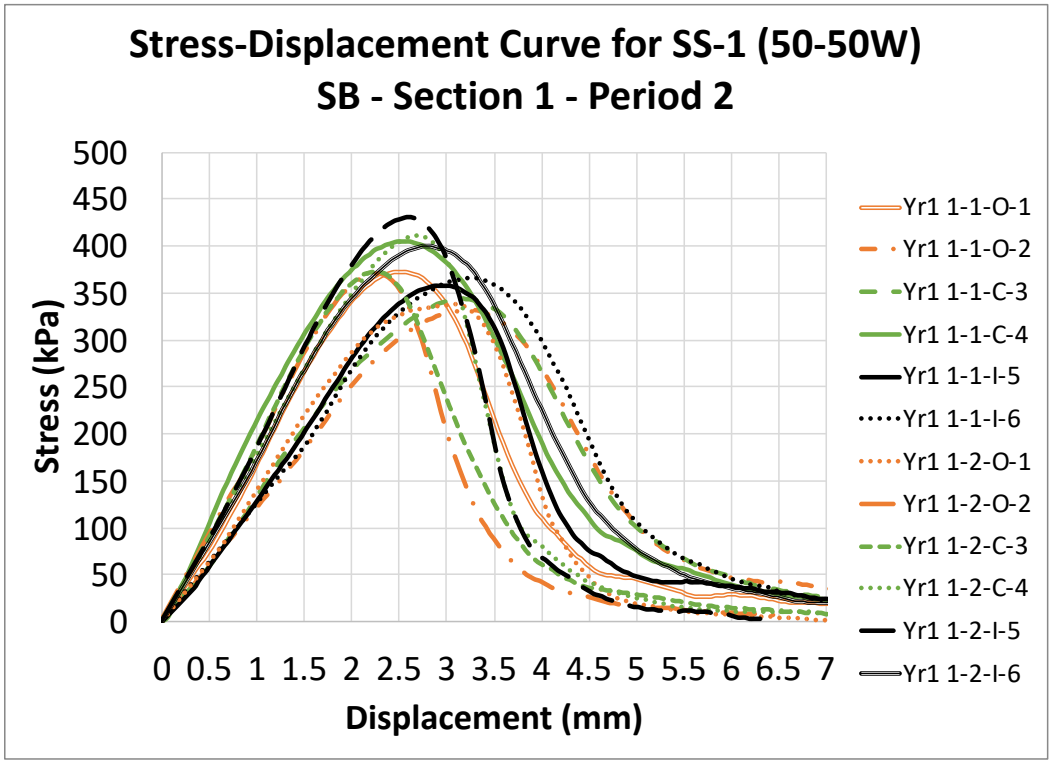


**Figure 5.28 Stress-Displacement Curve for SS-1 (50-50W) SB One Year Cores – Section 1**

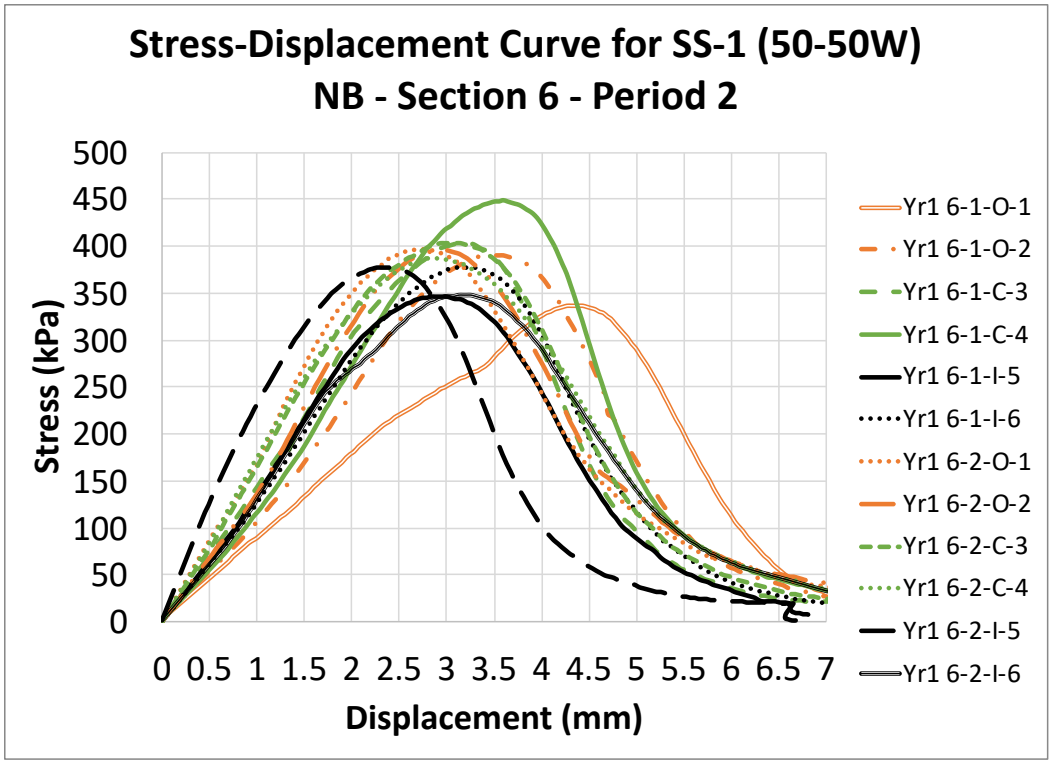


**Figure 5.29 Stress-Displacement Curve for SS-1 (50-50W) NB One Year Cores – Section 6**

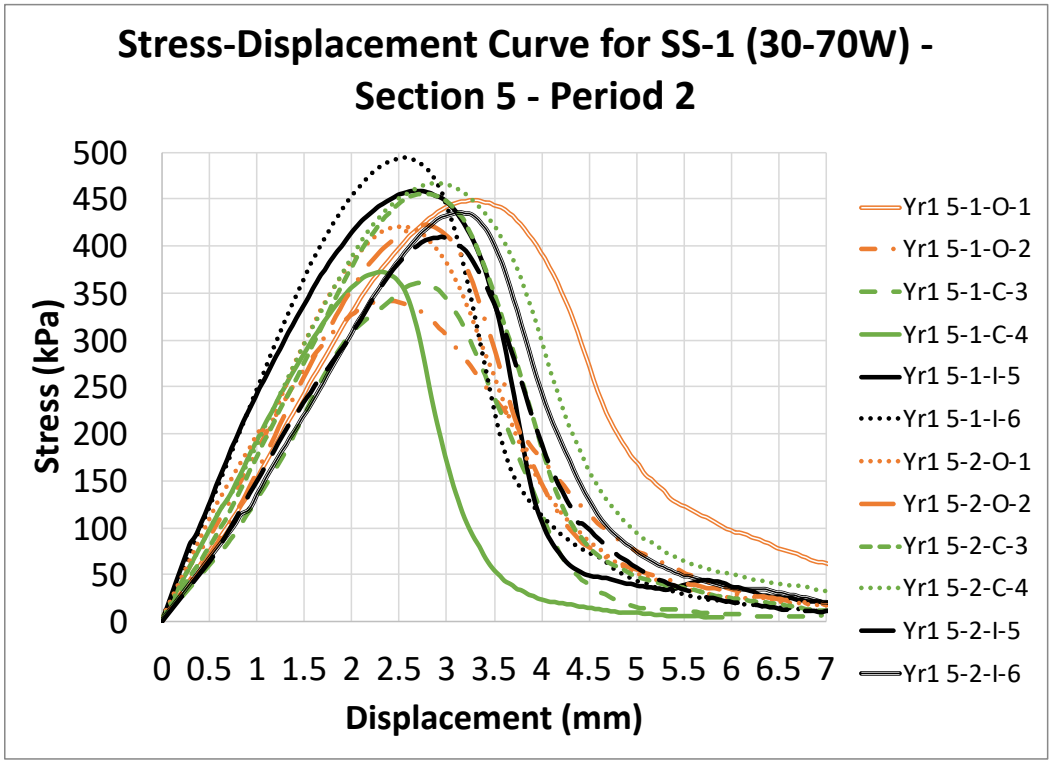


**Figure 5.30 Stress-Displacement Curve for SS-1 (30-70W) One Year Cores – Section 5**

Figure 5.31 (Section 2) and Figure 5.32 (Section 9) shows the stress-displacement curves for SS-1h for year one cores. For Figure 5.31 (Section 2), the ISS values ranged from 340.1kPa to 452.2kPa and the displacement at bond failure ranged from 2.37mm to 3.39mm. For Figure 5.32 (Section 9), the ISS values ranged from 303.31Pa to 406.0kPa and the displacement at bond failure ranged from 2.42mm to 3.21mm. For SS-1h SB, the highest shear strength is achieved by a sample that was extracted from the inner wheel path and the lowest is achieved in a sample that was extracted from the outer wheel path. For SS-1h NB, the highest shear strength is achieved by a sample that was extracted from the outer wheel path and the lowest is achieved in a sample that was extracted from the inner wheel path.

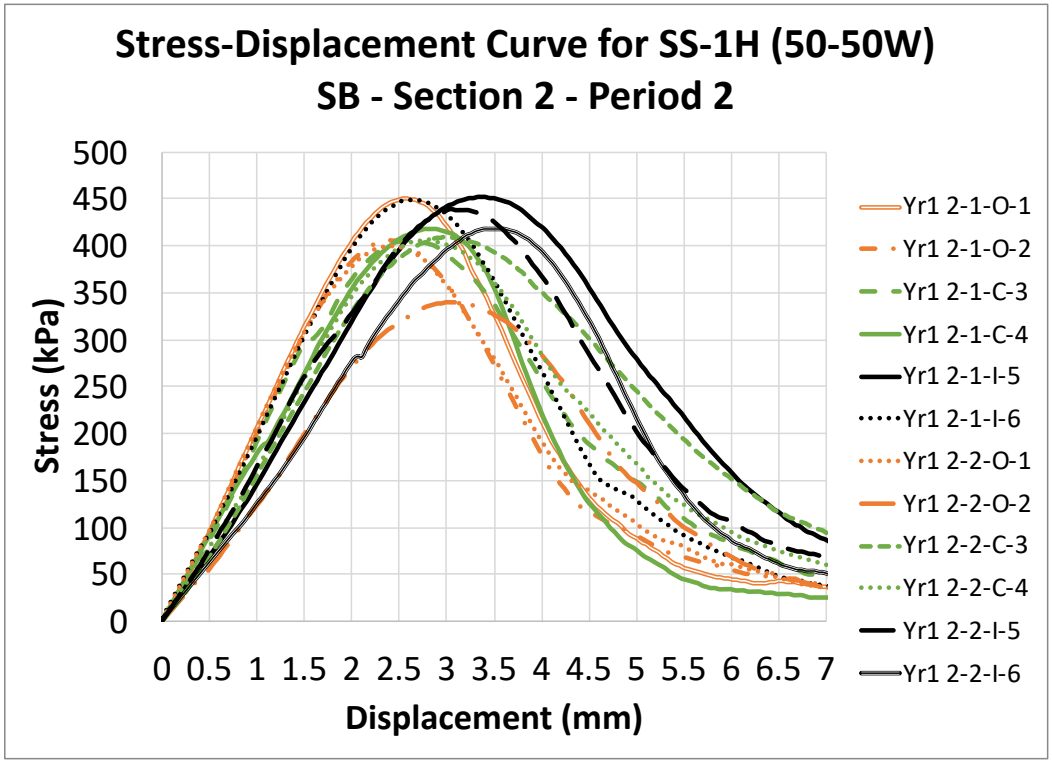


**Figure 5.31 Stress-Displacement Curve for SS-1h (50-50W) SB One Year Cores – Section 2**

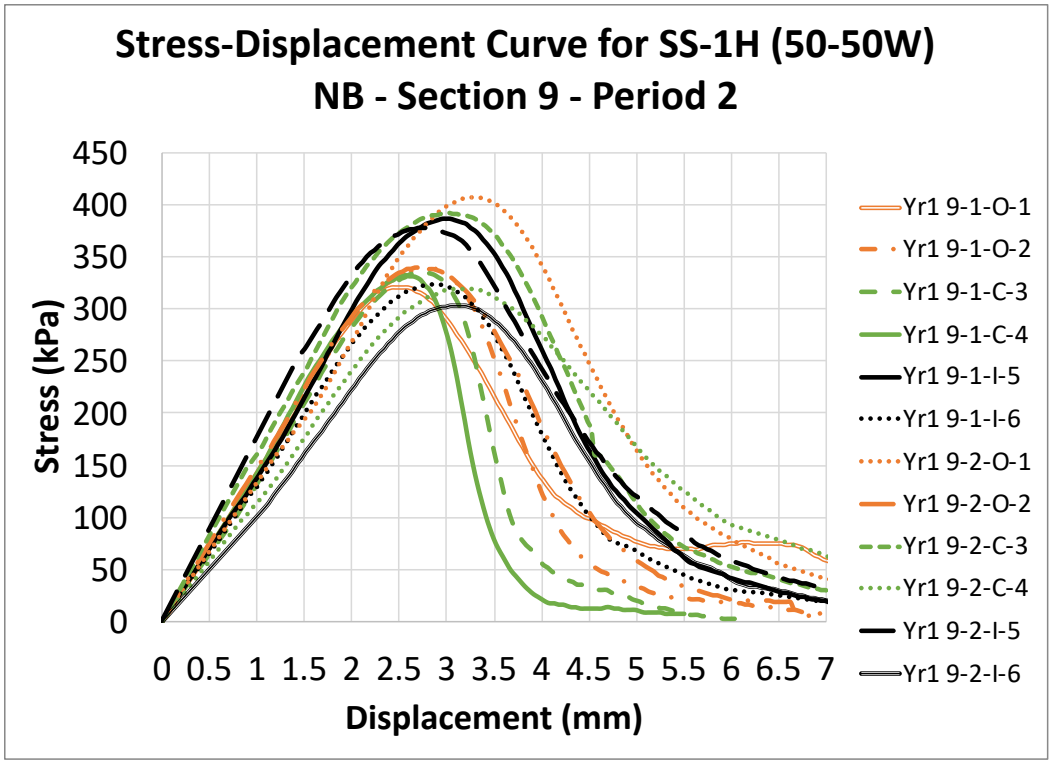


**Figure 5.32 Stress-Displacement Curve for SS-1h (50-50W) NB One Year Cores – Section 9**

Figure 5.33 (Section 4) shows the stress-displacement curves for MS-1 for year one cores. For MS-1 the ISS values ranged from 320.4kPa to 439.8kPa and the displacement at bond failure ranged from 2.39mm to 3.03mm. The highest shear strength is achieved by a sample that was extracted from the inner wheel path and the lowest is achieved in a sample that was extracted from the outer wheel path. The core samples for MS-1 show considerably less variation in k modulus and in displacement at peak stress than the sections of SS-1 and SS-1h.

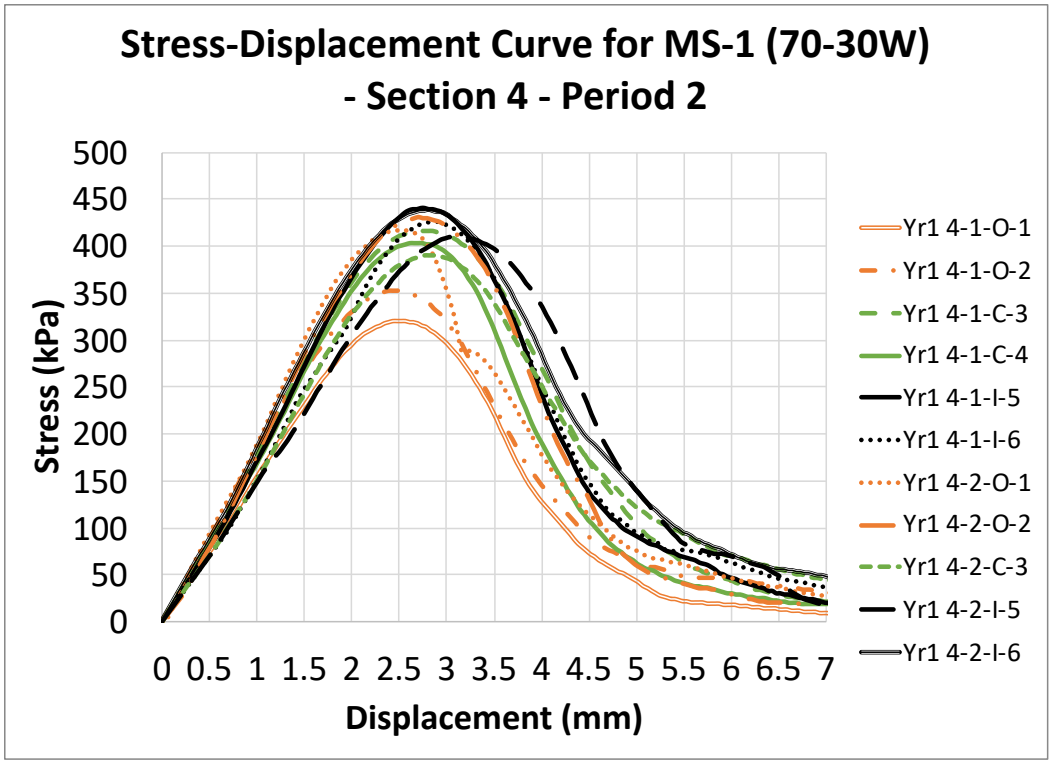


**Figure 5.33 Stress-Displacement Curve for MS-1 (70-30W) One Year Cores – Section 4**

Figure 5.34 (Section 7) shows the stress-displacement curves for CSS-1h for year one cores. For CSS-1h the ISS values ranged from 345.2kPa to 426.2kPa and the displacement at bond failure ranged from 2.39mm to 3.39mm. The highest shear strength is achieved by a sample that was extracted from the inner wheel path and the lowest is achieved in a sample that was extracted from the centre of the lane.

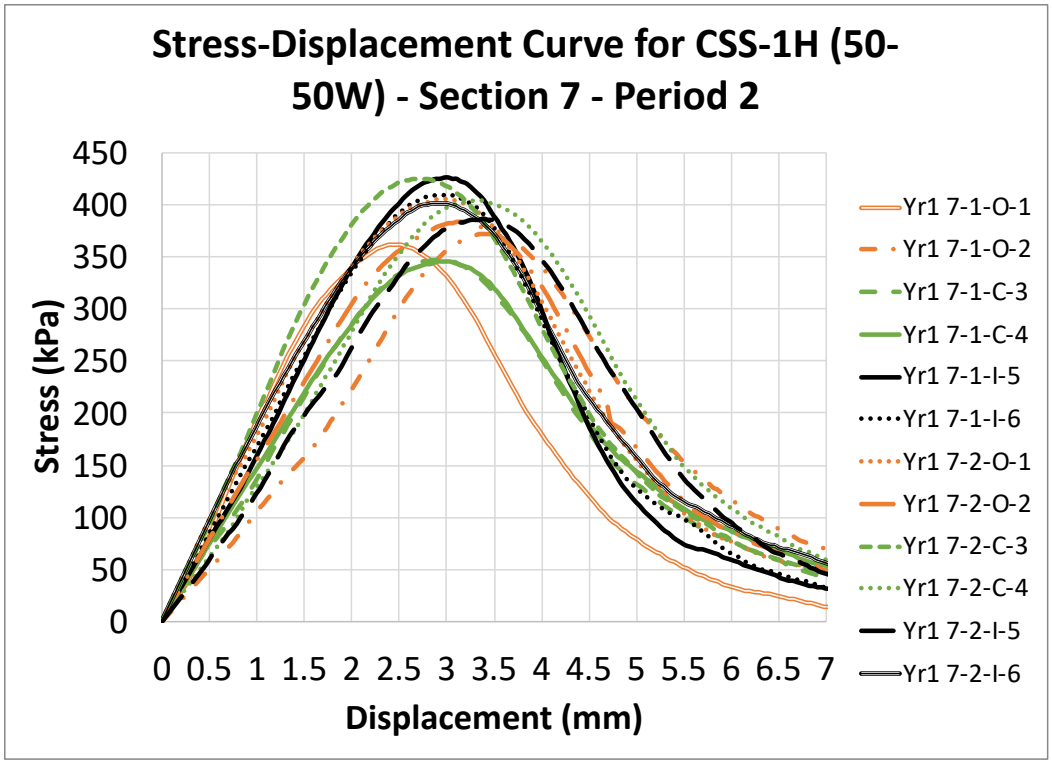


**Figure 5.34 Stress-Displacement Curve for CSS-1h (50-50W) One Year Cores – Section 7**

Figure 5.35 (Section 3) shows the stress-displacement curves for TackMax™ for year one cores. For TackMax™ the ISS values ranged from 292.7kPa to 455.4kPa and the displacement at bond failure ranged from 2.37mm to 3.18mm. The highest shear strength is achieved by a sample that was extracted from the inner wheel path and the lowest is achieved in a sample that was extracted from the centre of the lane.

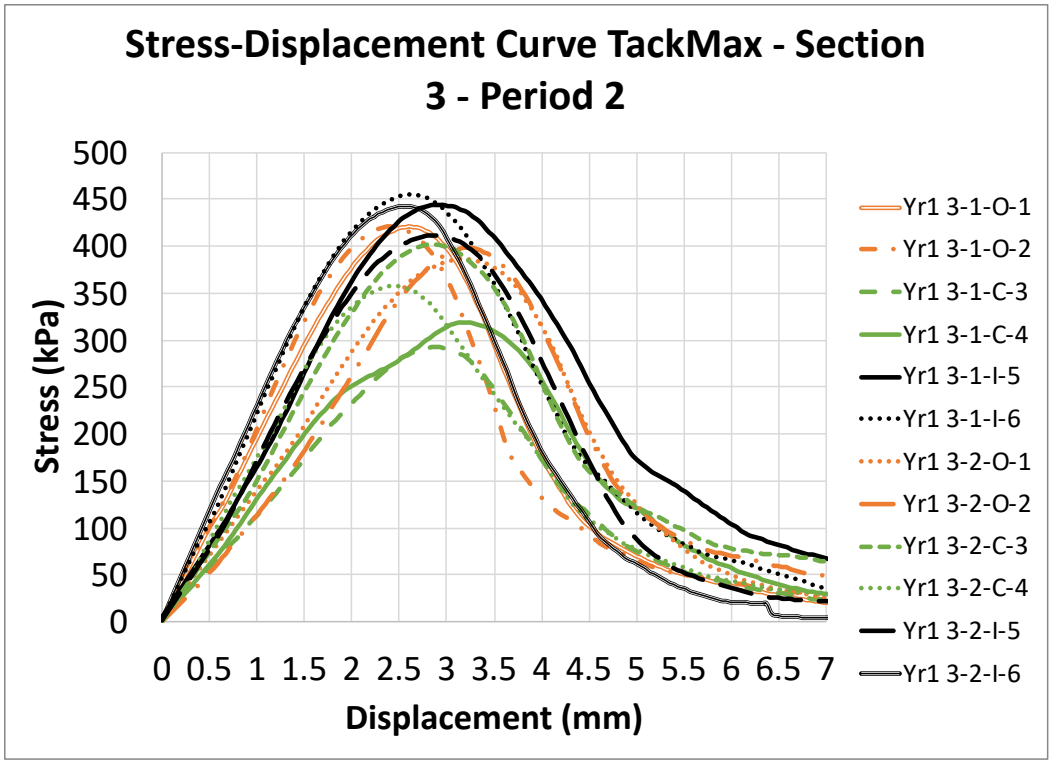


**Figure 5.35 Stress-Displacement Curve for TackMax™ One Year Cores – Section 3**

Figure 5.36 (Section 10) shows the stress-displacement curves for Clean Bond for year one cores. For Clean Bond the ISS values ranged from 356.6kPa to 427.3kPa and the displacement at bond failure ranged from 2.66mm to 3.84mm. The highest shear strength is achieved by a sample that was extracted from the centre of the lane and the lowest is achieved in a sample that was extracted from the outer wheel path.

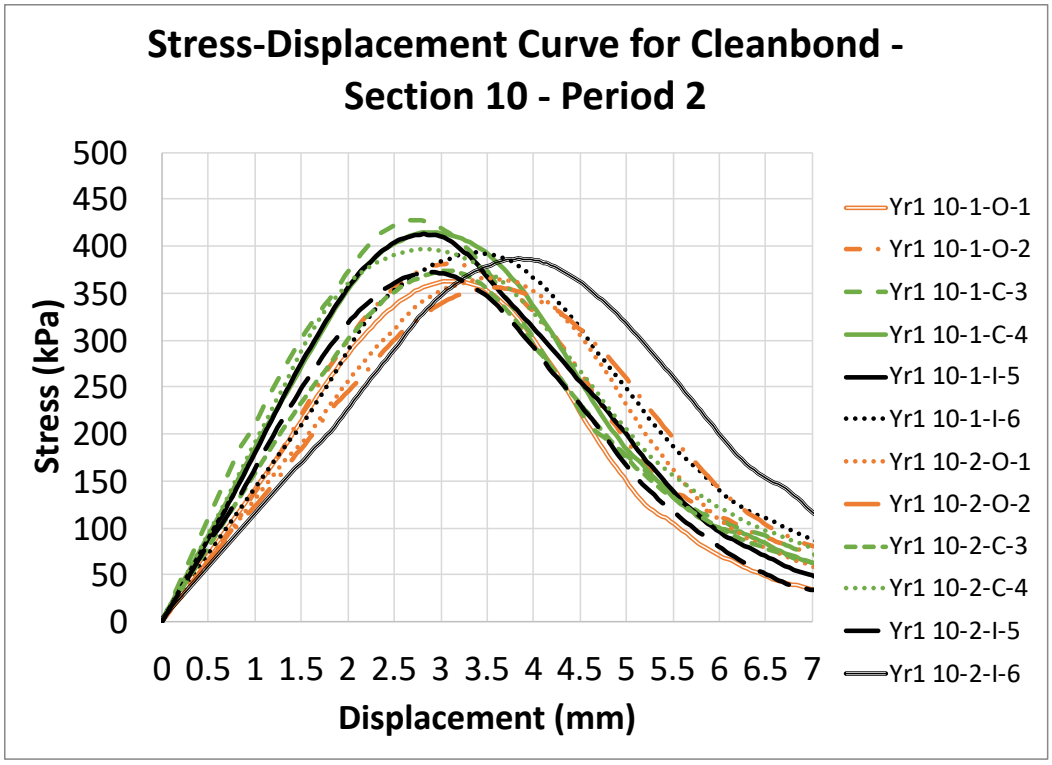


**Figure 5.36 Stress-Displacement Curve for Clean Bond One Year Cores – Section 10**

Figure 5.37 (Section 8) shows the stress-displacement curves for Colasphalt Tack for year one cores. For Colasphalt Tack the ISS values ranged from 261.9kPa to 463.0kPa and the displacement at bond failure ranged from 2.19mm to 3.38mm. The highest shear strength is achieved by a sample that was extracted from the centre of the lane and the lowest is achieved in a sample that was extracted from the outer wheel path.

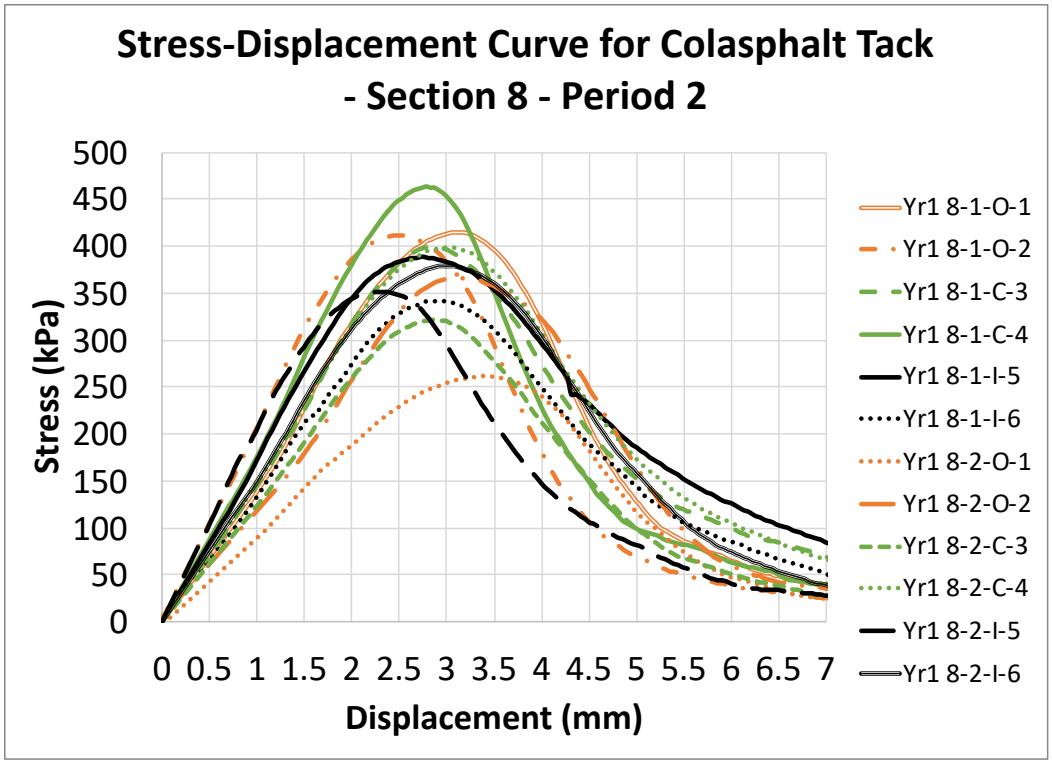


**Figure 5.37 Stress-Displacement Curve for Colasphalt Tack One Year Cores – Section 8**

Table 5.11 shows the ISS values for the year one cores divided by wheel path location, the CV, and % change from the baseline core ISS value. The % change for all groups is positive indicating that the ISS has increased with time and exposure to road traffic loading and environmental conditioning. This increase in strength could be due to continuous curing of tack coat materials. The range of % change values is from 1% to 46% from the original baseline core ISS values.

Six of the ten test sections have the highest ISS from the average of the four samples located in the inner wheel path, two test sections have the highest ISS from the centre of the lane, and two test sections have the highest ISS from the outer wheel paths. Five of the ten test sections have the lowest ISS from the average of the four samples located in the outer wheel path, three test sections have the lowest ISS from the centre of the lane, and two test sections have the lowest ISS from the inner wheel paths. These results indicate that the bond between AC layers may be stronger in the inner wheel path and weaker in the outer wheel path although not all test sections show this pattern.

Using the overall average ISS for each test section, the test sections with the highest ISS values are SS-1 (30-70W), SS-1h SB, and MS-1. The test sections with the lowest ISS values are SS-1h NB, SS-1 SB, and SS-1 NB.

**Table 5.11 Interlayer Shear Strength for Year One Cores**

| | | Overall | | | Inner Wheel Path | | | Outer Wheel Path | | | Centre of Lane | | |
|---|---|---|---|---|---|---|---|---|---|---|---|---|---|
| **Section** | **Material** | **Average ISS (kPa)** | **CV (%)** | **% Change** | **Average ISS (kPa)** | **CV (%)** | **% Change** | **Average ISS (kPa)** | **CV (%)** | **% Change** | **Average ISS (kPa)** | **CV (%)** | **% Change** |
| 1 | SS-1 (50-50W) SB | 375.0 | 8.2 | 40 | 388.7 | 8.5 | 46 | 353.1 | 6.2 | 32 | 383.3 | 8.0 | 44 |
| 6 | SS-1 (50-50W) NB | 384.1 | 8.1 | 18 | 361.8 | 4.9 | 12 | 380.1 | 7.8 | 17 | 410.4 | 6.5 | 27 |
| 5 | SS-1 (30-70W) | 424.0 | 10.8 | 32 | 449.8 | 7.9 | 40 | 408.8 | 11.3 | 27 | 413.3 | 13.2 | 29 |
| 2 | SS-1h (50-50W) SB | 416.2 | 7.4 | 18 | 439.2 | 3.5 | 25 | 399.2 | 11.3 | 13 | 410.4 | 1.3 | 17 |
| 9 | SS-1h (50-50W) NB | 347.7 | 9.7 | 5 | 347.6 | 11.7 | 5 | 350.9 | 10.7 | 6 | 344.7 | 9.4 | 4 |
| 4 | MS-1 (70-30W) | 404.1 | 9.2 | 18 | 428.8 | 3.3 | 25 | 380.2 | 13.8 | 11 | 403.2 | 3.2 | 17 |
| 7 | CSS-1h (50-50W) | 388.8 | 7.1 | 11 | 405.8 | 4.1 | 15 | 380.4 | 4.9 | 8 | 380.1 | 10.5 | 8 |
| 3 | TackMax™ | 395.8 | 12.7 | 27 | 438.1 | 4.4 | 41 | 406.8 | 4.2 | 31 | 342.6 | 13.9 | 10 |
| 10 | Clean Bond | 386.9 | 5.8 | 6 | 391.3 | 4.3 | 7 | 366.4 | 3.0 | 1 | 403.1 | 5.7 | 11 |
| 8 | Colasphalt Tack | 385.0 | 10.2 | 20 | 365.3 | 6.1 | 14 | 396.9 | 6.8 | 24 | 395.7 | 14.7 | 24 |

Table 5.12 shows the average strain at bond failure for each section and for each wheel path location, the CV, and % change from the baseline core strain value. Overall, the year one cores showed an increase in strain meaning the ability of the AC samples to deform has increased with time which is shown by the positive % change in strain value. The range of % change in strain is from -7% to 32% from the original baseline core strain values but the majority of the test sections showed a positive increase. When referring to the overall average for each test section, the three products with the highest strain values are Clean Bond, SS-1 NB, and CSS-1h. The three products with the lowest strain values are SS-1 SB, SS-1 (30-70W), and MS-1. CSS-1h and Colasphalt Tack were the products that showed the least amount of change between the baseline core samples and the year one core samples.

**Table 5.12 Average Strain at Bond Failure for Year One Cores**

| | | Overall | | | Inner Wheel Path | | | Outer Wheel Path | | | Centre of Lane | | |
|---|---|---|---|---|---|---|---|---|---|---|---|---|---|
| **Section** | **Material** | **Strain at Peak (%)** | **CV (%)** | **% Change** | **Strain at Peak (%)** | **CV (%)** | **% Change** | **Strain at Peak (%)** | **CV (%)** | **% Change** | **Strain at Peak (%)** | **CV (%)** | **% Change** |
| 1 | SS-1 (50-50W) SB | 2.7 | 12.8 | 15 | 2.8 | 9.0 | 20 | 2.7 | 16.5 | 15 | 2.6 | 14.6 | 10 |
| 6 | SS-1 (50-50W) NB | 3.1 | 16.4 | 14 | 2.8 | 14.0 | 4 | 3.3 | 21.1 | 23 | 3.1 | 11.2 | 15 |
| 5 | SS-1 (30-70W) | 2.7 | 11.0 | 21 | 2.8 | 9.8 | 25 | 2.7 | 15.3 | 21 | 2.6 | 8.8 | 17 |
| 2 | SS-1h (50-50W) SB | 2.8 | 12.1 | 10 | 3.1 | 12.3 | 21 | 2.6 | 11.3 | 1 | 2.8 | 5.3 | 10 |
| 9 | SS-1h (50-50W) NB | 2.8 | 8.1 | 30 | 2.8 | 5.1 | 32 | 2.7 | 12.1 | 28 | 2.8 | 7.8 | 31 |
| 4 | MS-1 (70-30W) | 2.7 | 6.9 | 22 | 2.8 | 4.6 | 30 | 2.5 | 5.8 | 15 | 2.7 | 2.9 | 22 |
| 7 | CSS-1h (50-50W) | 3.0 | 9.7 | -2 | 3.0 | 7.8 | 1 | 2.9 | 13.6 | -3 | 2.9 | 9.2 | -3 |
| 3 | TackMax™ | 2.8 | 10.0 | 23 | 2.7 | 5.8 | 19 | 2.8 | 14.0 | 25 | 2.8 | 10.6 | 24 |
| 10 | Clean Bond | 3.1 | 11.8 | 17 | 3.2 | 15.1 | 22 | 3.2 | 7.4 | 23 | 2.8 | 5.1 | 6 |
| 8 | Colasphalt Tack | 2.8 | 9.2 | -3 | 2.6 | 12.1 | -7 | 2.8 | 12.2 | -1 | 2.8 | 2.5 | 0 |

Table 5.13 shows the type of failure for all tack coat materials for the one year post construction cores. All SS-1 products were consistent after one year and produced failure type A, failure at the tack coat surface. Products CSS-1h, SS-1h SB, and Clean Bond maintained a strong bond indicated by failure Type B. Products SS-1h NB, MS-1, and TackMax™ had some cores that maintained failure Type B and some cores that experienced failure Type A. These results may indicate that these products become weaker over time compared to other products which maintained a failure type B.

**Table 5.13 Failure Type for Year One Cores**

| Section | Material | Baseline | Year 1 | Year 1 IWP | Year 1 OWP | Year 1 Centre |
|---|---|---|---|---|---|---|
| 1 | SS-1 (50-50W) SB | A | A | A | A | A |
| 6 | SS-1 (50-50W) NB | A | A | A | A | A |
| 5 | SS-1 (30-70W) | A | A | A | A | A |
| 2 | SS-1h (50-50W) SB | B | B | B | B | B |
| 9 | SS-1h (50-50W) NB | B | A/B | A/B | A/B | A/B |
| 4 | MS-1 (70-30W) | B | A/B | A/B | A/B | A/B |
| 7 | CSS-1h (50-50W) | B | B | B | B | B |
| 3 | TackMax™ | B | A/B | A/B | A/B | A/B |
| 10 | Clean Bond | B | B | B | B | B |
| 8 | Colasphalt Tack | B | A/B | A/B | A/B | A/B |

Some materials showed an increase in the interlayer tangential modulus and some products showed a decrease in tangential modulus between year one cores and baseline cores as shown in Table 5.14. The range for the % change values is from -29% to 24%. When referring to the overall average k modulus values, the three products with the highest k modulus values are SS-1 (30-70W), MS-1, and SS-1h SB. The three products with the lowest k modulus values are SS-1h NB, SS-1 NB, and Clean Bond. SS-1 NB, SS-1 (30-70W), SS-1h SB, and CSS-1h were the sections that showed the most amount of change between the baseline k modulus values and year one k modulus values. SS-1h NB, Colasphalt Tack, and SS-1 SB were the sections showing the most change between baseline k modulus values and year one k modulus values.

**Table 5.14 Interlayer Tangential Modulus for Year One Cores**

| | | Overall | | | Inner Wheel Path | | | Outer Wheel Path | | | Centre of Lane | | |
|---|---|---|---|---|---|---|---|---|---|---|---|---|---|
| **Section** | **Material** | **k Modulus ($N/mm^3$)** | **CV (%)** | **% Change** | **k Modulus ($N/mm^3$)** | **CV (%)** | **% Change** | **k Modulus ($N/mm^3$)** | **CV (%)** | **% Change** | **k Modulus ($N/mm^3$)** | **CV (%)** | **% Change** |
| 1 | SS-1 (50-50W) SB | 0.140 | 17.9 | 16 | 0.138 | 16.7 | 15 | 0.133 | 22.5 | 10 | 0.149 | 17.6 | 24 |
| 6 | SS-1 (50-50W) NB | 0.127 | 17.0 | -1 | 0.131 | 19.0 | 1 | 0.119 | 25.6 | -8 | 0.133 | 5.0 | 3 |
| 5 | SS-1 (30-70W) | 0.157 | 11.6 | 1 | 0.162 | 16.9 | 4 | 0.152 | 7.8 | -3 | 0.158 | 10.3 | 1 |
| 2 | SS-1h (50-50W) SB | 0.150 | 13.7 | -1 | 0.144 | 15.2 | -5 | 0.158 | 18.6 | 4 | 0.147 | 5.3 | -3 |
| 9 | SS-1h (50-50W) NB | 0.124 | 9.3 | -28 | 0.122 | 14.5 | -29 | 0.128 | 2.9 | -26 | 0.122 | 9.6 | -29 |
| 4 | MS-1 (70-30W) | 0.151 | 7.1 | -11 | 0.151 | 7.5 | -10 | 0.151 | 9.7 | -11 | 0.150 | 5.3 | -11 |
| 7 | CSS-1h (50-50W) | 0.132 | 11.8 | 1 | 0.134 | 10.1 | 2 | 0.131 | 13.5 | 1 | 0.131 | 15.1 | 0 |
| 3 | TackMax™ | 0.145 | 18.4 | -9 | 0.164 | 8.7 | 3 | 0.147 | 18.2 | -7 | 0.125 | 20.5 | -22 |
| 10 | Clean Bond | 0.127 | 15.4 | -15 | 0.123 | 15.8 | -17 | 0.113 | 9.2 | -24 | 0.144 | 10.3 | -3 |
| 8 | Colasphalt Tack | 0.140 | 13.5 | 17 | 0.139 | 12.1 | 16 | 0.142 | 17.2 | 19 | 0.139 | 16.1 | 16 |

All test sections showed a significant increase in average energy to peak stress between the baseline core samples and the one year core samples as shown in Table 5.15. This increase in energy to peak stress is due to the change in shape of the stress-displacement curve. Due to the increase in strain and increase in ISS values, and decrease in k, the area under the stress strain curve before reaching peak stress is larger. This means that it takes more energy to achieve bond failure. The range for the % change values are from 11% to 88% with all % change values being positive. When referring to the overall average energy values, the four products with the highest average energy to peak stress are Clean Bond, CSS-1h, SS-1 NB, and SS-1h SB. The three products with the lowest average energy to peak stress SS-1h NB, SS-1 SB, and Colasphalt Tack. The section with the lowest % change from the baseline value was CSS-1h with a % change of 16%. The section with the highest % change was SS-1 (30-70W) with a % change of 71%. Eight of the ten test sections have the highest energy to peak stress from the average of the four samples located in the inner wheel path, two test sections have the highest ISS from the centre of the lane, and no test sections have the highest ISS from the outer wheel paths. Four of the ten test sections have the lowest energy to peak stress from the average of the four samples located in the outer wheel path, four test sections have the lowest ISS from the centre of the lane, and two test sections have the lowest ISS from the inner wheel paths. These results indicate that the bond between AC layers may be stronger in the inner wheel path and weaker in the outer wheel path although not all test sections show this pattern.

**Table 5.15 Energy to Peak Stress for Year One Cores**

| | | Overall | | | Inner Wheel Path | | | Outer Wheel Path | | | Centre of Lane | | |
|---|---|---|---|---|---|---|---|---|---|---|---|---|---|
| **Section** | **Material** | **Energy to Peak ($J/m^2$)** | **CV (%)** | **% Change** | **Energy to Peak ($J/m^2$)** | **CV (%)** | **% Change** | **Energy to Peak ($J/m^2$)** | **CV (%)** | **% Change** | **Energy to Peak ($J/m^2$)** | **CV (%)** | **% Change** |
| 1 | SS-1 (50-50W) SB | 1861 | 11.4 | 68 | 1971 | 7.5 | 78 | 1767 | 13.0 | 59 | 1845 | 13.5 | 66 |
| 6 | SS-1 (50-50W) NB | 2127 | 13.5 | 40 | 1884 | 8.5 | 24 | 2190 | 10.2 | 44 | 2306 | 13.6 | 52 |
| 5 | SS-1 (30-70W) | 2091 | 17.3 | 71 | 2289 | 5.4 | 88 | 2042 | 23.4 | 67 | 1942 | 19.9 | 59 |
| 2 | SS-1h (50-50W) SB | 2127 | 13.3 | 32 | 2407 | 10.7 | 49 | 1866 | 7.9 | 15 | 2107 | 4.5 | 30 |
| 9 | SS-1h (50-50W) NB | 1763 | 15.3 | 34 | 1792 | 11.7 | 37 | 1729 | 20.9 | 32 | 1766 | 16.7 | 35 |
| 4 | MS-1 (70-30W) | 1958 | 13.1 | 43 | 2160 | 4.7 | 58 | 1763 | 18.0 | 29 | 1947 | 3.9 | 42 |
| 7 | CSS-1h (50-50W) | 2129 | 11.2 | 16 | 2300 | 3.1 | 25 | 2050 | 14.5 | 12 | 2038 | 11.8 | 11 |
| 3 | TackMax™ | 1988 | 12.8 | 46 | 2200 | 4.1 | 62 | 2041 | 6.9 | 50 | 1724 | 13.5 | 27 |
| 10 | Clean Bond | 2234 | 8.7 | 32 | 2350 | 12.5 | 38 | 2198 | 6.8 | 29 | 2155 | 1.3 | 27 |
| 8 | Colasphalt Tack | 1925 | 12.9 | 21 | 1801 | 14.6 | 13 | 1992 | 10.8 | 25 | 1999 | 13.5 | 26 |

### 5.8 Discussion

A correlation between baseline ISS and the residual application rate was found with an $R^2$ value of 0.56. A 2nd order polynomial curve was fitted to the data set as shown in Figure 5.38. For this particular data set, an increase in residual application rate results in an increase in ISS up to a residual application rate of 0.1L/m$^2$ and then a decrease in ISS results from any further increase in residual application rate. Although the $R^2$ value is not particularly high, the observed trend for ISS change with the increase of residual application rate provides a guideline that can be validated with future testing data.

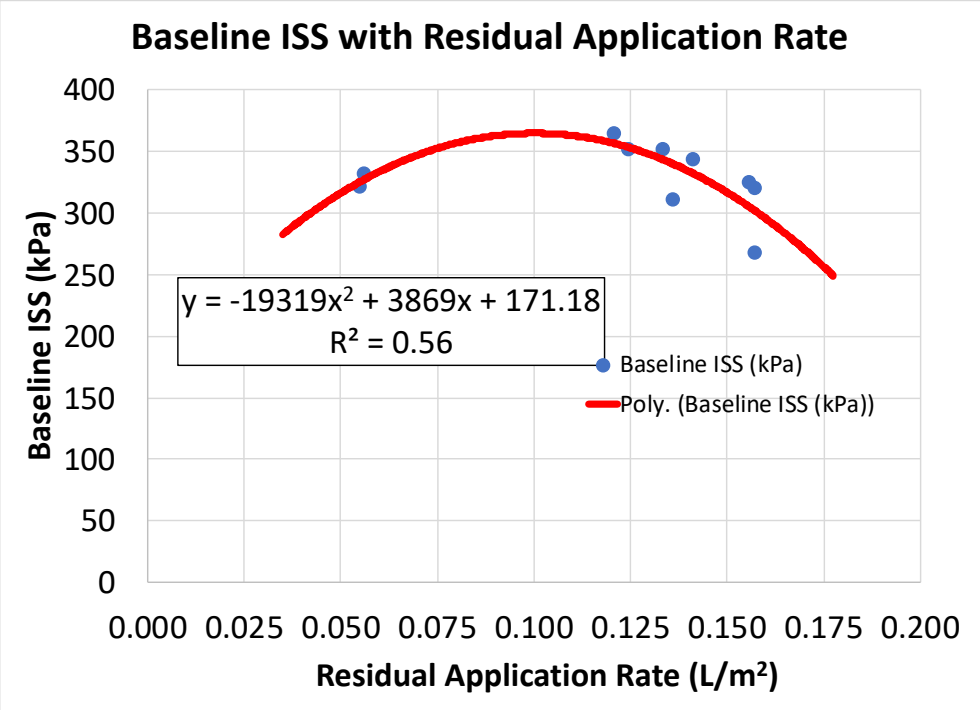


**Figure 5.38 Baseline ISS with Residual Application Rate**

The parameters used in this research to quantify the bond quality created by tack coat materials were ISS, strain, failure type, interlayer tangential modulus, and energy. Each of these parameters is shown as a comparison between baseline cores, core exposed to 15 FT cycles, and cores collected one year post construction.

ISS values from the baseline cores are lower than those of the cores collected at year one. This means that the tack coat is curing over time due to evaporation of water. This trend is short term

and the bond between layers will cease to strengthen once the tack coat has cured completely. This trend is shown in Figure 5.39. There is also an overall increase in ISS of the FT cycled cores compared to the baseline cores though there are some sections that have higher baseline ISS. There is no notable increase or decrease trend between the 3, 9, and 15 FT cores which is why the 15 FT core group is shown in Figure 5.39.

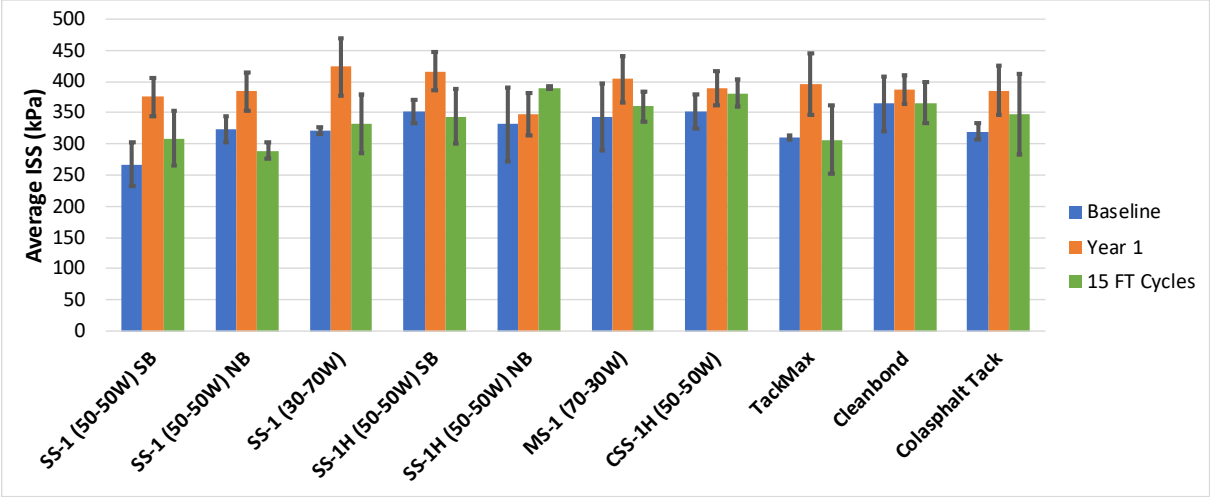


**Figure 5.39 Average Interlayer Shear Strength for Baseline, Year One, and 15 FT Cores**

Strain values from the baseline cores are lower than those of the cores collected at year one and lab conditioned cores as shown in Figure 5.40. This is due to an increase in displacement in the stress-displacement curve because of increase in deformation and a change in viscoelastic behaviour of the material with time. The cores exposed to lab conditioning had a larger increase than the year one cores.

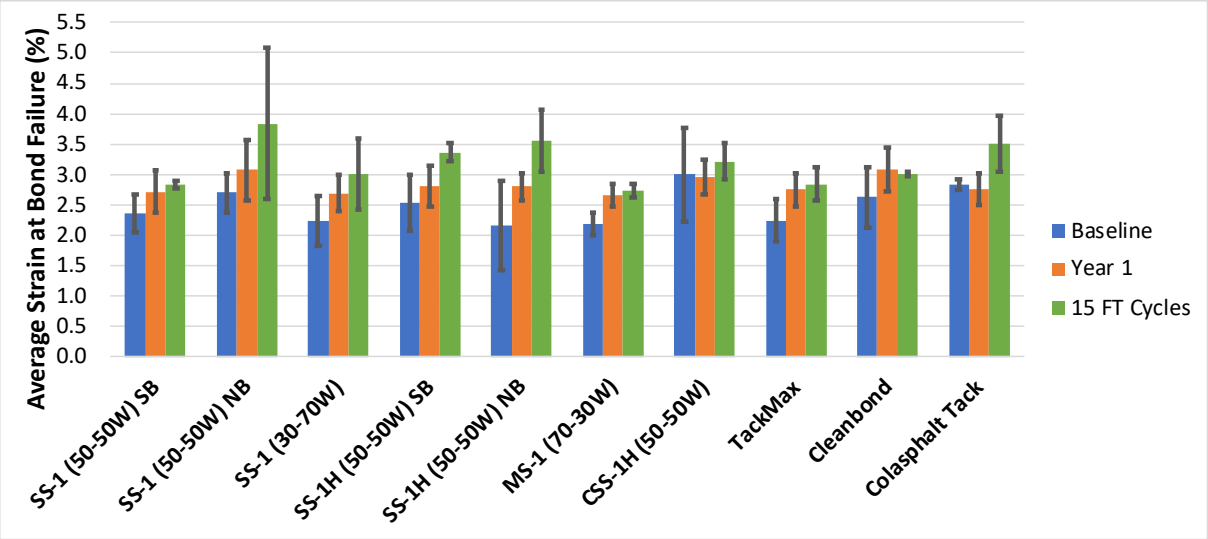


**Figure 5.40 Average Strain at Bond Failure for Baseline, Year One, and 15 FT Cores**

Some of the interlayer tangential modulus values from the baseline cores are higher than those of the cores collected at year one and lab conditioned cores as shown in Figure 5.41. Both the ISS and displacement of core samples increased in the year one and lab conditioned cores over the baseline cores. Since the k modulus is a ratio of the ISS and the displacement, some samples had a lower k modulus in year one or lab conditioned cores than the baseline cores if they experienced more growth in the displacement than in the ISS.

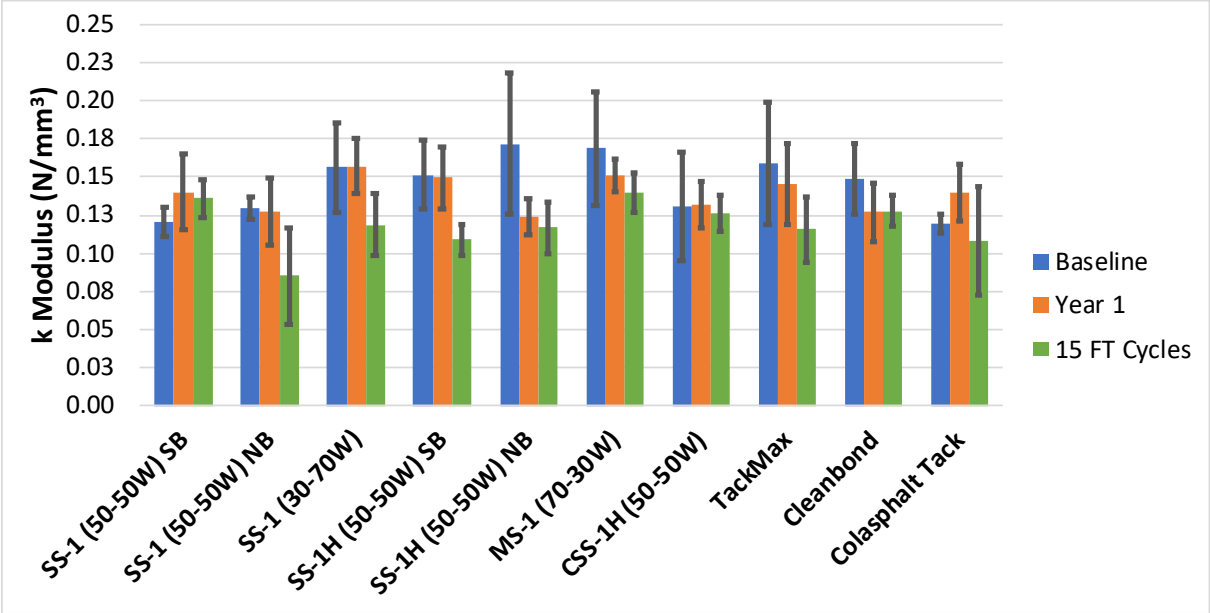


**Figure 5.41 Average Interlayer Tangential Modulus for Baseline, Year One, and 15 FT Cores**

Energy to peak shear stress values from the baseline cores are lower than those of the cores collected at year one and lab conditioned cores as shown in Figure 5.42. Due to an increase in ISS, and an increase in displacement in the stress-displacement curve, more energy is needed to reach bond failure. For most test sections the year one cores required the most energy to attain peak shear stress, followed by the lab conditioned cores, and then the baseline cores.

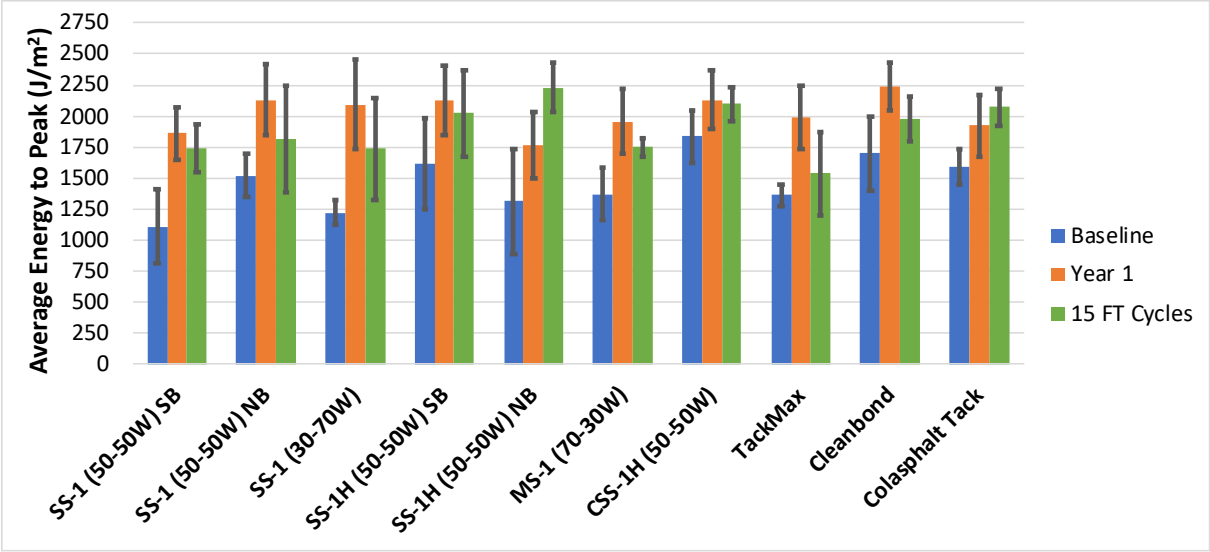


**Figure 5.42 Average Energy to Peak Stress Per Unit Area for Baseline, Year One, and 15 FT Cores**

Additional tables and figures compiling all of the data for each of the parameters including ISS, strain, energy, and tangential modulus can be found in Appendix H.

Table 5.16 to Table 5.18 show the ranking of the tack coat materials based on the parameters of ISS, strain at peak shear stress, the failure type, k modulus, and energy to peak shear stress. The parameters of focus in this discussion will be the ISS, failure type, and energy rank. Since the energy to peak shear stress is the area under the stress-displacement graph, this parameter takes into account the ISS, displacement (and therefore strain), as well as the slope of the curve which is the k modulus.

The materials ranked by parameters for the baseline cores are shown in Table 5.16. CSS-1h had the highest average energy to reach peak shear stress and was ranked third according to ISS. Clean Bond had the highest average ISS value and was ranked second according to the average energy to reach peak shear stress. SS-1SB had the lowest ISS and the lowest average energy to reach peak shear stress among all the tested materials. Although there are differences between the rankings according to the two criteria, there is an agreement between the two criteria in identifying the three products with the highest ISS and the product with the lowest ISS. In addition, Table 5.16 shows that the three products with the highest ISS and average energy (SS-

1h SB, CSS-1h, and Clean Bond) had failure type B; while the product with the lowest ISS and average energy (SS-1 SB) had failure type A.

**Table 5.16 Materials Ranked by Parameters for Baseline Cores**

| Material | Dilution | ISS Rank | Strain Rank | Failure Type | k Modulus Rank | Energy Rank |
|---|---|---|---|---|---|---|
| SS-1 SB | 50-50W | 10 | 6 | A | 9 | 10 |
| SS-1 NB | 50-50W | 6 | 3 | A | 8 | 5 |
| SS-1 | 30-70W | 7 | 8 | A | 4 | 9 |
| SS-1h SB | 50-50W | 2 | 5 | B | 5 | 3 |
| SS-1h NB | 50-50W | 5 | 10 | B | 1 | 8 |
| MS-1 | 70-30W | 4 | 9 | B | 2 | 6 |
| CSS-1h | 50-50W | 3 | 1 | B | 7 | 1 |
| TackMax™ | No dilution | 9 | 7 | B | 3 | 7 |
| Clean Bond | No dilution | 1 | 4 | B | 6 | 2 |
| Colasphalt Tack | No dilution | 8 | 2 | B | 10 | 4 |

The materials ranked by parameters for lab conditioned cores (15 FT Cycles) are shown in Table 5.17. The same three products (although different sections) that were ranked as top three for the baseline cores also have the highest ISS ranking for lab conditioned cores. These products are SS-1h NB, CSS-1h, and Clean Bond. The product with the lowest ISS is SS-1 NB which is also the same product to rank last compared to the baseline cores. SS-1h NB and CSS-1h also ranked 1st and 2nd by the energy rank. The top three products according to ISS and the lowest product all have failure type B.

**Table 5.17 Materials Ranked by Parameters for Lab Conditioned Cores (15 FT Cycles)**

| Material | Dilution | ISS Rank | Strain Rank | Failure Type | k Modulus Rank | Energy Rank |
|---|---|---|---|---|---|---|
| SS-1 SB | 50-50W | 8 | 7 | A | 2 | 8 |
| SS-1 NB | 50-50W | 10 | 1 | B | 10 | 6 |
| SS-1 | 30-70W | 7 | 6 | A | 5 | 9 |
| SS-1h SB | 50-50W | 6 | 4 | B | 8 | 4 |
| SS-1h NB | 50-50W | 1 | 2 | B | 6 | 1 |
| MS-1 | 70-30W | 4 | 8 | B | 1 | 7 |
| CSS-1h | 50-50W | 2 | 5 | B | 4 | 2 |
| TackMax™ | No dilution | 9 | 7 | B | 7 | 10 |
| Clean Bond | No dilution | 3 | 6 | B | 3 | 5 |
| Colasphalt Tack | No dilution | 5 | 3 | B | 9 | 3 |

Note: Strain is ranked from 1 to 8 because there are multiple strain values that are the same. Failure type of A/B indicates that approximately half of the cores had failure type A and half had failure type B.

The materials ranked by parameters for year one cores are shown in Table 5.18. The rankings for this group of cores are much different from the rankings in the baseline cores and the lab conditioned cores. According to ISS the highest ranked products are SS-1 (30-70W), SS-1h SB, and MS-1. SS-1 (30-70W) and SS-1h also have high energy rankings but MS-1 does not. The lowest ranked product according to ISS is SS-1h NB which also has a very low energy ranking. The failure type for the highest ranked products according to ISS is type A, type B, and type A/B respectively. The failure type for the lowest ranked product according to ISS, SS-1h NB is type A/B. These results are not as consistent with the previous results as the strongest product ranked highest in ISS for the year one cores ranked low in the lab conditioned cores and baseline cores. Sections that consistently ranked low in the baseline cores, lab conditioned cores, and year one cores are the SS-1 SB and SS-1 NB. MS-1 consistently ranked 3$^{rd}$ or 4$^{th}$ according to ISS.

**Table 5.18 Materials Ranked by Parameters for Year One Cores (Overall)**

| Material | Dilution | ISS Rank | Strain Rank | Failure Type | k Modulus Rank | Energy Rank |
|---|---|---|---|---|---|---|
| SS-1 SB | 50-50W | 9 | 4 | A | 5 | 8 |
| SS-1 NB | 50-50W | 8 | 1 | A | 7 | 3 |
| SS-1 | 30-70W | 1 | 4 | A | 1 | 4 |
| SS-1h SB | 50-50W | 2 | 3 | B | 3 | 3 |
| SS-1h NB | 50-50W | 10 | 3 | A/B | 8 | 9 |
| MS-1 | 70-30W | 3 | 4 | A/B | 2 | 6 |
| CSS-1h | 50-50W | 5 | 2 | B | 6 | 2 |
| TackMax™ | No dilution | 4 | 3 | A/B | 4 | 5 |
| Clean Bond | No dilution | 6 | 1 | B | 7 | 1 |
| Colasphalt Tack | No dilution | 7 | 3 | A/B | 5 | 7 |

*Note: Strain is ranked from 1 to 4 because there are multiple strain values that are the same. Failure type of A/B indicates that approximately half of the cores had failure type A and half had failure type B.

k Modulus is ranked from 1-8 because there are multiple k modulus values that are the same.

Energy is ranked from 1-9 because there are two energy values that are the same.

# CHAPTER 6: SUMMARY, CONCLUSIONS, AND RECOMMENDATIONS

## 6.1 Summary of Research

The tack coat project began in 2017 on Highway 12 near Blaine Lake Saskatchewan. The purpose of the project was to evaluate the performance of several types of tack coat materials available in Saskatchewan. The basic SS-1 emulsion is typically used on all Saskatchewan Ministry of Highways & Infrastructure projects and expanding the repertoire of products used as tack coats may be beneficial. Products selected for the trial included SS-1, SS-1h, CSS-1h, MS-1, and three proprietary products. The performance of these products was analyzed to see which products offer faster curing times, less tracking and pickup on construction equipment, higher bond strength between pavement layers, and better long-term performance. Improving the bond between pavement layers is beneficial to pavement life and can help reduce the strain placed on the pavement management system and extend the lifespan of the road by reducing the need for corrective maintenance and rehabilitation. This research is significant because it fills a gap in the literature pertaining to tack coat material research. An extensive study into the performance of tack coat materials in cold climate has not been performed and this research will help to fill this void.

To analyze the performance of the tack coat materials a field and laboratory testing program was established. The field study program comprised of analyzing field performance during construction including monitoring curing times and pickup on construction equipment, and post-construction and yearly distress surveys, and core sample collection post-construction and yearly. The laboratory testing program included testing core samples for interlayer shear strength and analyzing other computed parameters such as strain, energy required for the samples to reach peak stress and a displacement of 5mm, and stress/displacement slope to peak stress. Cores were divided into three groups: post-construction cores, environmentally conditioned post-construction cores, and year one cores. A portion of the core samples collected post-construction were environmentally conditioned in a chamber to experience freeze-thaw cycling to mimic the FT cycling experienced in Saskatchewan. These cores were subjected to 3, 9, and 15 FT cycles A comparison of results from three separate core groups is presented.

The research in this thesis includes the analysis of the core samples collected after construction, and the core samples collected one year after construction. This is an ongoing project and further analysis will be completed.

### 6.2 Conclusions

The results of the field study and laboratory testing component are as follows:

- Proprietary non-tracking products perform well in the field in terms of breaking and setting. Their quick setting properties allow for the tack coat to remain intact where it is needed more in the wheel paths and allow for a strong bond to form between layers.
- All other products perform better, in terms of breaking and setting, than the basic SS-1 emulsion.
- Weather conditions including temperature and humidity affect the speed of breaking and setting of tack coat materials. Hot dry weather will result in the fastest breaking and setting.
- The first two distress surveys, shortly after construction and one year post-construction, did not show any distresses due to the poor bond between pavement layers.
- Core samples collected after one year showed higher ISS than baseline cores. Lab conditioned core samples had higher ISS than baseline cores but lower ISS than one year cores. The increase in bond strength after one year and conditioning can be attributed to the continuous curing of tack coat materials.
- SS-1 products with 50-50W dilution consistently ranked low in terms of ISS among the three core groups.
- The lab conditioned cores showed higher strain at bond failure than the baseline cores, which indicates an increase in the ability for samples to deform after conditioning. The same observation was recorded for core samples collected after one year. The increase in displacement to reach peak stress can be attributed to the change in viscoelastic behaviour and interface characteristics of tack coat materials with FT conditioning and exposure to environmental conditions. SS-1 NB and Colasphalt consistently have high strain values among all three core groups.
- Failure type of core samples sheared using the LISST can be a good indicator for quality of bond between AC layers. For the baseline cores, all products except the three sections of SS-1 experienced failure type B (failure within the mix) indicating that SS-1 may be

an inferior product in terms of providing good bond between layers. SS-1 cores collected one year post-construction maintained a failure type A (failure at the tack coat surface), similar to the performance of baseline cores. Products CSS-1h, SS-1h SB, and Clean Bond maintained a strong bond indicated by failure type B. Products SS-1h NB, MS-1, and TackMax$^{TM}$ had some cores that maintained failure type B and some cores that experienced failure type A. These results indicate that these products became weaker over time compared to other products that maintained a failure type B at one year.

- There were no noticeable differences in failure type based on position within the outer wheel path, inner wheel path, or centre of the lane.
- The interlayer tangential modulus (k modulus) of core samples decreased for the year one cores and the lab conditioned cores compared to the baseline cores. This decreases in k modulus can be attributed to the increase in the ability for samples to deform with conditioning. Overall, the lab conditioned cores experienced a larger decrease in k modulus than the year one cores. MS-1 had a consistently high k modulus value for all three core groups.
- The energy required to reach the peak shear stress is a comprehensive parameter that accounts for both the applied stress and the amount of deformation that the sample undergoes before reaching bond failure. For the FT conditioned and one year cores, an increase in the energy required to reach peak shear stress was observed when compared to the baseline cores. SS-1 SB had a consistently low energy rank for all three core groups and CSS-1h had a consistently high energy rank for all three core groups.
- The lab conditioned cores did not show significant degradation in bond behaviour due to FT cycling. The lab conditioned cores were not saturated before FT cycling to avoid failure of the AC mixture. A higher number of FT cycles than the number used in this study may be required to cause degradation in bond strength.
- The ISS and energy values are affected by the placement of the core in the inner wheel path, centre of the lane, or outer wheel path. The cores in the inner wheel path showed higher ISS and energy than the core samples in the outer wheel paths.
- Five parameters including the ISS, strain at bond failure, failure type, interlayer tangential modulus, and energy to bond failure were studied and showed merit in quantifying the quality of bond between two AC layers. Using these parameters allows for a greater understanding of the bond quality than using ISS only.

- Overall, SS-1h, MS-1, CSS-1h, and the three proprietary products showed better performance than SS-1 emulsion according to the test results of the baseline and year one cores.
- An optimum residual application rate of 0.1L/$m^2$ was found to reach the maximum post-construction ISS for this set of data. The correlation value was not strong with an $R^2$ value of 0.56.

### 6.3 Recommendations for Applications

With this research, the Saskatchewan Ministry of Highways & Infrastructure can implement performance based specifications for tack coat materials according to bond strength in terms of ISS value, failure type of the samples tested in shear strength, and energy/displacement at peak stress. With the completion of the study in three years, the change in bond strength between AC layers will be fully characterized and acceptance limits can be established for bond strength of tack coat materials in cold regions.

### 6.4 Recommendations for Future Research

Monitoring of the test sections should continue for at least three more years. Monitoring should include collection of core samples for bond strength testing and field distress surveys. The FT cycling completed in this study did not cause significant change in bond strength. Samples were not saturated before FT cycling to avoid failure within the AC mixture. More research should be completed to investigate the impact of higher number of FT cycling and different methods for sample conditioning. Further testing of non-tracking proprietary emulsions and products besides SS-1 should be considered as these products appear to have better performance based on year 1 results. Testing monitoring the placement of core samples in the wheel paths and centre of the lane should be continued because the placement of the cores may yield different results in future testing.

## REFERENCES

American Association of State Highway and Transportation Officials (AASHTO) T 283-14, "Standard Method of Test for Resistance of Compacted Asphalt Mixtures to Moisture-Induced Damage", Standard Specifications for Transportation Materials and Methods of Sampling and Testing, 2014 Edition, Washington, D.C. (2014).

American Association of State Highway and Transportation Officials (AASHTO) TP 114-15, "Standard Method of Test for Determining the Interlayer Shear Strength (ISS) of Asphalt Pavement Layers", Standard Specifications for Transportation Materials and Methods of Sampling and Testing, 2015 Edition, Washington, D.C. (2015).

Amini, B., Tehrani, S., "Simultaneous Effects of Salted Water and Water Flow on Asphalt Concrete Pavement Deterioration Under Freeze–Thaw Cycles", International Journal of Pavement Engineering, 15:5, 383-391 (2014).

Arnfield, J., "Köppen Climate Classification", <https://www.britannica.com/science/Koppen-climate-classification> (2009).

Asphalt Institute, "Tack Coat Best Practice," Webinar, Federal Highway Administration (FHWA), Office of Asset Management, Pavements and Construction (2014).

Asphalt Institute, "Tack Coat Best Practices Tech Brief", Federal Highway Administration (FHWA), Office of Asset Management, Pavements and Construction (2016).

ASTM International (ASTM) C666/C666M-15, "Standard Test Method for Resistance of Concrete to Rapid Freezing and Thawing", Annual Book of ASTM Standards, Concrete and Aggregates, 04-02, West Conshohocken, Pennsylvania (2015).

ASTM International (ASTM) D5/D5M-13, "Standard Test Method for Penetration of Bituminous Materials", Annual Book of ASTM Standards, Road and Paving Materials; Vehicle-Pavement Systems, 04-03, West Conshohocken, Pennsylvania (2013).

ASTM International (ASTM) D88-07 (Reapproved 2013), “Standard Test Method for Saybolt Viscosity”, Annual Book of ASTM Standards, Roofing and Waterproofing, 04-04, West Conshohocken, Pennsylvania (2013).

ASTM International (ASTM) D113-17, “Standard Test Method for Ductility of Asphalt Materials”, Annual Book of ASTM Standards, Road and Paving Materials; Vehicle-Pavement Systems, 04-03, West Conshohocken, Pennsylvania (2017).

ASTM International (ASTM) D139-16, “Standard Test Method for Float Test for Bituminious Materials”, Annual Book of ASTM Standards, Road and Paving Materials; Vehicle-Pavement Systems, 04-03, West Conshohocken, Pennsylvania (2016).

ASTM International (ASTM) D244(09)-17, “Standard Test Methods and Practices for Emulsified Asphalts”, Annual Book of ASTM Standards, Road and Paving Materials; Vehicle-Pavement Systems, 04-03, West Conshohocken, Pennsylvania (2017).

ASTM International (ASTM) D560/D560M-16, “Standard Test Methods for Freezing and Thawing Compacted Soil-Cement Mixtures”, Annual Book of ASTM Standards, Road and Paving Materials; Vehicle-Pavement Systems, 04-03, West Conshohocken, Pennsylvania (2016).

ASTM International (ASTM) D977-17, “Standard Specification for Emulsified Asphalt”, Annual Book of ASTM Standards, Road and Paving Materials; Vehicle-Pavement Systems, 04-03, West Conshohocken, Pennsylvania (2017).

ASTM International (ASTM) D1645-16, “Standard Test Method for Freeze-Thaw and De-Icing Salt Durability of Solid Concrete Interlocking Paving Units”, Annual Book of ASTM Standards, Road and Paving Materials; Vehicle-Pavement Systems, 04-03, West Conshohocken, Pennsylvania (2016).

ASTM International (ASTM) D2042-15, “Standard Test Method for Solubility of Asphalt Materials in Trichloroethylene”, Annual Book of ASTM Standards, Road and Paving Materials; Vehicle-Pavement Systems, 04-03, West Conshohocken, Pennsylvania (2015).

ASTM International (ASTM) D2170/D2170M-10, “Standard Test Method for Kinematic Viscosity of Asphalts (Bitumens)”, Annual Book of ASTM Standards, Road and Paving Materials; Vehicle-Pavement Systems, 04-03, West Conshohocken, Pennsylvania (2010).

ASTM International (ASTM) D2397/D2397M-17, “Standard Specification for Cationic Emulsified Asphalt”, Annual Book of ASTM Standards, Road and Paving Materials; Vehicle-Pavement Systems, 04-03, West Conshohocken, Pennsylvania (2017).

ASTM International (ASTM) D2995-14, “Standard Practice for Estimating Application Rate and Residual Application Rate of Bituminous Distributors”, Annual Book of ASTM Standards, Road and Paving Materials; Vehicle-Pavement Systems, 04-03, West Conshohocken, Pennsylvania (2014).

ASTM International (ASTM) D4212-16, “Standard Test Method for Viscosity by Dip-Type Viscosity Cups”, Annual Book of ASTM Standards, Paint—Tests for Chemical, Physical, and Optical Properties; Appearance, 06-01, West Conshohocken, Pennsylvania (2016).

ASTM International (ASTM) D4867/D4867M-09, “Standard Test Method for Effect of Moisture on Asphalt Concrete Paving Mixtures”, Annual Book of ASTM Standards, Road and Paving Materials; Vehicle-Pavement Systems, 04-03, West Conshohocken, Pennsylvania (2009).

ASTM International (ASTM) D4957-18, “Standard Test Method for Apparent Viscosity of Asphalt Emulsion Residues and Non- Newtonian Asphalts by Vacuum Capillary Viscometer”, Annual Book of ASTM Standards, Road and Paving Materials; Vehicle-Pavement Systems, 04-03, West Conshohocken, Pennsylvania (2018).

ASTM International (ASTM) D6930-10, “Standard Test Method for Settlement and Storage Stability of Emulsified Asphalts”, Annual Book of ASTM Standards, Road and Paving Materials; Vehicle-Pavement Systems, 04-03, West Conshohocken, Pennsylvania (2010).

ASTM International (ASTM) D6933-13, “Standard Test Method for Oversized Particles in Emulsified Asphalts (Sieve Test)”, Annual Book of ASTM Standards, Road and Paving Materials; Vehicle-Pavement Systems, 04-03, West Conshohocken, Pennsylvania (2013).

ASTM International (ASTM) D6934-08 (Reapproved 2016), “Standard Test Method for Residue by Evaporation of Emulsified Asphalt”, Annual Book of ASTM Standards, Road and Paving Materials; Vehicle-Pavement Systems, 04-03, West Conshohocken, Pennsylvania (2016).

ASTM International (ASTM) D6935-17, “Standard Test Method for Determining Cement Mixing of Emulsified Asphalt”, Annual Book of ASTM Standards, Road and Paving Materials; Vehicle-Pavement Systems, 04-03, West Conshohocken, Pennsylvania (2017).

ASTM International (ASTM) D6936-17, “Standard Test Method for Determining Demulsibility of Emulsified Asphalt”, Annual Book of ASTM Standards, Road and Paving Materials; Vehicle-Pavement Systems, 04-03, West Conshohocken, Pennsylvania (2017).

ASTM International (ASTM) D6937-16, “Standard Test Method for Determining Density of Emulsified Asphalt”, Annual Book of ASTM Standards, Road and Paving Materials; Vehicle-Pavement Systems, 04-03, West Conshohocken, Pennsylvania (2016).

ASTM International (ASTM) D6997-12, “Standard Test Method for Distillation of Emulsified Asphalt”, Annual Book of ASTM Standards, Road and Paving Materials; Vehicle-Pavement Systems, 04-03, West Conshohocken, Pennsylvania (2012).

ASTM International (ASTM) D7175-15, “Standard Test Method for Determining the Rheological Properties of Asphalt Binder Using a Dynamic Shear Rheometer”, Annual Book of ASTM Standards, Road and Paving Materials; Vehicle-Pavement Systems, 04-03, West Conshohocken, Pennsylvania (2015).

ASTM International (ASTM) D7226-13 (Reapproved 2017), “Standard Test Method for Determining the Viscosity of Emulsified Asphalts Using a Rotational Paddle Viscometer”, Annual Book of ASTM Standards, Road and Paving Materials; Vehicle-Pavement Systems, 04-03, West Conshohocken, Pennsylvania (2017).

ASTM International (ASTM) D7402-17, “Standard Practice for Identifying Cationic Emulsified Asphalts”, Annual Book of ASTM Standards, Road and Paving Materials; Vehicle-Pavement Systems, 04-03, West Conshohocken, Pennsylvania (2017).

ASTM International (ASTM) D7404-07 (Reapproved 2016), “Standard Test Method for Determination of Emulsified Asphalt Residue by Moisture Analyzer”, Annual Book of ASTM Standards, Road and Paving Materials; Vehicle-Pavement Systems, 04-03, West Conshohocken, Pennsylvania (2016).

ASTM International (ASTM) D7496-17, “Standard Test Method for Viscosity of Emulsified Asphalt by Saybolt Furol Viscometer”, Annual Book of ASTM Standards, Road and Paving Materials; Vehicle-Pavement Systems, 04-03, West Conshohocken, Pennsylvania (2017).

Attia, M., Abdelrahman, M., “Sensitivity of Untreated Reclaimed Asphalt Pavement to Moisture, Density, and Freeze Thaw”, Journal of Materials in Civil Engineering, 22(12): 1260-1269 (2010).

Badeli, S., Carter, A., Doré, G., “Complex Modulus and Fatigue Analysis of Asphalt Mix After Daily Rapid Freeze-Thaw Cycles”, Journal of Materials in Civil Engineering, 30(4) (2018).

Badeli, S., Carter, A., Doré, G., “Effect of Laboratory Compaction on the Viscoelastic Characteristics of an Asphalt Mix Before and After Rapid Freeze-Thaw Cycles”, Cold Regions Science and Technology, 146: 98-109 (2018).

Badeli, S., Carter, A., Doré, G., Saliani, S., “Evaluation of the Durability and the Performance of an Asphalt Mix Involving Aramid Pulp Fiber (APF): Complex Modulus Before and After Freeze-Thaw Cycles, Fatigue, and TSRST Tests, Construction and Building Materials, 174: 60–71 (2018).

Bae, A., Mohammad, L., Elseifi, M., Button, J. Patel, N. “Effects of Temperature on Interface Shear Strength of Emulsified Tack Coats and Its Relationship to Rheological Properties,” Transportation Research Record: Journal of the Transportation Research Board, 2180: 102-109 (2010).

Barlas, G., “Material Characteristics of Hot Mix Asphalt and Binder Using Freeze-Thaw Conditioning”, M.S. Thesis, Department of Civil Engineering, University of New Mexico, Albuquerque, NM, (2013).

Colasphalt, “Emulsion Product Data Sheet Typical Analysis and Specifications – Colasphalt Tack”, Acheson, Alberta (June 2017).

Colasphalt, “Pavement Bonding – Colasphalt Fast Tack.” Acheson, Alberta (2018).

Das, R., Mohammad, L.N., Elsei, M., “Effects of Tack Coat Application on Interface Bond Strength and Short-Term Pavement Performance”, Transportation Research Record: Journal of the Transportation Research Board, 2633: 1–8 (2017).

Davidson, J. Keith, McAsphalt Industries Limited, “Introduction to Asphalt Emulsions”, Public Works Canada Seminar, Charlottetown, Prince Edward Island (November 1995).

Destrée, A., De Visscher, J., “Impact of Tack Coat Application Conditions on the Interlayer Bond Strength”, European Journal of Environmental and Civil Engineering, 21:sup1, 3-13 (2017).

Doré, G., Zubeck, H., Cold Regions Pavement Engineering, ASCE Press, Reston, Va., New York, N.Y (2009).

Federal Highway Administration, “Tack Coat Best Practices”, Office of Asset Management, Pavements, and Construction, FHWA-HIF-16-017 (2016).

Feng, D., Yi, J., Wang, L., Wang, D., “Impact of Gradation Types on Freeze-Thaw Performance of Asphalt Mixtures in Seasonal Frozen Region”, Proc., 9th Int. Conference of Chinese Transportation Professionals, ASCE, Reston, VA, 1–7 (2009).

Feng, D., Yi, J., Wang, D., Chen, L., “Impact of Salt and Freeze–Thaw Cycles on Performance of Asphalt Mixtures in Coastal Frozen Region of China”, Cold Regions Science and Technology 62, 34–41 (2010).

Gilmore, D., Darland, J., Girdler, L., Wilson, L., Scherocman, J., “Changes in Asphalt Concrete Durability Resulting from Exposure to Multiple Cycles of Freezing and Thawing", Evaluation and Prevention of Water Damage of Asphalt Pavement Materials, ASTM STP 899, B.E. Ruth, Ed., American Society for Testing and Materials, Philadelphia, pp. 73-88 (1985).

Goh, S. W., You, Z., “Evaluation of Hot-Mix Asphalt Distress Under Rapid Freeze-Thaw Cycles Using Image Processing Technique.” CICTP 2012: Multimodal Transportation Systems—Convenient, Safe, Cost-Effective, Efficient, ASCE, Reston, VA, 3305–3315 (2012).

Gubler, R., Partl, M., Canestrari, F., Grilli, A., “Influence of Water and Temperature on Mechanical Properties of Selected Asphalt Pavements, Materials and Structures, 38 (5): 523–532 (2005).

Hajj, E., Morian, N., El Tannoury, G., Manoharan, S., Sebaaly, P., “Impact of Lime Application Method on Ravelling and Moisture Sensitivity in HMA Mixtures”, International Journal of Pavement Engineering, 12:02, 149-160 (2011).

Hakimzadeh, S., Buttlar, W.G., Santarromana, R., “Shear- and Tension-Type Tests to Evaluate Bonding of Hot-Mix Asphalt Layers with Different Tack Coat Application Rates”, Transportation Research Record: Journal of the Transportation Research Board, 2295: 54-62 (2012).

Hamzah, M., Kakar, M., Quadri, S., Valentin, J., “Quantification of Moisture Sensitivity of Warm Mix Asphalt Using Image Analysis Technique”, Journal of Cleaner Production, 68: 200-208 (2014).

Hamzah, M., Yee, T., Golchin, B. Voskuilen, J., “Use of Imaging Technique and Direct Tensile Test to Evaluate Moisture Damage Properties of Warm Mix Asphalt Using Response Surface Method”, Construction and Building Materials, 132: 323–334 (2017).

Hassn, A., Aboufoul, M., Wu, Y., Dawson, A., Garcia, A., “Effect of Air Voids Content on Thermal Properties of Asphalt Mixtures”, Construction and Building Materials, 115: 327–335 (2016).

Huining, X., Fengche, C., Xingao, Y., Yiqiu, T., “Micro-Scale Moisture Distribution and Hydrologically Active Pores in Partially Saturated Asphalt Mixtures by X-ray Computed Tomography”, Construction and Building Materials, 160: 653–667 (2018).

Islam, M., Tarefder, R., “Effects of Large Freeze-Thaw Cycles on Stiffness and Tensile Strength of Asphalt Concrete”, Journal of Cold Regions Engineering, 30(1) (2016).

James, A., “Overview of Asphalt Emulsion”, Asphalt Emulsion Technology, Transportation Research Circular, Number E-C102, Washington, DC (August 2006).

Kutay, M., Aydilek A., “Dynamic Effects on Moisture Transport in Asphalt Concrete”, Journal of Transportation Engineering, 133: 406–414 (2007).

Lachance-Tremblay, E., Perraton, D., Vaillancourt, M., Di Benedetto, H., “Effect of Hydrated Lime on Linear Viscoelastic Properties of Asphalt Mixtures with Glass Aggregates Subjected to Freeze-Thaw Cycles”, Construction and Building Materials, 184: 58–67 (2018).

Lachance-Tremblay, E., Perraton, D., Vaillancourt, M., Di Benedetto, H., “Degradation of Asphalt Mixtures with Glass Aggregates Subjected to Freeze-Thaw Cycles”, Cold Regions Science and Technology, 141: 8-15 (2017).

Lamothe, S., Perraton D., & Di Benedetto, H., “Contraction and Expansion of Partially Saturated Hot Mix Asphalt Samples Exposed to Freeze–Thaw Cycles, Road Materials and Pavement Design, 16:2, 277-299 (2015).

LTPP (Long-Term Pavement Performance), “Virtual Weather Station Temperature Annual - CLM_VWS_TEMP_ANNUAL”, Station 90-0901, Accessed January 2019.

Ma, B., Si, W., Zhu, D., Wang, H., “Applying Method of Moments to Model the Reliability of Deteriorating Performance to Asphalt Pavement Under Freeze-Thaw Cycles in Cold Regions”, Journal of Materials in Civil Engineering, 25(1) (2015).

Mahmoud, A., Coleri, E., Batti, J., Covey, D., “Development of a Field Torque Test to Evaluate In-Situ Tack Coat Performance”, Construction and Building Materials, 135: 377-385 (2017).

Mauduit, C., Hammoum, F., Piau, J., Maudui, V., Ludwig, S., Hamon, D., “Quantifying Expansion Effects Induced by Freeze-Thaw Cycles in Partially Water Saturated Bituminous Mix”, Road Materials and Pavement Design, 11:sup1, 443-457 (2010).

McAsphalt Industries Limited, “Product Data Sheet – Clean Bond Coat.” Toronto, ON (September 2017).

McCann, M., Sebaaly, P., "Evaluation of Moisture Sensitivity and Performance of Lime in Hot-Mix Asphalt: Resilient Modulus, Tensile Strength, and Simple Performance Tests", Transportation Research Record: Journal of the Transportation Research Board, 1832: 9-16 (2003).

Mohammad, L.N., Bae, A., Elseifi, M., Button, J., Patel, N., “Effects of Pavement Surface Type and Sample Preparation Method on Tack Coat Interface Shear Strength”, Transportation Research Record: Journal of the Transportation Research Board, 2180: 93-101 (2010).

Mohammad, L.N., Bae, A., Elseifi, M.A., Button, J., Scherocman, J.A., "Evaluation of Bond Strength of Tack Coat Materials in Field Development of Pull-Off Test Device and Methodology", Transportation Research Record: Journal of the Transportation Research Board, 2126: 1-11 (2009).

Mohammad, L. N., Elseifi, M. A., Bae, A., Patel, N., Button, J., Scheroconan, J. A., "Optimization of Tack Coat for HMA Placement", National Cooperative Highway Research Program (NCHRP) Report 712, Transportation Research Board, National Research Council, National Academies, Washington, D.C. (2012).

Mohammad, L.N., Hassan, M., and Patel, N., "Effects of Shear Bond Characteristics of Tack Coats on Pavement Performance at the Interface", Transportation Research Record: Journal of the Transportation Research Board, 2209: 1–8 (2011).

Mohammad, L.N., Raqib, M.A., Huang, B.H., "Influence of Asphalt Tack Coat Materials on Interface Shear Strength", Transportation Research Record: Journal of the Transportation Research Board, 1789: 56-65 (2002).

Natural Resources Canada, Reference Maps, Political Map of Saskatchewan (2001).

Obaidat, M., Abo-Qudais, S., Obaidat, A., "Evaluation of Stripping in Bituminous Mixtures Using Conventional and Image Processing Techniques", Journal of Testing and Evaluation, 33(6) (2005).

O'Connor, D., "Properties and Uses for High Float Emulsions", State Department of Highways and Public Transportation, Materials and Tests Division, Paris, Texas (January 1982).

Özgan, E.,Serin, S., "Investigation of Certain Engineering Characteristics of Asphalt Concrete Exposed to Freeze–Thaw Cycles", Cold Regions Science and Technology, 85: 131–136 (2013).

Pavement Interactive. “Dynamic Shear Rheometer”, <https://www.pavementinteractive.org/reference-desk/testing/binder-tests/dynamic-shear-rheometer/> (2019).

Porras, J., Hajj, E., Sebaaly, P., Kass, S., Liske, T., “Performance Evaluation of Field-Produced Warm-Mix Asphalt Mixtures in Manitoba, Canada”, Transportation Research Record: Journal of the Transportation Research Board, 2294: 64–73 (2012).

Pounder Emulsions, A Division of Husky Oil Operations Limited. “Specifications and Typical Analyses – CSS-1h”, Saskatoon, Saskatchewan (March 2018).

Pounder Emulsions, A Division of Husky Oil Operations Limited. “Specifications and Typical Analyses – MS-1”, Saskatoon, Saskatchewan (March 2018).

Pounder Emulsions, A Division of Husky Oil Operations Limited. “Specifications and Typical Analyses - SS-1”, Saskatoon, Saskatchewan (March 2018).

Pounder Emulsions, A Division of Husky Oil Operations Limited. “Specifications and Typical Analyses - SS-1h”, Saskatoon, Saskatchewan (March 2018).

Pounder Emulsions, A Division of Husky Oil Operations Limited. “Specifications and Typical Analyses – TackMax™”, Saskatoon, Saskatchewan (March 2018).

Qiao, Y., Flintsch, G., Dawson, A., Parry, T., “Examining Effects of Climatic Factors on Flexible Pavement Performance and Service Life, Transportation Research Record: Journal of the Transportation Research Board, 2349: 100–107 (2013).

Raab, C., Grenfell, J., El Halim A.O.A, Partl, M.N., “The Influence of Age on Interlayer Shear Properties”, International Journal of Pavement Engineering, 16:6, 559-569 (2015).

Rahman, A., Ai, C., Xin, C., Gao, X., Lu, Y., "State-of-the-Art Review of Interface Bond Testing Devices for Pavement Layers: Toward the Standardization Procedure", *Journal of Adhesion Science and Technology*, 31:2, 109-126 (2017).

Romanoschi, S.A., "Characterization of Pavement Layer Interfaces", LSU Historical Dissertations and Theses, 7008 (1999).

Salinas, A., Al-Qadi, I.L., Hasiba, K.I., Ozer, H., Leng, Z., Parish, D.C. Interface Layer Tack Coat Optimization. Transportation Research Record: Journal of the Transportation Research Board, 2372: 53-60 (2013).

Saskatchewan Ministry of Highways & Infrastructure, "Annual Report for 2015-16", Saskatchewan (2016).

Saskatchewan Ministry of Highways & Infrastructure, "Pavement Distress Legend", Saskatchewan (1995).

Saskatchewan Ministry of Highways & Infrastructure, "Surface Defects Mapping Form", Saskatchewan (2017).

Saskatchewan Ministry of Highways & Infrastructure, "Surfacing Design Report C.S. 12-02 km 13.50 – 38.21, Saskatchewan (June 2017).

Si, W., Ma, B., Li, N., Ren, J. P., and Wang, H. N., "Reliability-Based Assessment of Deteriorating Performance to Asphalt Pavement Under Freeze-Thaw Cycles in Cold Regions." Construction and Building Materials, 68, 572–579 (2014).

Statistics Canada, "Census Profile, 2016 Census, Saskatchewan [Province] and Canada [County]", <https://www12.statcan.gc.ca/census-recensement/2016/dp-pd/prof/details/Page.cfm?Lang=E&Geo1=PR&Code1=47&Geo2=&Code2=&Data=Count&SearchText=Saskatchewan&SearchType=Begins&SearchPR=01&B1=All&GeoLevel=PR&GeoCode=47> (2016).

Stasiuk, L., Soliman, H., Anthony, A., Dechkoff, C., Penner, J., “Evaluating the Performance of Tack Coat Materials in Saskatchewan Climate”, Transportation Association of Canada Conference Proceedings, Saskatoon, SK (2018).

Damage and corrosion of conductive asphalt concrete subjected to freeze–thaw cycles and salt Tang, N., Sun, C., Huang, S., Wu, S., “Damage and Corrosion of Conductive Asphalt Concrete Subjected to Freeze–Thaw Cycles and Salt”, Materials Research Innovations, 17:sup1, 240-245 (2013).

Tarefder, R., Islam, Mh. R., “Measuring Fatigue Damages from an Instrumented Pavement Section due to Day-Night and Yearly Temperature Rise and Fall in Desert Land of the West”, Climatic Effects on Pavement and Geotechnical Infrastructure, 78-88 (2013).

Tarefder, R., Faisal, H., Barlas, G., “Freeze-Thaw Effects on Fatigue Life of Hot Mix Asphalt and Creep Stiffness of Asphalt Binder”, Cold Regions Science and Technology, 153:197-204 (2018).

Teguedi, M., Toussaint, E., Blaysat, B., Moreira, S., Liandrat, S., Grédiac, M., “Towards the Local Expansion and Contraction Measurement of Asphalt Exposed to Freeze-Thaw Cycles, Construction and Building Materials, 154: 438–450 (2017).

Yi, Y., Shen, S., Muhunthan, B., Feng, D., “Viscoelastic–Plastic Damage Model for Porous Asphalt Mixtures: Application to Uniaxial Compression and Freeze–Thaw Damage, Mechanics of Materials, 70: 67–75 (2014).

Young Seo, A., Sakhaeifar, M.S., Wilson, B.T., “Evaluating Tack Properties of Trackless Tack Coats Through Dynamic Shear Rheometer”, Transportation Research Record: Journal of the Transportation Research Board, 2632: 119-129 (2017).

WSP, “Patch Test Form” (2017).

Xu, H., Guo, W., Tan, Y., “Permeability of Asphalt Mixtures Exposed to Freeze–Thaw Cycles”, Cold Regions Science and Technology, 123, 99-106 (2016).

Xu, H., Guo, W., Tan, Y., “Internal Structure Evolution of Asphalt Mixtures During Freeze–Thaw Cycles”, Materials and Design, 86: 436-446 (2015).

## CONTRIBUTIONS

1) Stasiuk, L., Soliman, H., Anthony, A., Dechkoff, C., Penner, J., “Evaluating the Performance of Tack Coat Materials in Saskatchewan Climate”, Transportation Association of Canada Conference Proceedings, Saskatoon, SK (2018).

2) Anthony, A., Dechkoff, C., Stasiuk, L., Soliman, H., Prosko, N. “Characterizing Bond Strength Behaviour of Tack Coat Materials in Saskatchewan Climate”, Canadian Technical Asphalt Association Conference Proceedings, Regina, SK (2018).

3) Stasiuk, L., Soliman, H., Anthony, A. “Effect of Emulsion Type on Bond Behavior of Asphalt Concrete Layers in Cold Regions”, Transportation Research Record: Journal of the Transportation Research Board, 2673: 368-378 (2019).

# APPENDIX A: Construction Parameter Plots

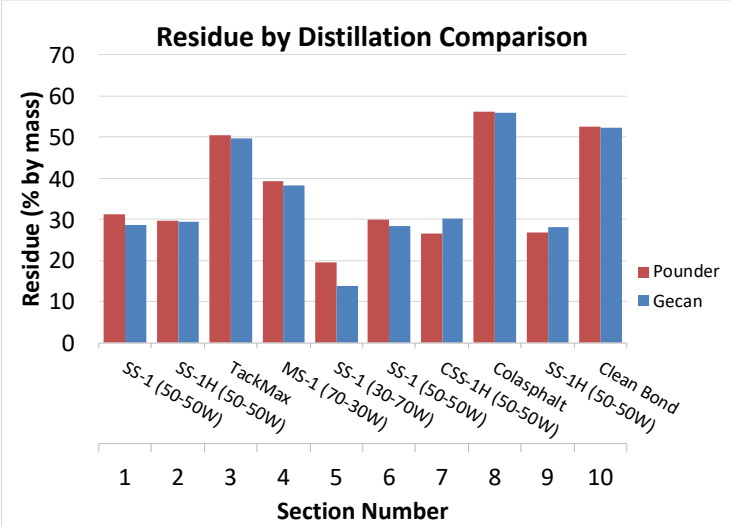


**Figure A.1 Post Trial Residue by Distillation Comparison**

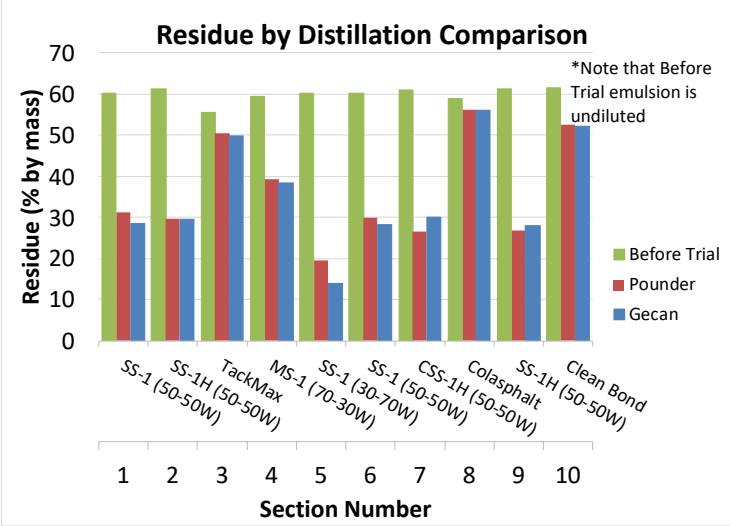


**Figure A.2 Residue by Distillation Comparison including Before Trial Results**

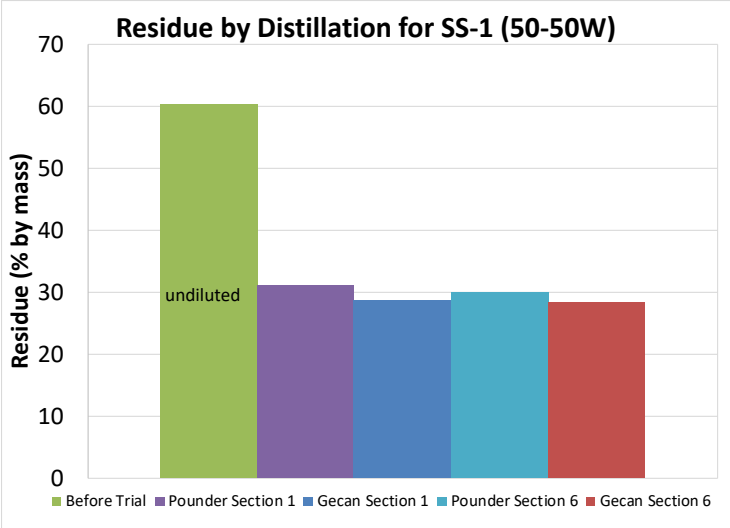


**Figure A.3 Residue by Distillation Comparison for SS-1**

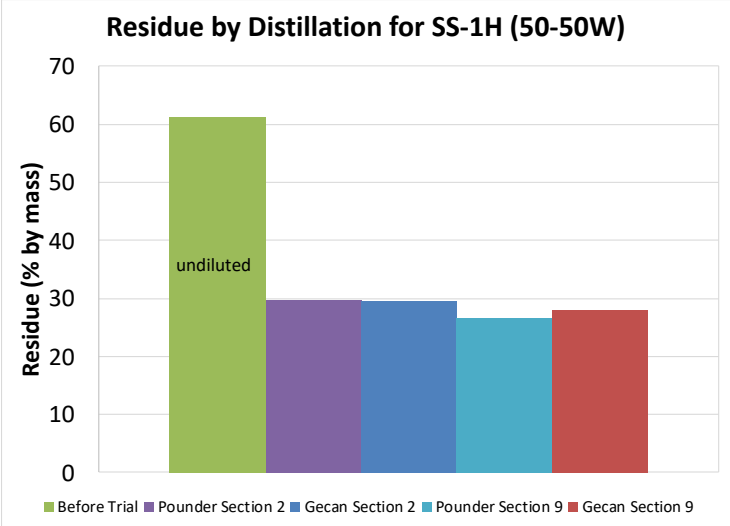


**Figure A.4 Residue by Distillation Comparison for SS-1h**

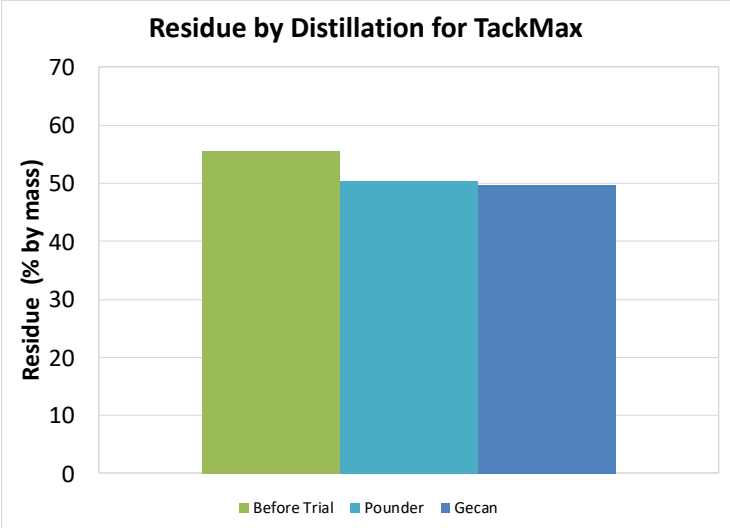


**Figure A.5 Residue by Distillation Comparison for TackMax™**

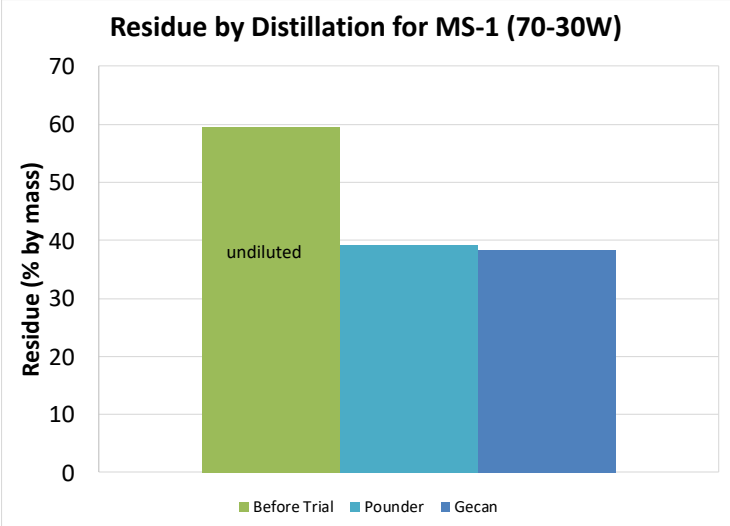


**Figure A.6 Residue by Distillation Comparison for MS-1**

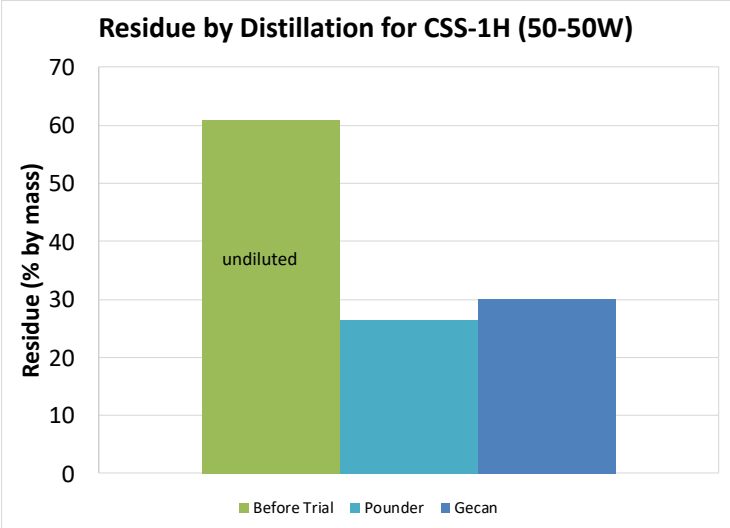


**Figure A.7 Residue by Distillation Comparison for CSS-1h**

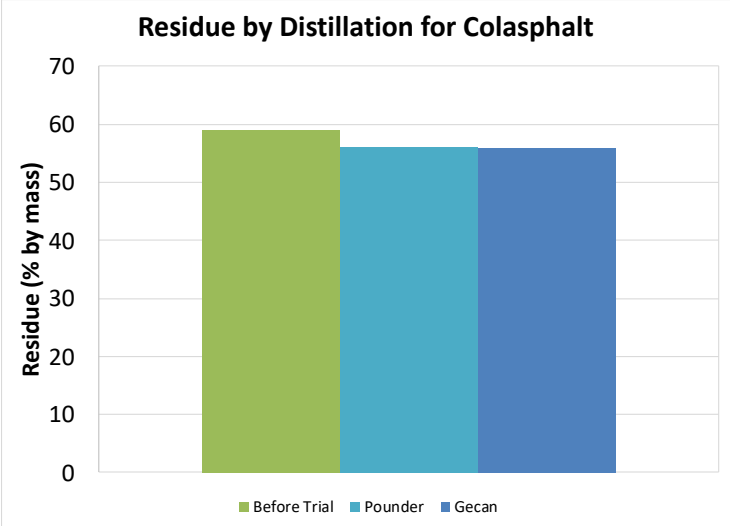


**Figure A.8 Residue by Distillation Comparison for Colasphalt Tack**

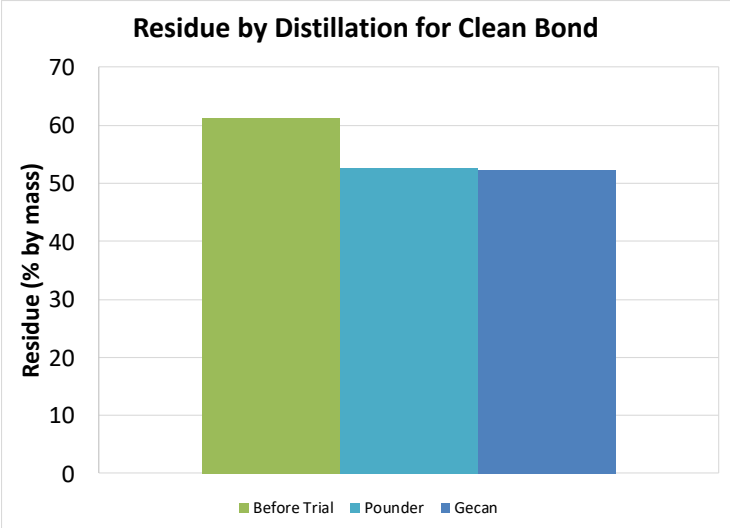


**Figure A.9 Residue by Distillation Comparison for Clean Bond**

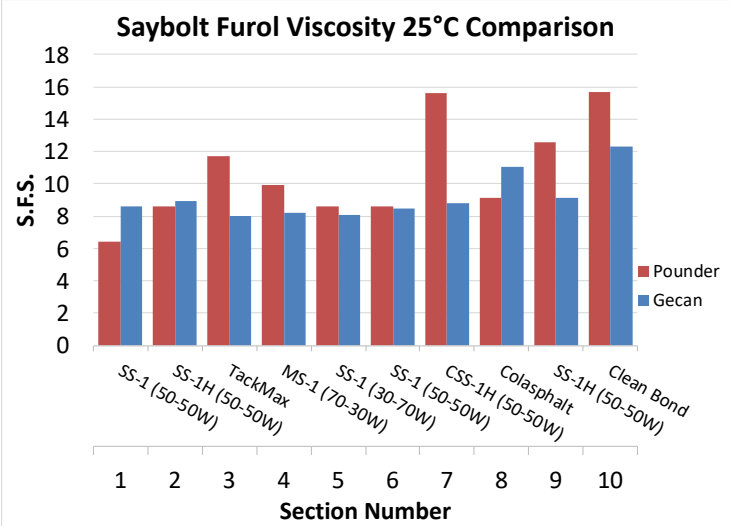


**Figure A.10 Saybolt Furol Viscosity Comparison**

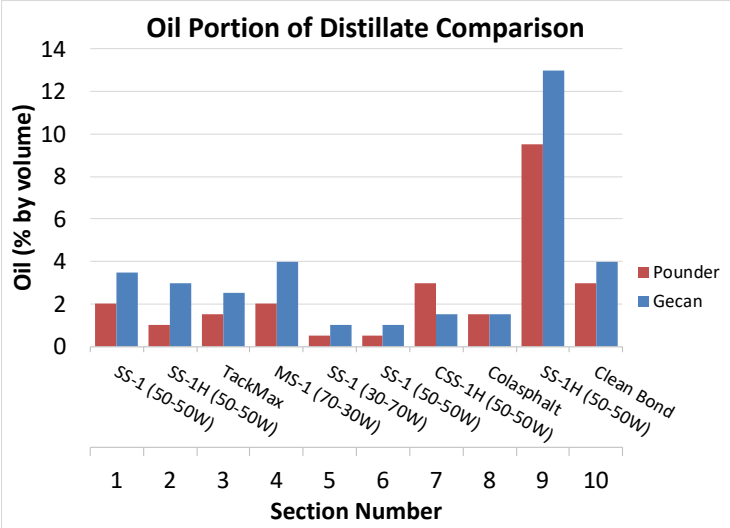


**Figure A.11 Oil Portion of Distillate Comparison**

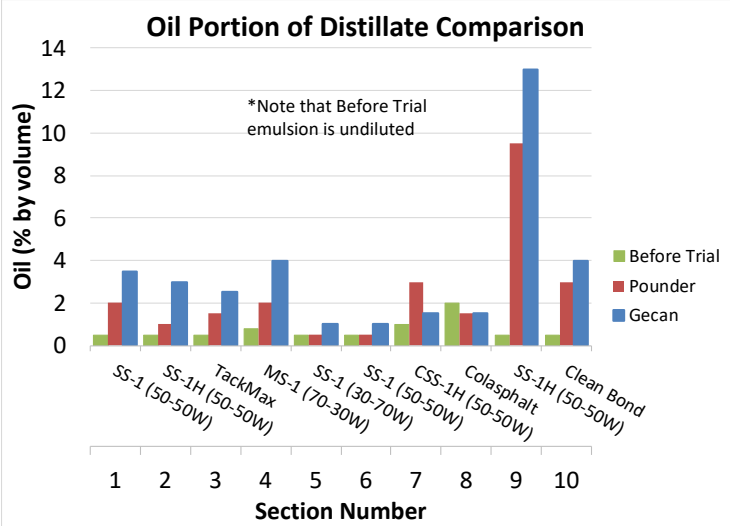


**Figure A.12 Oil Portion of Distillate Comparison including Before Trial Results**

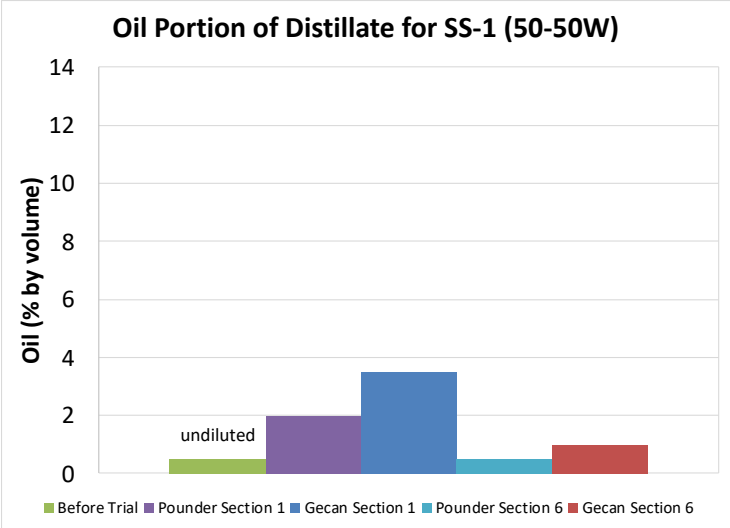


**Figure A.13 Oil Portion of Distillate Comparison for SS-1**

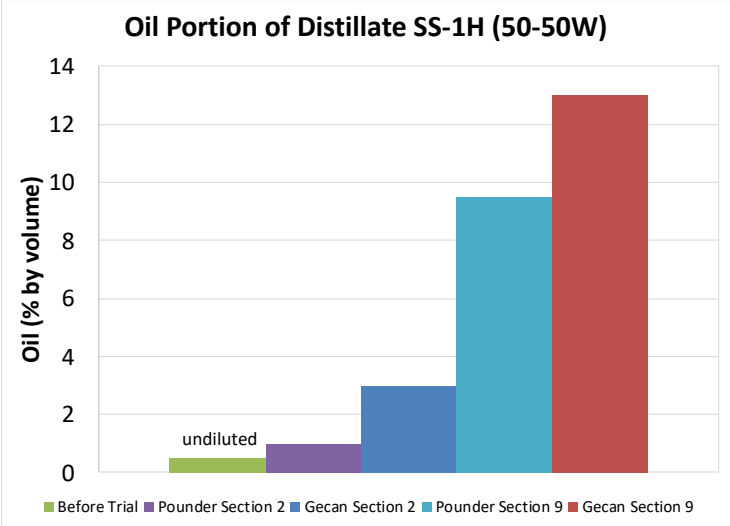


**Figure A.14 Oil Portion of Distillate Comparison for SS-1h**

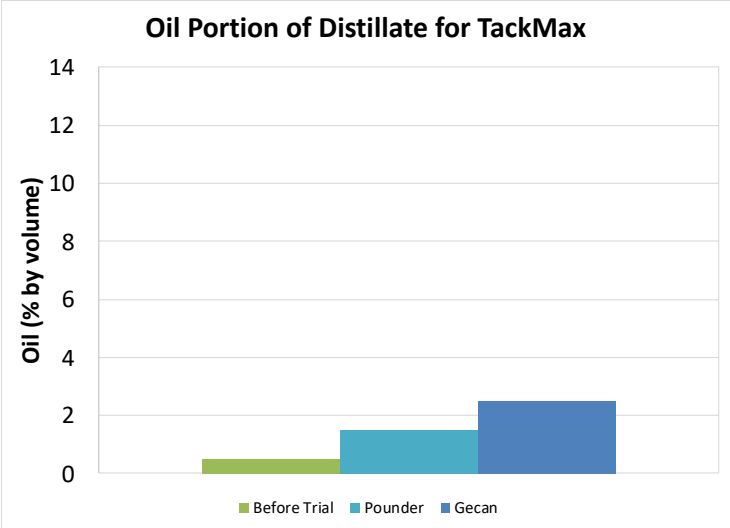


**Figure A.15 Oil Portion of Distillate Comparison for TackMax™**

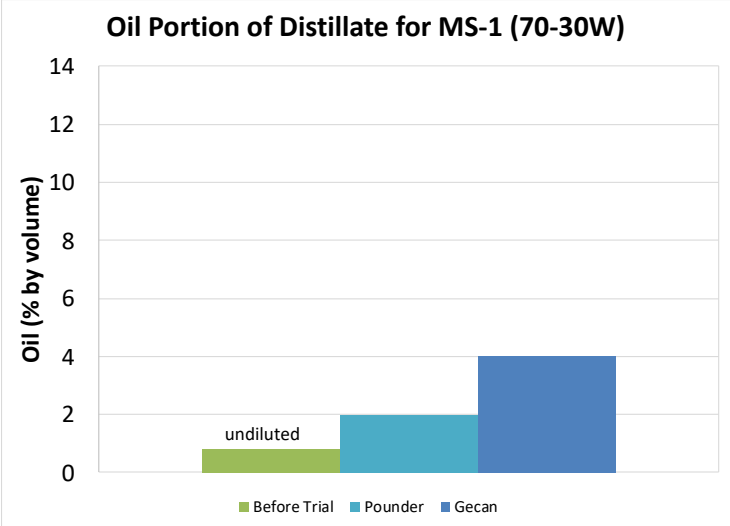


**Figure A.16 Oil Portion of Distillate Comparison for MS-1**

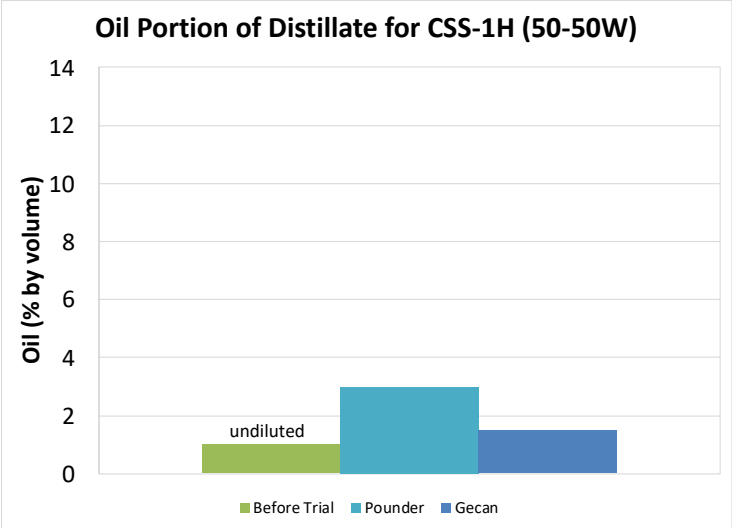


**Figure A.17 Oil Portion of Distillate Comparison for CSS-1h**

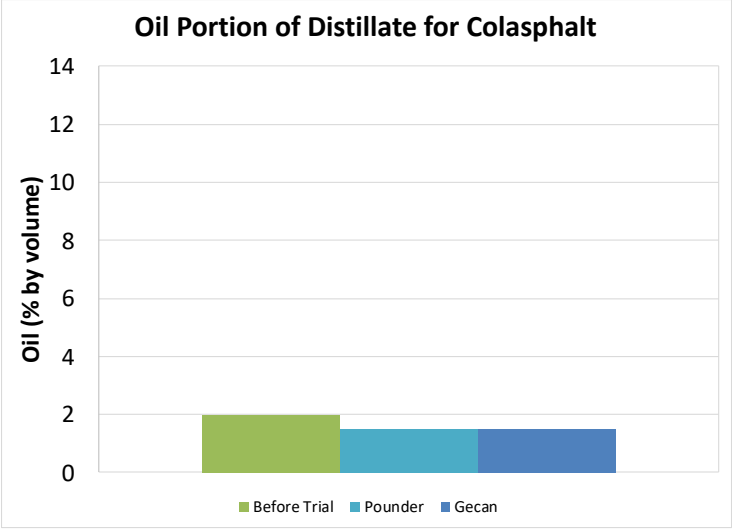


**Figure A.18 Oil Portion of Distillate Comparison for Colapshalt Tack**

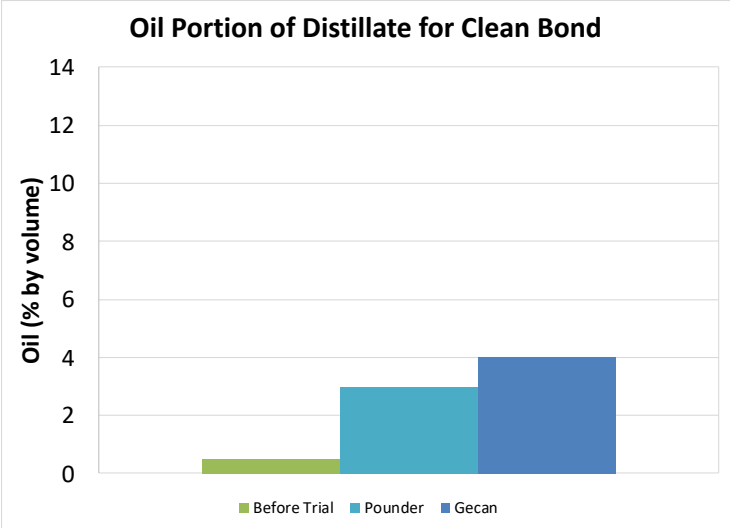


**Figure A.19 Oil Portion of Distillate Comparison for Clean Bond**

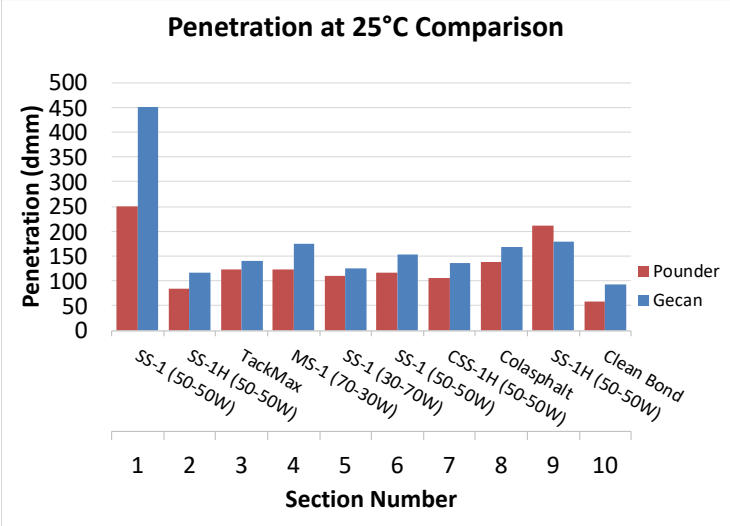


**Figure A.20 Post Trial Penetration Comparison**

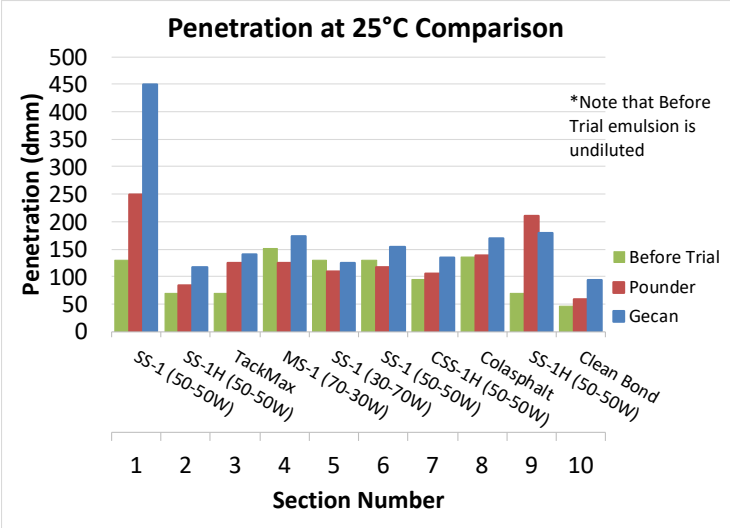


**Figure A.21 Penetration Comparison including Before Trial Results**

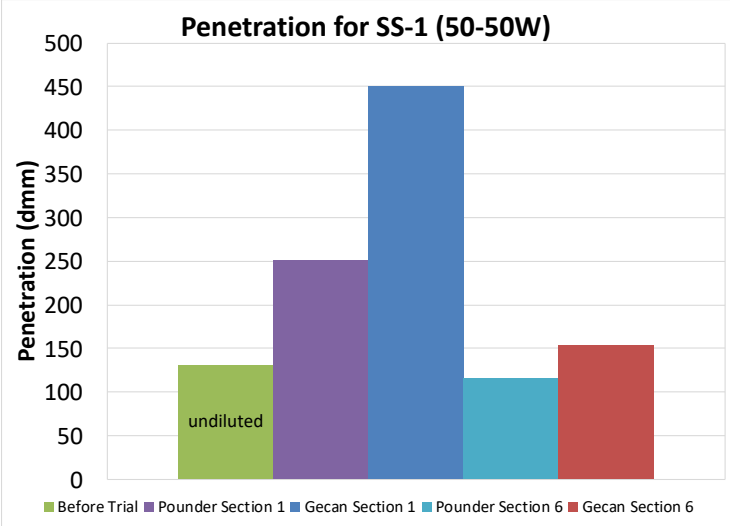


**Figure A.22 Penetration Comparison for SS-1**

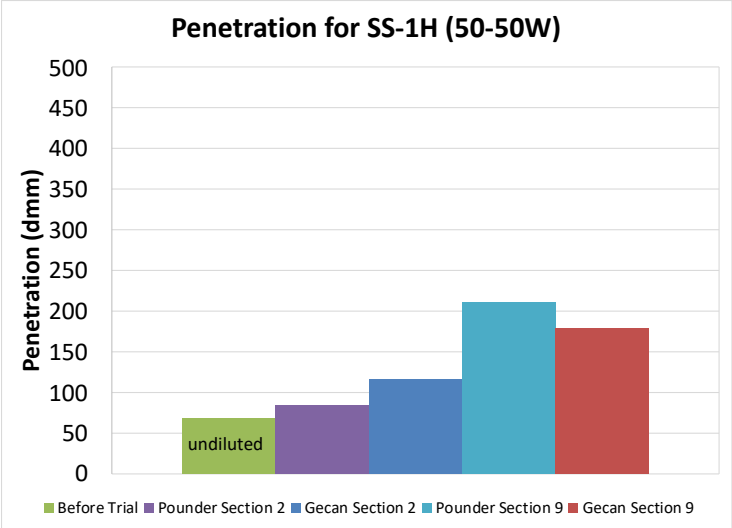


**Figure A.23 Penetration Comparison for SS-1h**

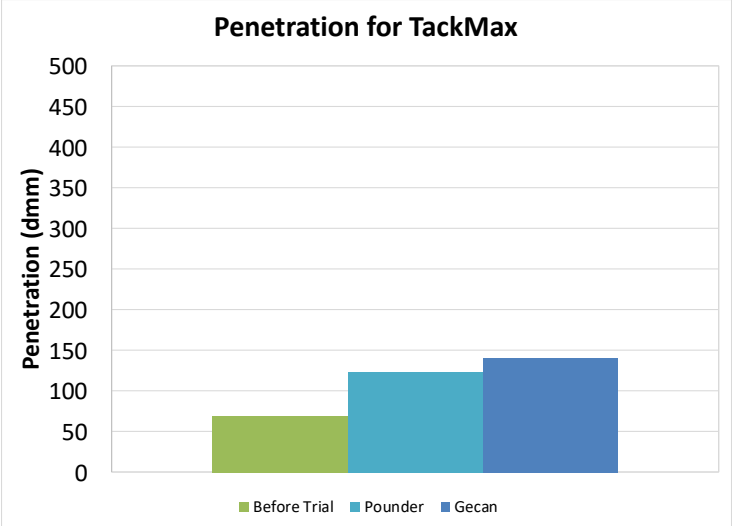


**Figure A.24 Penetration Comparison for TackMax™**

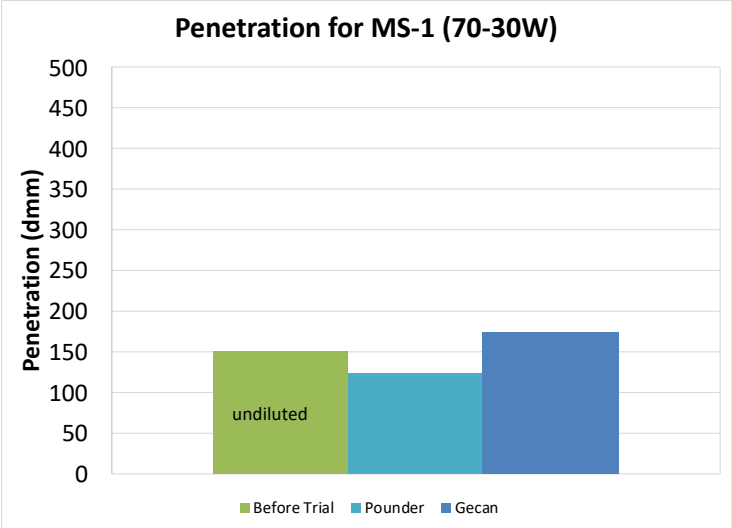


**Figure A.25 Penetration Comparison for MS-1**

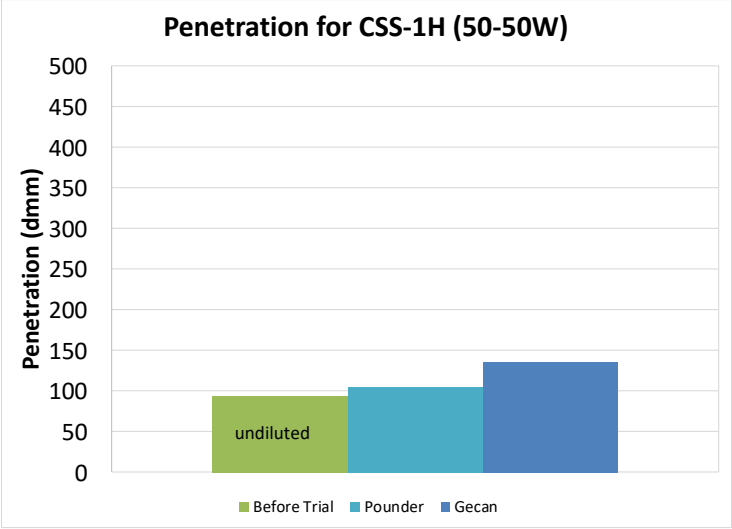


**Figure A.26 Penetration Comparison for CSS-1h**

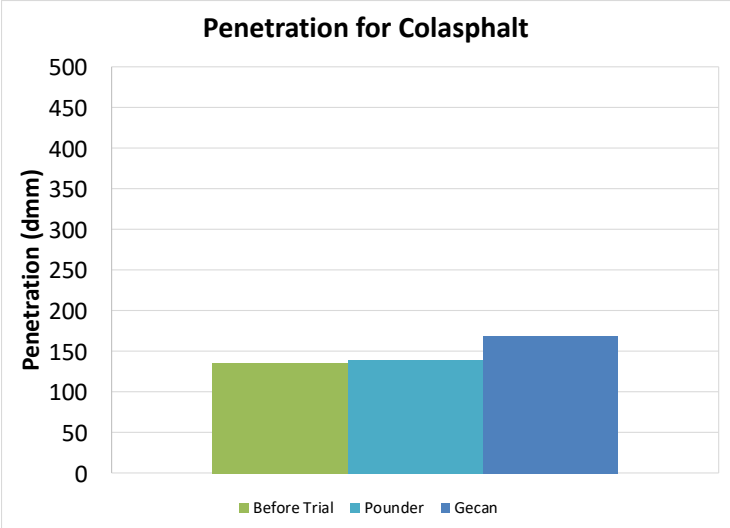


**Figure A.27 Penetration Comparison for Colasphalt Tack**

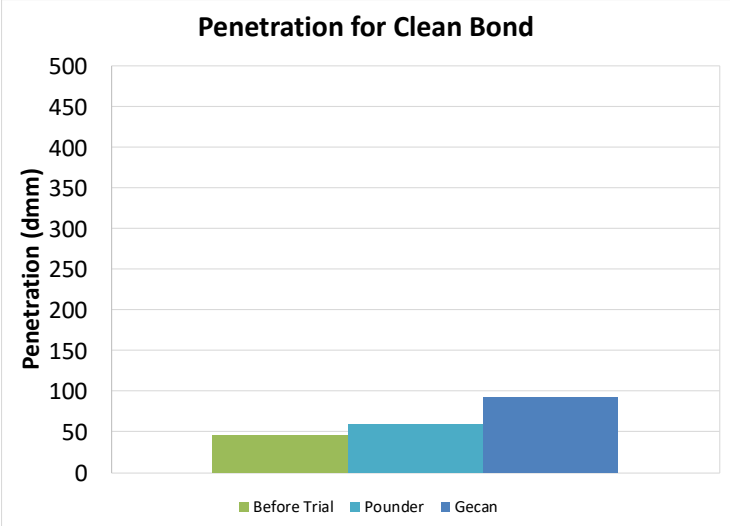


**Figure A.28 Penetration Comparison for Clean Bond**

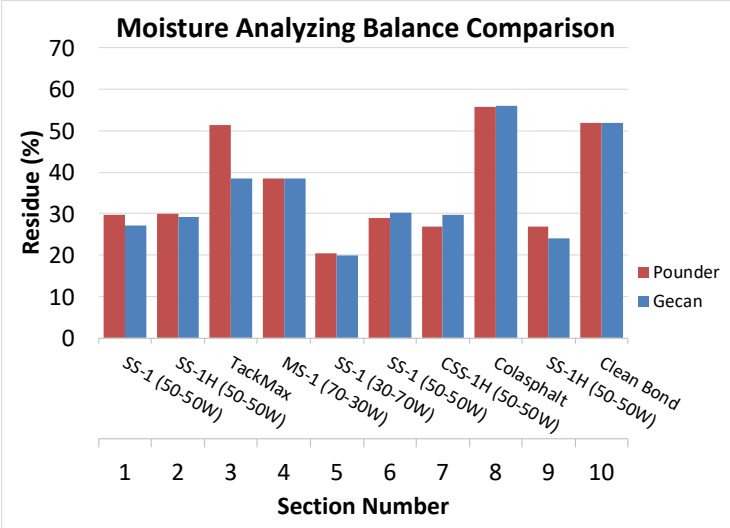


**Figure A.29 Post Trial Moisture Analyzing Balance Comparison**

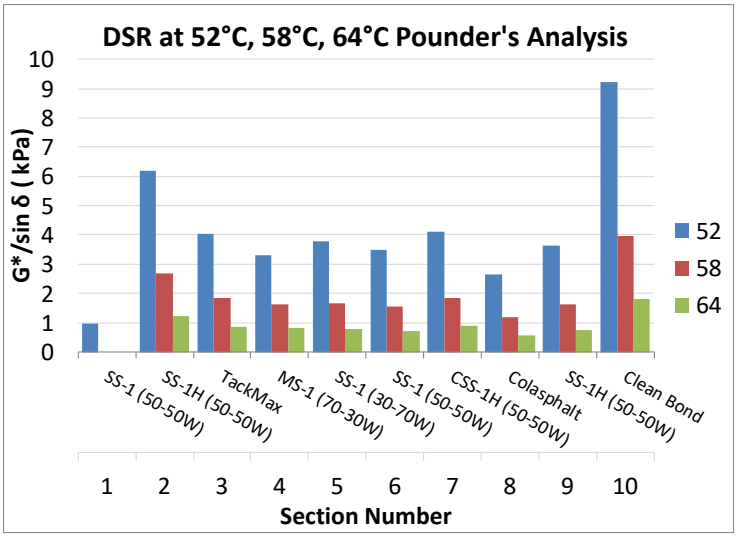


**Figure A.30 Pounder Emulsion Dynamic Shear Rheometer G*/sinδ Results**

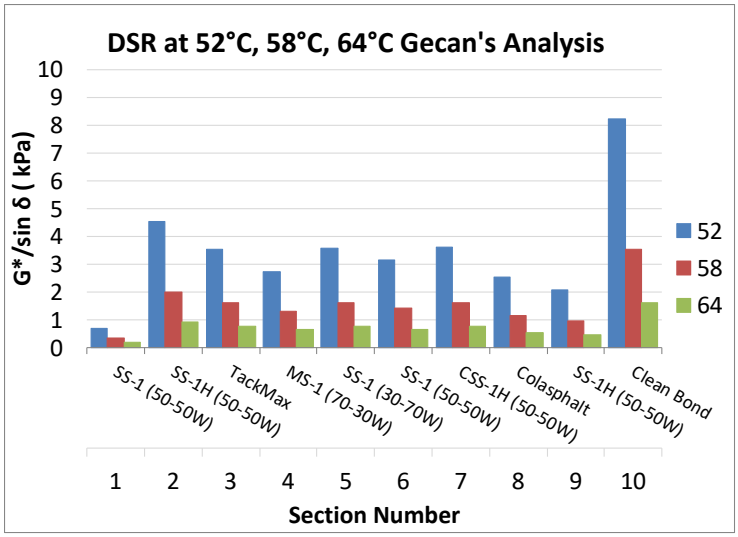


**Figure A.31 Gecan Dynamic Shear Rheometer G*/sinδ Results**

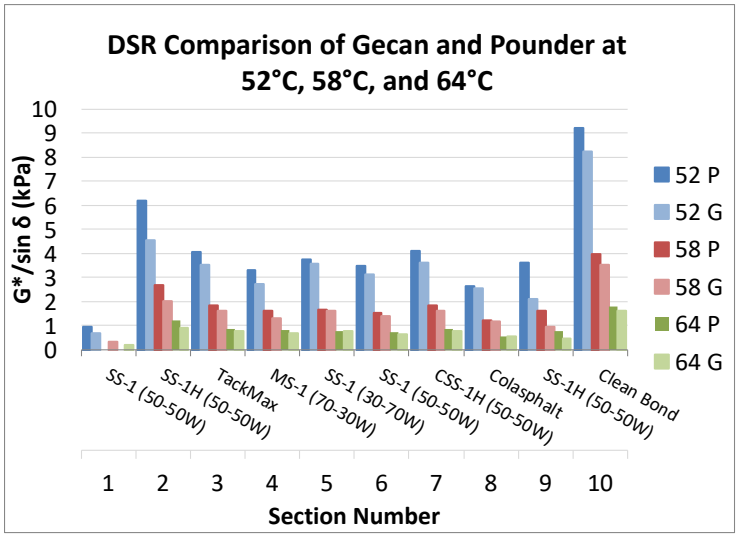


**Figure A.32 Dynamic Shear Rheometer G*/sinδ Results Comparison**

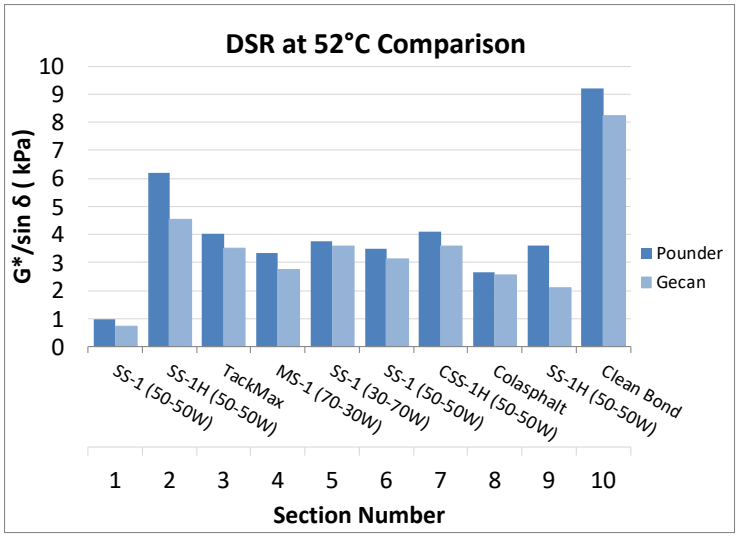


**Figure A.33 Dynamic Shear Rheometer G*/sinδ Results at 52°C Comparison**

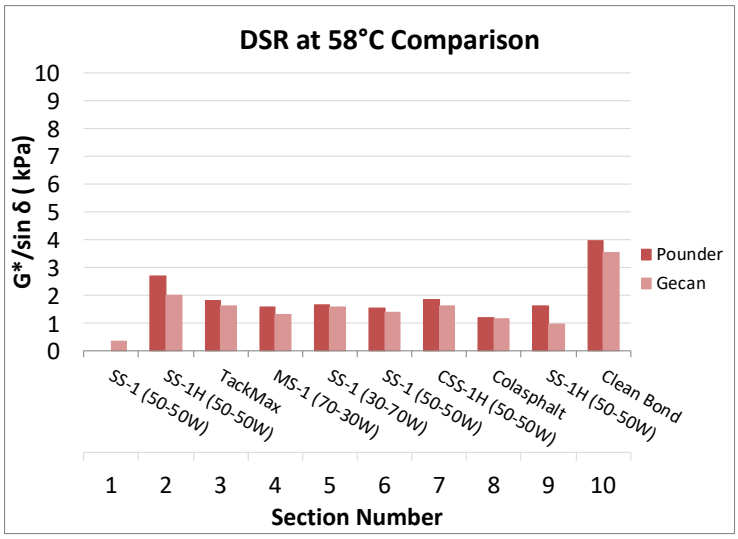


**Figure A.34 Dynamic Shear Rheometer G*/sinδ Results at 58°C Comparison**

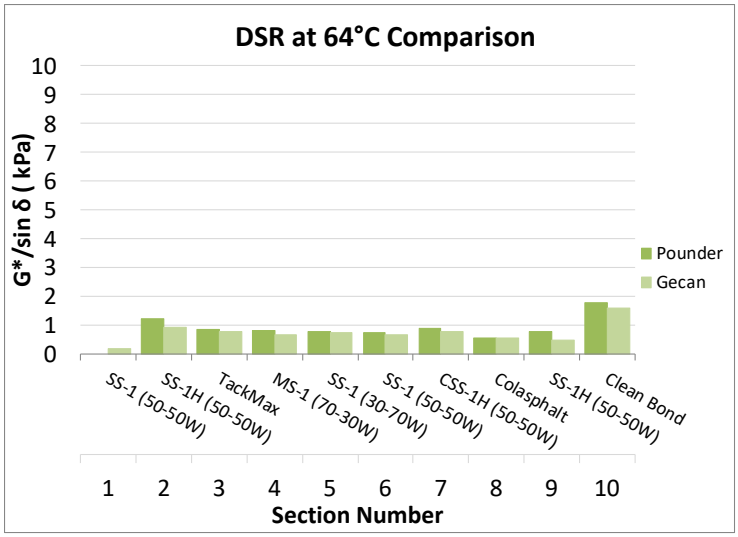


**Figure A.35 Dynamic Shear Rheometer G*/sinδ Results at 64°C Comparison**

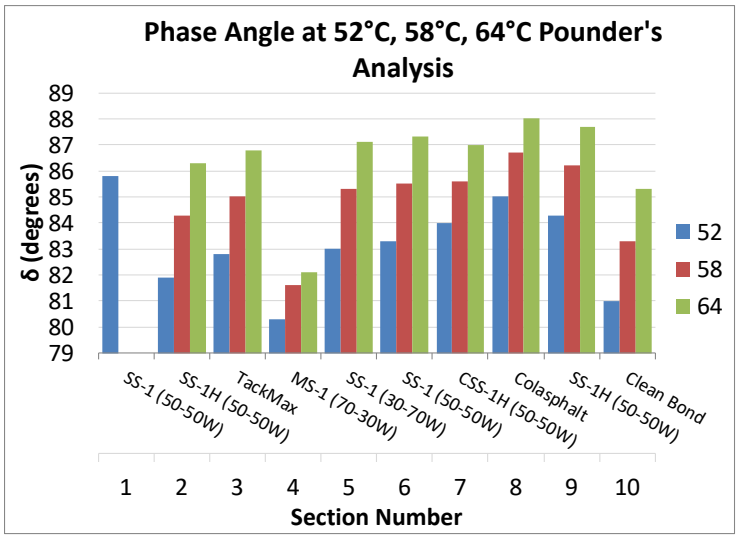


**Figure A.36 Pounder Emulsion Phase Angles**

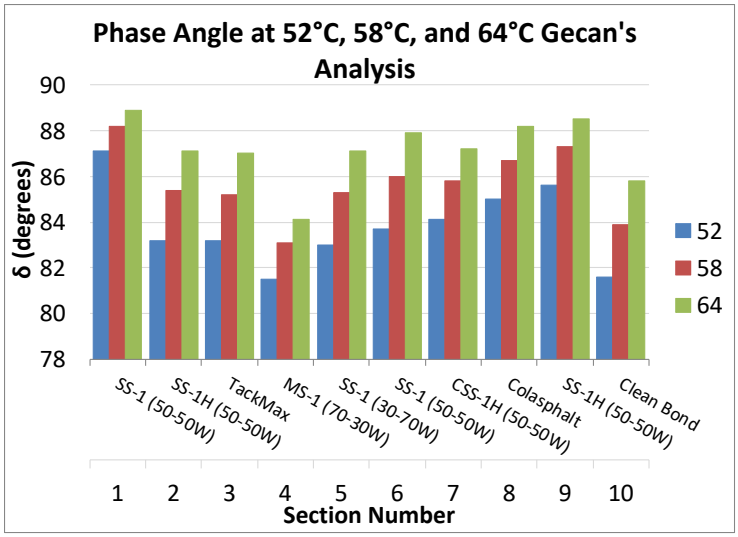


**Figure A.37 Gecan Phase Angles**

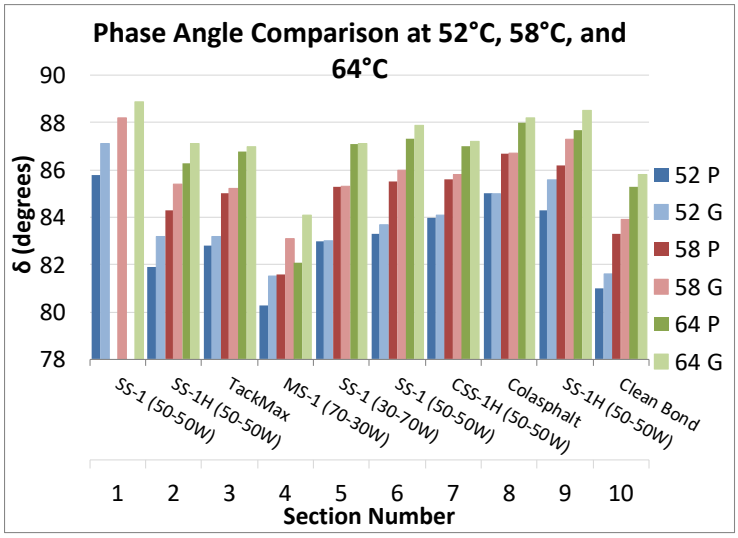


**Figure A.38 Phase Angle Comparison**

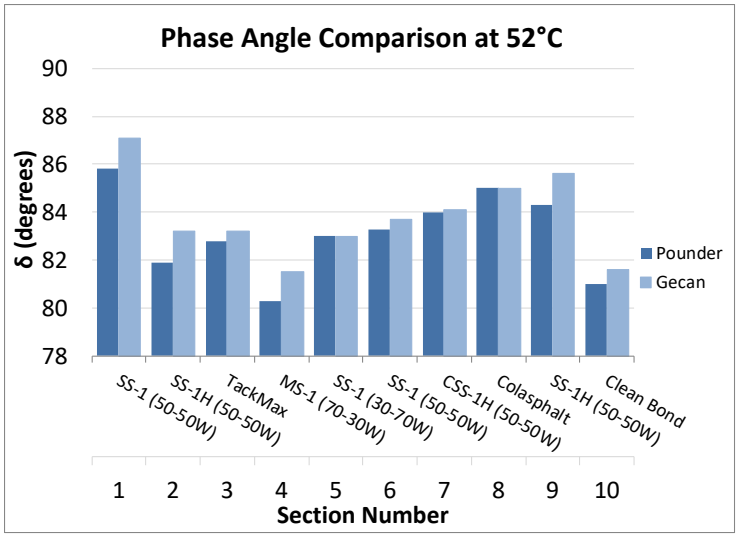


**Figure A.39 Phase Angle at 52°C Comparison**

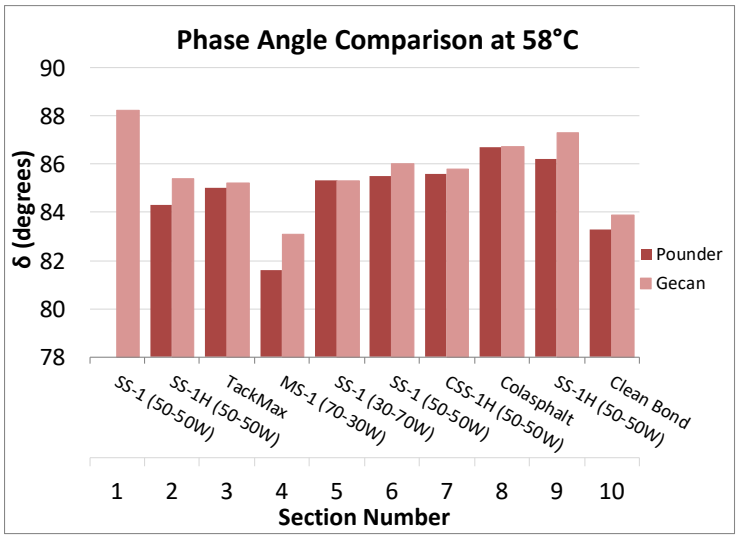


**Figure A.40 Phase Angle at 58°C Comparison**

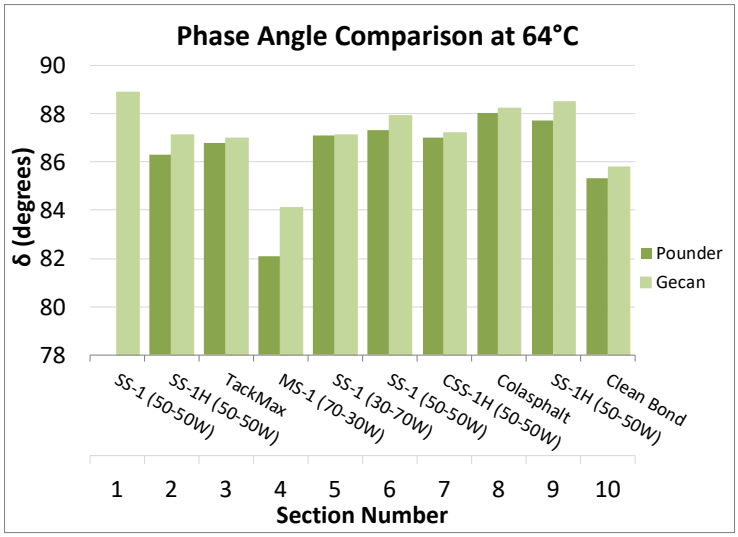


**Figure A.41 Phase Angle at 64°C Comparison**

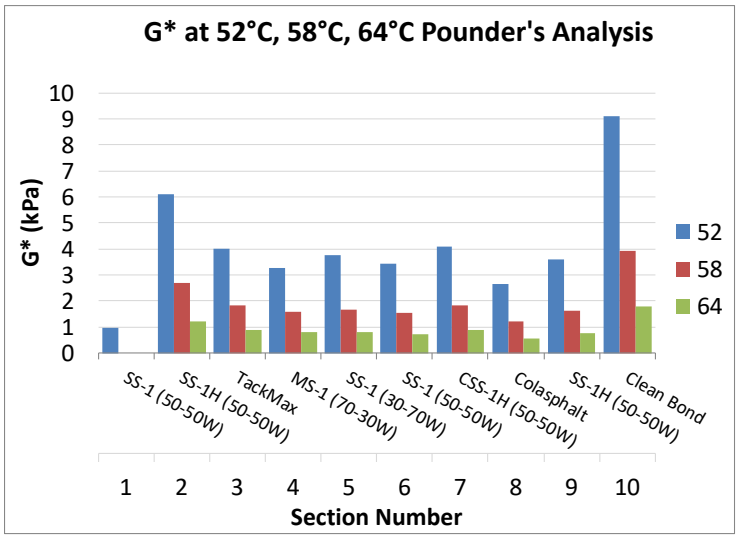


**Figure A.42 Pounder Emulsion G* Results**

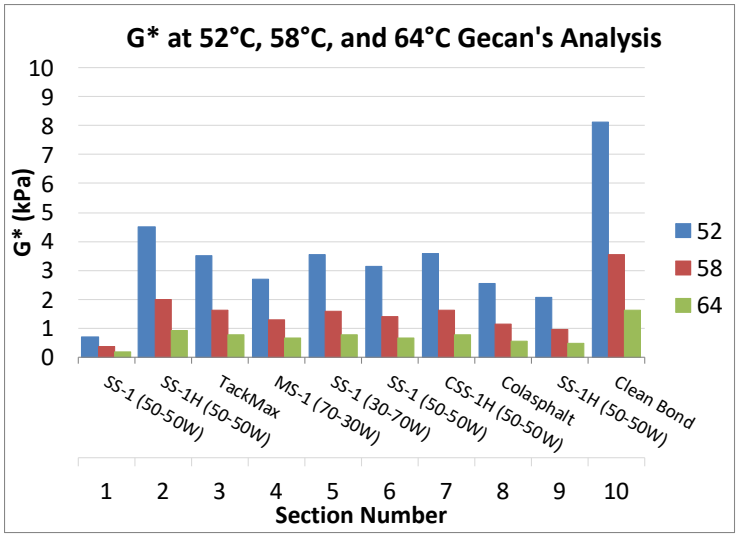


**Figure A.43 Gecan G* Results**

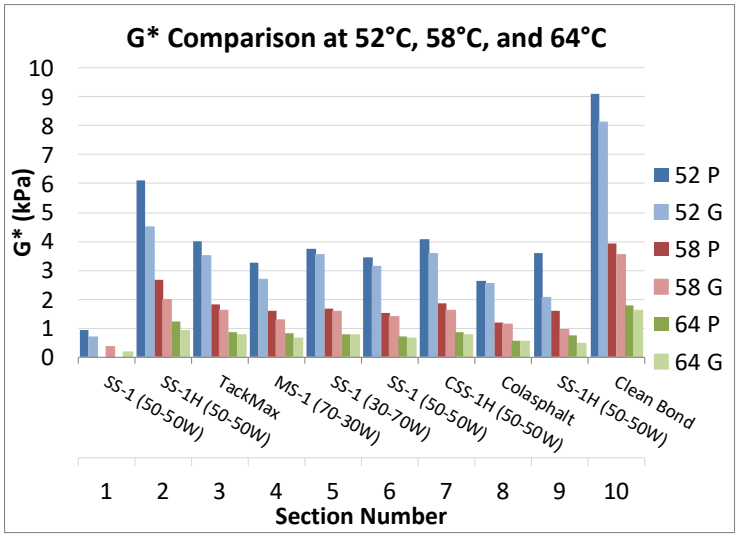


**Figure A.44 G* Comparison**

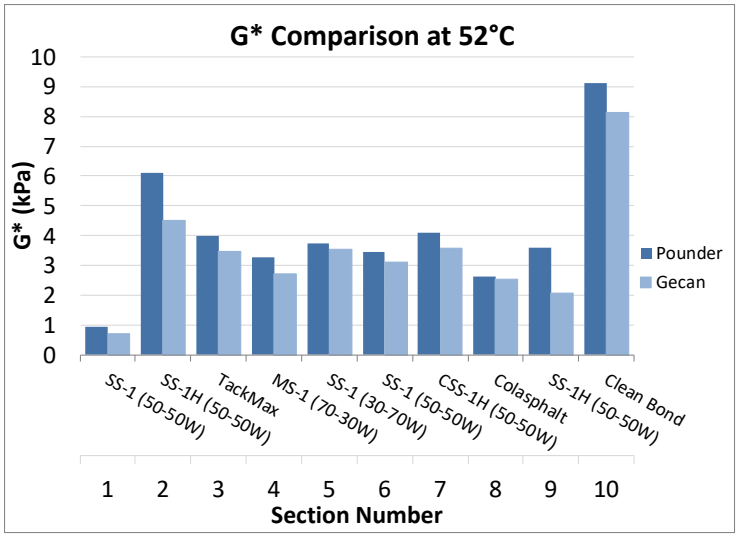


**Figure A.45 G* at 52°C Comparison**

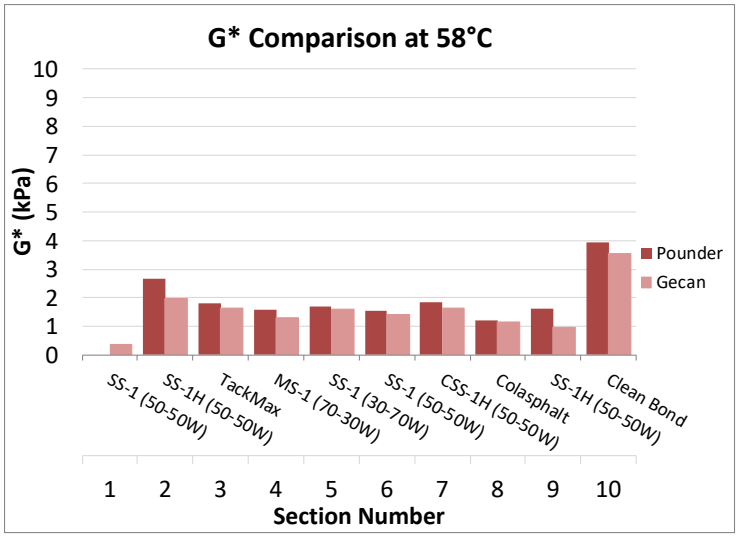


**Figure A.46 G* at 58°C Comparison**

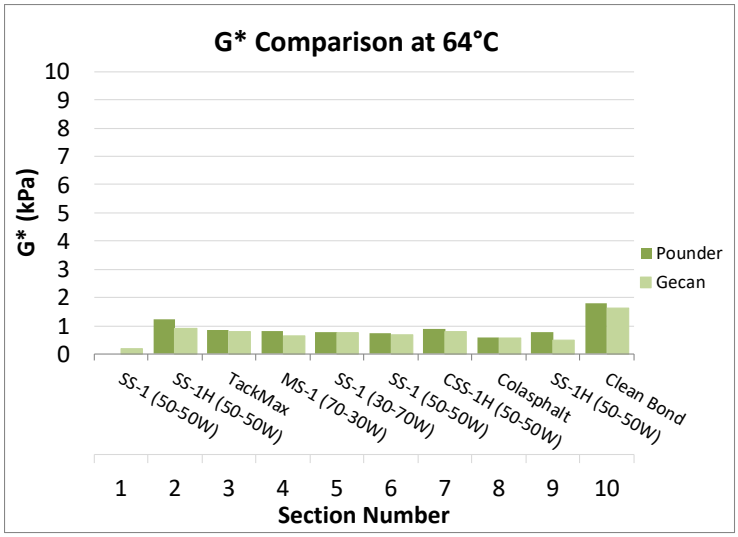


**Figure A.47 G* at 64°C Comparison**

## Table A.1 Application Rate Comparison

| Product | Dilution | Section | Target Application Rate ($L/m^2$) | Target Residual Application Rate ($L/m^2$) | Distributor Average ($L/m^2$) | Patch Test Overall Avg Spray Rate ($L/m^2$) | Patch Test Inner Wheel Path Avg (Patches 6,7,8) ($L/m^2$) | Patch Test Outer Wheel Path Avg (Patches 9,10,11) ($L/m^2$) | Patch Test Middle Value Avg (Patches 6,7,9,10) ($L/m^2$) | Patch Test Avg Rate Along Spray Bar (Patches 1-5) ($L/m^2$) |
|---|---|---|---|---|---|---|---|---|---|---|
| SS-1 | 50-50W | 1 | 0.5 | 0.16 | 0.52 | 0.5 | 0.52 | 0.54 | 0.52 | 0.48 |
| SS-1H | 50-50W | 2 | 0.5 | 0.16 | 0.55 | 0.45 | 0.46 | 0.49 | 0.46 | 0.41 |
| TackMax | - | 3 | 0.36 | 0.18 | 0.36 | 0.27 | 0.29 | 0.31 | 0.29 | 0.24 |
| MS-1 | 70-30W | 4 | 0.41 | 0.16 | 0.41 | 0.36 | 0.37 | 0.4 | 0.39 | 0.33 |
| SS-1 | 30-70W | 5 | 0.5 | 0.11 | 0.54 | 0.28 | 0.17 | 0.56 | 0.28 | 0.18 |
| SS-1 | 50-50W | 6 | 0.5 | 0.16 | 0.54 | 0.52 | 0.53 | 0.59 | 0.55 | 0.48 |
| CSS-1H | 50-50W | 7 | 0.5 | 0.13 | | 0.47 | 0.56 | 0.48 | 0.51 | 0.41 |
| Colasphalt Tack | - | 8 | 0.33 | 0.2 | 0.36 | 0.28 | 0.32 | 0.29 | 0.3 | 0.25 |
| SS-1H | 50-50W | 9 | 0.5 | 0.15 | 0.54 | 0.21 | 0.29 | 0.27 | 0.22 | 0.12 |
| Clean Bond | - | 10 | 0.33 | 0.21 | | 0.23 | 0.25 | 0.23 | 0.25 | 0.21 |

Note: Data is based on construction notes

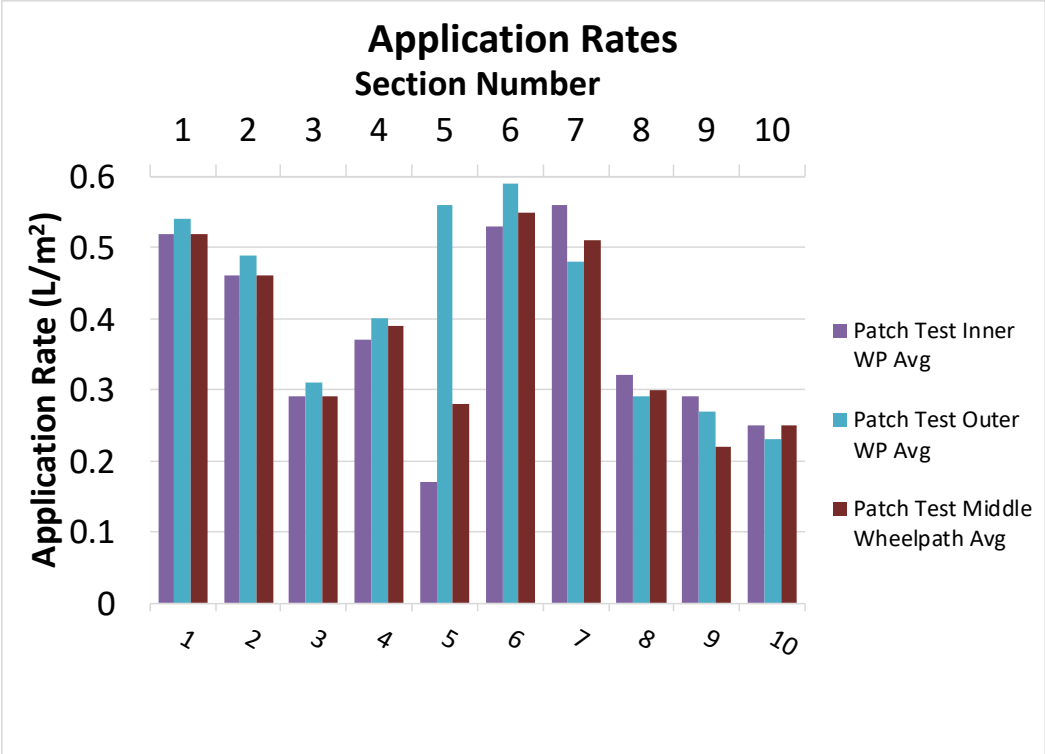


**Figure A.48 Application Rates in the Wheel Paths of the Patch Test**

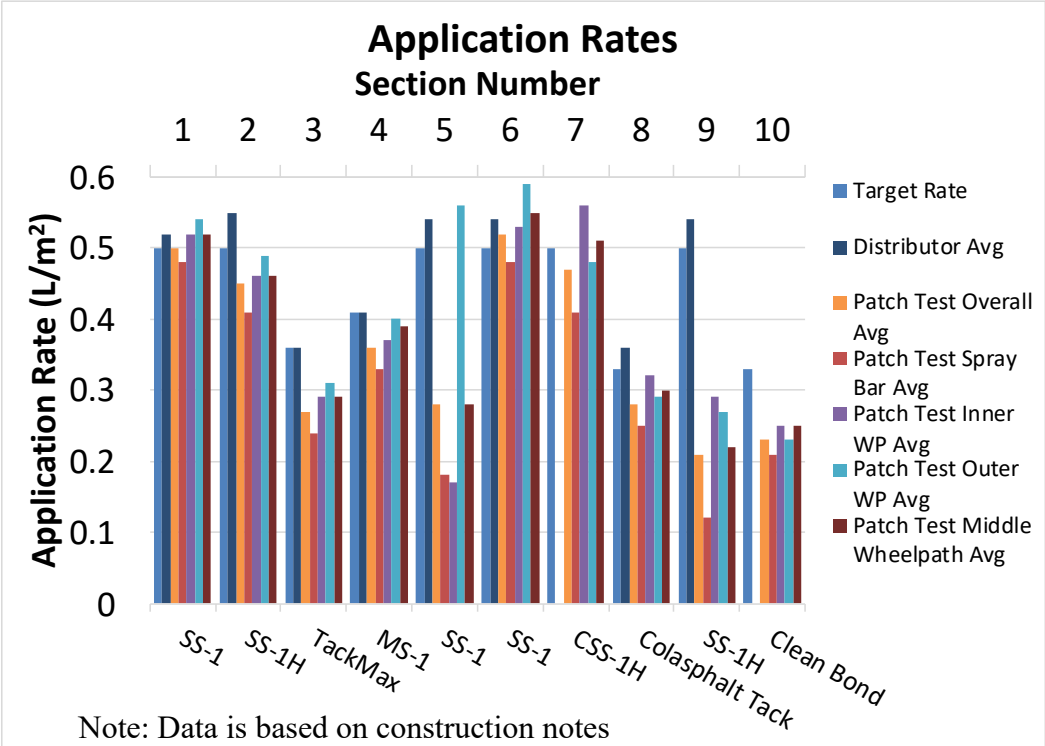


Note: Data is based on construction notes

**Figure A.49 Comparison of Application Rates**

# APPENDIX B: Test Section Maps

# Test Section Product Map

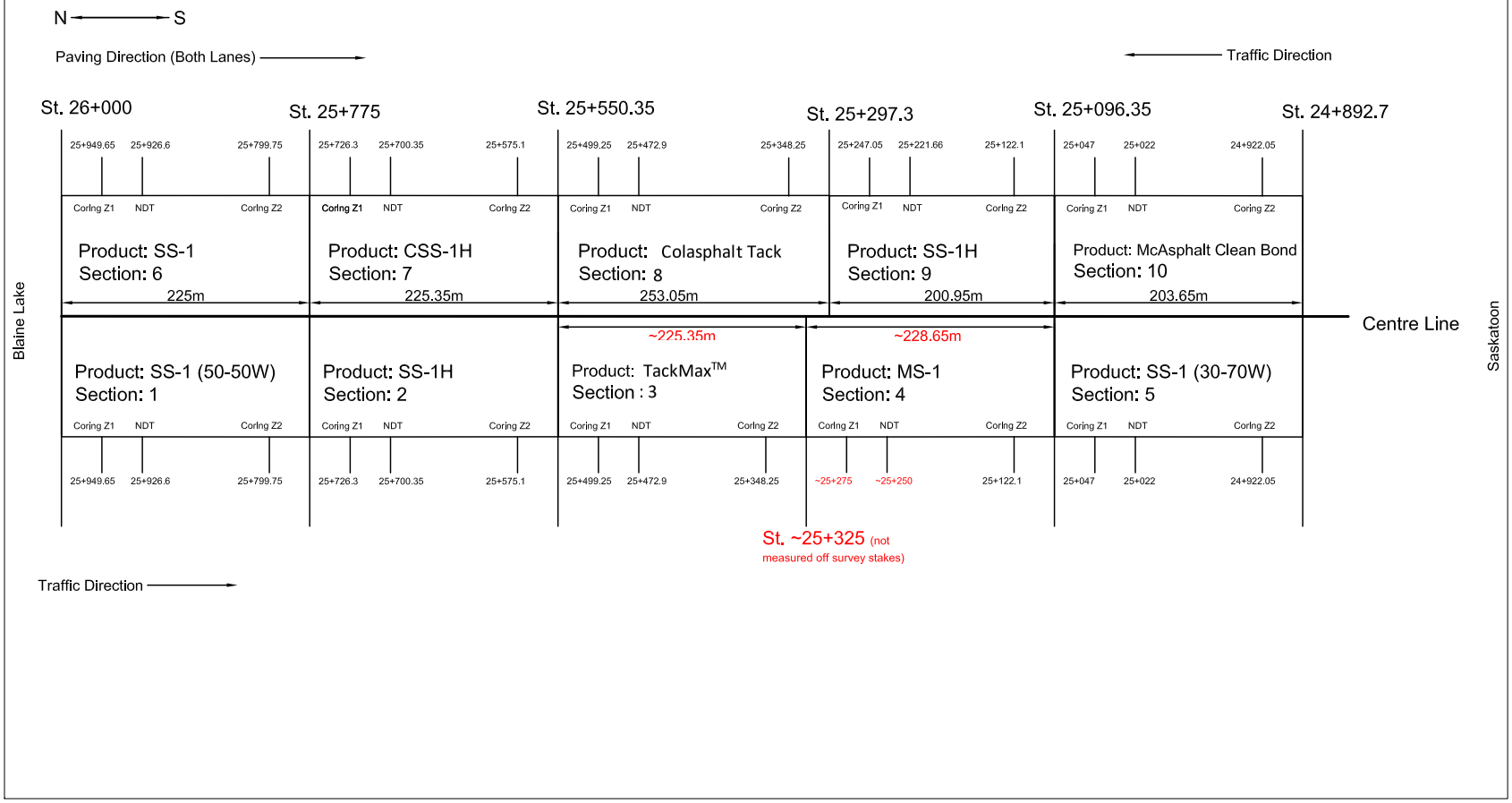

# Test Section Product Map

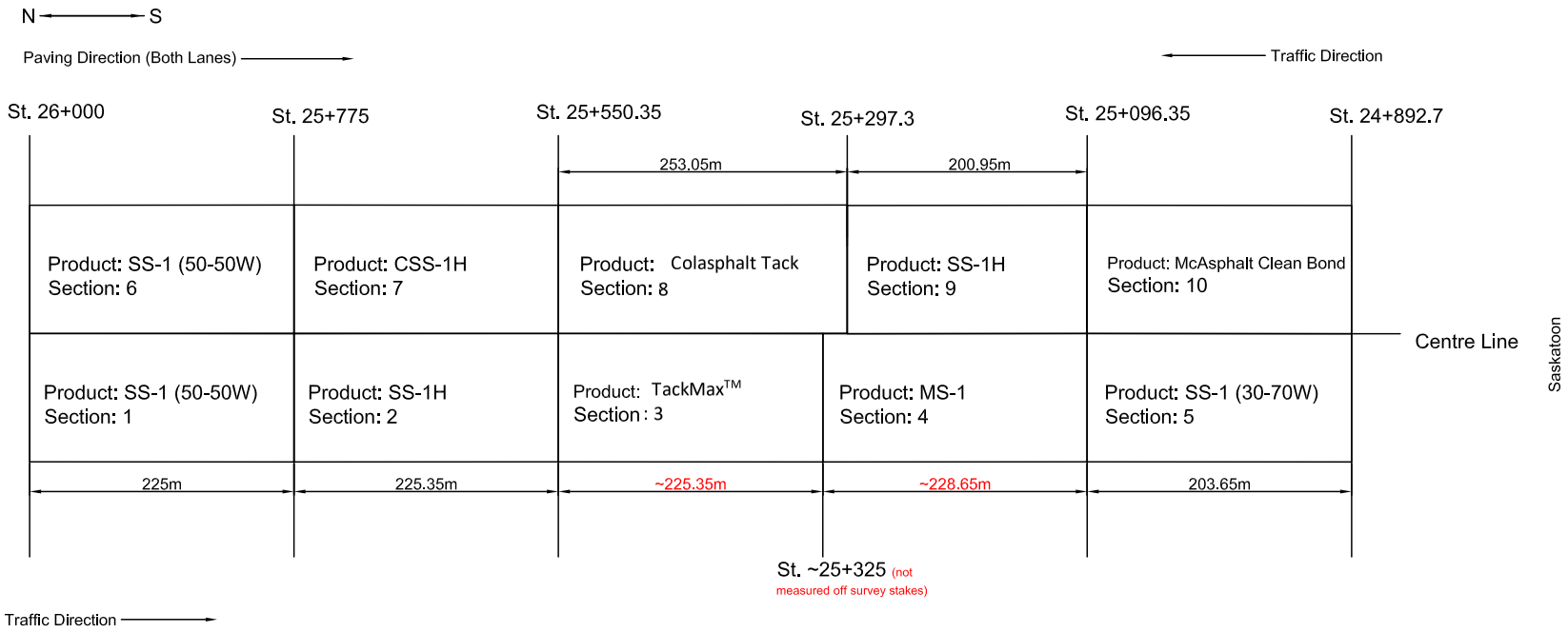

# Test Section Schematic
# Section 1: SS-1 (50-50W)

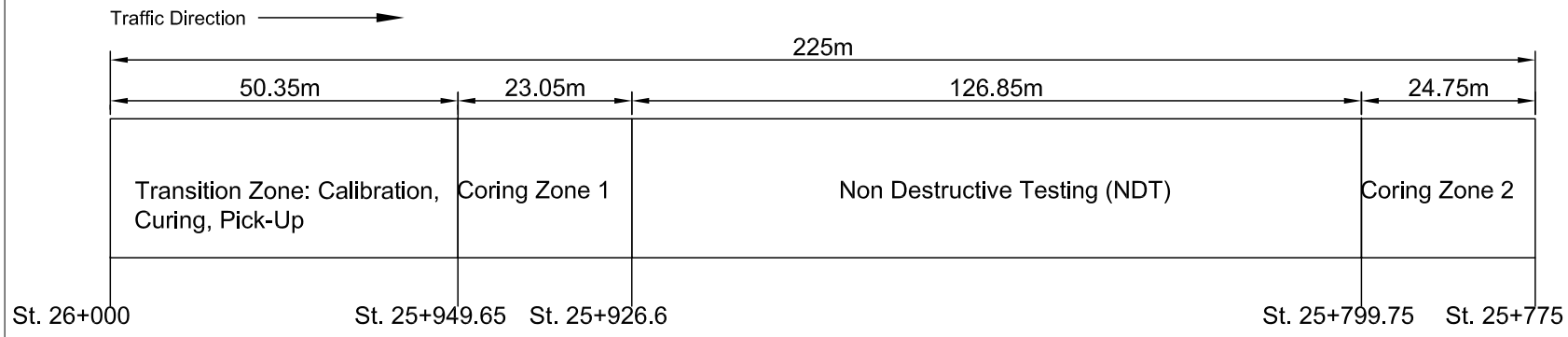

# Test Section Schematic
# Section 2: SS-1H

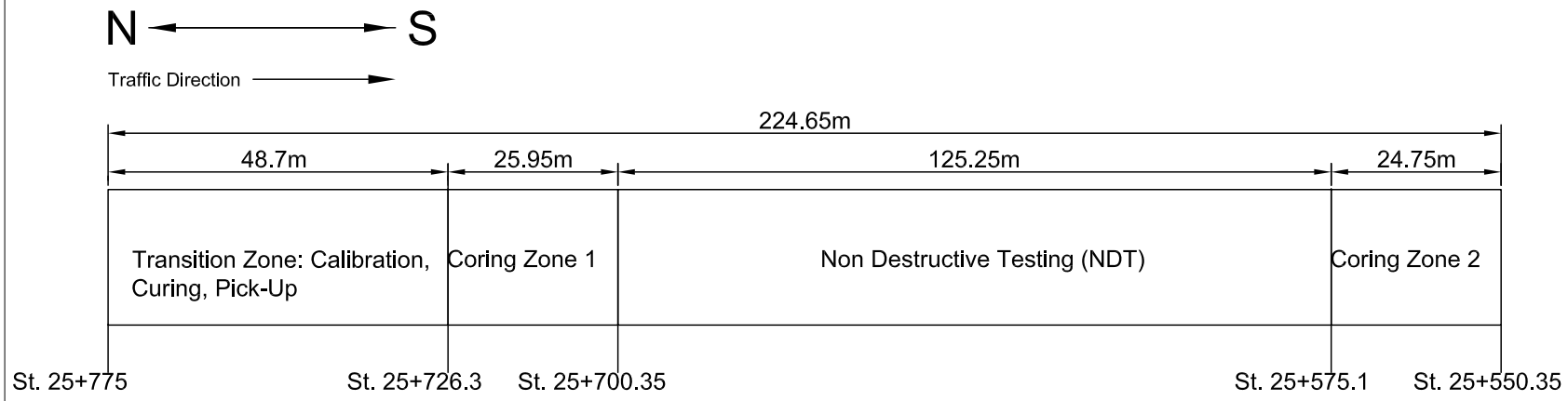

# Test Section Schematic

## Section 3: TackMax™

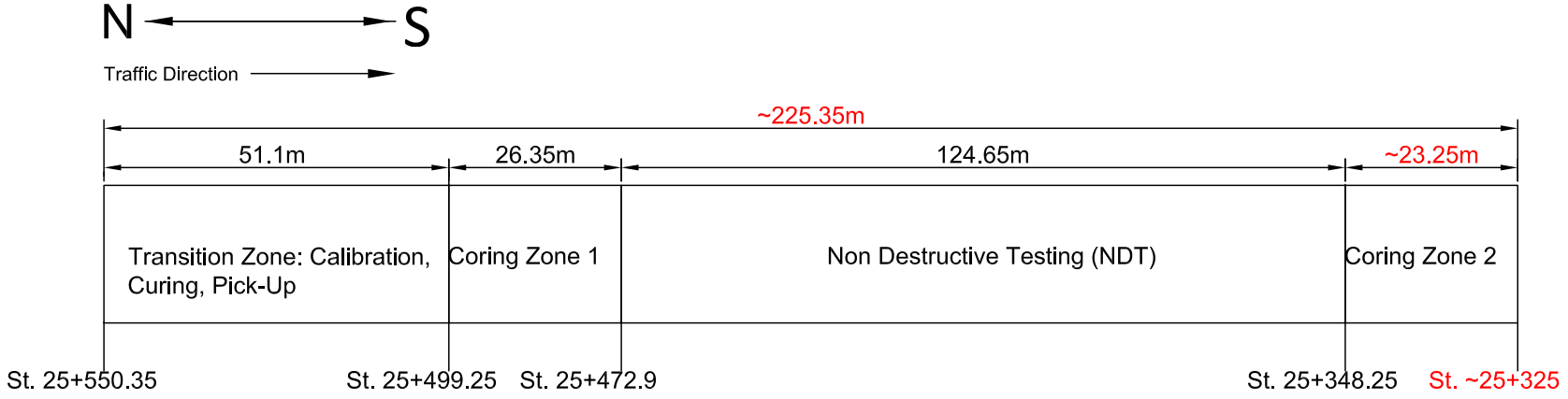

# Test Section Schematic
# Section 4: MS-1

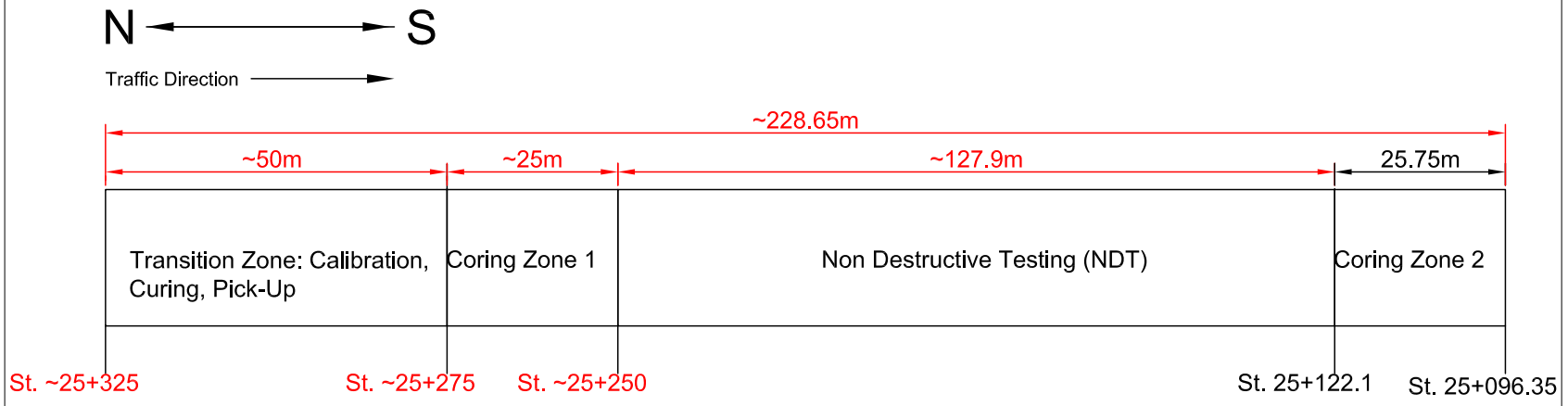

# Test Section Schematic
# Section 5: SS-1 (30-70W)

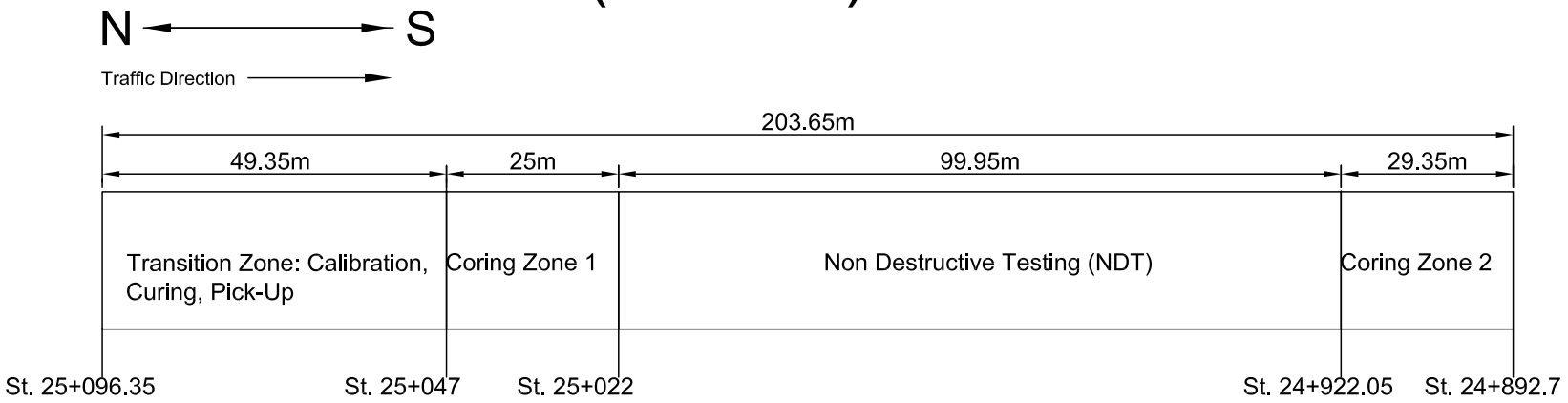

# Test Section Schematic
# Section 6: SS-1 (50-50W)

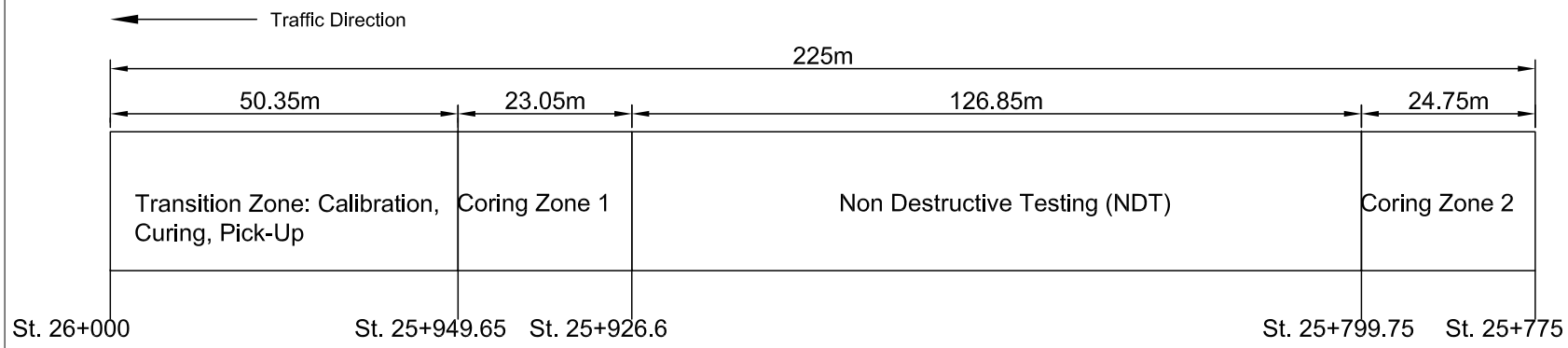

# Test Section Schematic
# Section 7: CSS-1H

N ◄——————► S

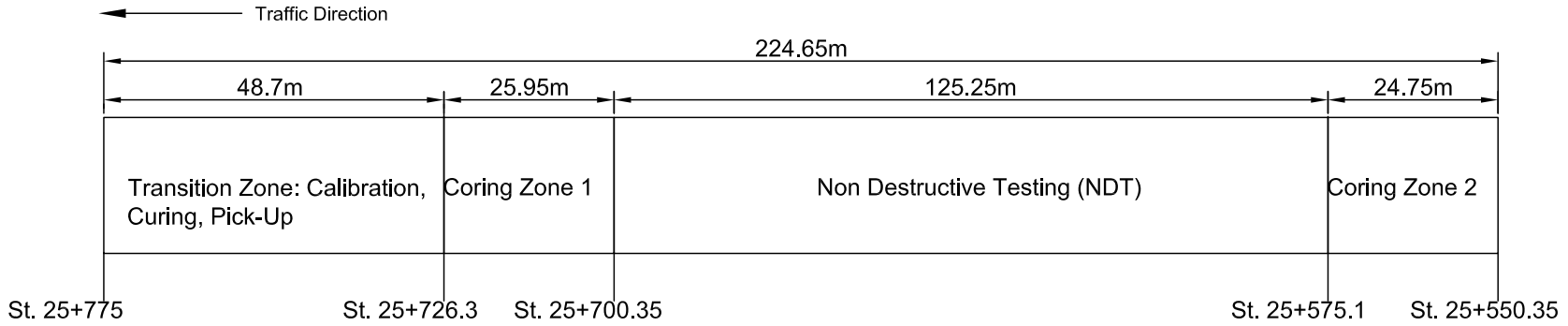

# Test Section Schematic

## Section 8: Colasphalt Tack

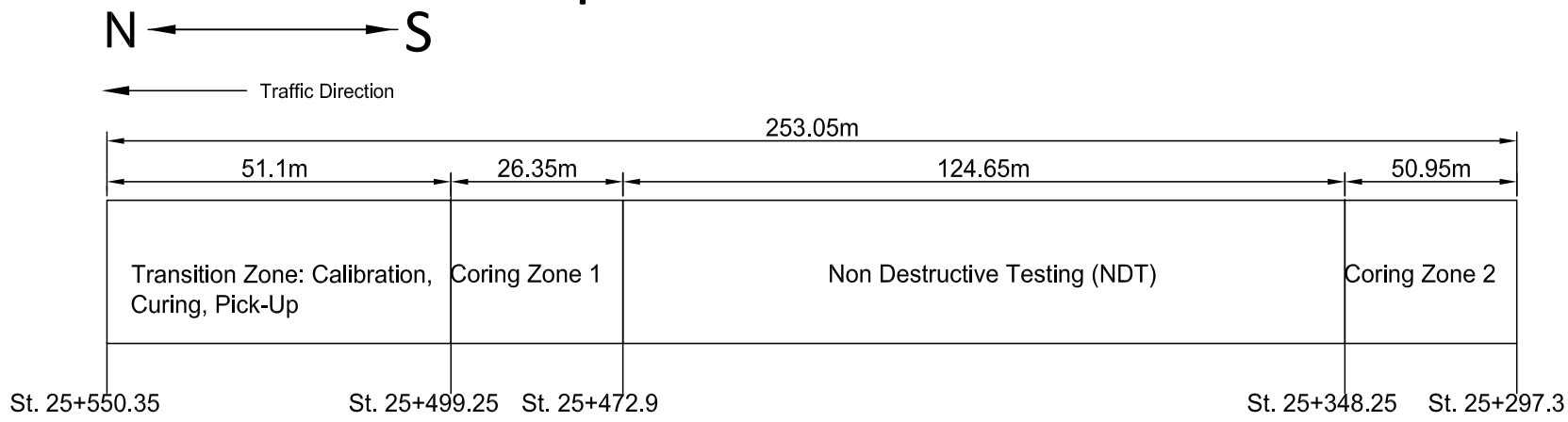

# Test Section Schematic
# Section 9: SS-1H

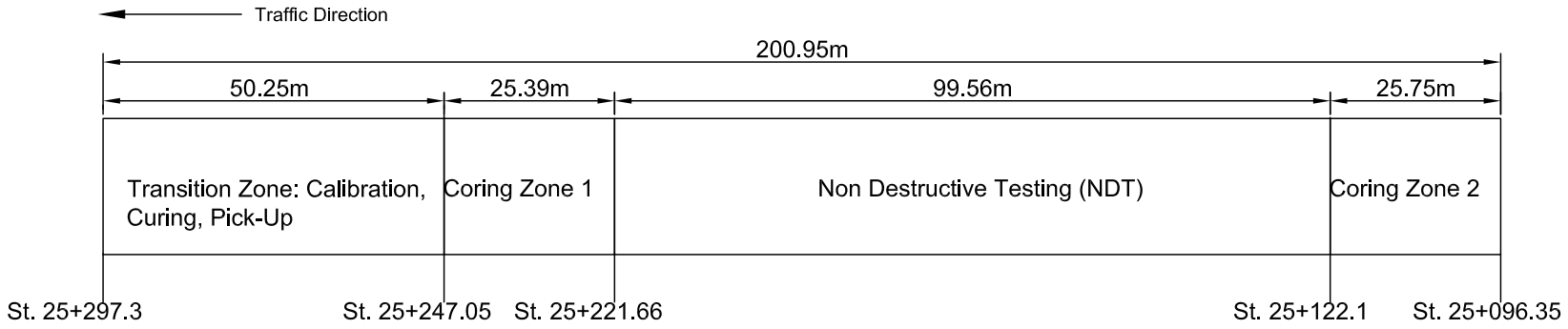

# Test Section Schematic
# Section 10: McAsphalt Clean Bond

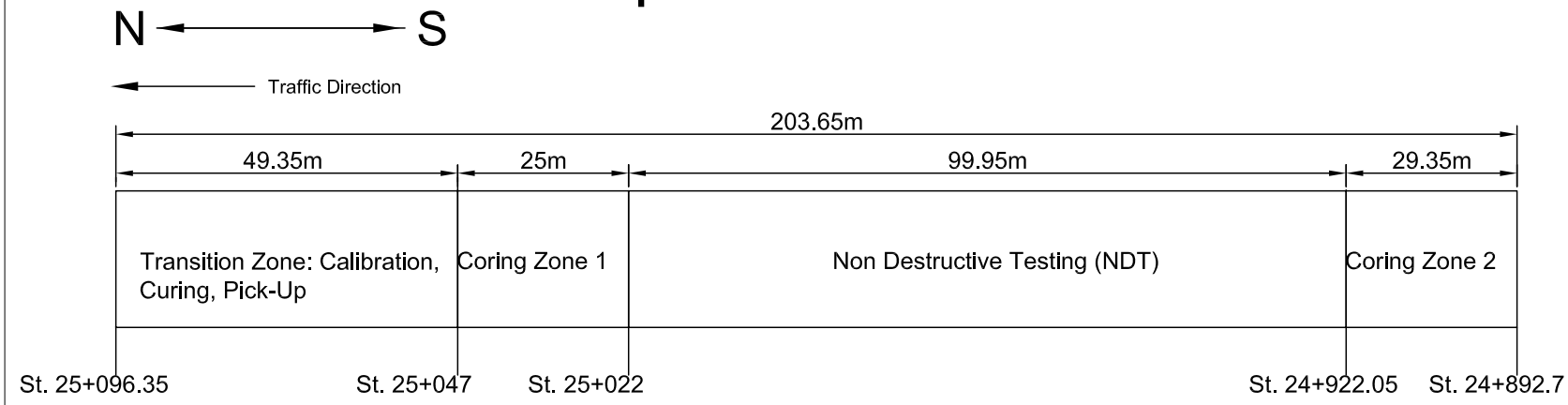

## APPENDIX C: Pictures from Road Construction






# APPENDIX D: Coring Maps

# Coring Map Sections 1-5

**Section - Zone - I/O/C - Core #**

Cores will be taken in the direction of paving (Southbound)

Cores will be taken starting in the OWP (O), then centre (C), then IWP (I)

| For Period 1 core #s are: | | For Periods 2-5 core #s are: | |
|---|---|---|---|
| OWP | 6, 7, 8 | OWP | 5, 6 |
| C | 4, 5 | C | 3, 4 |
| IWP | 1, 2, 3 | IWP | 1, 2 |

| Key | | |
|---|---|---|
| 3 Week | Period 1 | 16 Cores |
| Spring 2018 | Period 2 | 12 Cores |
| Spring 2019 | Period 3 | 12 Cores |
| Spring 2020 | Period 4 | 12 Cores |
| Spring 2021 | Period 5 | 12 Cores |
| Total | | 64 Cores |

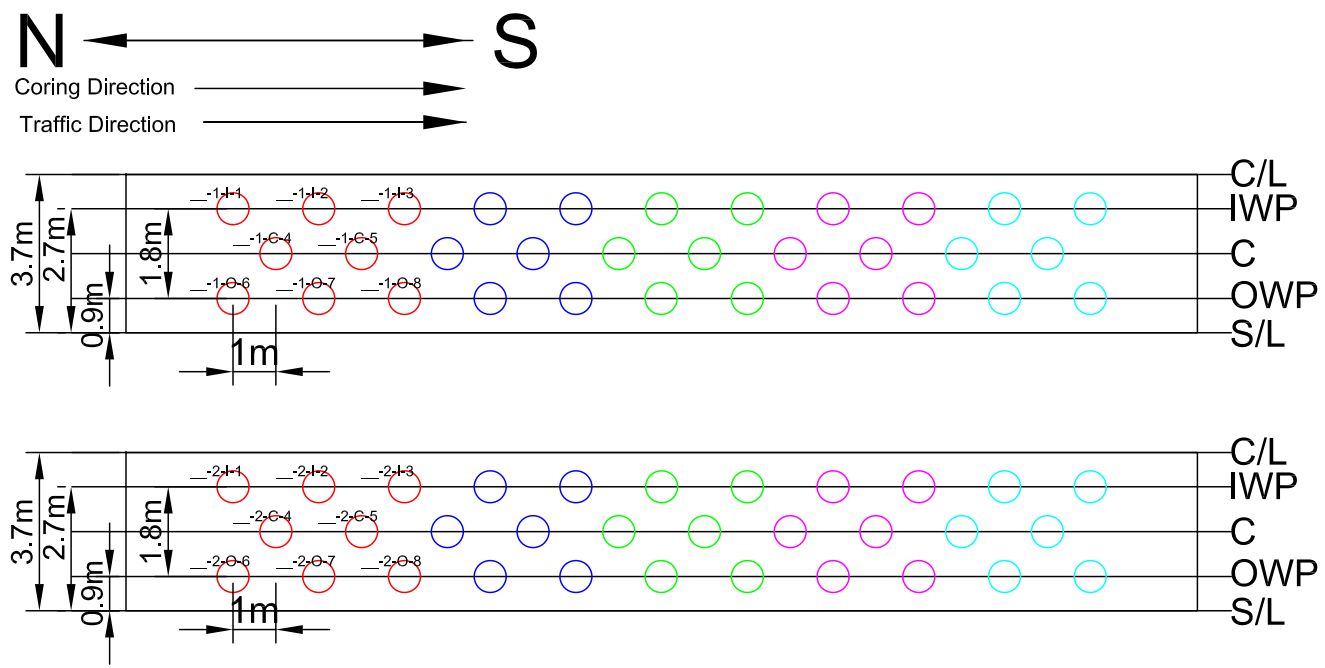

# Coring Map Sections 6-10

**Section - Zone - I/O/C - Core #**

Cores will be taken in the direction of paving (Southbound)

Cores will be taken starting in the OWP (O), then centre (C), then IWP (I)

| For Period 1 core #s are: | | For Periods 2-5 core #s are: | |
|---|---|---|---|
| OWP | 1, 2, 3 | OWP | 1, 2 |
| C | 4, 5 | C | 3, 4 |
| IWP | 6, 7, 8 | IWP | 5, 6 |

| Key | | |
|---|---|---|
| 3 Week | Period 1 | 16 Cores |
| Spring 2018 | Period 2 | 12 Cores |
| Spring 2019 | Period 3 | 12 Cores |
| Spring 2020 | Period 4 | 12 Cores |
| Spring 2021 | Period 5 | 12 Cores |
| Total | | 64 Cores |

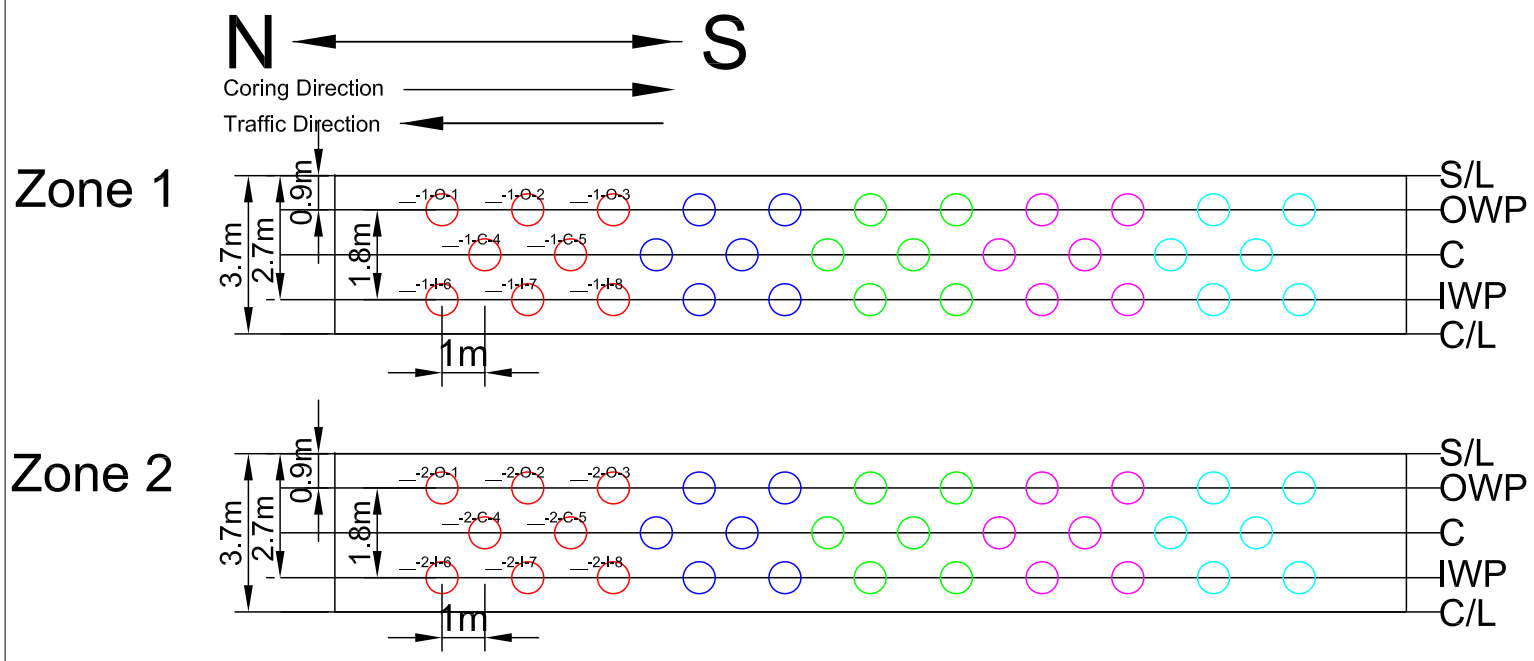

# Coring Map
# Section 1

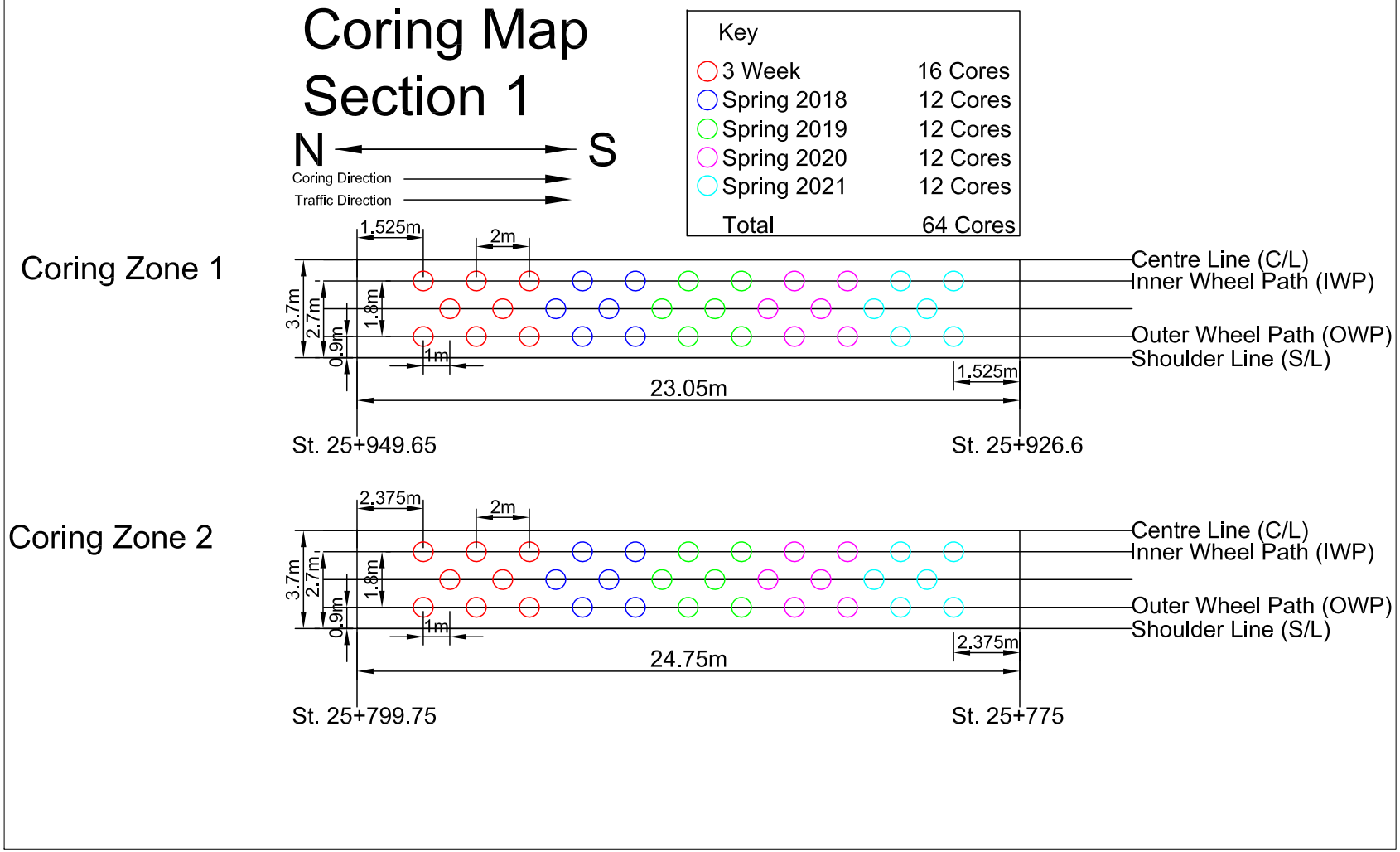

# Coring Map
# Section 2

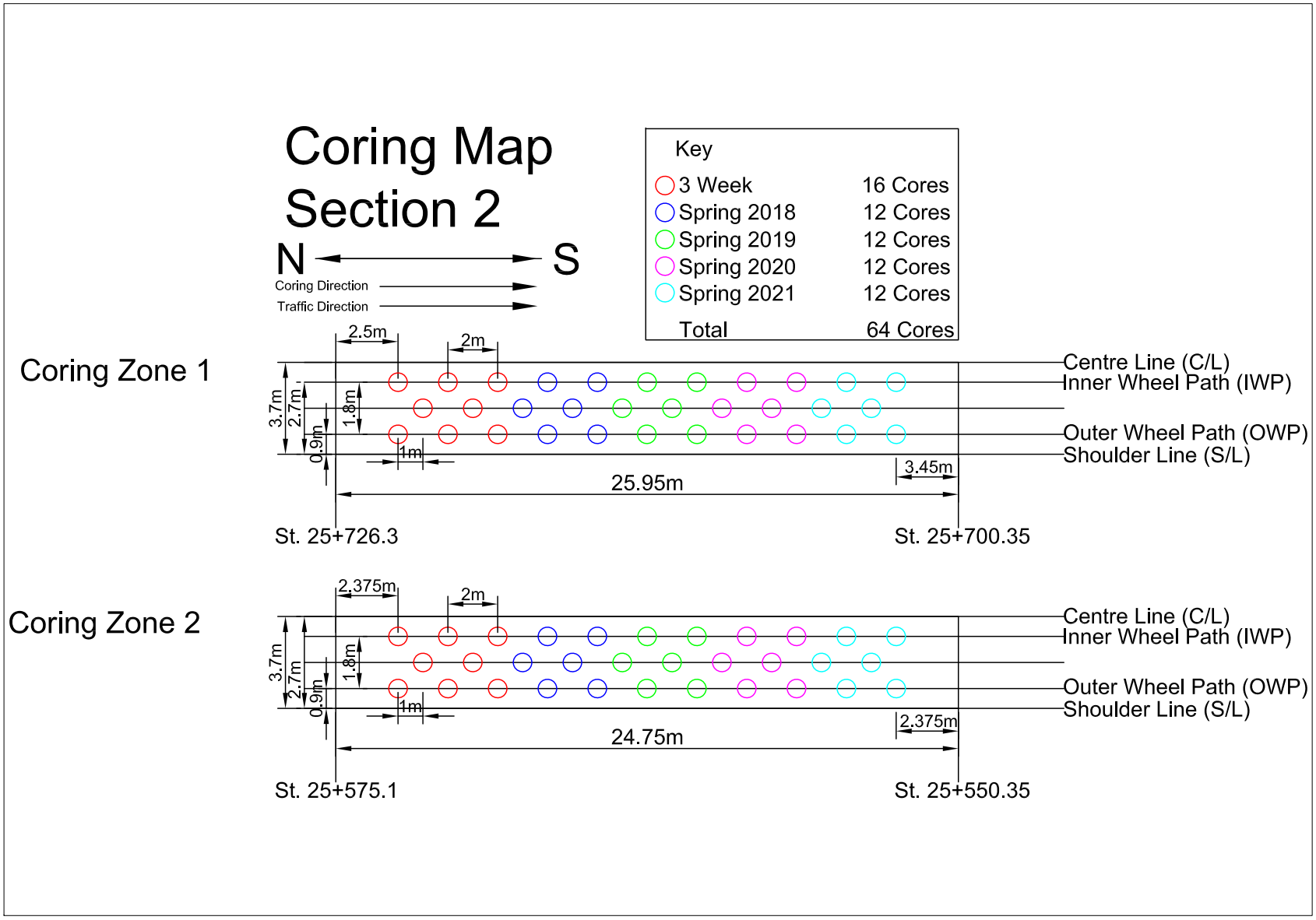

# Coring Map
# Section 3

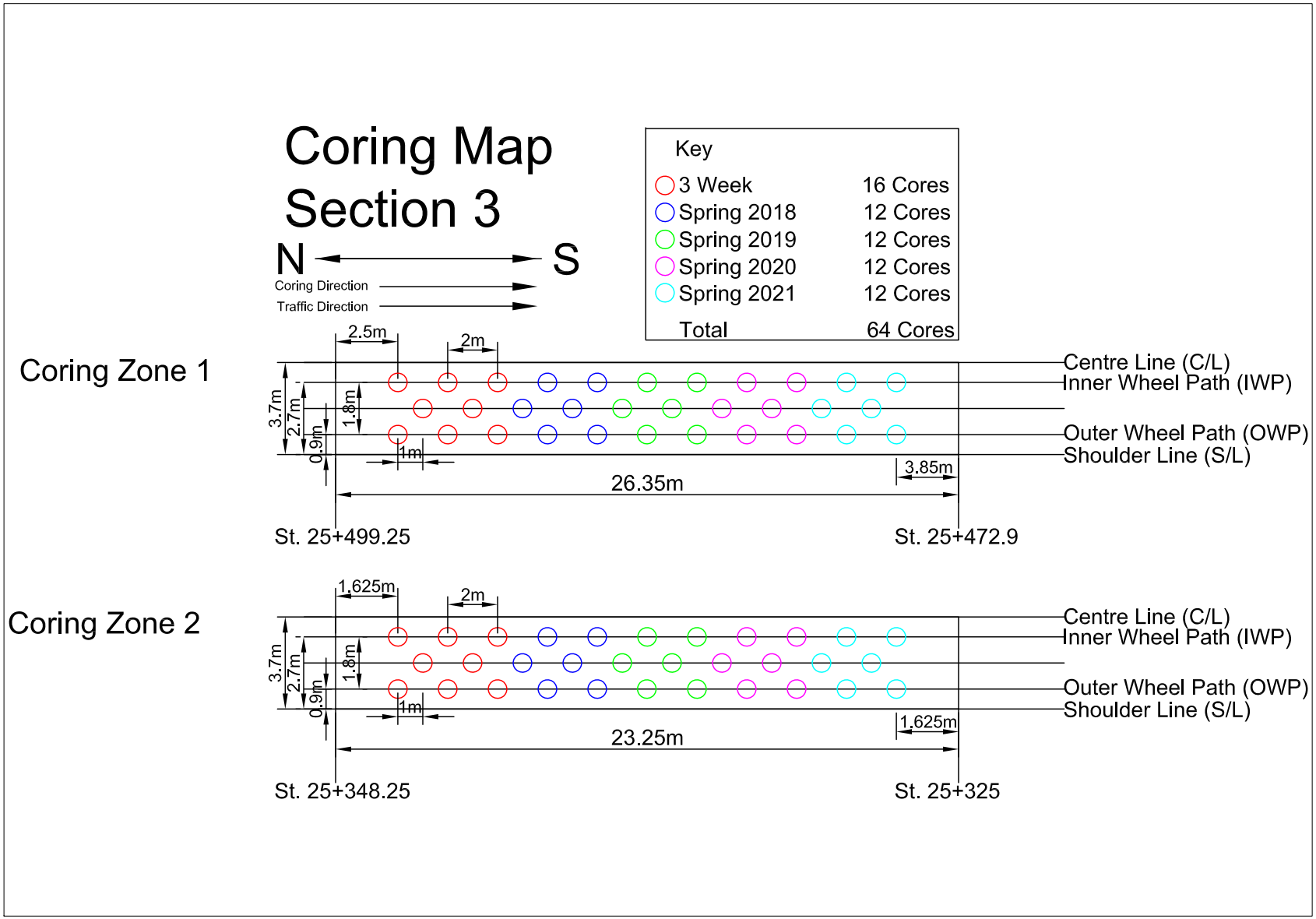

# Coring Map
# Section 4

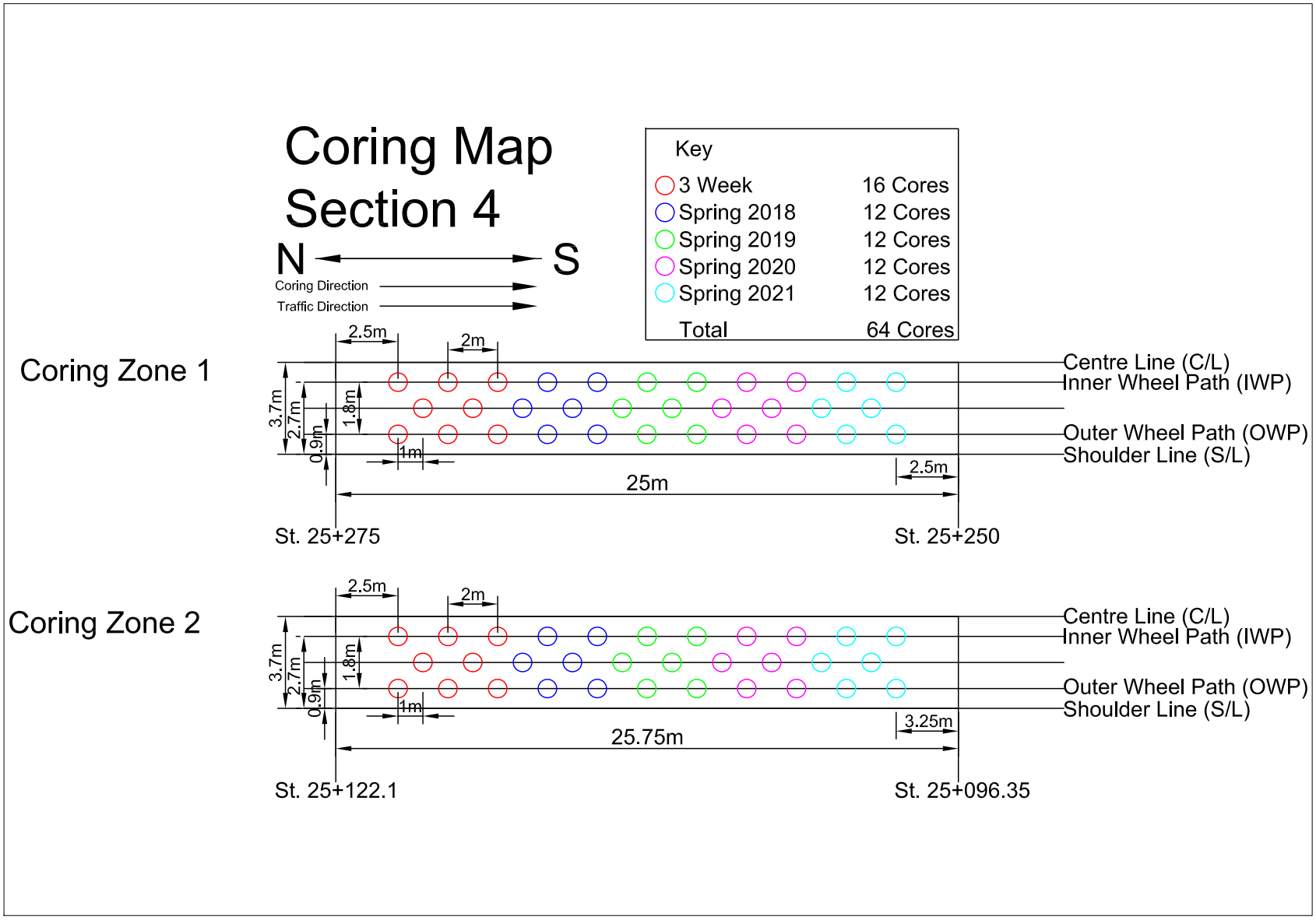

# Coring Map
# Section 5

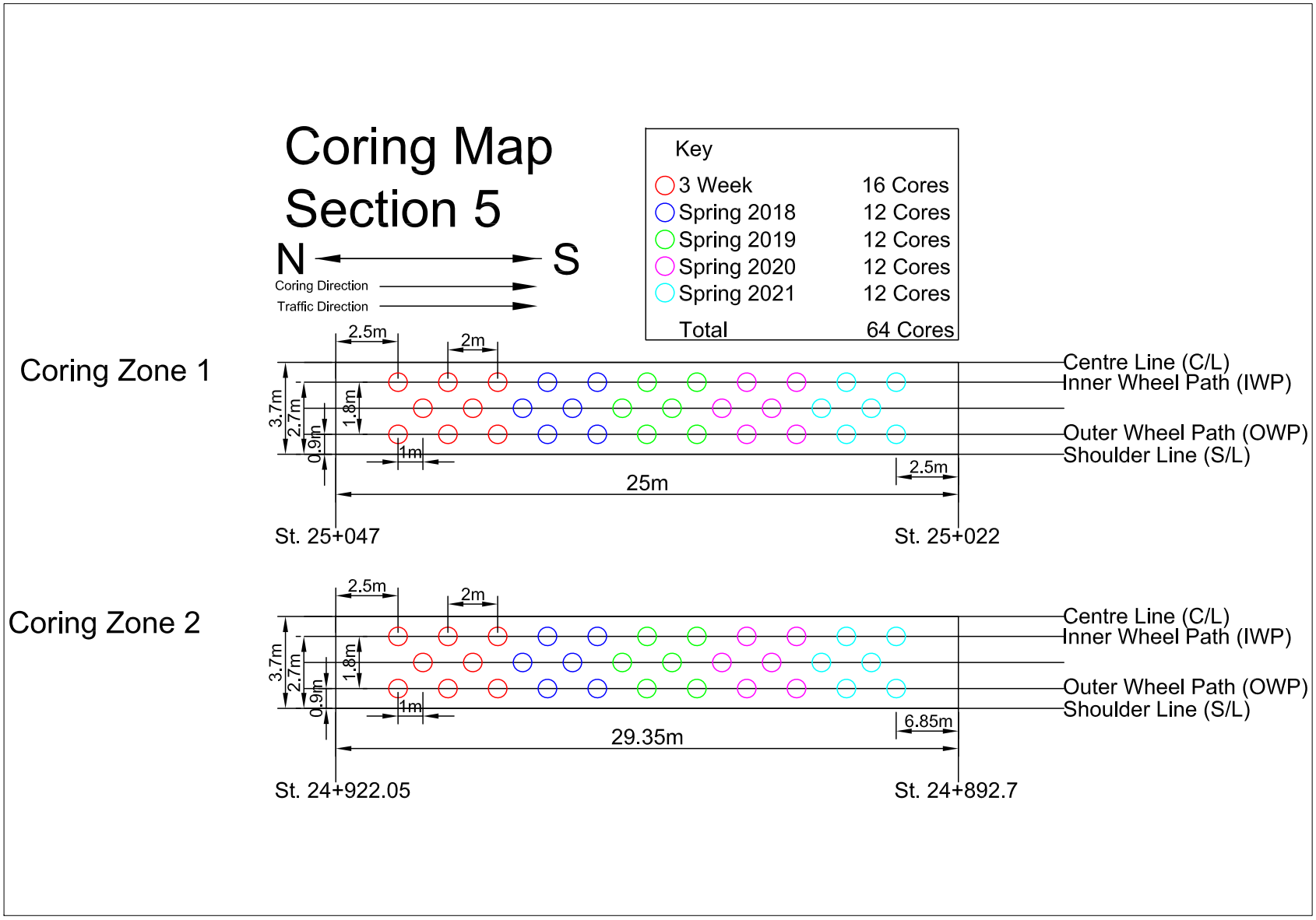

# Coring Map
# Section 6

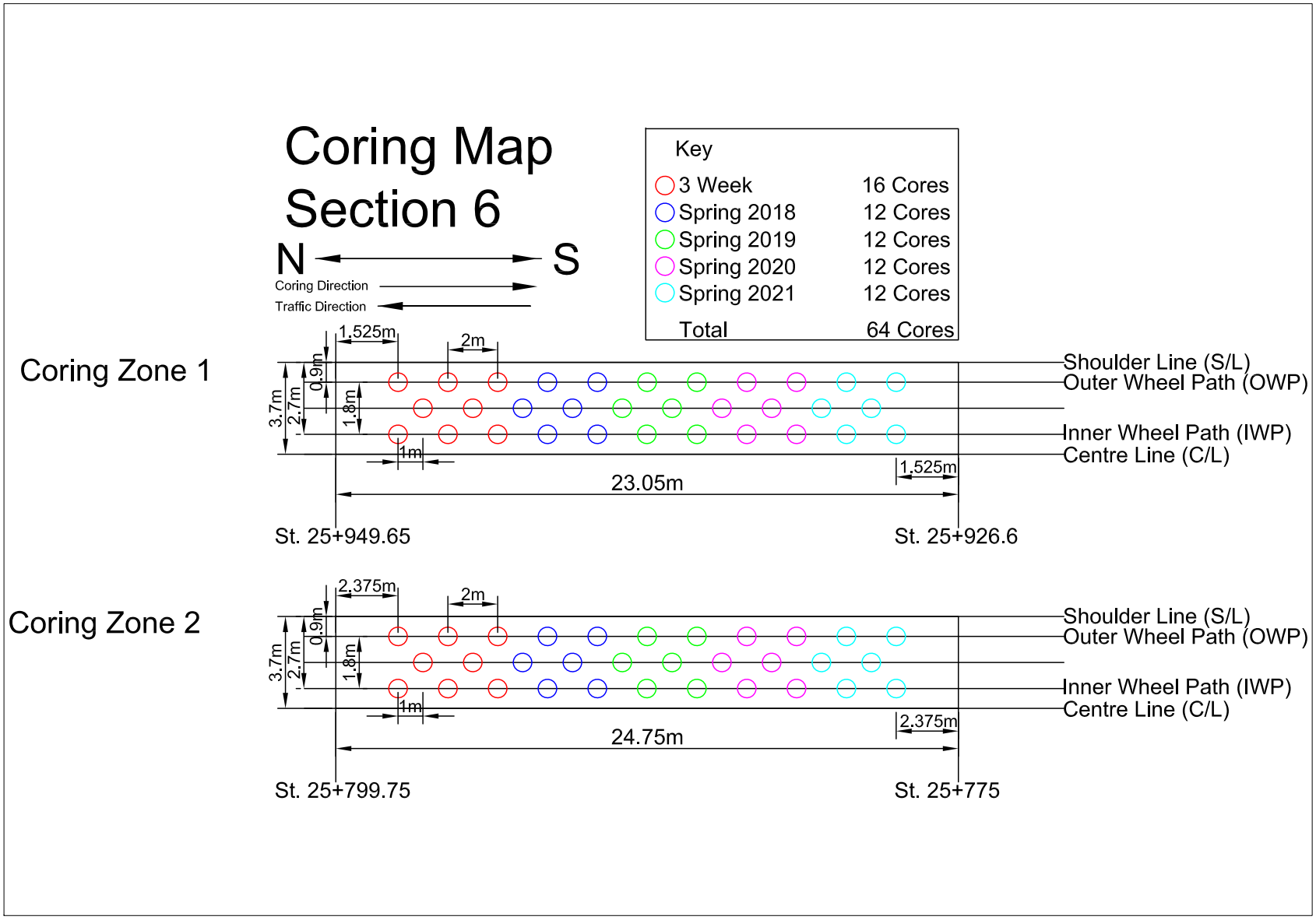

# Coring Map
# Section 7

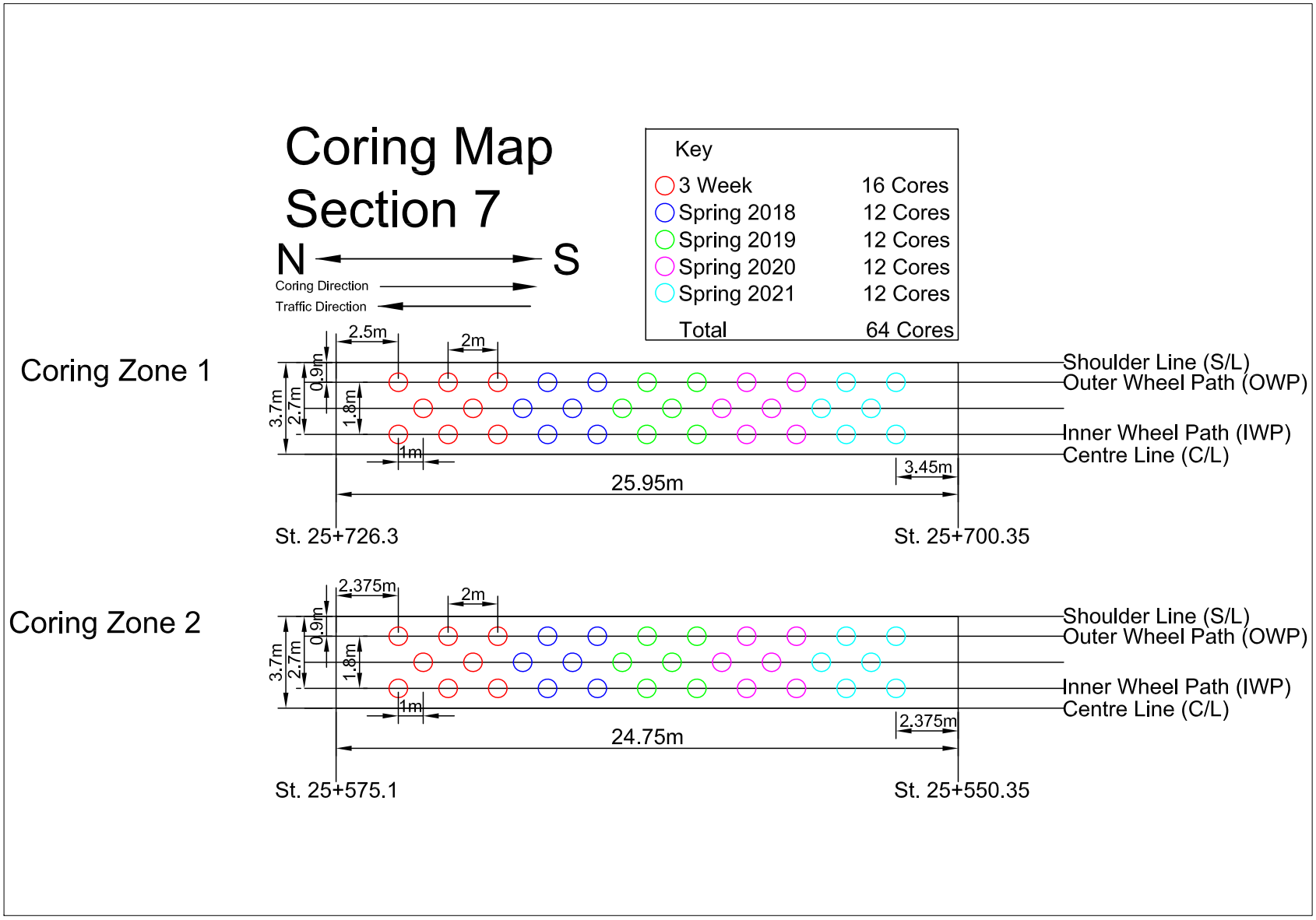

# Coring Map
# Section 8

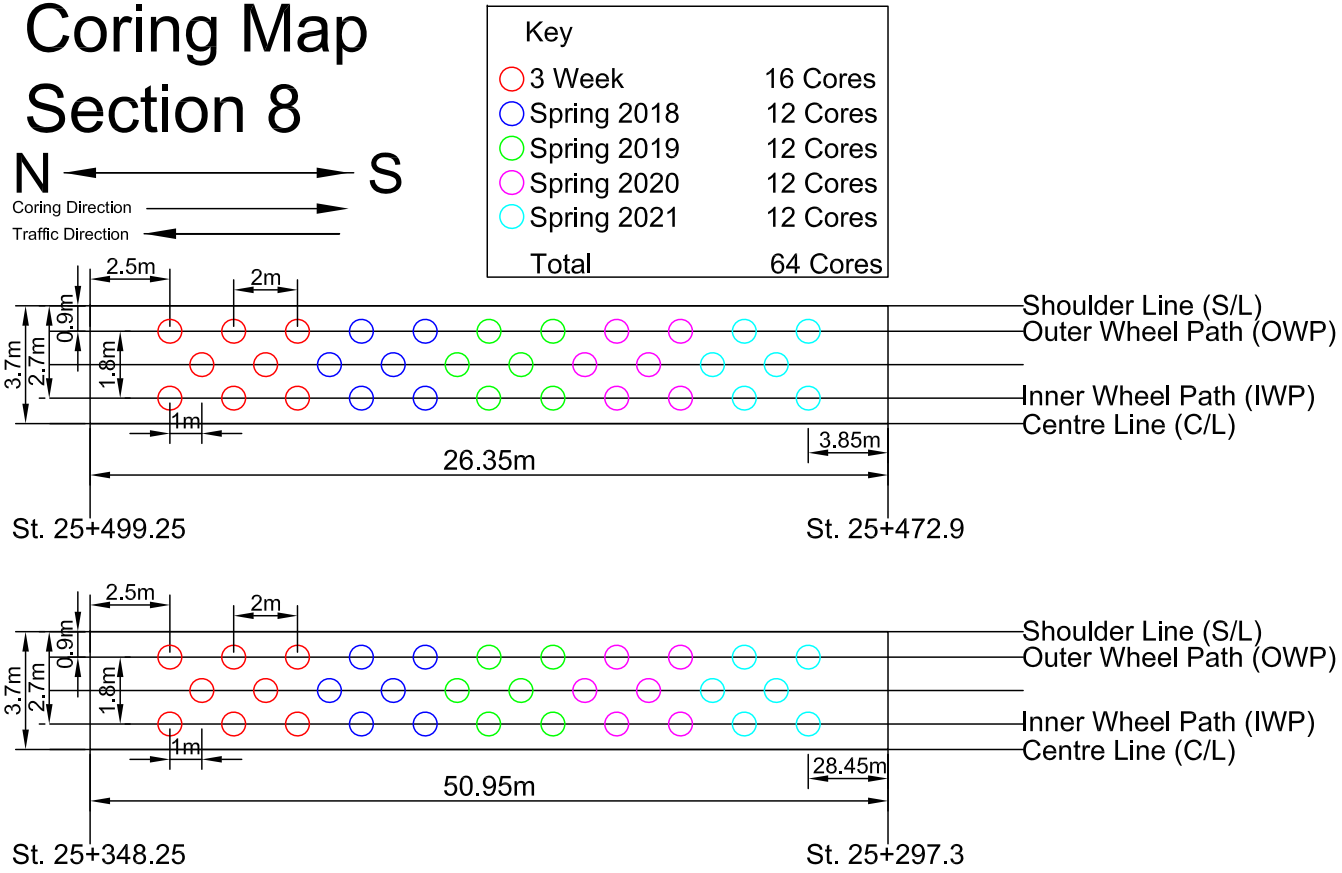

# Coring Map
# Section 9

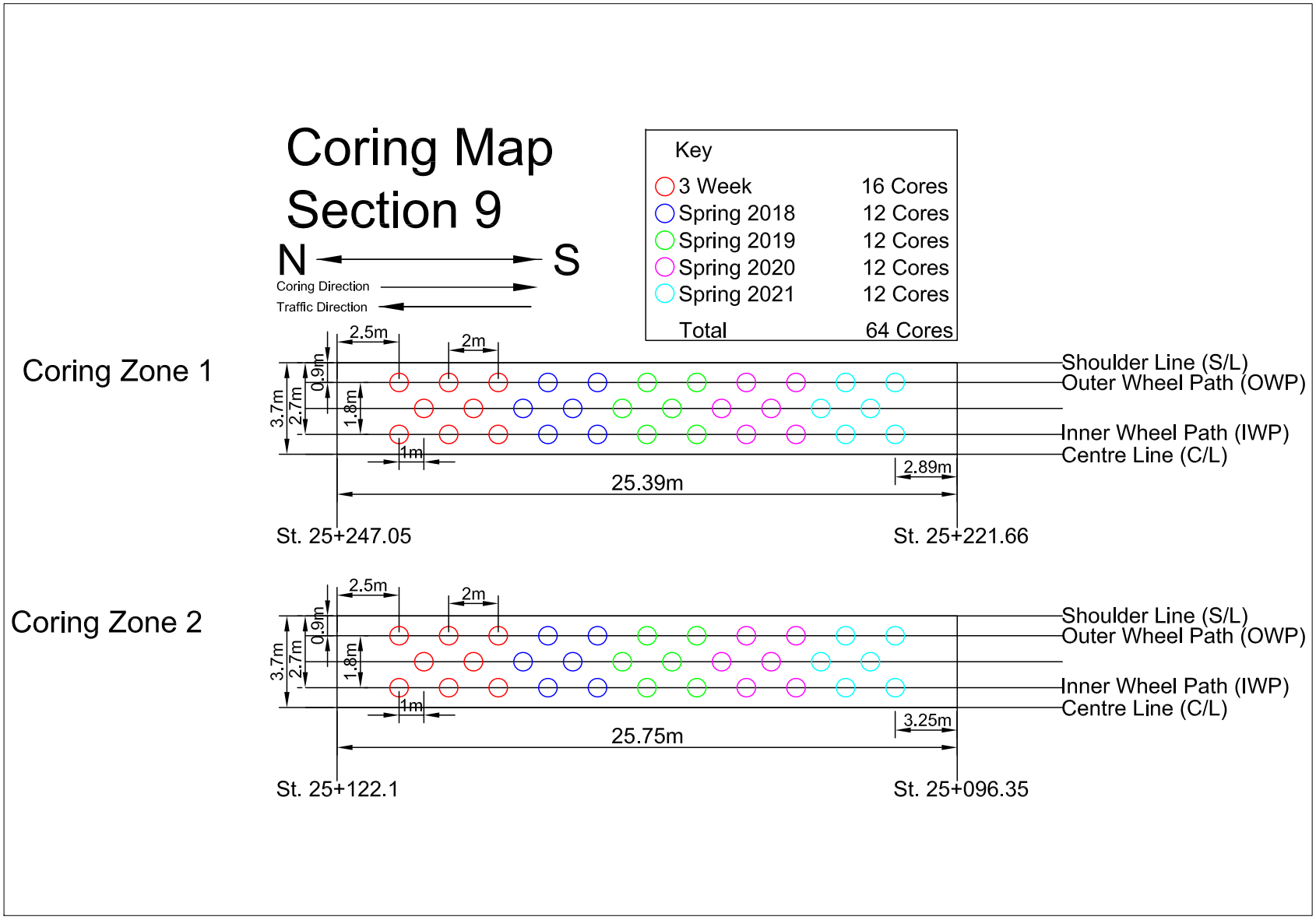

# Coring Map
# Section 10

N ⟷ S

Coring Direction →

Traffic Direction ←

| Key | |
|---|---|
| 3 Week | 16 Cores |
| Spring 2018 | 12 Cores |
| Spring 2019 | 12 Cores |
| Spring 2020 | 12 Cores |
| Spring 2021 | 12 Cores |
| Total | 64 Cores |

## Coring Zone 1

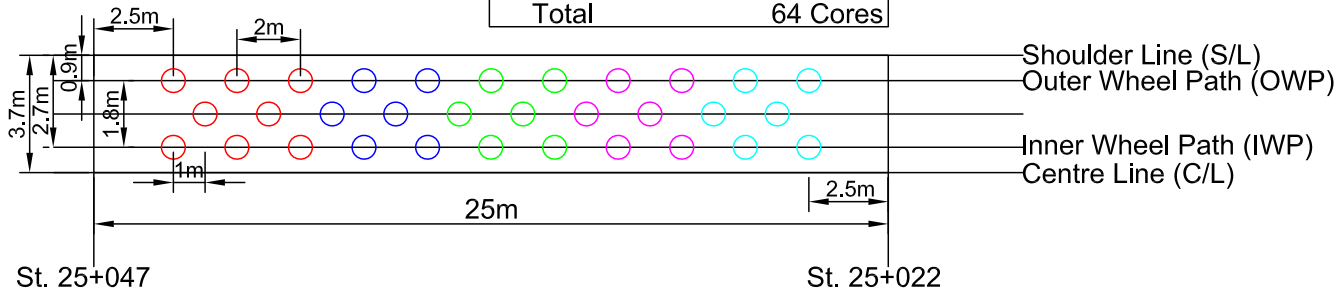


## Coring Zone 2

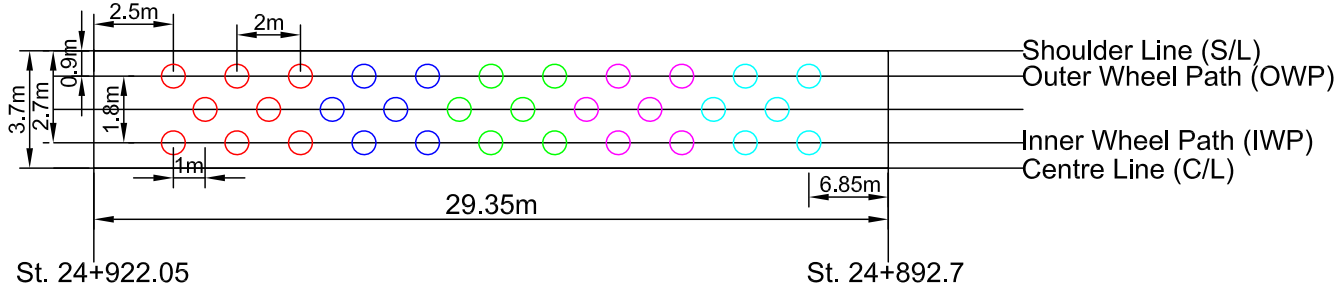

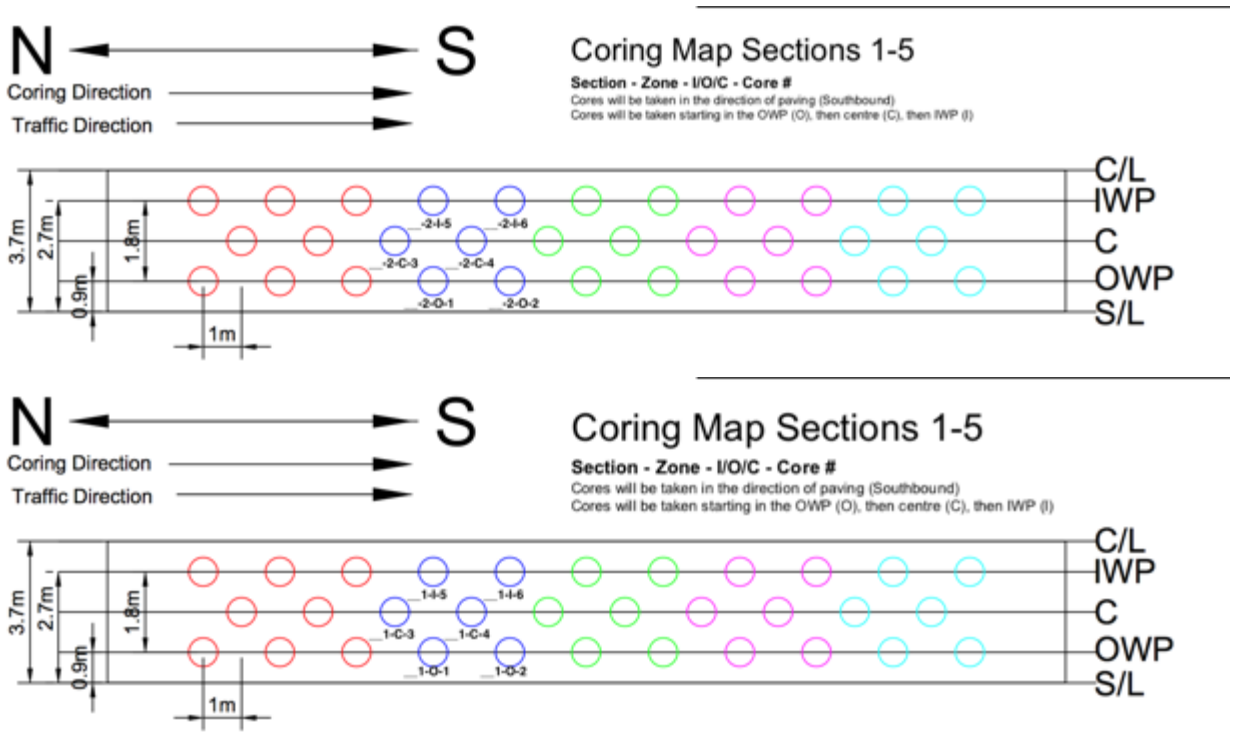


Period 2 – One Year After Construction

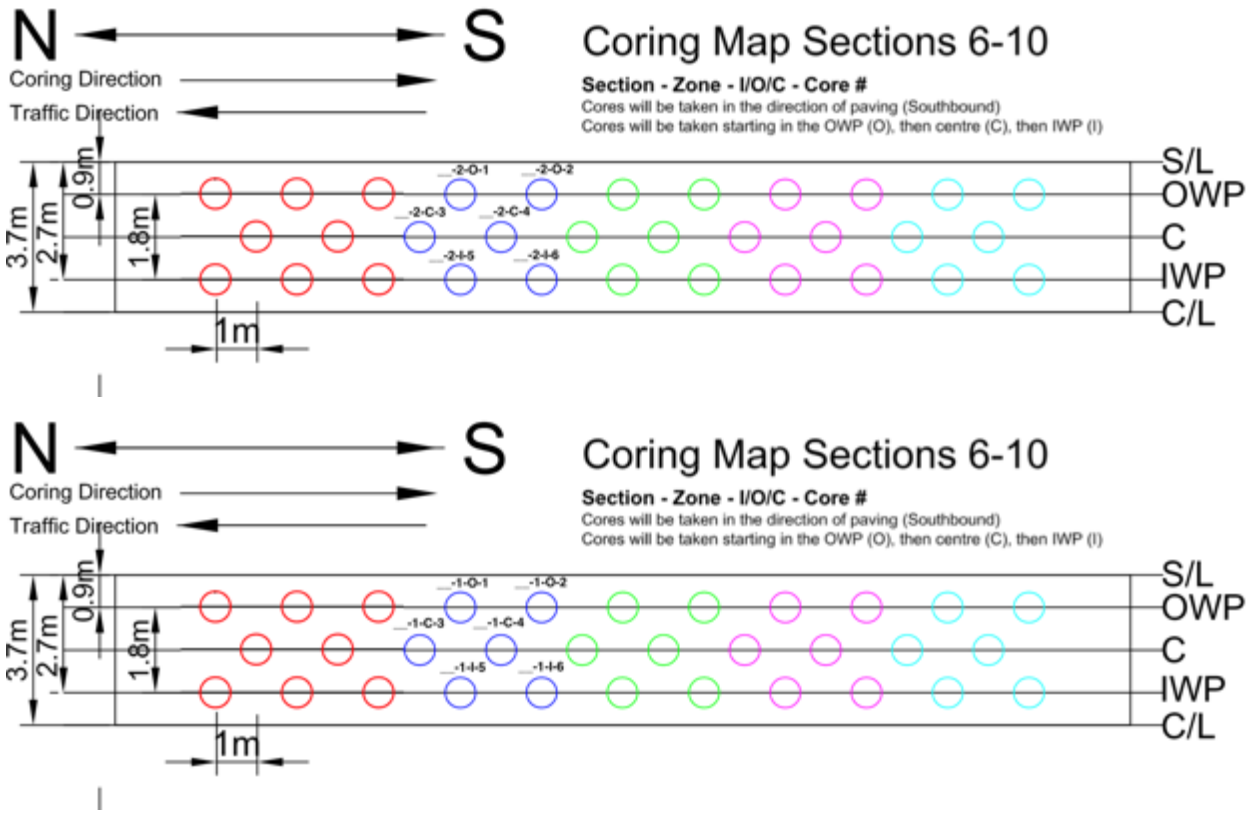


Period 2 – One Year After Construction

# APPENDIX E: Distress Survey Form



**Surface Defects Mapping Form**

| | |
|---|---|
| **Treatment** | |
| **Segment Name** | |
| **Road # or Description** | |
| **Site Location** | |
| **GPS Coordinates** | |

**Survey Date :** _____

**Time:**

**Localized Defects**

Monitored wheelpaths determined to be @ 0.9m and 2.7m from outside edge of shoulderline (Road Science)


| UNIFORM DEFECTS | | |
|---|---|---|
| **Type** | **Severity** | **Extent** |
| | | |

**REMARKS**

Rutting measured with a 1.5m and 1.8m rut bar in that order

Rutting measured in wheelpaths determined to be at 0.9m and 2.7m from outside edge of shoulderline.

Actual Rutting measurements recorded in millimeters below the rutting classification.

- Classification severity change
- Old Defect
- New Defect
- Under Seal not visible yet

**Signature**

## APPENDIX F: Construction Forms

**Product Preparation & Installation Form**

Product Name: _____

Date: _____

Dilution %: _____

Product Pre-Heated: Yes / No (Circle)

Application Temperature (C ): _____

Application Rate: _____

Air Temperature (C ): _____

Humidity: _____

Section Location (Start & end stations of the test section): _____

**Notes:**

**Tack Coat Break, Set, Cure Form**

| | |
|---|---|
| Test Section: | Comments: |
| Product: | |
| Date: | |
| Spray Time: | |
| Air Temp at Spray (C ): | |
| Humidity at Spray: | |
| Tack Coat Temp (C ): | |
| Set Time: | |
| Break Time: | |
| Cure Time: | |

**Pick-Up on Truck Tires Form**

**Test Section:** _____

**Product:** _____

| Date | Time | Severity of Pick-Up (Low, Med, High) | Stage When Measured (AB, BS, AS, AC) | Comments |
|---|---|---|---|---|
| | | | | |

## APPENDIX G: 2018 Distress Survey – One Year After Construction


**Figure G.1 Section 1 - Full Transverse Cracks, Crack Width <5mm & Coarse Aggregate Loss <5%**


**Figure G.2 Section 2 - Full Transverse Cracks, Crack Width <5mm & Coarse Aggregate Loss <5%**


**Figure G.3 Section 3 - Full Transverse Cracks, Crack Width <5mm & Coarse Aggregate Loss <5% & Ravelling <5%**


**Figure G.4 Section 4 - Full Transverse Cracks, Crack Width <5mm & Coarse Aggregate Loss <5%**


**Figure G.5 Section 5 - Coarse Aggregate Loss <5%**


**Figure G.6 Section 6 - Full Transverse Cracks, Crack Width <5mm & Coarse Aggregate Loss <5% & Ravelling <5%**


55-1
50-50W
SECTION 6


55-1
50-50W
SECTION 6

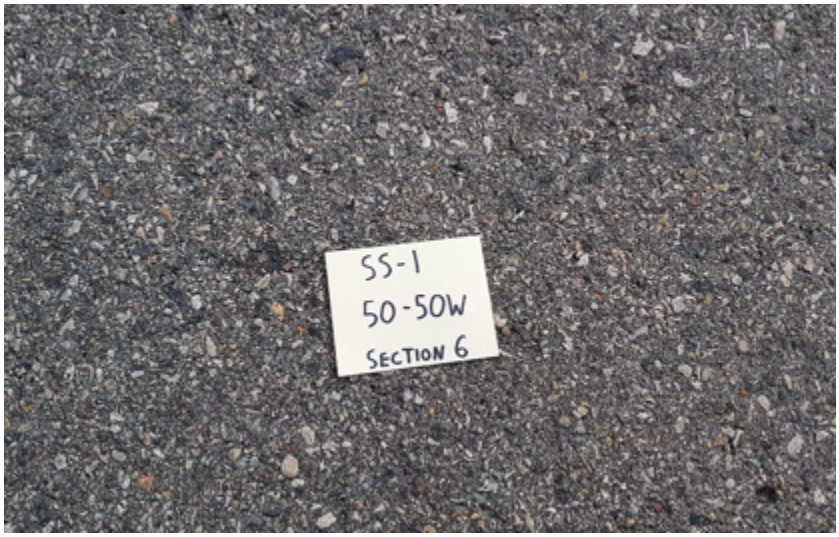


**Figure G.7 Section 6 - Full Transverse Cracks, Crack Width <5mm & Coarse Aggregate Loss <5% & Ravelling <5% (Cont'd)**


**Figure G.8 Section 7 – Full and Half Transverse Cracks, Crack Width <5mm & Coarse Aggregate Loss <5%**


**Figure G.9 Section 8 - Full Transverse Cracks, Crack Width <5mm & Coarse Aggregate Loss <5% & Ravelling <5%**


**Figure G.10 Section 9 – Full and Half Transverse Cracks, Crack Width <5mm & Coarse Aggregate Loss <5%**


**Figure G.11 Section 10 - Coarse Aggregate Loss <5%**

## APPENDIX H: Additional Tables and Plots

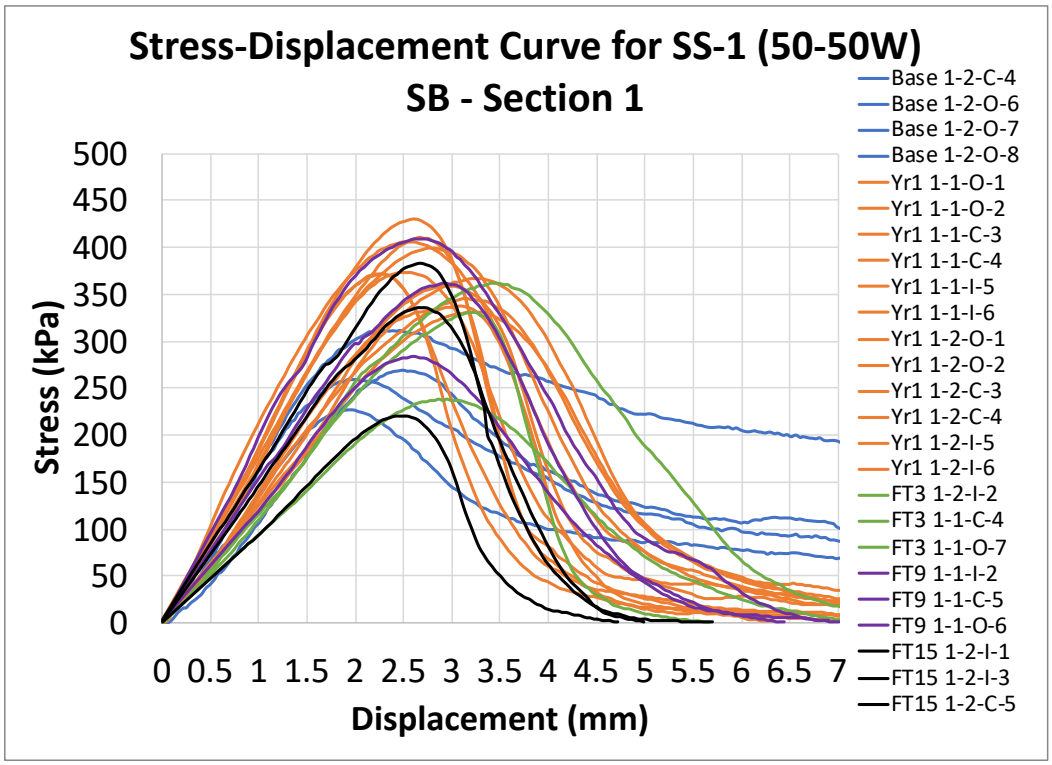


**Figure H.1 Stress-Displacement Curve for All Cores in Section 1 - SS-1 (50-50W) SB**

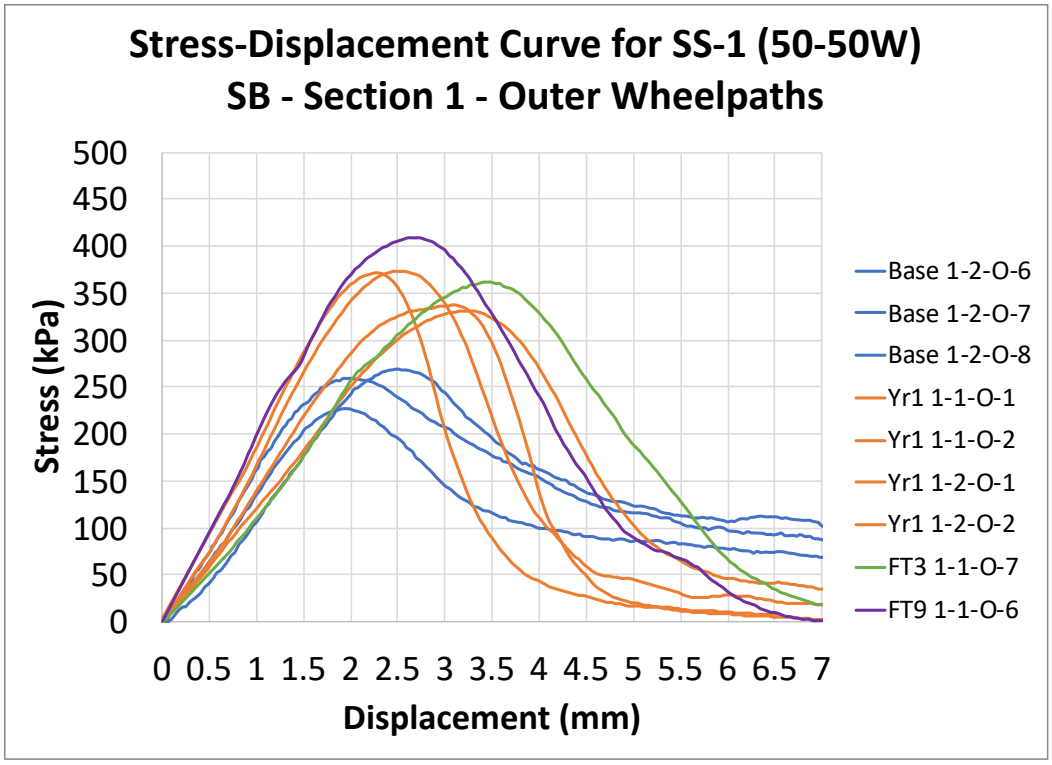


**Figure H.2 Stress-Displacement Curve for Outer Wheel Path Cores in Section 1 - SS-1 (50-50W) SB**

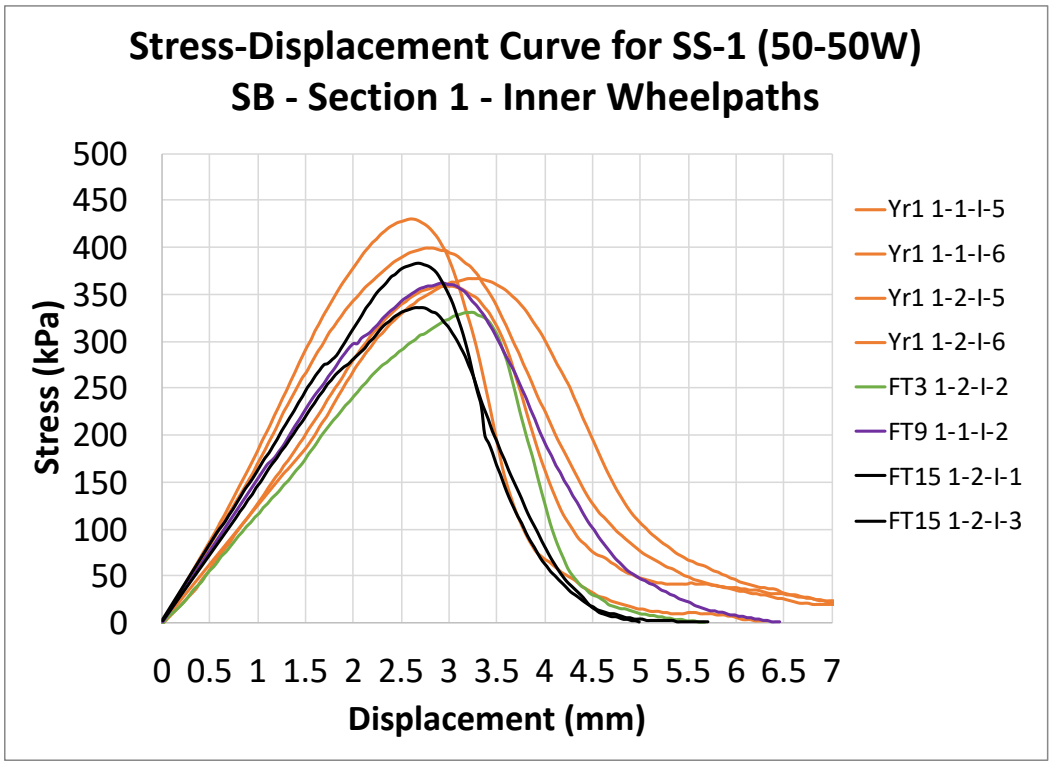


**Figure H.3 Stress-Displacement Curve for Inner Wheel Path Cores in Section 1 - SS-1 (50-50W) SB**

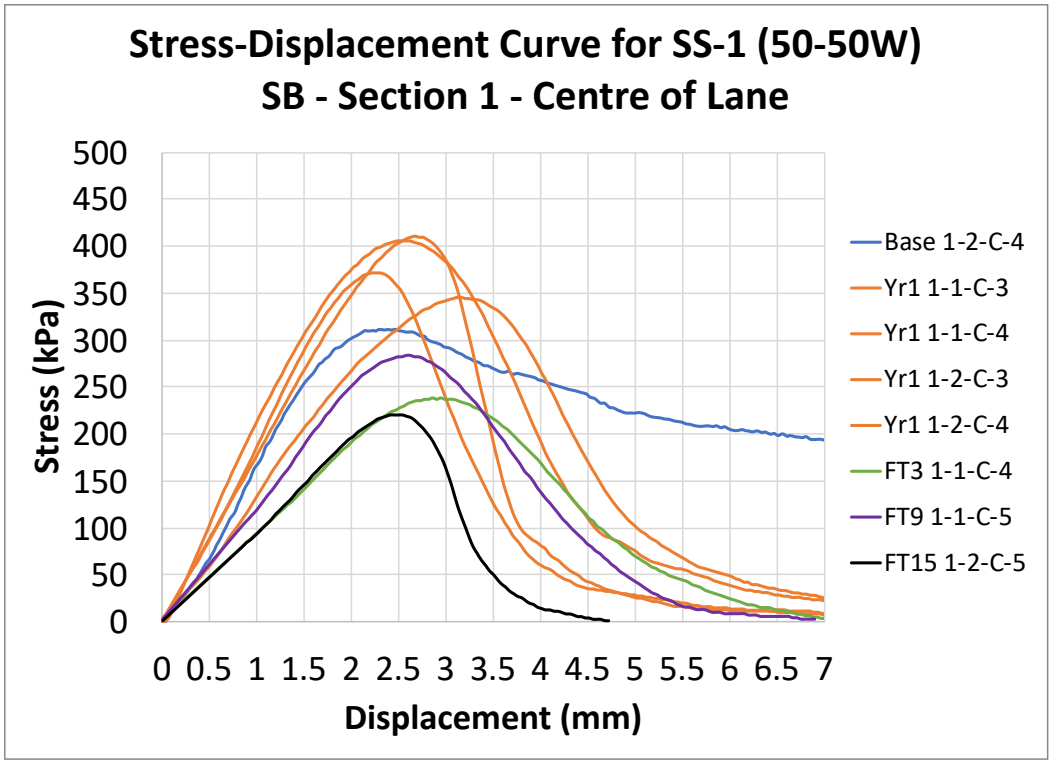


**Figure H.4 Stress-Displacement Curve for Centre of the Lane Cores in Section 1 - SS-1 (50-50W) SB**

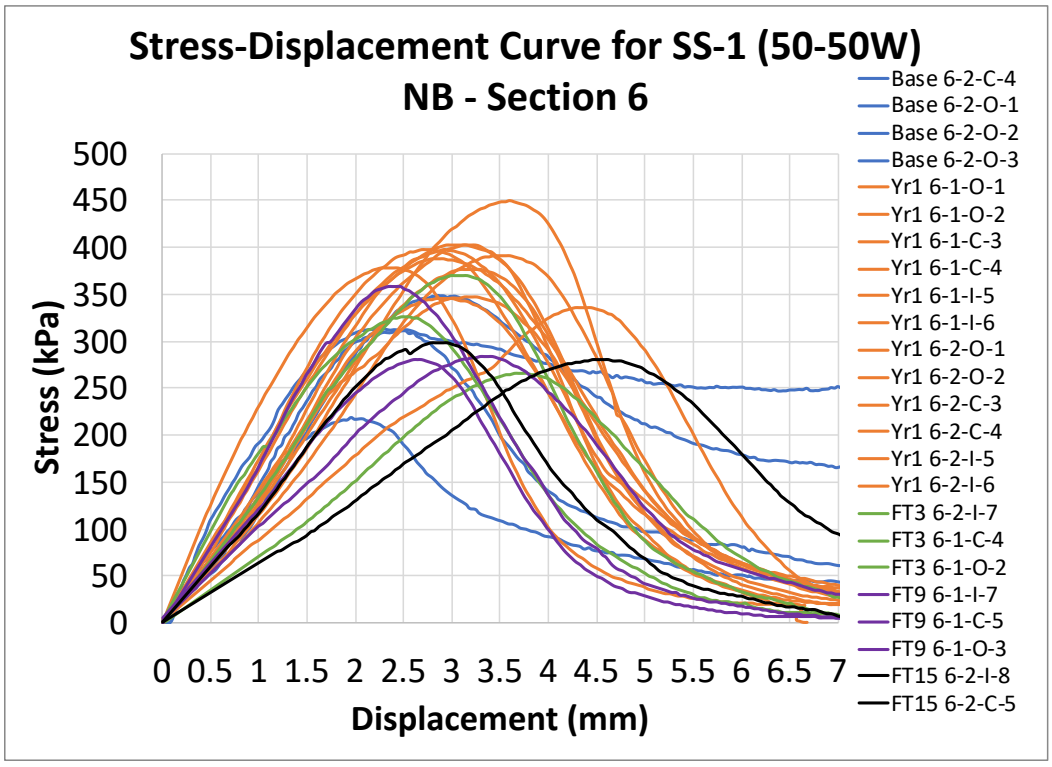


**Figure H.5 Stress-Displacement Curve for All Cores in Section 6 - SS-1 (50-50W) NB**

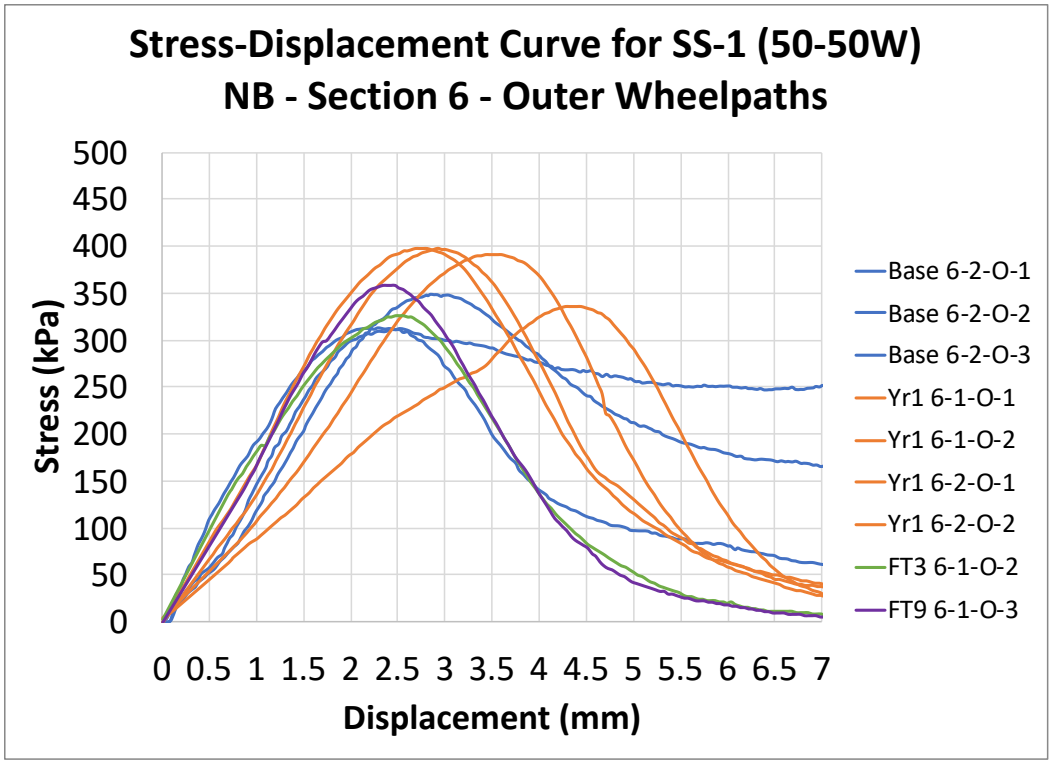


**Figure H.6 Stress-Displacement Curve for Outer Wheel Path Cores in Section 6 - SS-1 (50-50W) NB**

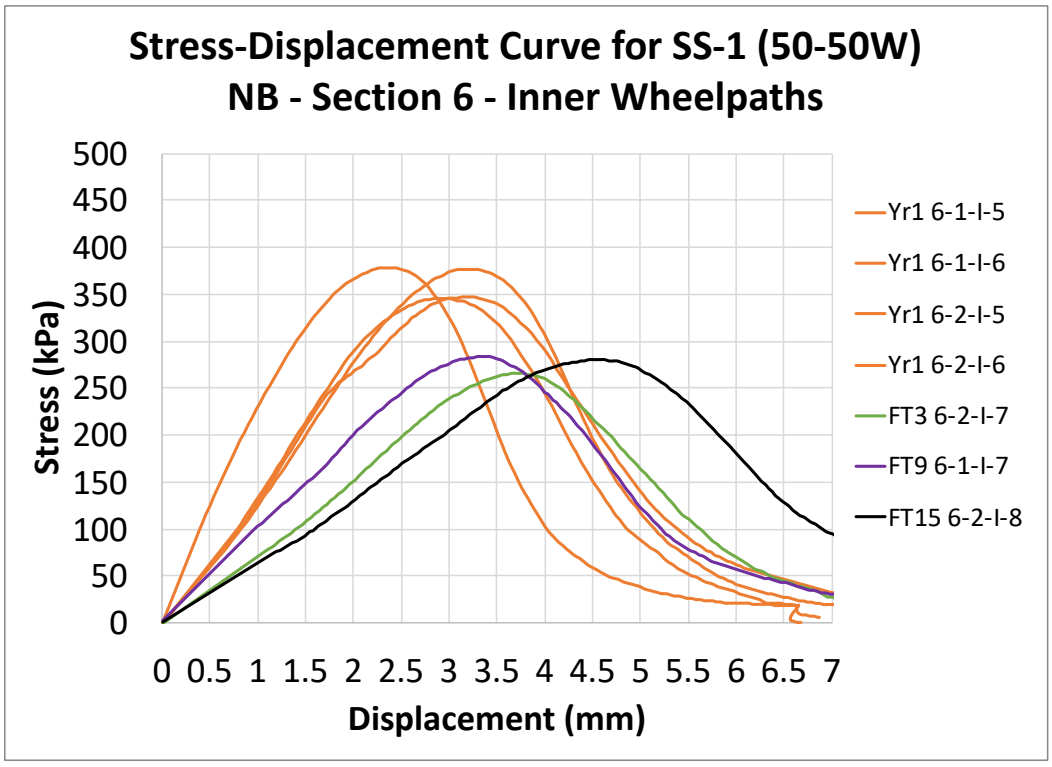


**Figure H.7 Stress-Displacement Curve for Inner Wheel Path Cores in Section 6 - SS-1 (50-50W) NB**

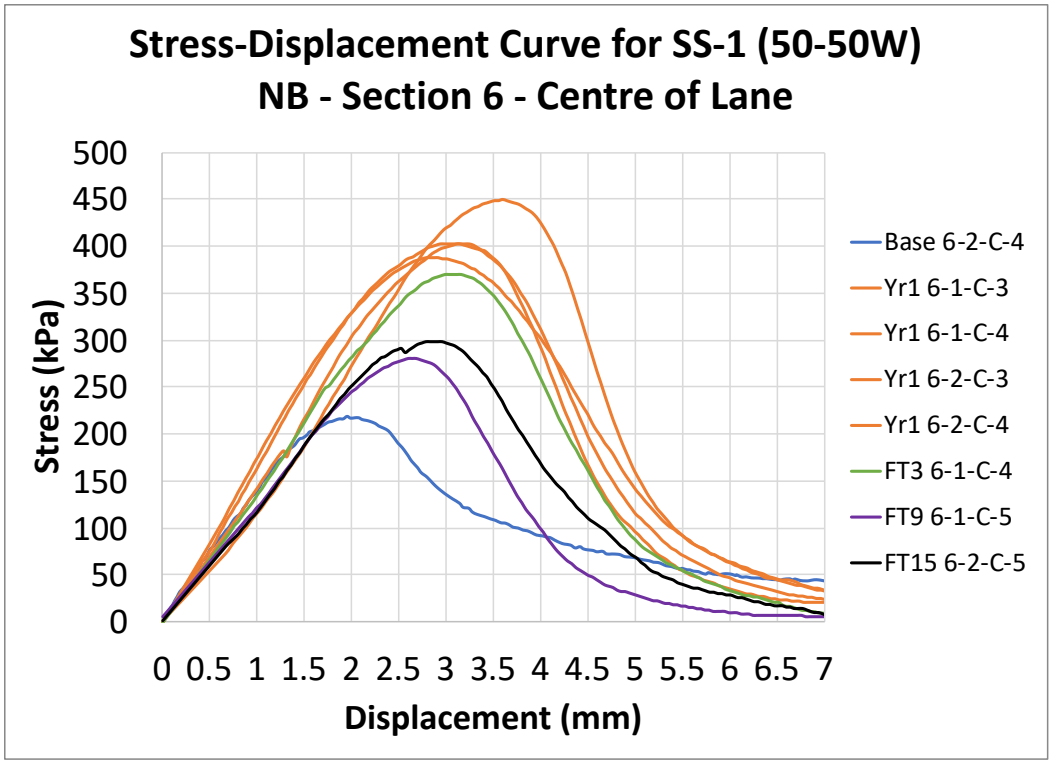


**Figure H.8 Stress-Displacement Curve for Centre of the Lane Cores in Section 6 - SS-1 (50-50W) NB**

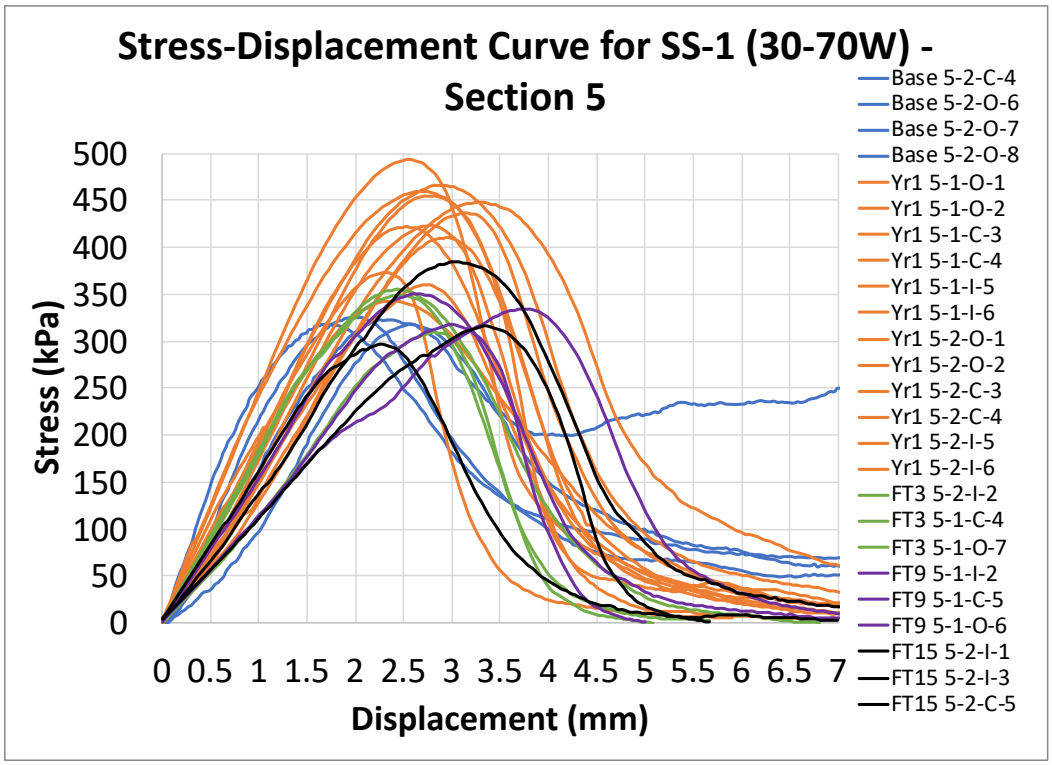


**Figure H.9 Stress-Displacement Curve for All Cores in Section 5 - SS-1 (30-70W)**

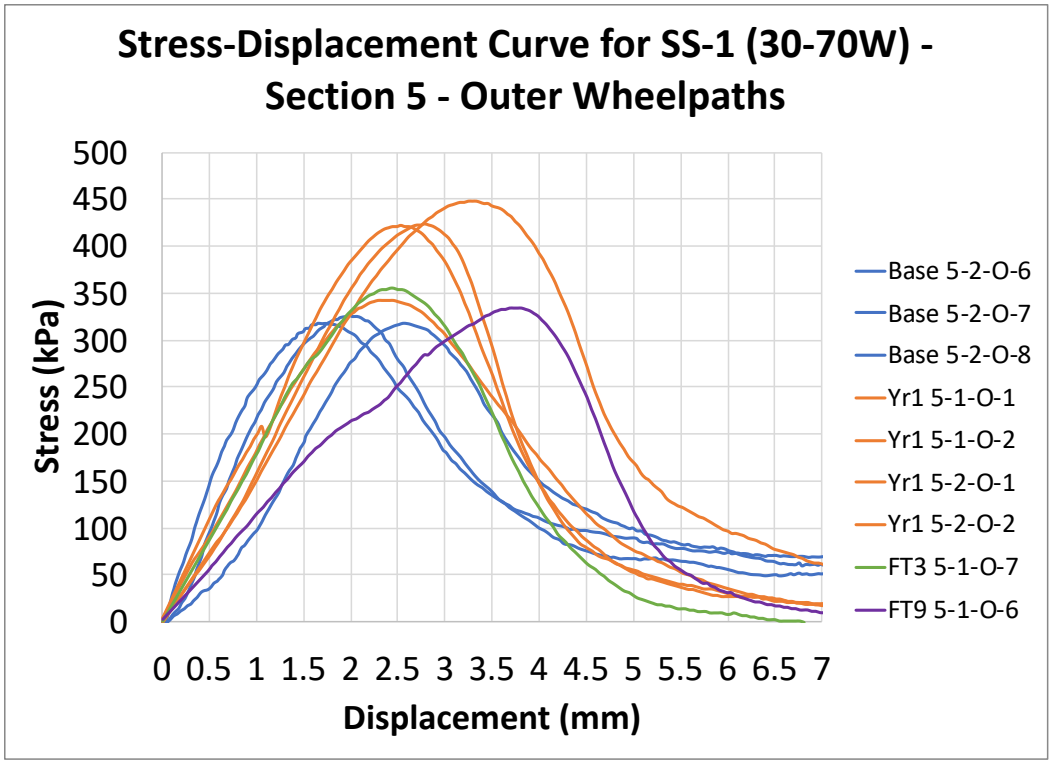


**Figure H.10 Stress-Displacement Curve for Outer Wheel Path Cores in Section 5 - SS-1 (30-70W)**

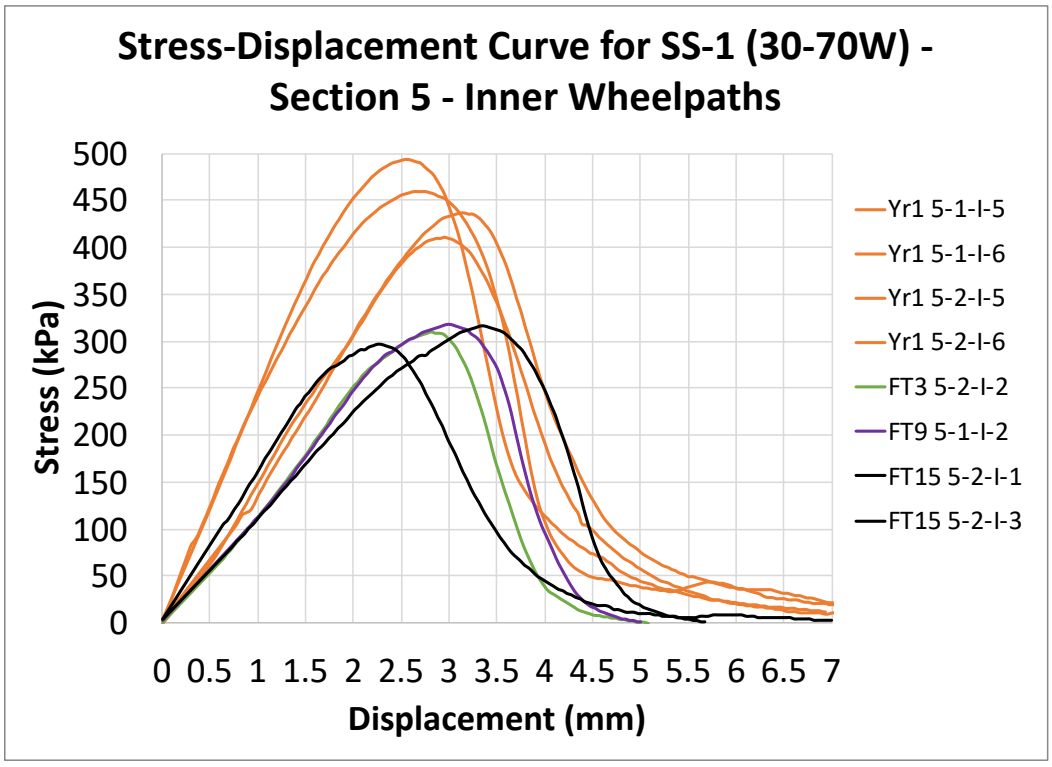


**Figure H.11 Stress-Displacement Curve for Inner Wheel Path Cores in Section 5 - SS-1 (30-70W)**

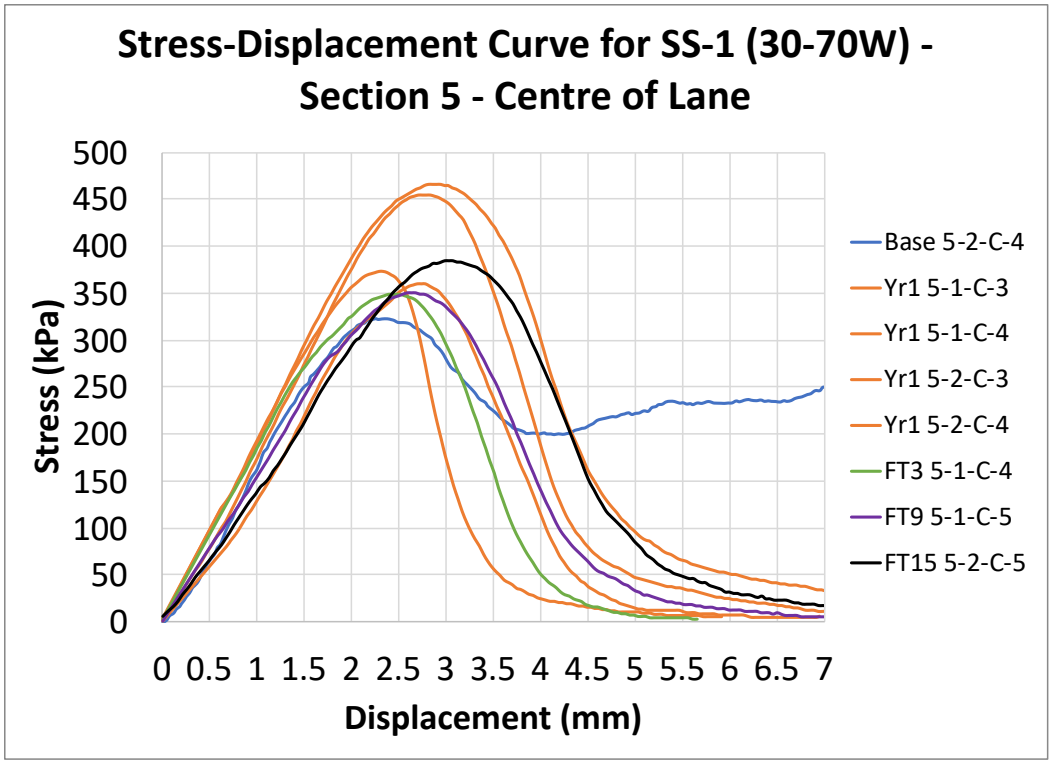


**Figure H.12 Stress-Displacement Curve for Centre of the Lane Cores in Section 5 - SS-1 (30-70W)**

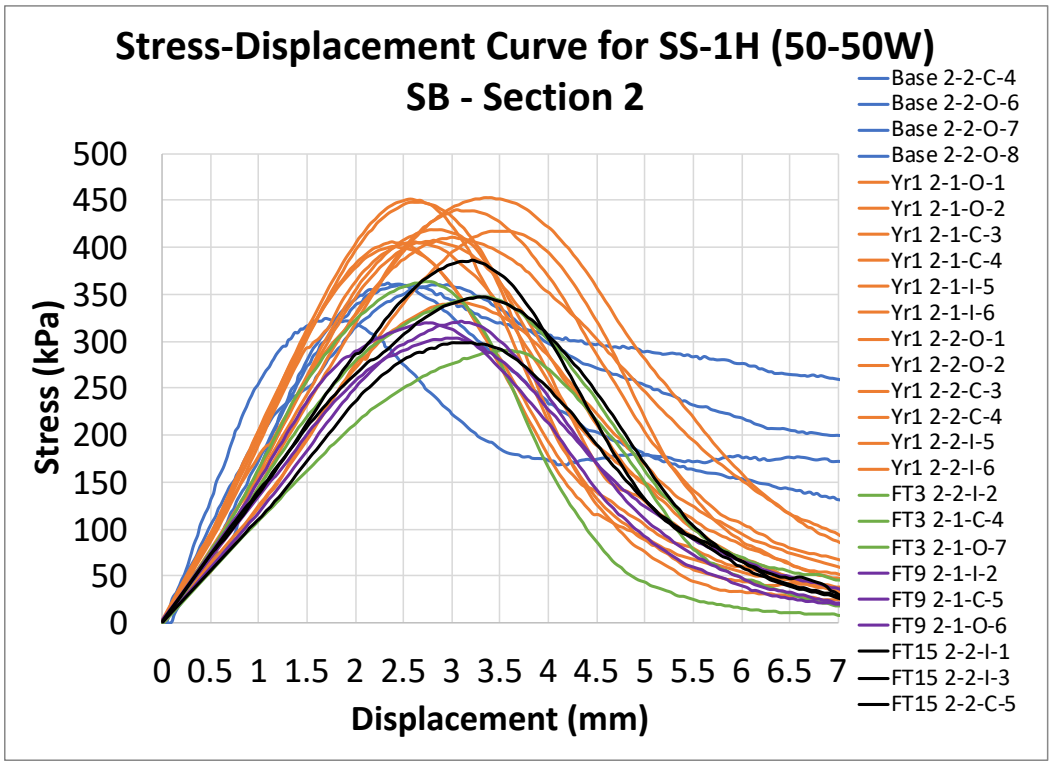


**Figure H.13 Stress-Displacement Curve for All Cores in Section 2 - SS-1h (50-50W) SB**

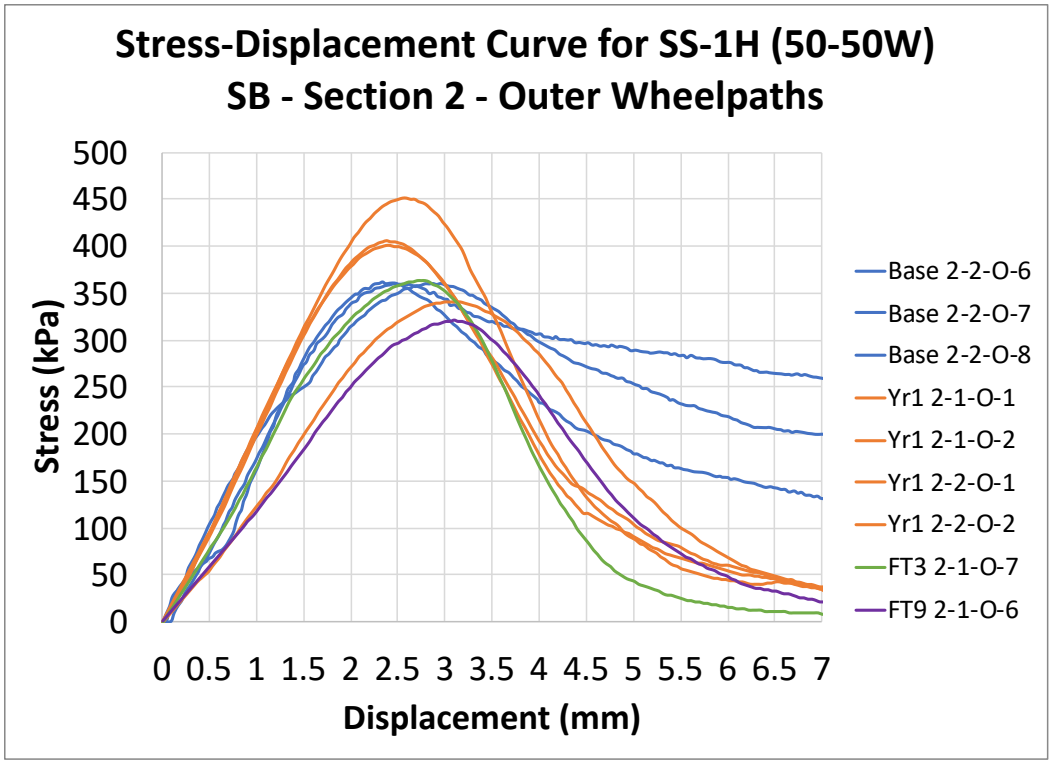


**Figure H.14 Stress-Displacement Curve for Outer Wheel Path Cores in Section 2 - SS-1h (50-50W) SB**

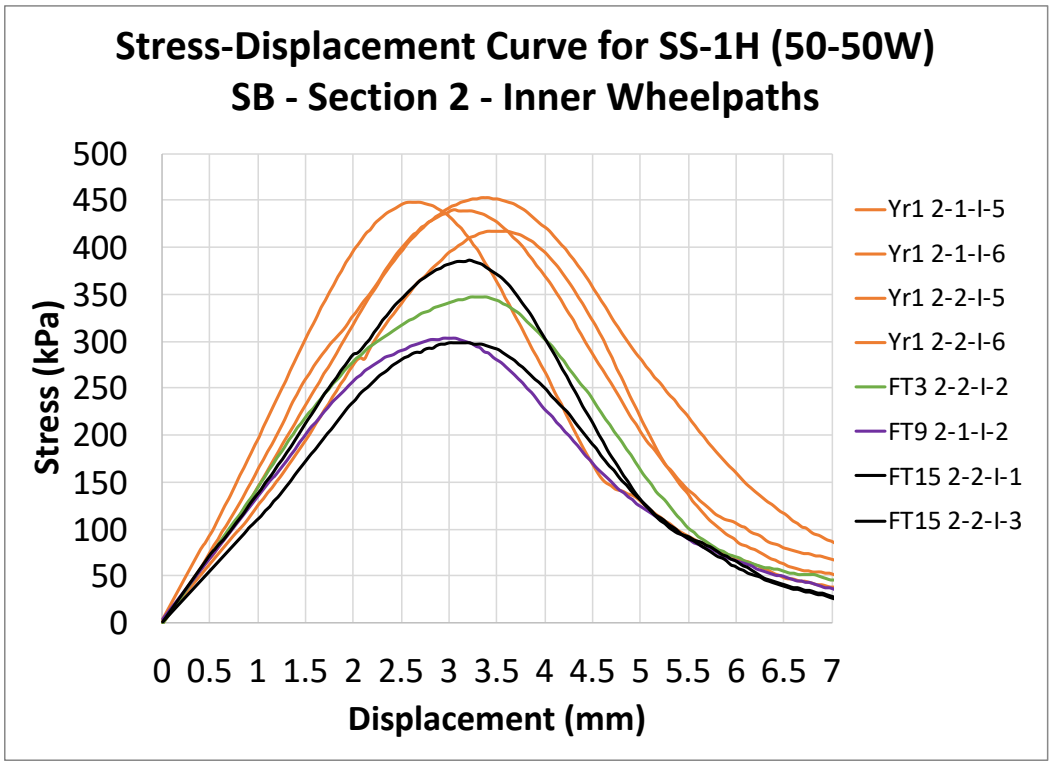


**Figure H.15 Stress-Displacement Curve for Inner Wheel Path Cores in Section 2 - SS-1h (50-50W) SB**

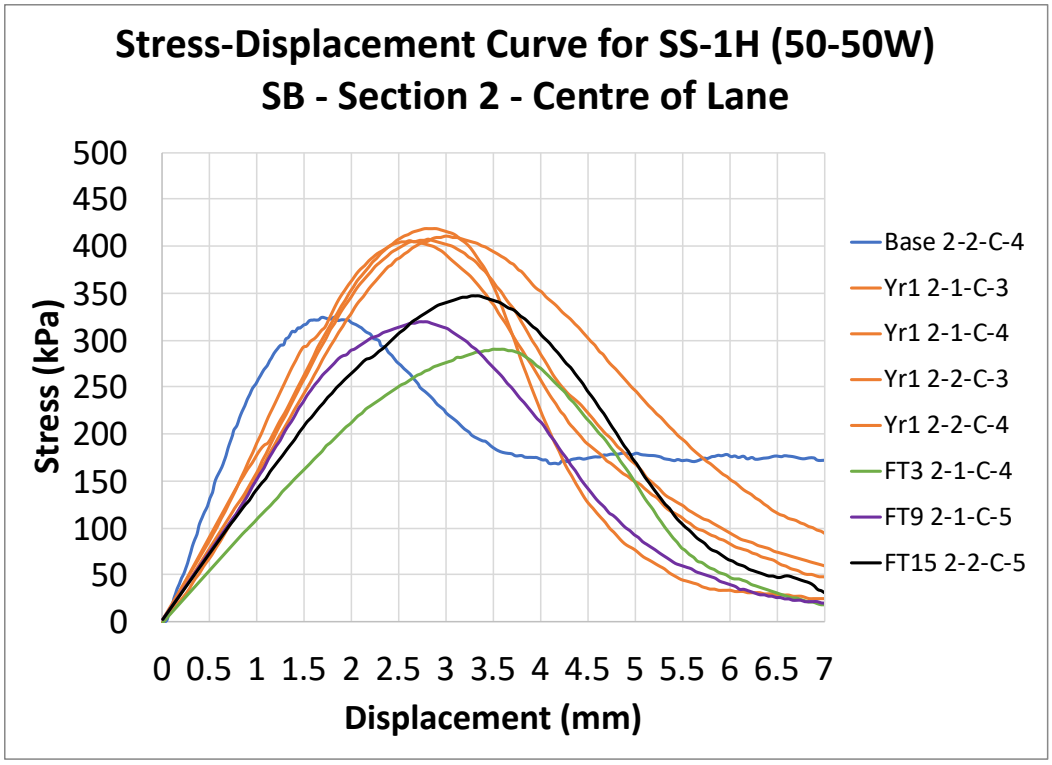


**Figure H.16 Stress-Displacement Curve for Centre of the Lane Cores in Section 2 - SS-1h (50-50W) SB**

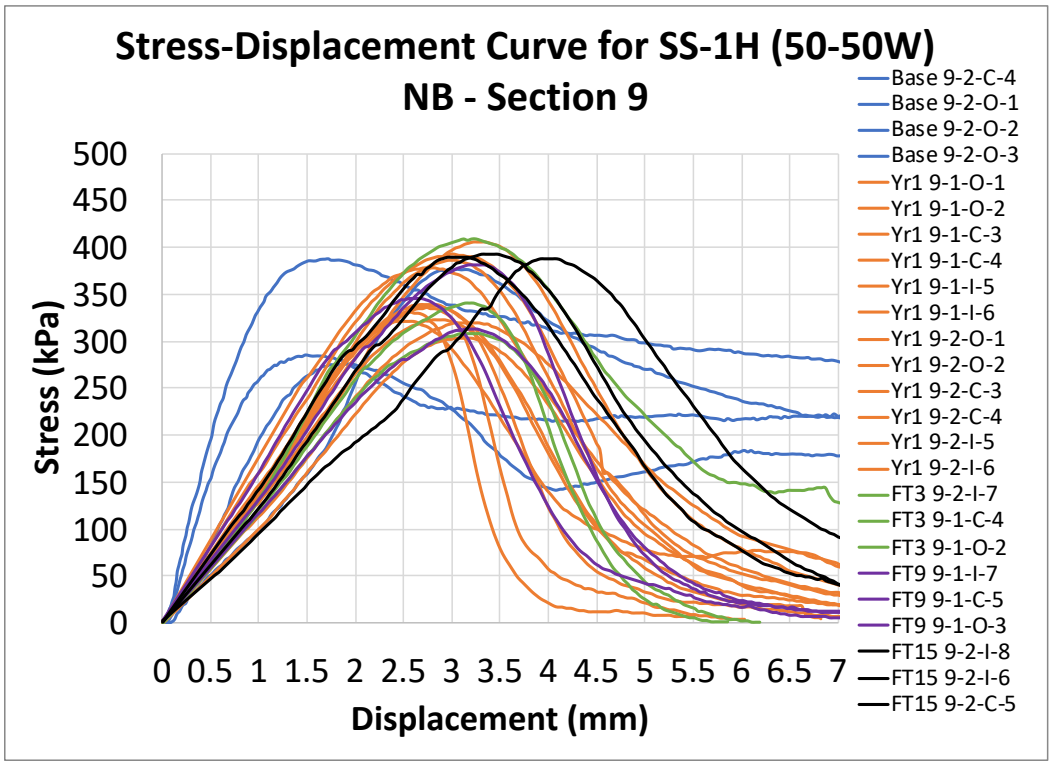


**Figure H.17 Stress-Displacement Curve for All Cores in Section 9 - SS-1h (50-50W) NB**

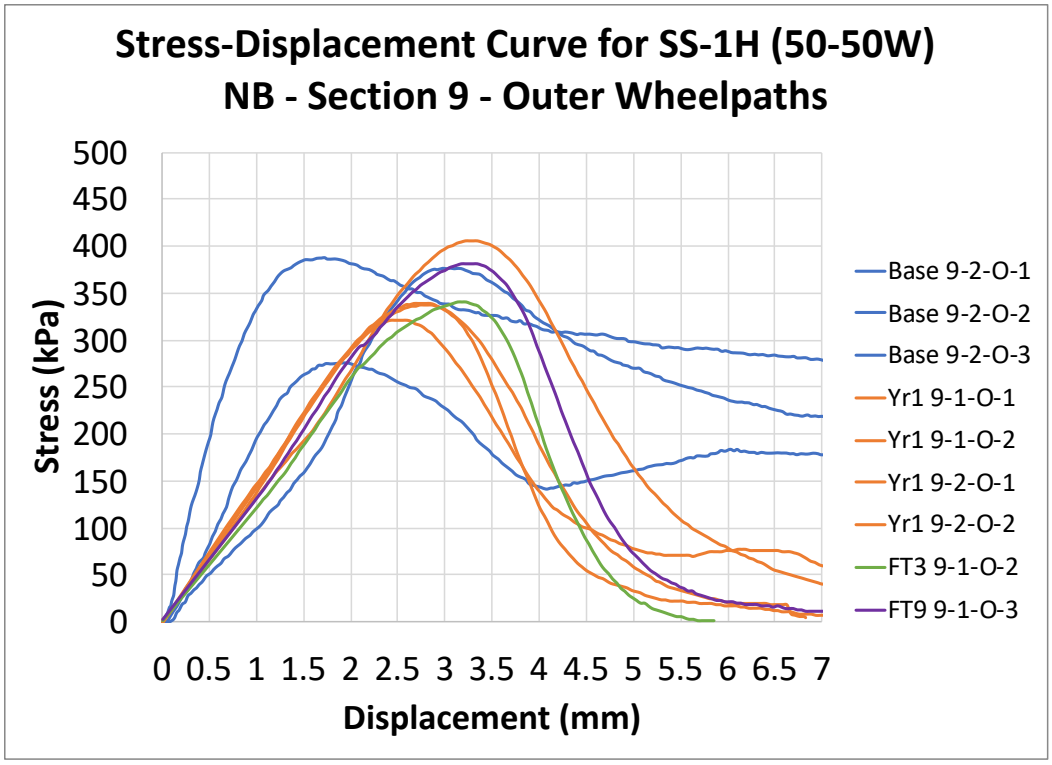


**Figure H.18 Stress-Displacement Curve for Outer Wheel Path Cores in Section 9 - SS-1h (50-50W) NB**

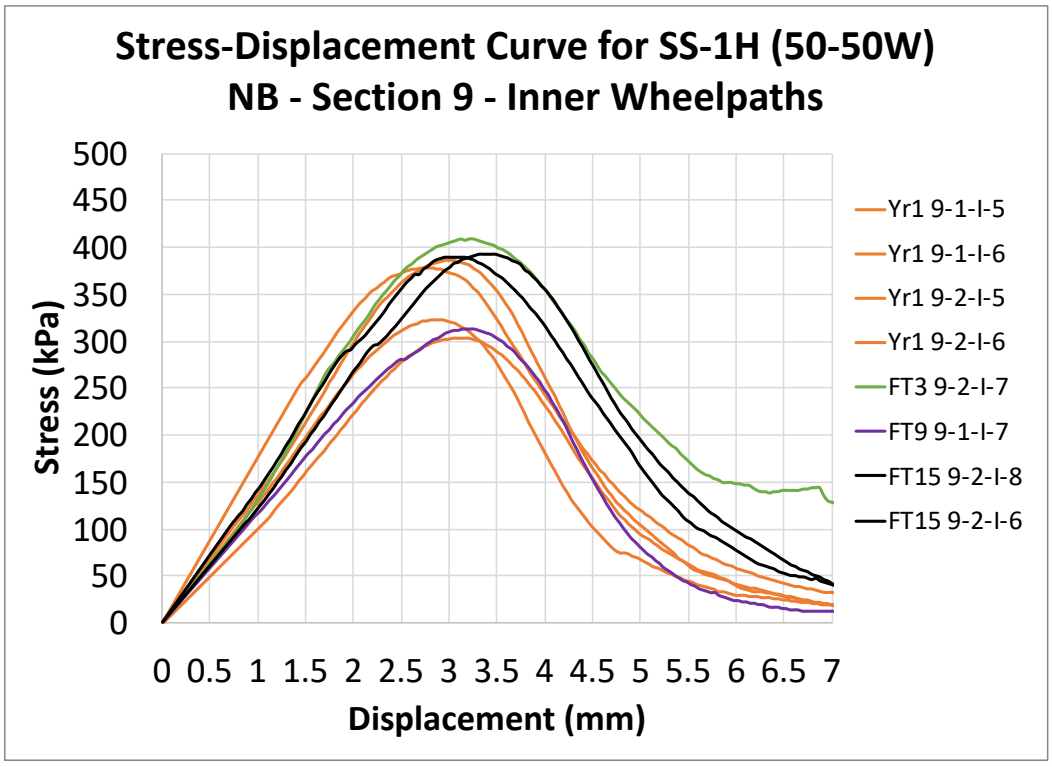


**Figure H.19 Stress-Displacement Curve for Inner Wheel Path Cores in Section 9 - SS-1h (50-50W) NB**

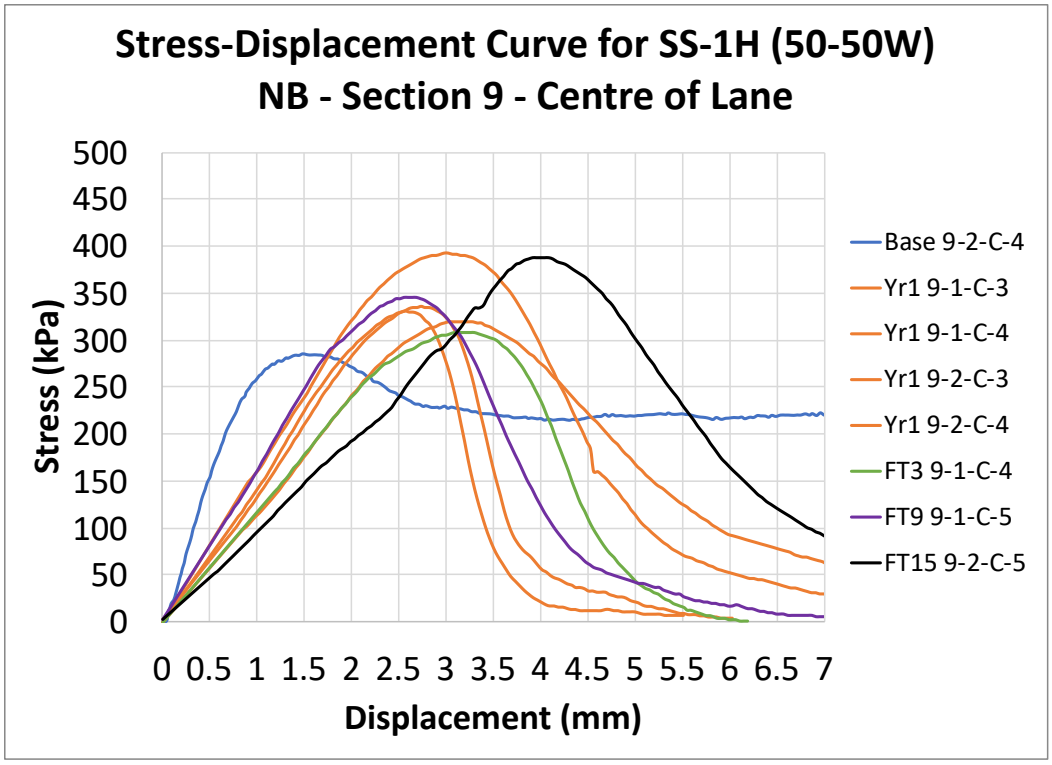


**Figure H.20 Stress-Displacement Curve for Centre of the Lane Cores in Section 9 - SS-1h (50-50W) NB**

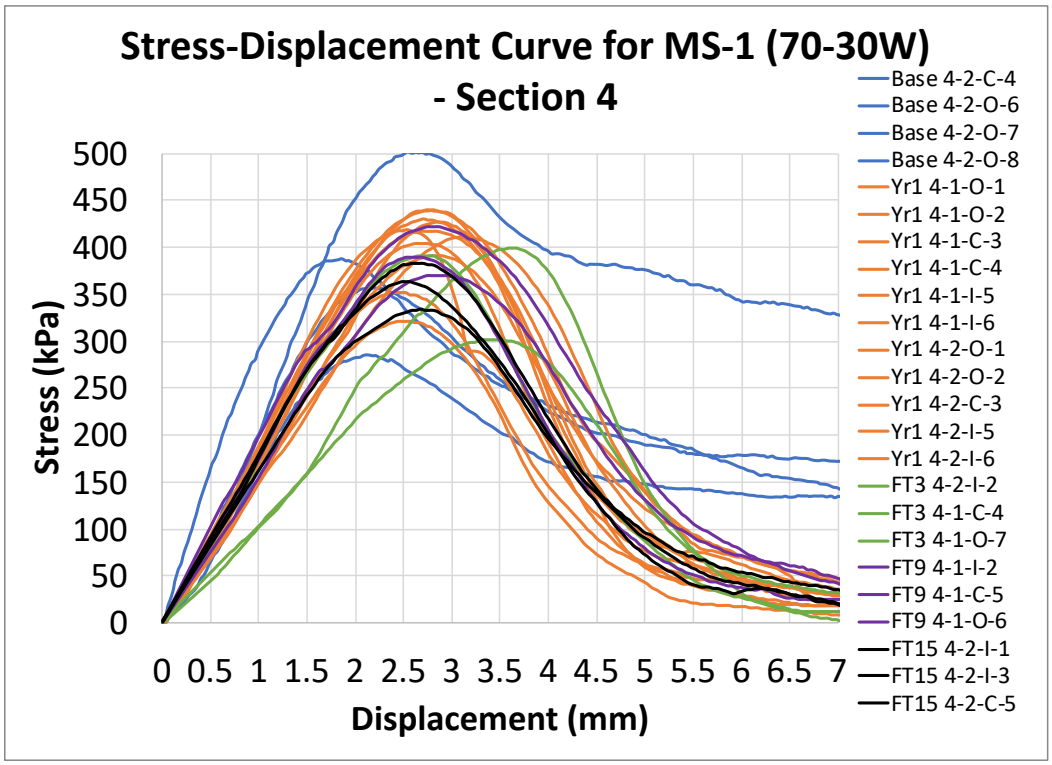


**Figure H.21 Stress-Displacement Curve for All Cores in Section 4 - MS-1 (70-30W)**

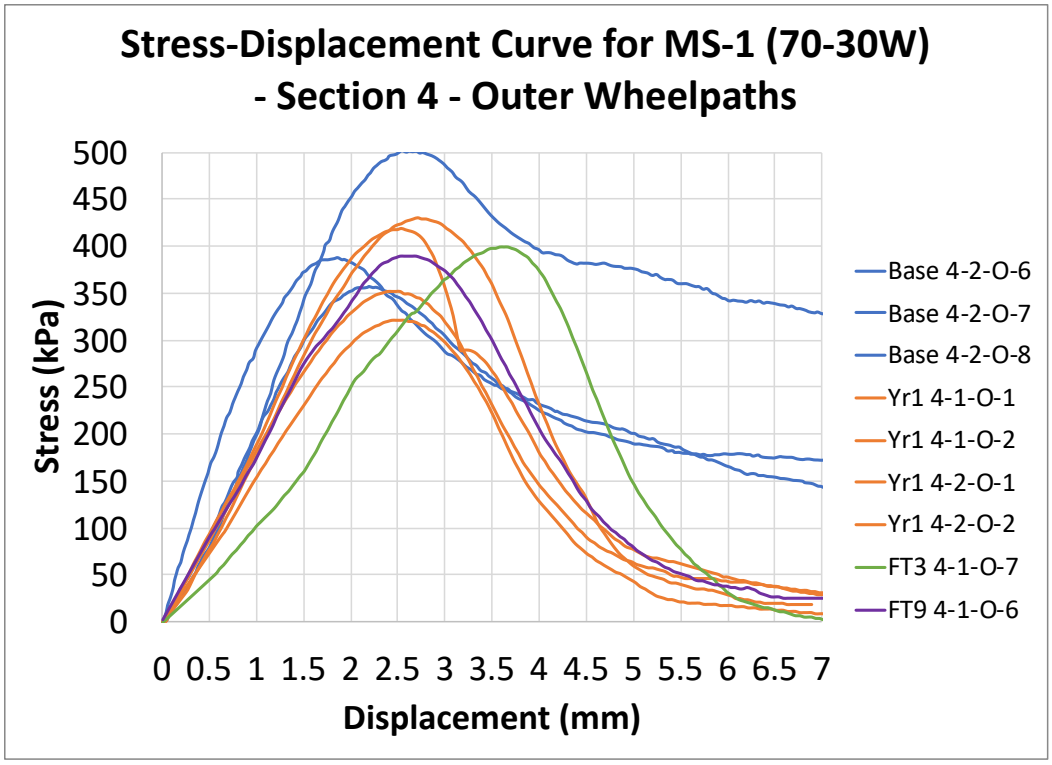


**Figure H.22 Stress-Displacement Curve for Outer Wheel Path Cores in Section 4 - MS-1 (70-30W)**

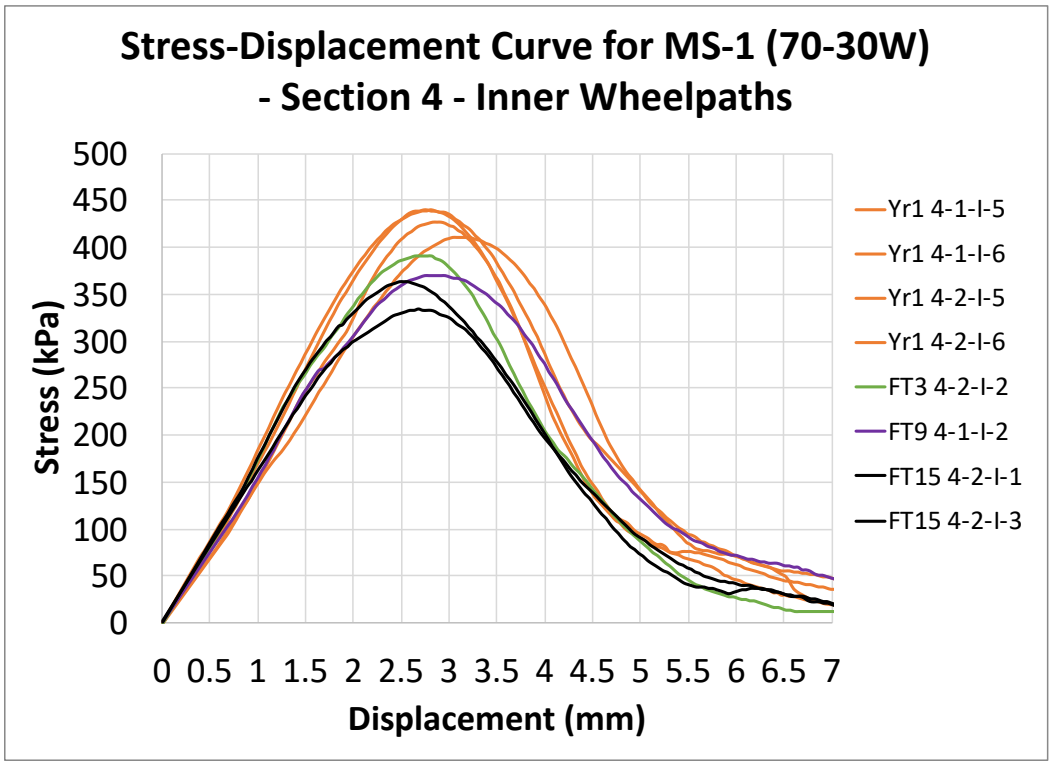


**Figure H.23 Stress-Displacement Curve for Inner Wheel Path Cores in Section 4 - MS-1 (70-30W)**

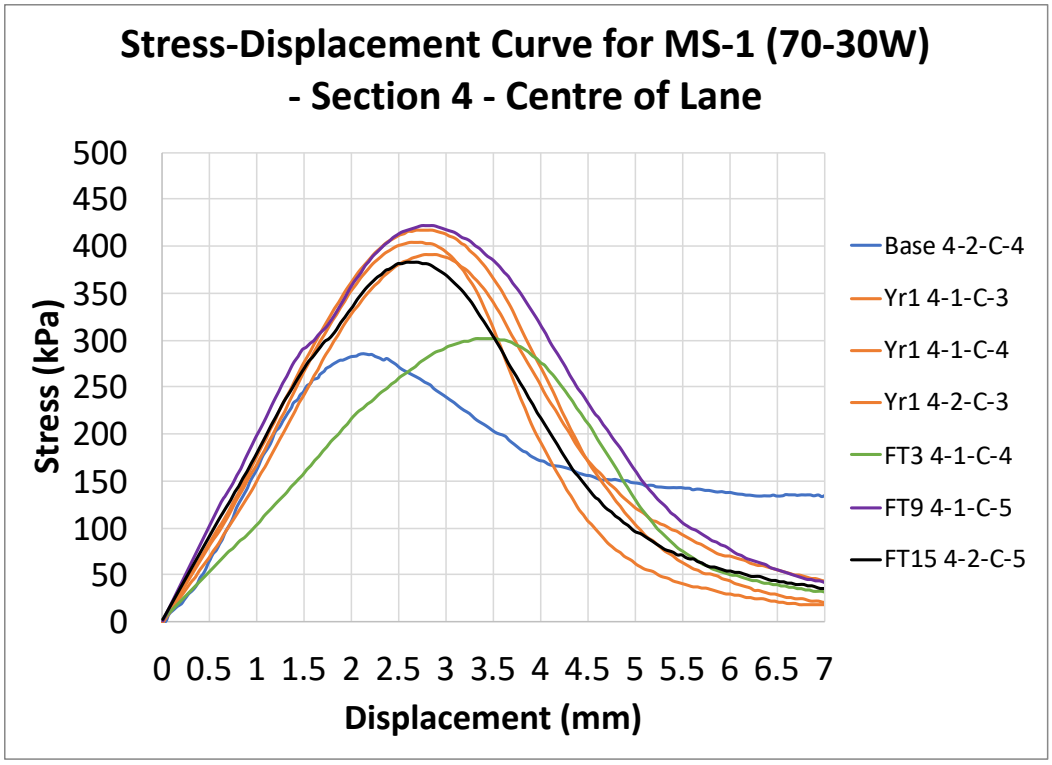


**Figure H.24 Stress-Displacement Curve for Centre of the Lane Cores in Section 4 - MS-1 (70-30W)**

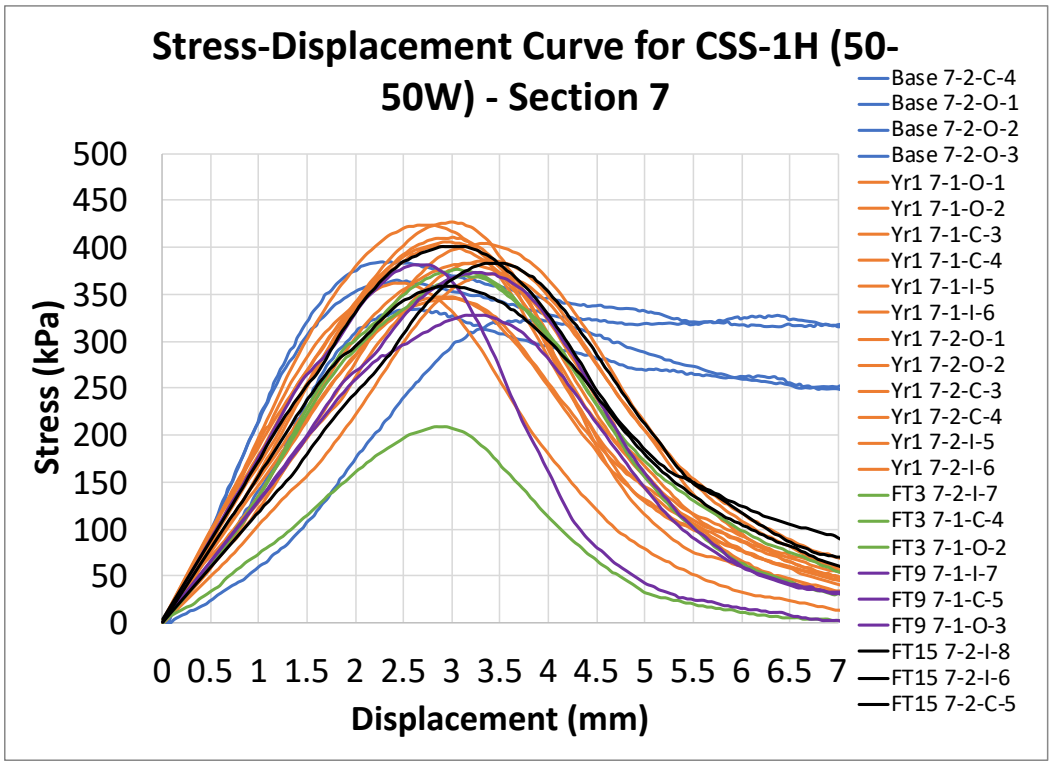


**Figure H.25 Stress-Displacement Curve for All Cores in Section 7 - CSS-1h (50-50W)**

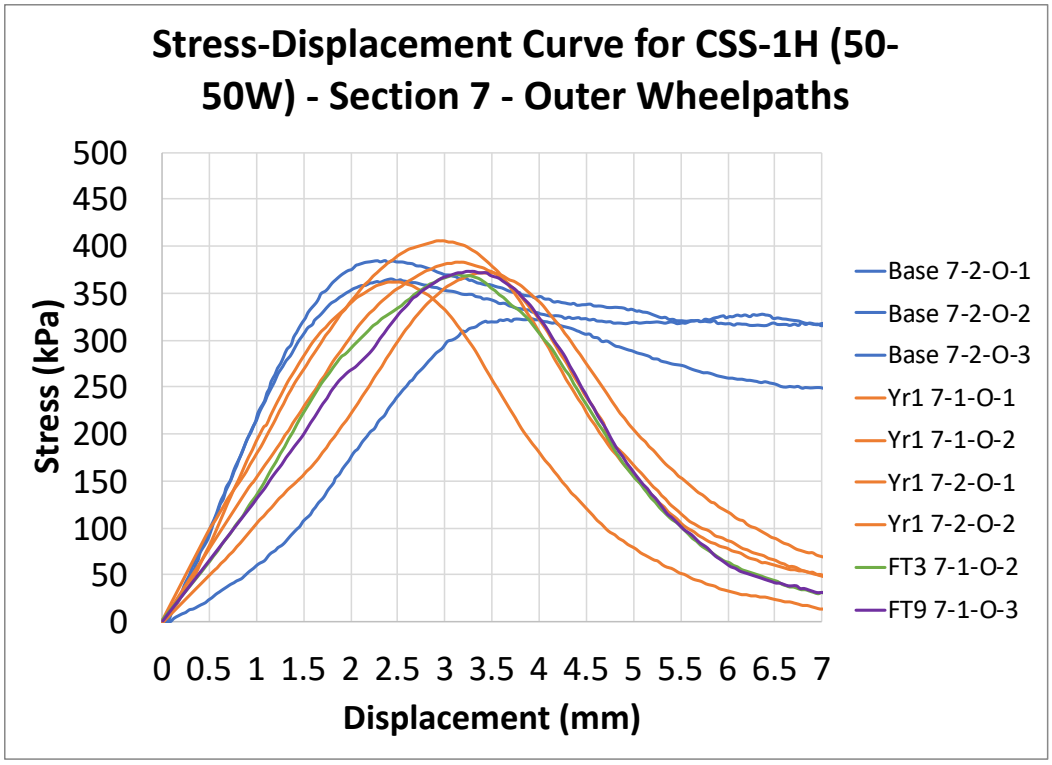


**Figure H.26 Stress-Displacement Curve for Outer Wheel Path Cores in Section 7 - CSS-1h (50-50W)**

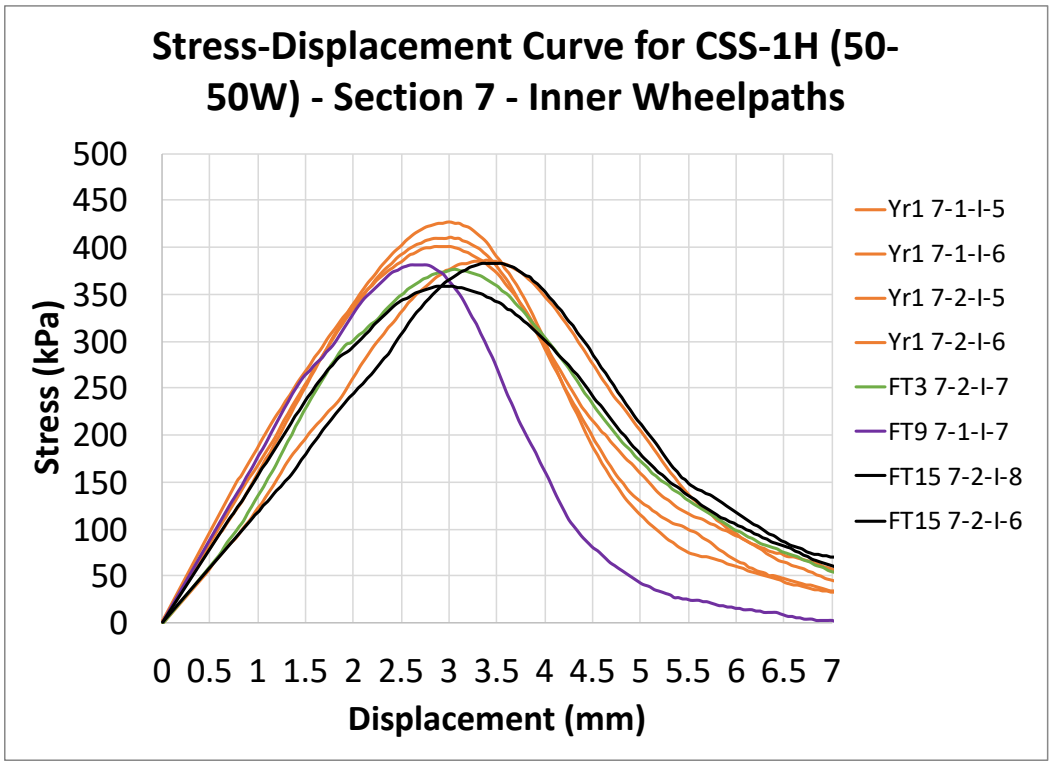


**Figure H.27 Stress-Displacement Curve for Inner Wheel Path Cores in Section 7 - CSS-1h (50-50W)**

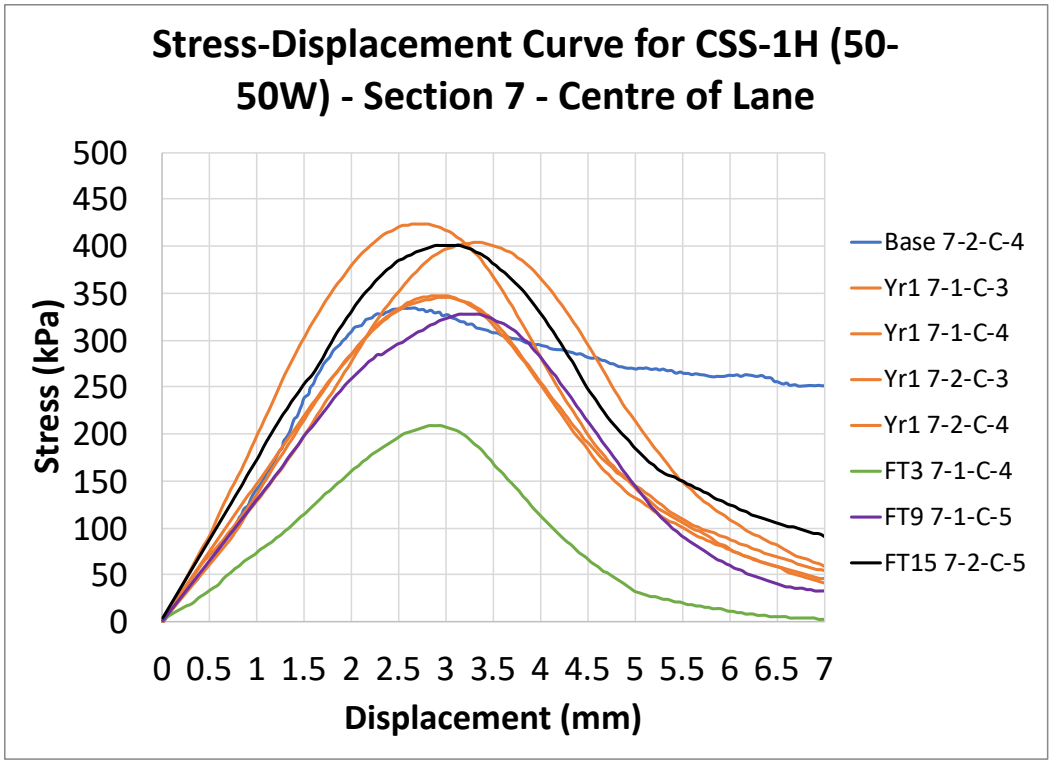


**Figure H.28 Stress-Displacement Curve for Centre of the Lane Cores in Section 7 - CSS-1h (50-50W)**

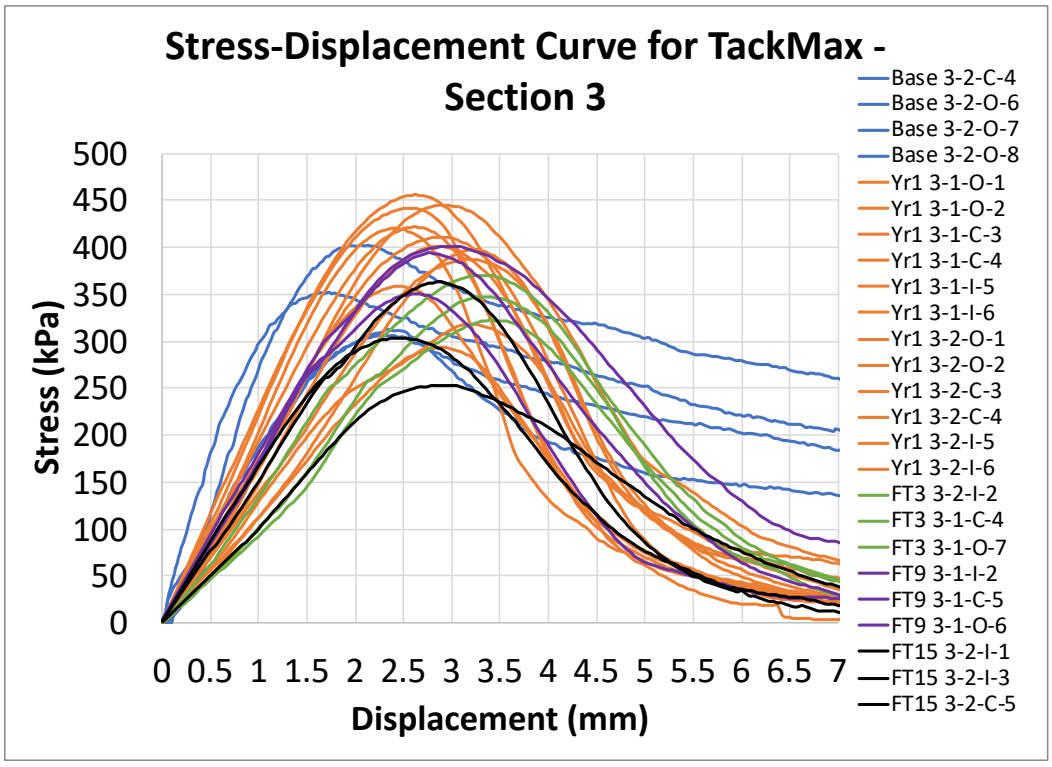


**Figure H.29 Stress-Displacement Curve for All Cores in Section 3 - TackMax™**

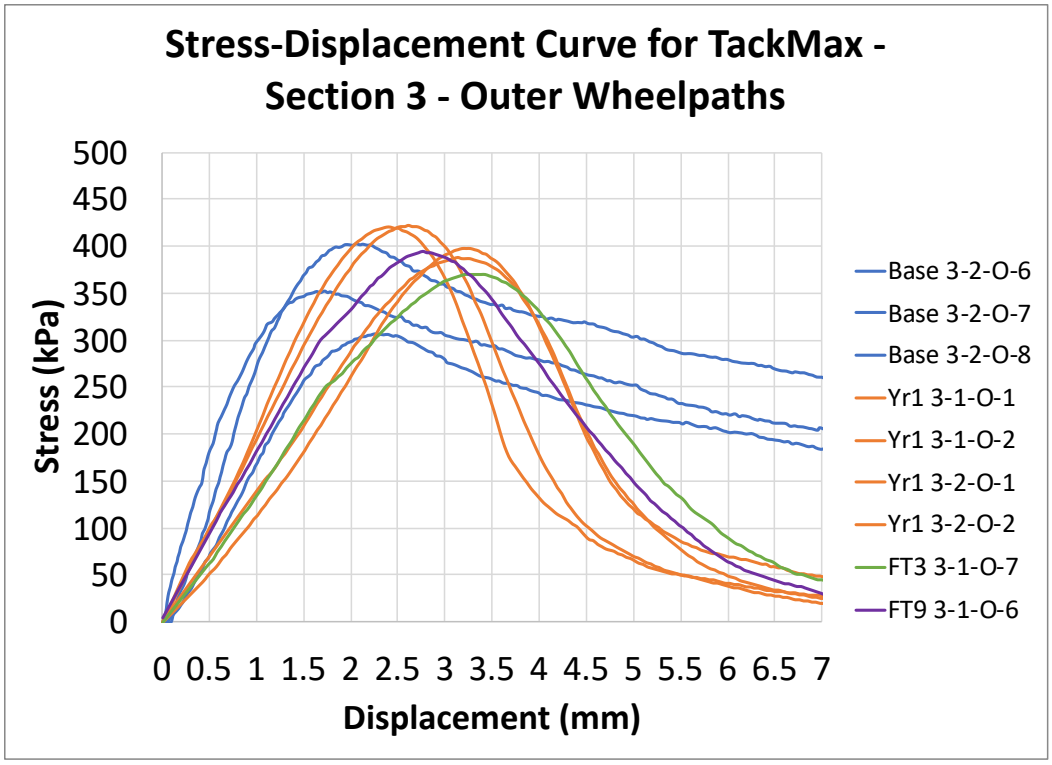


**Figure H.30 Stress-Displacement Curve for Outer Wheel Path Cores in Section 3 - TackMax™**

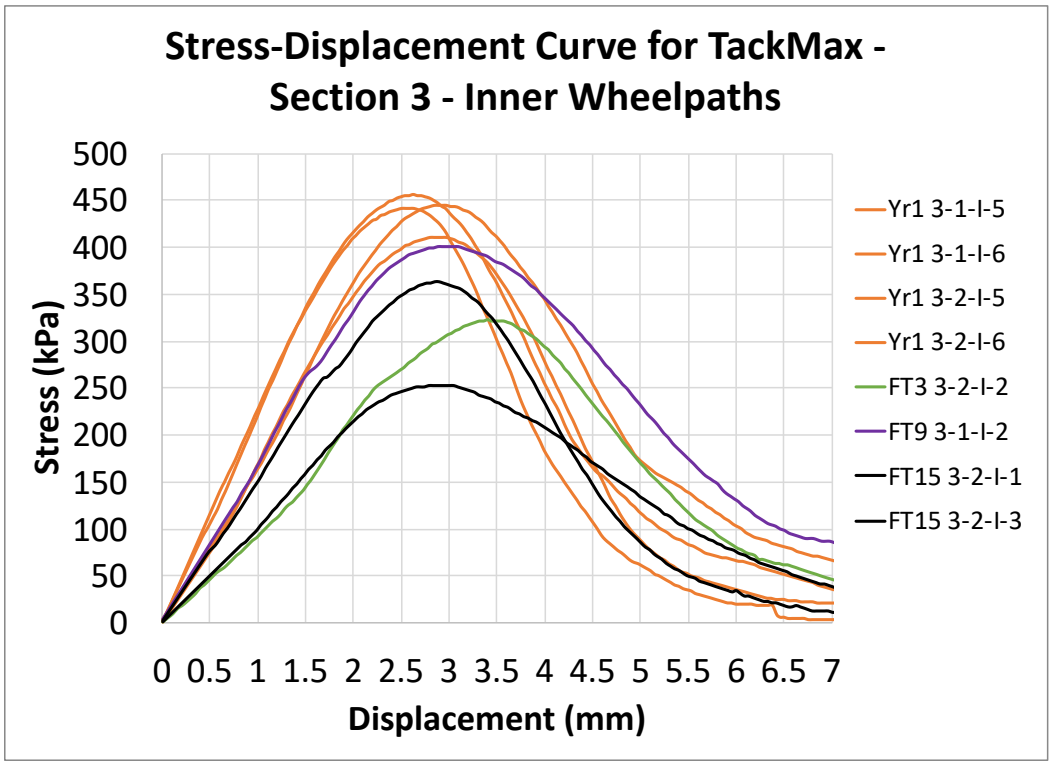


**Figure H.31 Stress-Displacement Curve for Inner Wheel Path Cores in Section 3 - TackMax™**

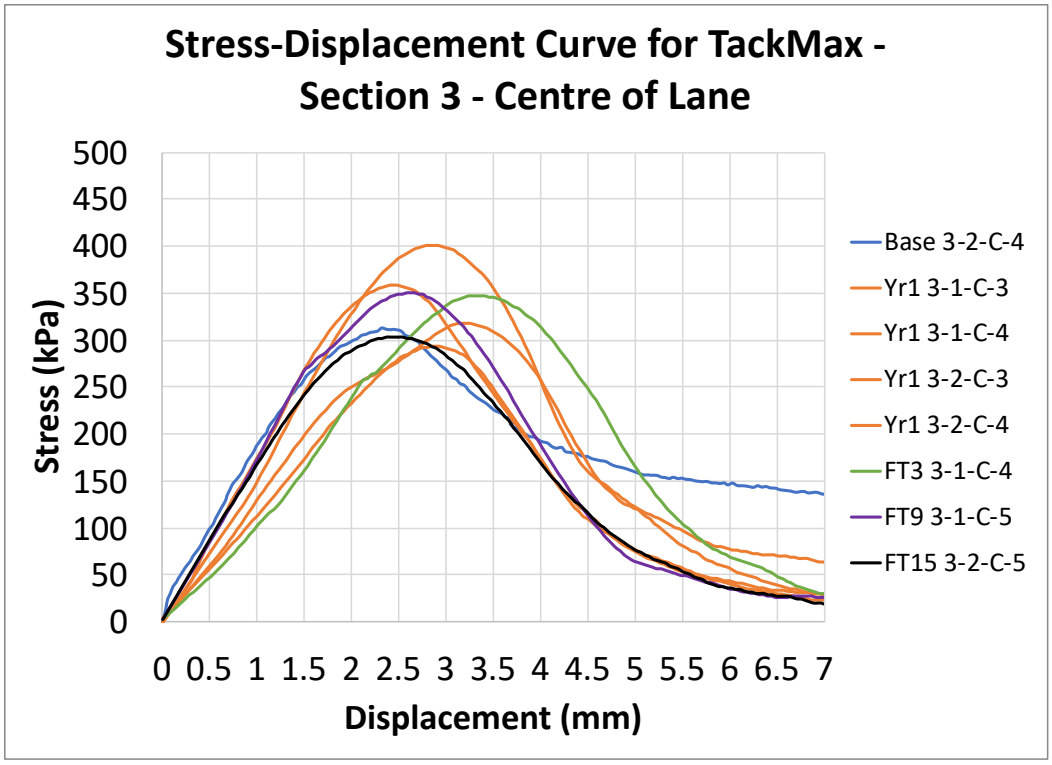


**Figure H.32 Stress-Displacement Curve for Centre of the Lane Cores in Section 3 - TackMax™**

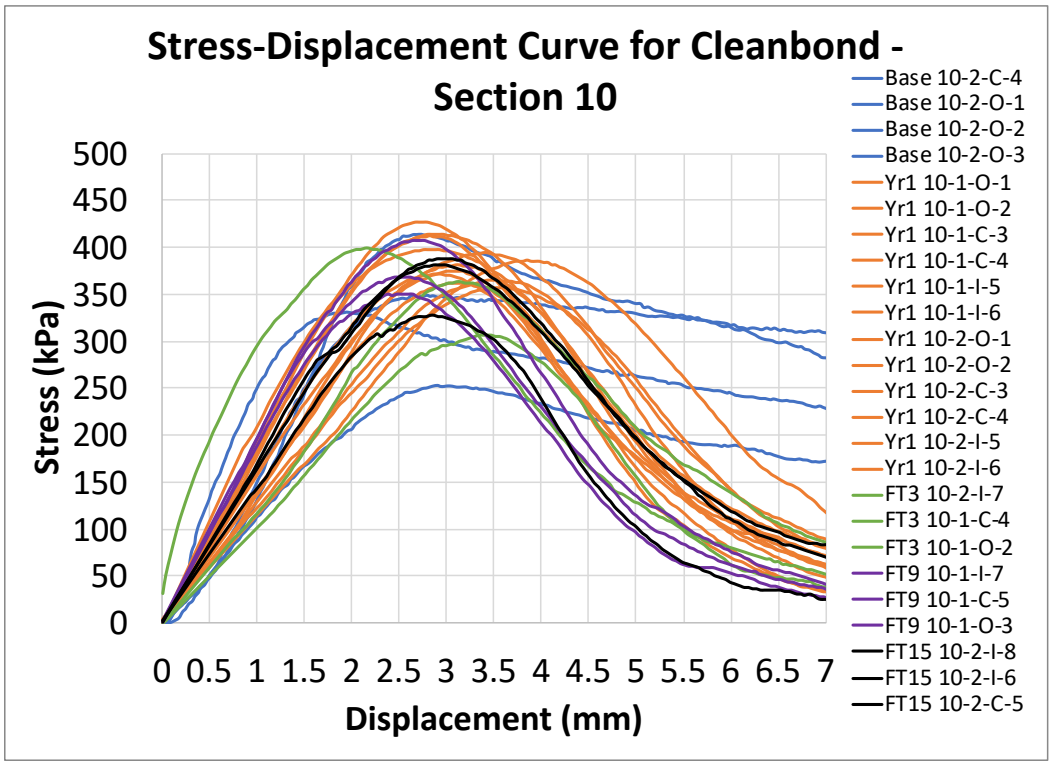


**Figure H.33 Stress-Displacement Curve for All Cores in Section 10 - Clean Bond**

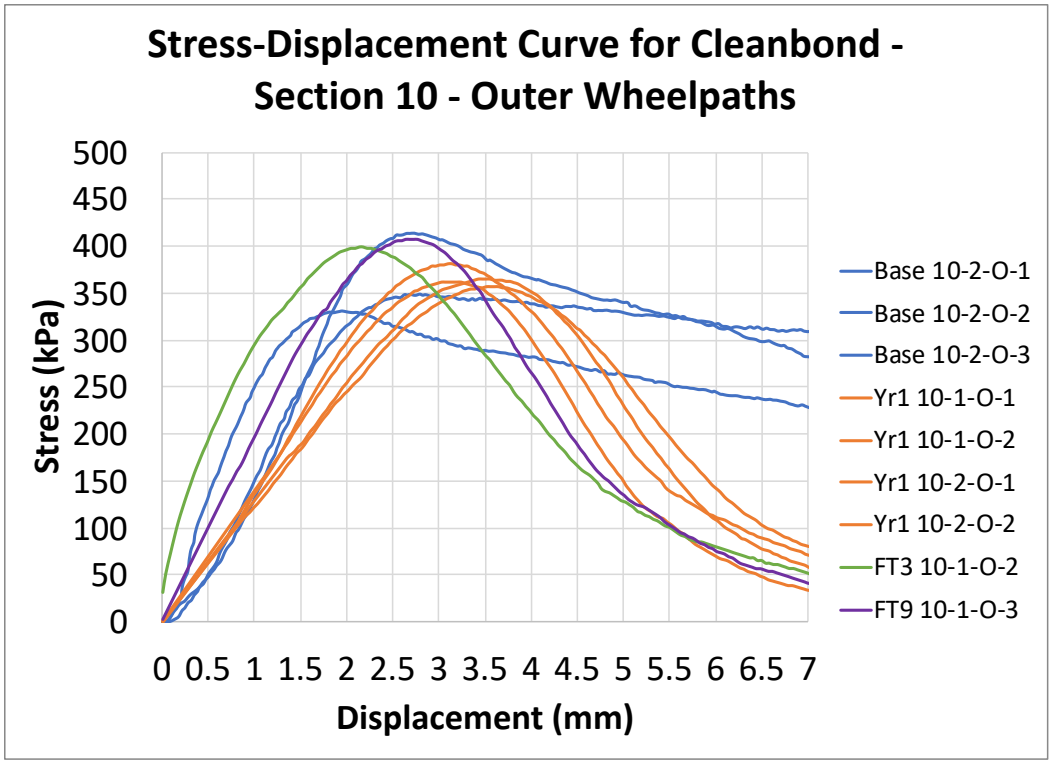


**Figure H.34 Stress-Displacement Curve for Outer Wheel Path Cores in Section 10 - Clean Bond**

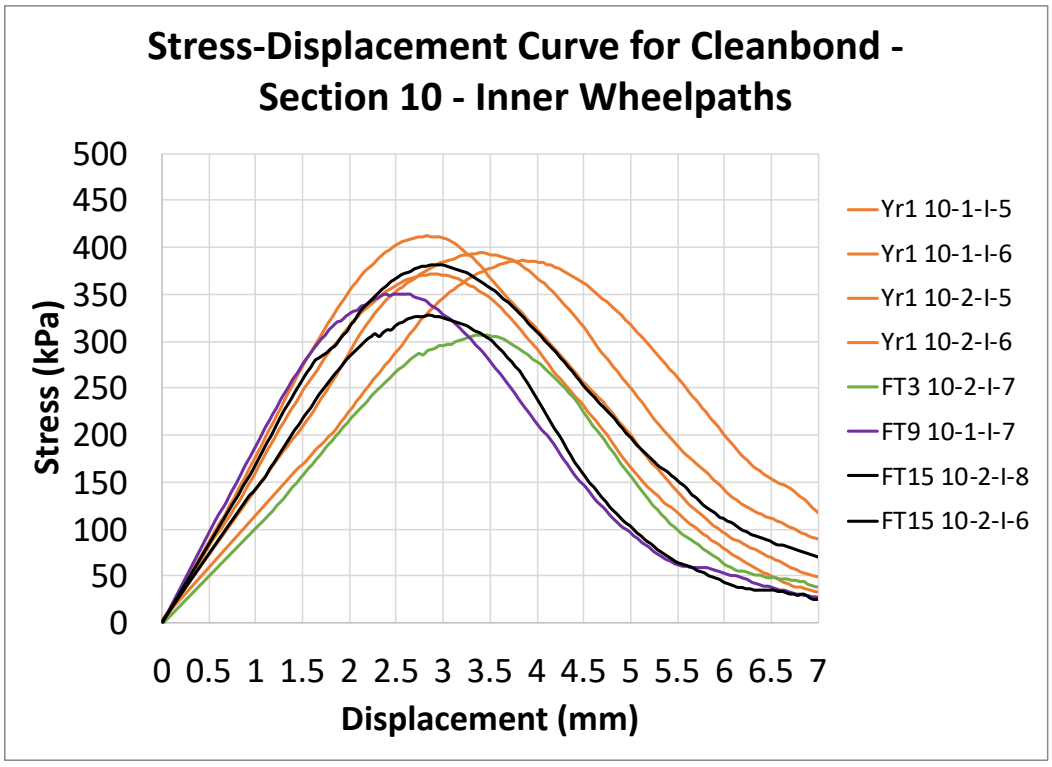


**Figure H.35 Stress-Displacement Curve for Inner Wheel Path Cores in Section 10 - Clean Bond**

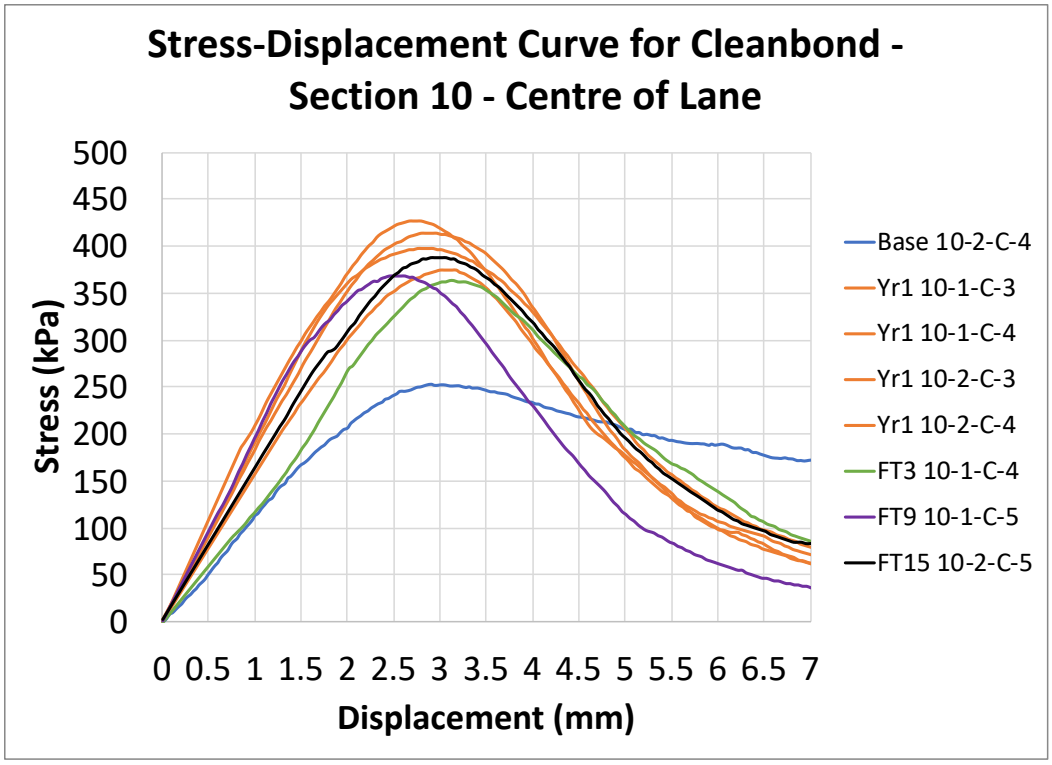


**Figure H.36 Stress-Displacement Curve for Centre of the Lane Cores in Section 10 - Clean Bond**

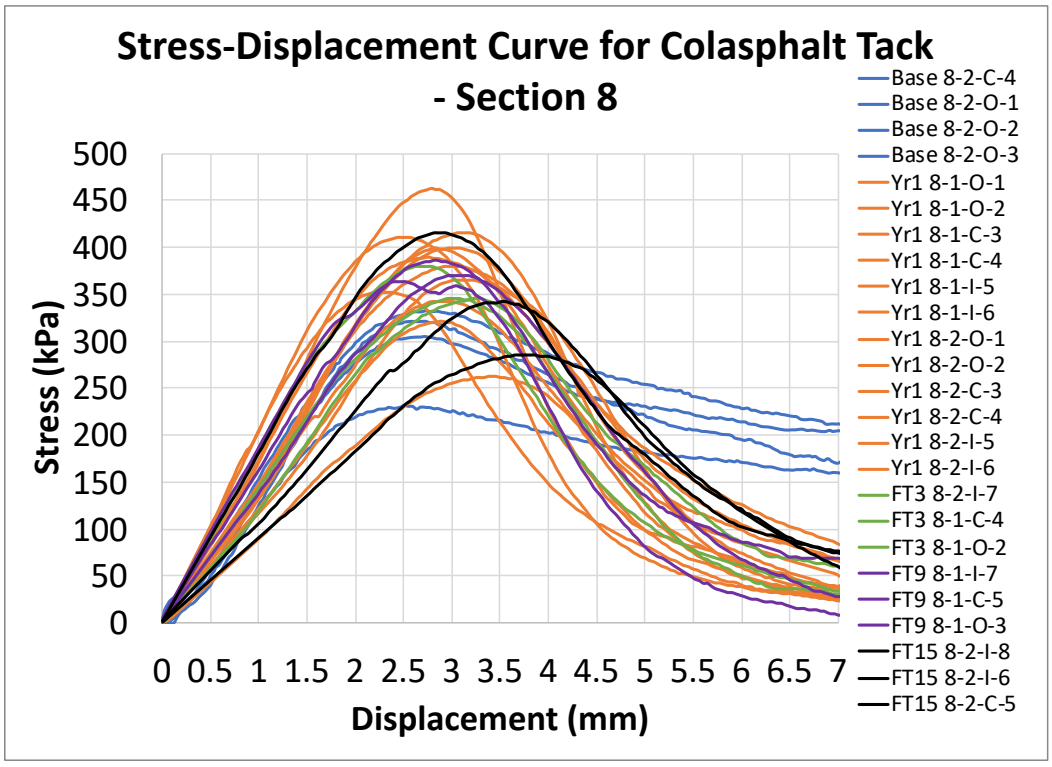


**Figure H.37 Stress-Displacement Curve for All Cores in Section 8 – Colasphalt Tack**

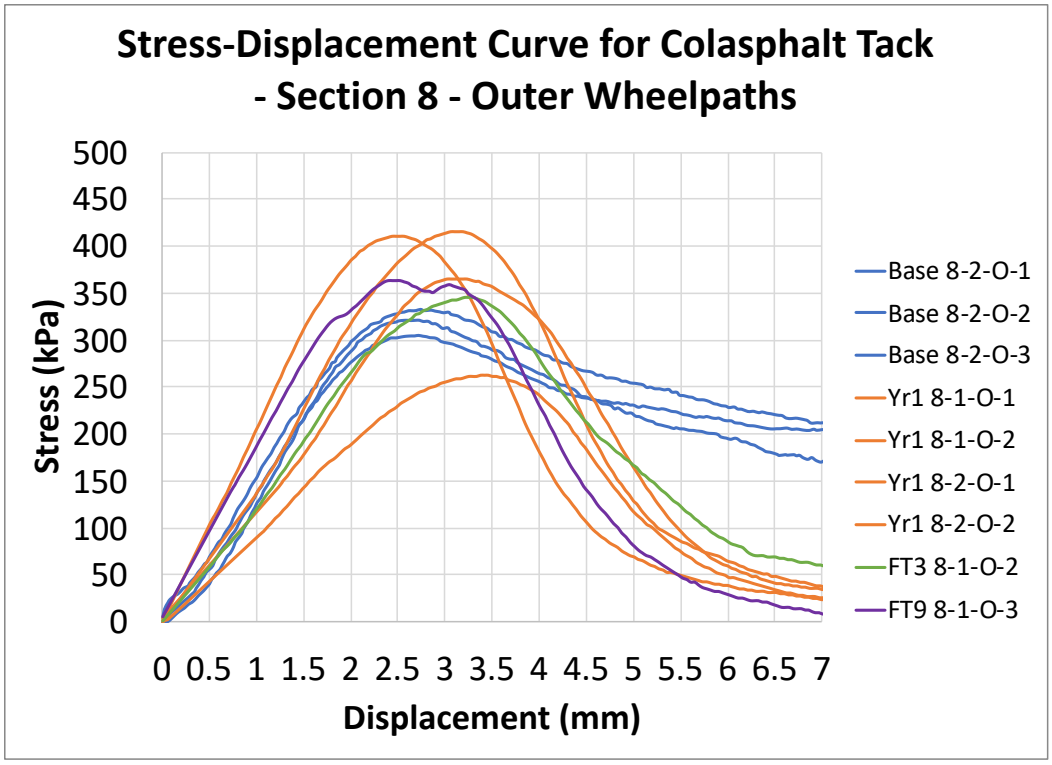


**Figure H.38 Stress-Displacement Curve for Outer Wheel Path Cores in Section 8 – Colasphalt Tack**

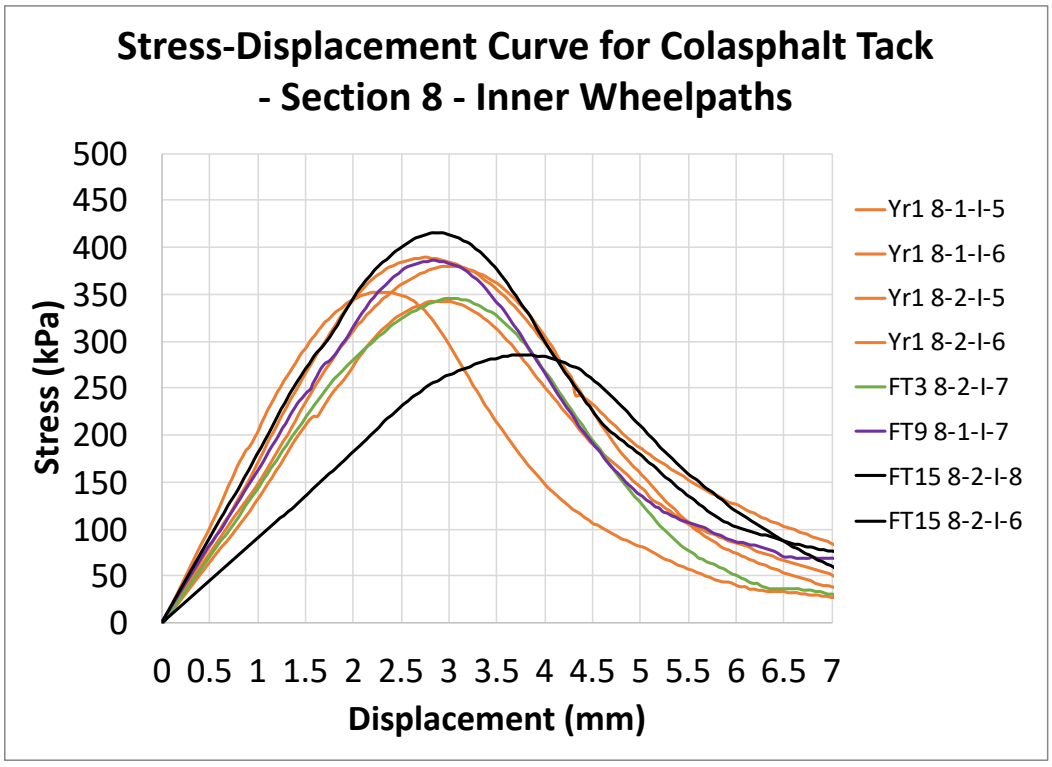


**Figure H.39 Stress-Displacement Curve for Outer Wheel Path Cores in Section 8 – Colasphalt Tack**

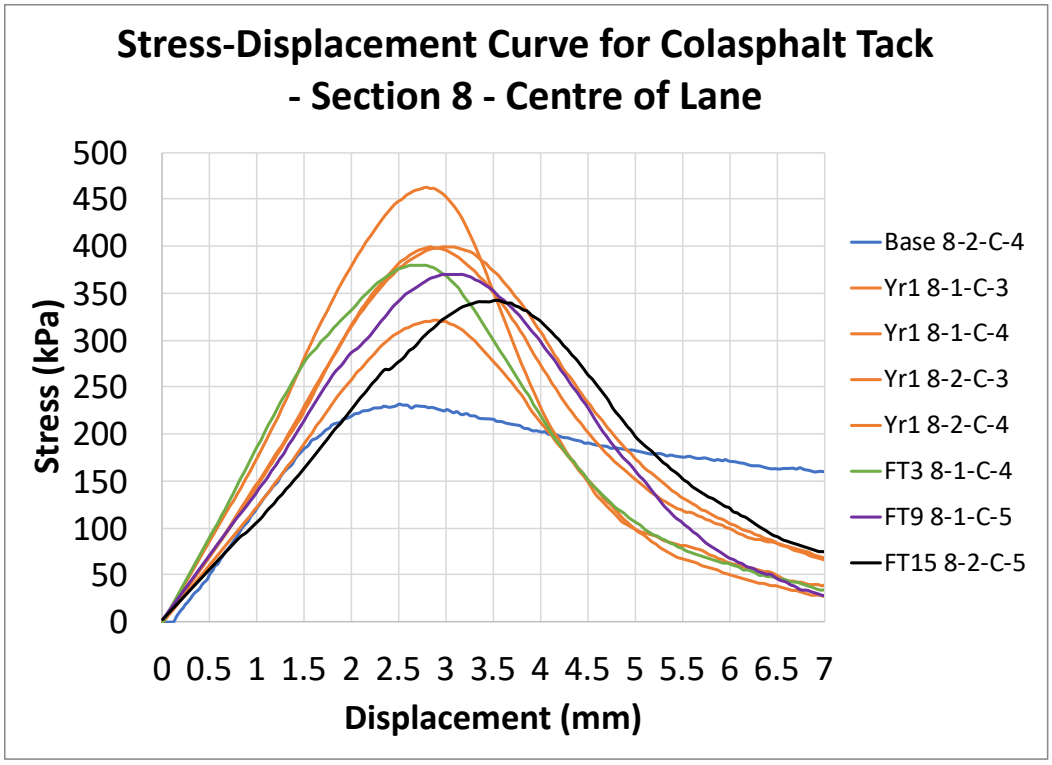


**Figure H.40 Stress-Displacement Curve for Centre of the Lane Cores in Section 8 – Colasphalt Tack**

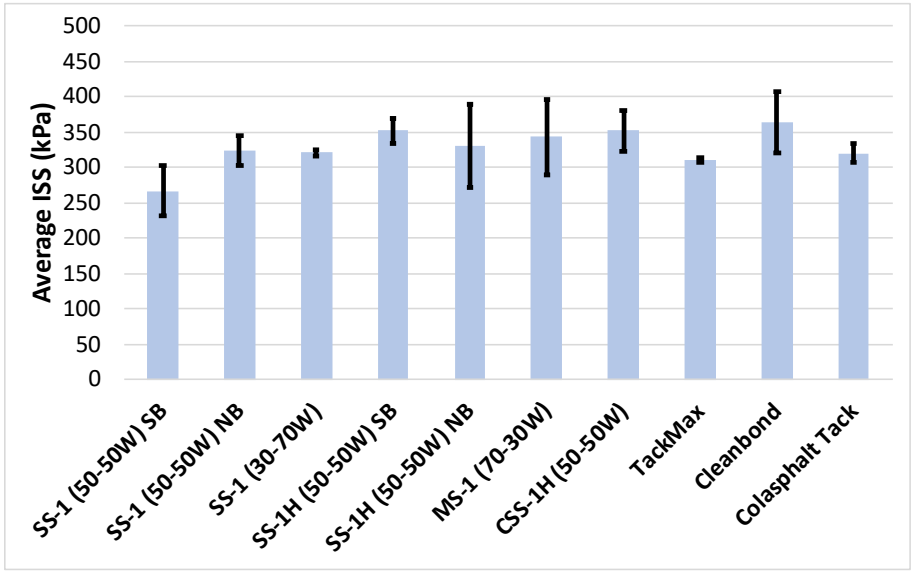


**Figure H.41 Average Interlayer Shear Strength for Baseline Cores**

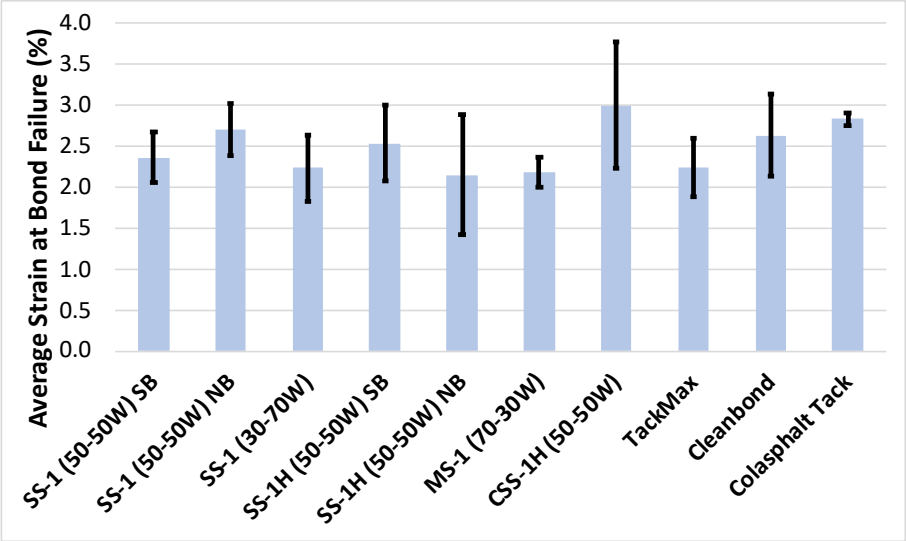


**Figure H.42 Average Strain at Bond Failure for Baseline Cores**

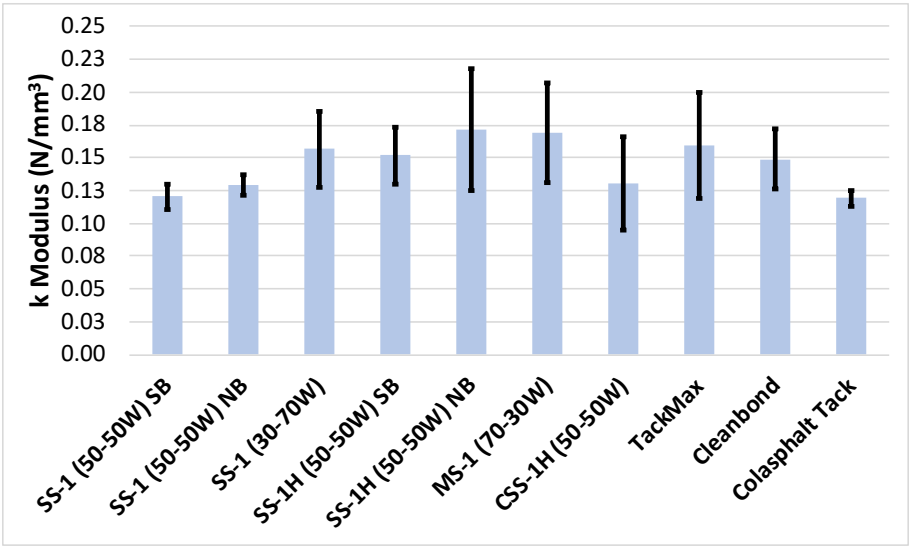


**Figure H.43 Average Interlayer Tangential Modulus for Baseline Cores**

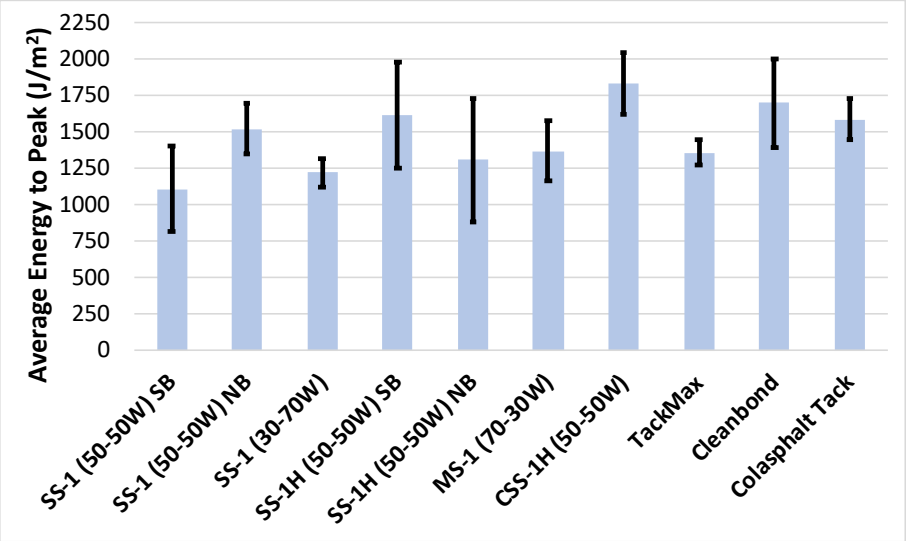


**Figure H.44 Average Energy to Peak Stress Per Unit Area for Baseline Cores**

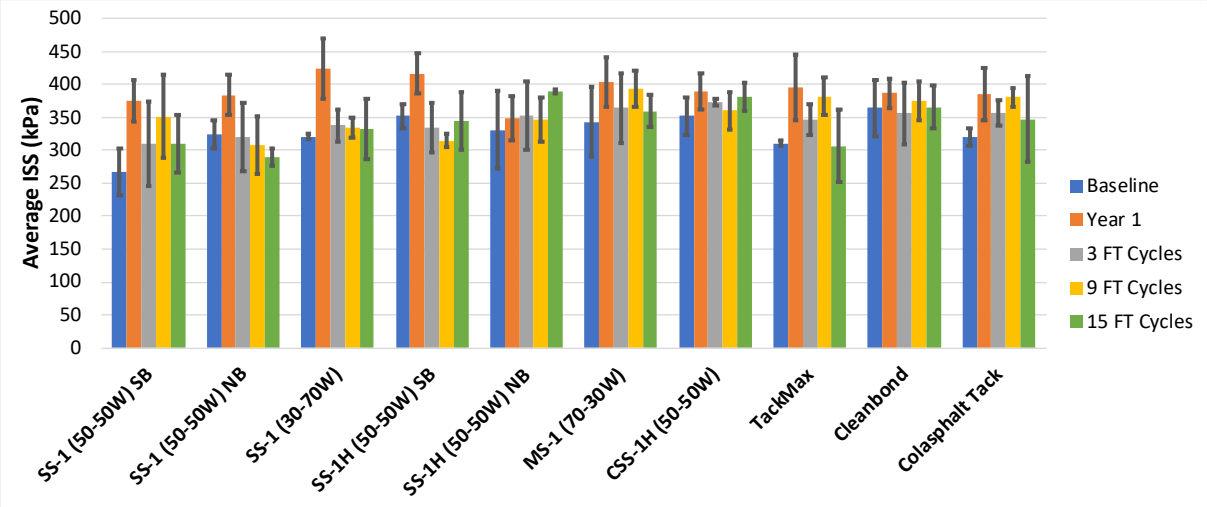


**Figure H.45 Average Interlayer Shear Strength for All Core Groups**

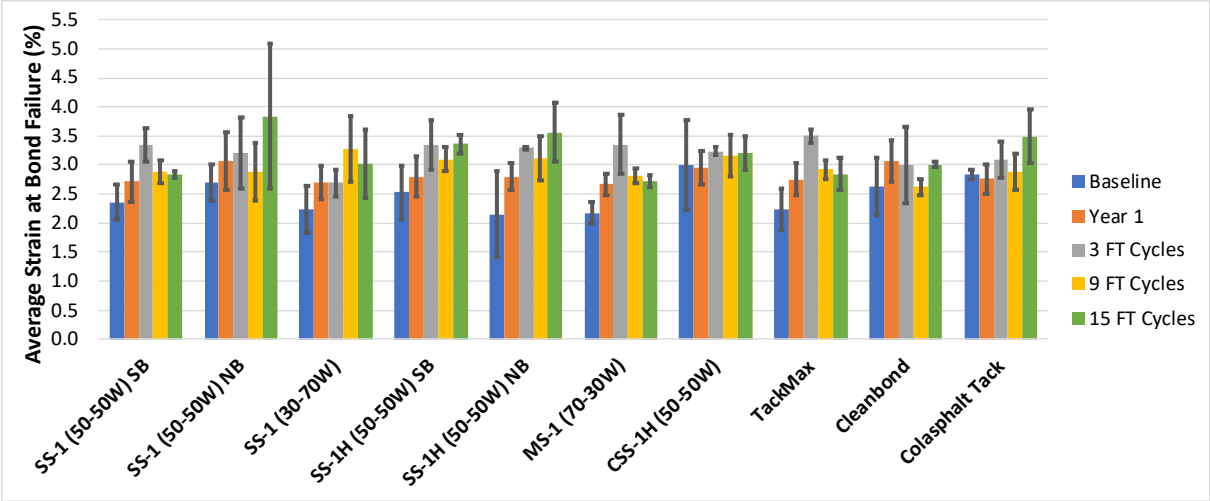


**Figure H.46 Average Strain at Bond Failure for All Core Groups**

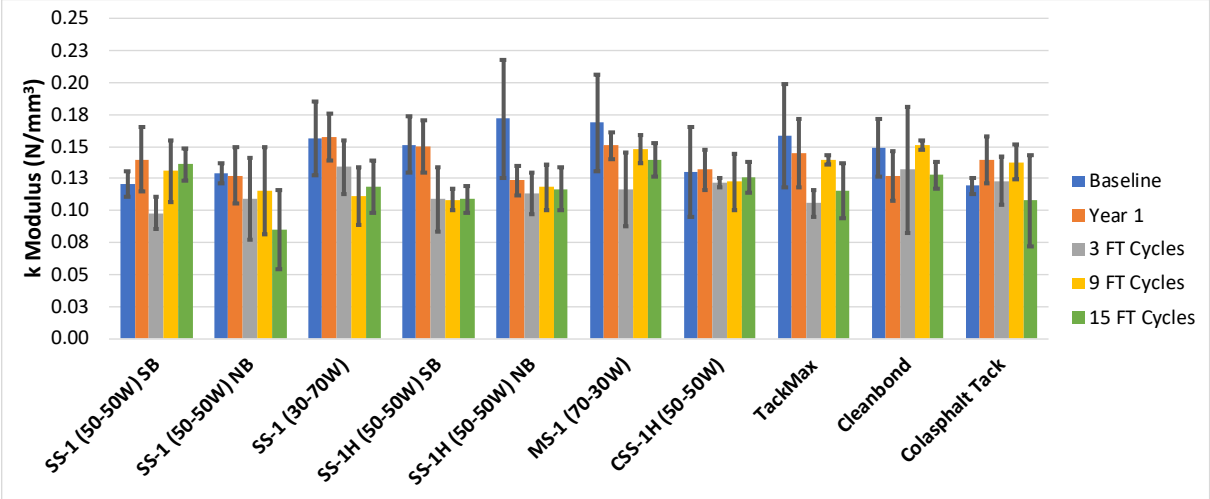


**Figure H.47 Average Interlayer Tangential Modulus for All Core Groups**

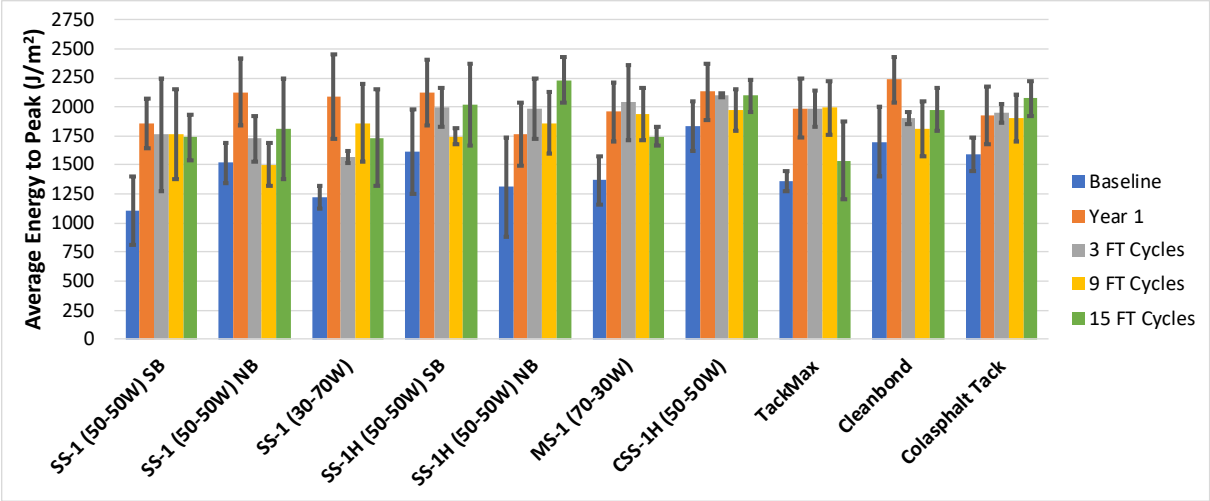


**Figure H.48 Average Energy to Peak Stress Per Unit Area for All Core Groups**

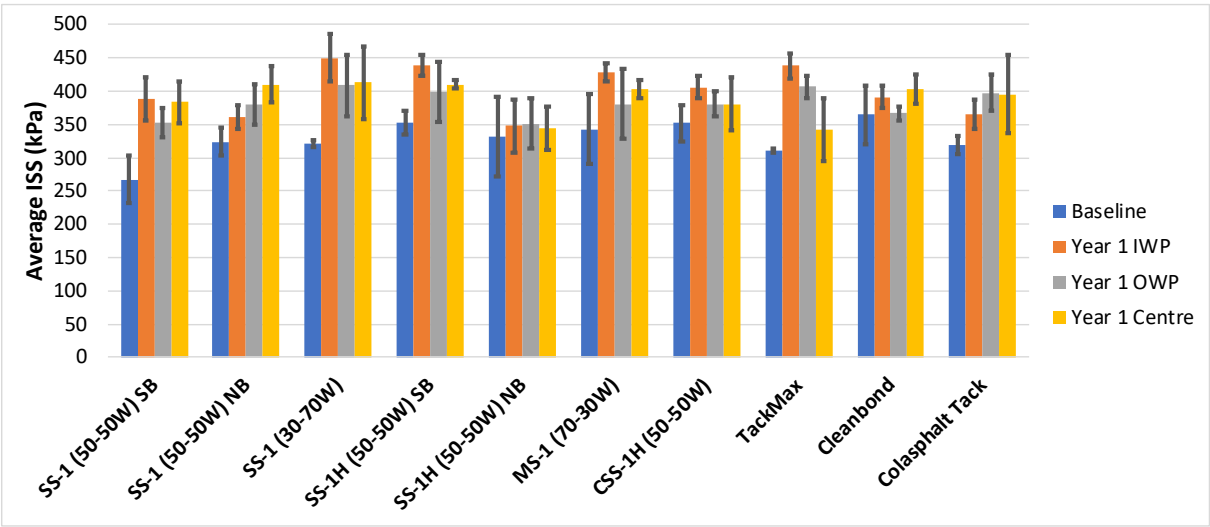


**Figure H.49 Average Interlayer Shear Strength for Year One Cores**

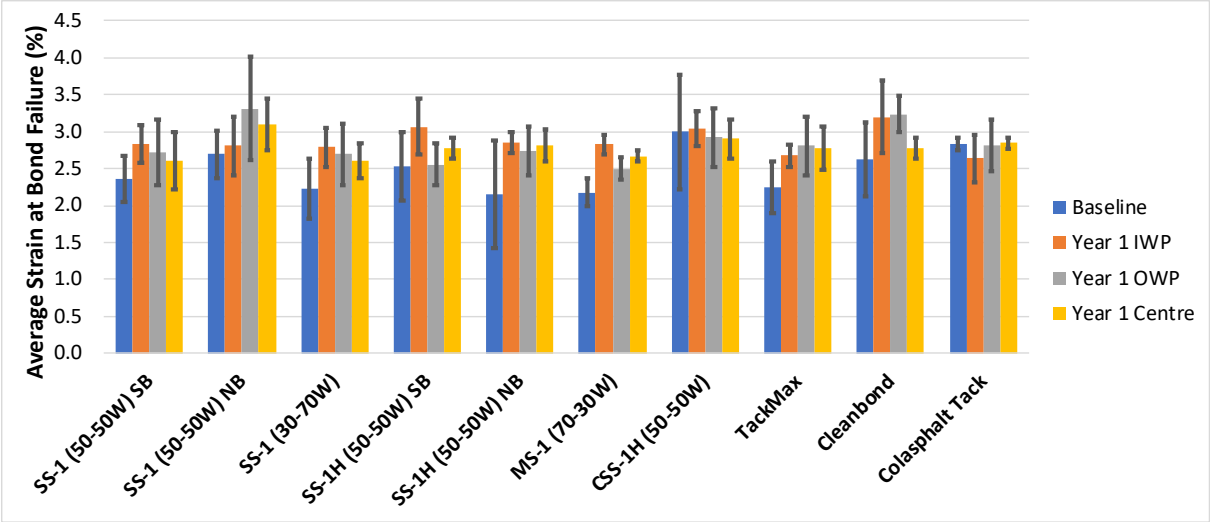


**Figure H.50 Average Strain at Bond Failure for Year One Cores**

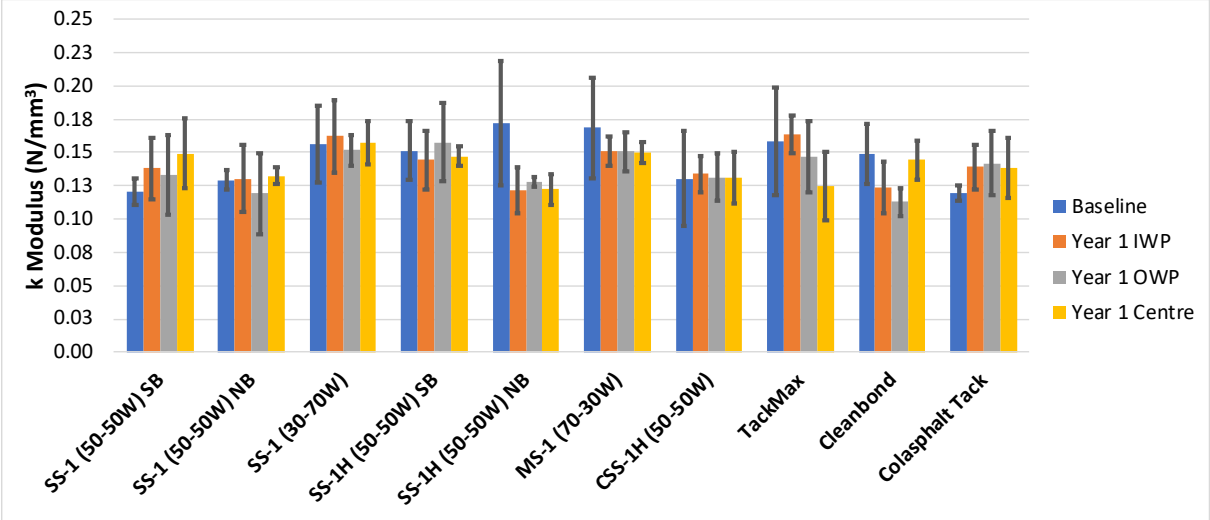


**Figure H.51 Average Interlayer Tangential Modulus for Year One Cores**

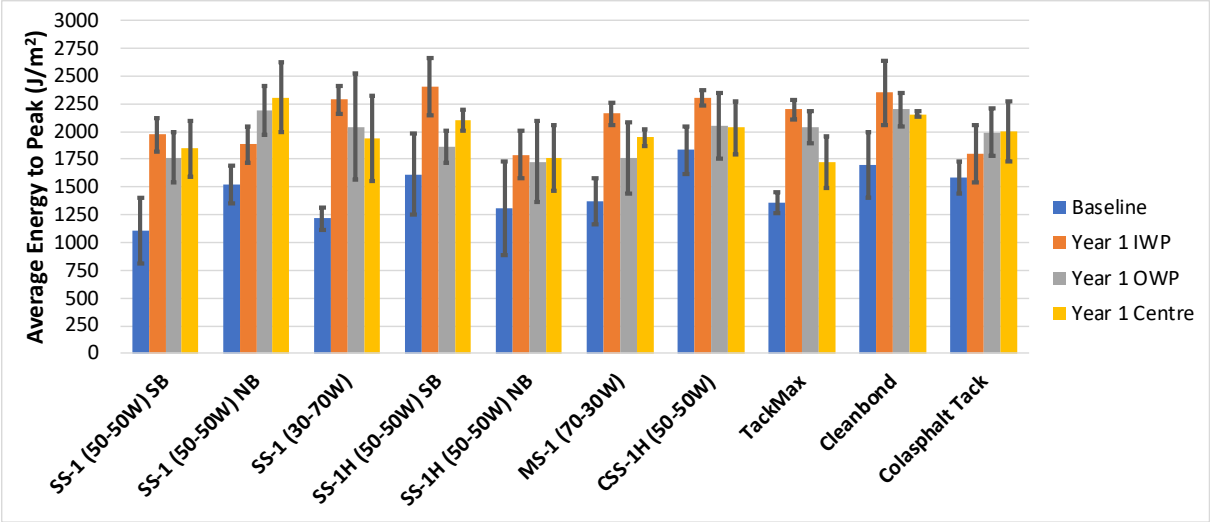


**Figure H.52 Average Energy to Peak Stress Per Unit Area for Year One Cores**

# Table H.1 Average Interlayer Shear Strength Results for All Core Groups

| | | Average ISS (kPa) | COV | Average ISS (kPa) | COV | % Change | Average ISS (kPa) | COV | % Change | Average ISS (kPa) | COV | % Change | Average ISS (kPa) | COV | % Change | Average ISS (kPa) | COV | % Change | Average ISS (kPa) | COV | % Change | Average ISS (kPa) | COV | % Change |
|---|---|---|---|---|---|---|---|---|---|---|---|---|---|---|---|---|---|---|---|---|---|---|---|---|
| Section | Material | Baseline | | Year 1 | | | Year 1 IWP | | | Year 1 OWP | | | Year 1 Centre | | | 3 FT Cycles | | | 9 FT Cycles | | | 15 FT Cycles | | |
| 1 | SS-1 (50-50W) SB | 267.0 | 13.3 | 375.0 | 8.2 | 40 | 388.7 | 8.5 | 46 | 353.1 | 6.2 | 32 | 383.3 | 8.0 | 44 | 310.5 | 20.6 | 16 | 351.7 | 18.1 | 32 | 309.1 | 14.2 | 16 |
| 6 | SS-1 (50-50W) NB | 324.1 | 6.4 | 384.1 | 8.1 | 18 | 361.8 | 4.9 | 12 | 380.1 | 7.8 | 17 | 410.4 | 6.5 | 27 | 320.5 | 16.2 | -1 | 307.5 | 14.1 | -5 | 289.2 | 4.6 | -11 |
| 5 | SS-1 (30-70W) | 321.1 | 1.5 | 424.0 | 10.8 | 32 | 449.8 | 7.9 | 40 | 408.8 | 11.3 | 27 | 413.3 | 13.2 | 29 | 337.6 | 7.3 | 5 | 334.5 | 4.8 | 4 | 332.5 | 14.0 | 4 |
| 2 | SS-1H (50-50W) SB | 351.9 | 5.1 | 416.2 | 7.4 | 18 | 439.2 | 3.5 | 25 | 399.2 | 11.3 | 13 | 410.4 | 1.3 | 17 | 334.1 | 11.5 | -5 | 314.8 | 3.1 | -11 | 343.9 | 12.8 | -2 |
| 9 | SS-1H (50-50W) NB | 331.4 | 17.9 | 347.7 | 9.7 | 5 | 347.6 | 11.7 | 5 | 350.9 | 10.7 | 6 | 344.7 | 9.4 | 4 | 352.4 | 14.7 | 6 | 346.3 | 9.8 | 5 | 389.8 | 0.7 | 18 |
| 4 | MS-1 (70-30W) | 343.2 | 15.4 | 404.1 | 9.2 | 18 | 428.8 | 3.3 | 25 | 380.2 | 13.8 | 11 | 403.2 | 3.2 | 17 | 364.0 | 14.8 | 6 | 393.7 | 6.8 | 15 | 359.7 | 6.7 | 5 |
| 7 | CSS-1H (50-50W) | 351.8 | 8.0 | 388.8 | 7.1 | 11 | 405.8 | 4.1 | 15 | 380.4 | 4.9 | 8 | 380.1 | 10.5 | 8 | 372.6 | 1.3 | 6 | 360.2 | 8.0 | 2 | 380.7 | 5.7 | 8 |
| 3 | TackMax | 310.6 | 1.2 | 395.8 | 12.7 | 27 | 438.1 | 4.4 | 41 | 406.8 | 4.2 | 31 | 342.6 | 13.9 | 10 | 346.1 | 6.7 | 11 | 382.0 | 7.4 | 23 | 306.9 | 18.0 | -1 |
| 10 | Cleanbond | 364.3 | 11.9 | 386.9 | 5.8 | 6 | 391.3 | 4.3 | 7 | 366.4 | 3.0 | 1 | 403.1 | 5.7 | 11 | 356.5 | 13.2 | -2 | 375.5 | 7.8 | 3 | 365.4 | 9.0 | 0 |
| 8 | Colasphalt Tack | 319.7 | 4.2 | 385.0 | 10.2 | 20 | 365.3 | 6.1 | 14 | 396.9 | 6.8 | 24 | 395.7 | 14.7 | 24 | 356.8 | 5.4 | 12 | 380.8 | 3.8 | 19 | 347.4 | 18.6 | 9 |

| | | Std Dev (kPa) | | | | | | | |
|---|---|---|---|---|---|---|---|---|---|
| Section | Material | Baseline | Year 1 | Year 1 IWP | Year 1 OWP | Year 1 Centre | 3 FT Cycles | 9 FT Cycles | 15 FT Cycles |
| 1 | SS-1 (50-50W) SB | 35.6 | 30.9 | 33.1 | 21.8 | 30.8 | 64.1 | 63.6 | 43.8 |
| 6 | SS-1 (50-50W) NB | 20.8 | 31.0 | 17.6 | 29.8 | 26.8 | 51.9 | 43.3 | 13.2 |
| 5 | SS-1 (30-70W) | 4.8 | 45.9 | 35.4 | 46.3 | 54.7 | 24.7 | 15.9 | 46.6 |
| 2 | SS-1H (50-50W) SB | 17.9 | 30.7 | 15.6 | 45.2 | 5.4 | 38.4 | 9.8 | 43.9 |
| 9 | SS-1H (50-50W) NB | 59.2 | 33.6 | 40.7 | 37.6 | 32.3 | 51.9 | 34.0 | 2.5 |
| 4 | MS-1 (70-30W) | 52.9 | 37.4 | 14.0 | 52.6 | 12.9 | 53.8 | 26.8 | 24.3 |
| 7 | CSS-1H (50-50W) | 28.1 | 27.7 | 16.8 | 18.6 | 39.9 | 4.9 | 28.9 | 21.6 |
| 3 | TackMax | 3.7 | 50.2 | 19.1 | 17.2 | 47.6 | 23.1 | 28.3 | 55.3 |
| 10 | Cleanbond | 43.3 | 22.6 | 16.9 | 10.9 | 23.0 | 46.9 | 29.4 | 32.7 |
| 8 | Colasphalt Tack | 13.3 | 39.4 | 22.3 | 27.2 | 58.0 | 19.4 | 14.6 | 64.6 |

## Table H.2 Average Strain at Bond Failure Results for All Core Groups

| | | Average Strain at Peak (%) | COV | Average Strain at Peak (%) | COV | % Change | Average Strain at Peak (%) | COV | % Change | Average Strain at Peak (%) | COV | % Change | Average Strain at Peak (%) | COV | % Change | Average Strain at Peak (%) | COV | % Change | Average Strain at Peak (%) | COV | % Change | Average Strain at Peak (%) | COV | % Change |
|---|---|---|---|---|---|---|---|---|---|---|---|---|---|---|---|---|---|---|---|---|---|---|---|---|
| Section | Material | Baseline | | Year 1 | | | Year 1 IWP | | | Year 1 OWP | | | Year 1 Centre | | | 3 FT Cycles | | | 9 FT Cycles | | | 15 FT Cycles | | |
| 1 | SS-1 (50-50W) SB | 2.36 | 13.0 | 2.7 | 12.8 | 15 | 2.8 | 9.0 | 20 | 2.7 | 16.5 | 15 | 2.6 | 14.6 | 10 | 3.3 | 8.9 | 42 | 2.9 | 6.8 | 22 | 2.8 | 1.8 | 20 |
| 6 | SS-1 (50-50W) NB | 2.70 | 11.9 | 3.1 | 16.4 | 14 | 2.8 | 14.0 | 4 | 3.3 | 21.1 | 23 | 3.1 | 11.2 | 15 | 3.2 | 19.2 | 19 | 2.9 | 17.5 | 7 | 3.8 | 32.3 | 42 |
| 5 | SS-1 (30-70W) | 2.23 | 18.3 | 2.7 | 11.0 | 21 | 2.8 | 9.8 | 25 | 2.7 | 15.3 | 21 | 2.6 | 8.8 | 17 | 2.7 | 8.8 | 21 | 3.3 | 17.6 | 47 | 3.0 | 19.3 | 35 |
| 2 | SS-1H (50-50W) SB | 2.54 | 18.2 | 2.8 | 12.1 | 10 | 3.1 | 12.3 | 21 | 2.6 | 11.3 | 1 | 2.8 | 5.3 | 10 | 3.3 | 12.7 | 32 | 3.1 | 6.4 | 22 | 3.4 | 4.6 | 32 |
| 9 | SS-1H (50-50W) NB | 2.15 | 34.2 | 2.8 | 8.1 | 30 | 2.8 | 5.1 | 32 | 2.7 | 12.1 | 28 | 2.8 | 7.8 | 31 | 3.3 | 0.9 | 53 | 3.1 | 11.9 | 45 | 3.6 | 14.4 | 66 |
| 4 | MS-1 (70-30W) | 2.18 | 8.6 | 2.7 | 6.9 | 22 | 2.8 | 4.6 | 30 | 2.5 | 5.8 | 15 | 2.7 | 2.9 | 22 | 3.4 | 15.3 | 54 | 2.8 | 4.7 | 29 | 2.7 | 4.0 | 25 |
| 7 | CSS-1H (50-50W) | 3.00 | 25.7 | 3.0 | 9.7 | -2 | 3.0 | 7.8 | 1 | 2.9 | 13.6 | -3 | 2.9 | 9.2 | -3 | 3.2 | 2.1 | 8 | 3.2 | 11.6 | 5 | 3.2 | 9.3 | 7 |
| 3 | TackMax | 2.24 | 15.7 | 2.8 | 10.0 | 23 | 2.7 | 5.8 | 19 | 2.8 | 14.0 | 25 | 2.8 | 10.6 | 24 | 3.5 | 3.1 | 56 | 2.9 | 5.4 | 31 | 2.8 | 9.6 | 27 |
| 10 | Cleanbond | 2.63 | 19.0 | 3.1 | 11.8 | 17 | 3.2 | 15.1 | 22 | 3.2 | 7.4 | 23 | 2.8 | 5.1 | 6 | 3.0 | 22.1 | 14 | 2.6 | 5.5 | 0 | 3.0 | 1.3 | 14 |
| 8 | Colasphalt Tack | 2.83 | 2.9 | 2.8 | 9.2 | -3 | 2.6 | 12.1 | -7 | 2.8 | 12.2 | -1 | 2.8 | 2.5 | 0 | 3.1 | 9.9 | 9 | 2.9 | 10.7 | 2 | 3.5 | 13.2 | 23 |

| | | Std Dev (%) | | | | | | | |
|---|---|---|---|---|---|---|---|---|---|
| Section | Material | Baseline | Year 1 | Year 1 IWP | Year 1 OWP | Year 1 Centre | 3 FT Cycles | 9 FT Cycles | 15 FT Cycles |
| 1 | SS-1 (50-50W) SB | 0.307 | 0.349 | 0.257 | 0.447 | 0.381 | 0.299 | 0.195 | 0.051 |
| 6 | SS-1 (50-50W) NB | 0.320 | 0.504 | 0.393 | 0.698 | 0.347 | 0.613 | 0.504 | 1.241 |
| 5 | SS-1 (30-70W) | 0.409 | 0.295 | 0.273 | 0.413 | 0.230 | 0.236 | 0.575 | 0.584 |
| 2 | SS-1H (50-50W) SB | 0.462 | 0.339 | 0.377 | 0.288 | 0.148 | 0.426 | 0.199 | 0.154 |
| 9 | SS-1H (50-50W) NB | 0.735 | 0.226 | 0.147 | 0.333 | 0.219 | 0.030 | 0.372 | 0.514 |
| 4 | MS-1 (70-30W) | 0.187 | 0.185 | 0.131 | 0.145 | 0.078 | 0.513 | 0.132 | 0.108 |
| 7 | CSS-1H (50-50W) | 0.772 | 0.285 | 0.236 | 0.398 | 0.267 | 0.068 | 0.366 | 0.297 |
| 3 | TackMax | 0.351 | 0.275 | 0.155 | 0.392 | 0.295 | 0.108 | 0.159 | 0.274 |
| 10 | Cleanbond | 0.500 | 0.361 | 0.483 | 0.241 | 0.142 | 0.663 | 0.143 | 0.040 |
| 8 | Colasphalt Tack | 0.082 | 0.255 | 0.320 | 0.342 | 0.071 | 0.305 | 0.310 | 0.463 |

**Table H.3 Failure Type Results for All Core Groups**

| | | Failure Type | | | | | | | |
|---|---|---|---|---|---|---|---|---|---|
| **Section** | **Material** | **Baseline** | **Year 1** | **Year 1 IWP** | **Year 1 OWP** | **Year 1 Centre** | **3 FT Cycles** | **9 FT Cycles** | **15 FT Cycles** |
| 1 | SS-1 (50-50W) SB | A | A | A | A | A | A | A/B | A |
| 6 | SS-1 (50-50W) NB | A | A | A | A | A | B | A/B | B |
| 5 | SS-1 (30-70W) | A | A | A | A | A | A | A | A |
| 2 | SS-1H (50-50W) SB | B | B | B | B | B | B | B | B |
| 9 | SS-1H (50-50W) NB | B | A/B | A/B | A/B | A/B | A | A | B |
| 4 | MS-1 (70-30W) | B | A/B | A/B | A/B | A/B | B | B | B |
| 7 | CSS-1H (50-50W) | B | B | B | B | B | B | A/B | B |
| 3 | TackMax | B | A/B | A/B | A/B | A/B | B | B | B |
| 10 | Cleanbond | B | B | B | B | B | B | B | B |
| 8 | Colasphalt Tack | B | A/B | A/B | A/B | A/B | B | B | B |

*Type A/B indicates that approximately half of the core samples had Failure Type A and half had Failure Type B.

## Table H.4 Interlayer Tangential Modulus Results for All Core Groups

| | | k Modulus ($N/mm^3$) | COV | k Modulus ($N/mm^3$) | COV | % Change | k Modulus ($N/mm^3$) | COV | % Change | k Modulus ($N/mm^3$) | COV | % Change | k Modulus ($N/mm^3$) | COV | % Change | k Modulus ($N/mm^3$) | COV | % Change | k Modulus ($N/mm^3$) | COV | % Change | k Modulus ($N/mm^3$) | COV | % Change |
|---|---|---|---|---|---|---|---|---|---|---|---|---|---|---|---|---|---|---|---|---|---|---|---|---|
| Section | Material | Baseline | | Year 1 | | | Year 1 IWP | | | Year 1 OWP | | | Year 1 Centre | | | 3 FT Cycles | | | 9 FT Cycles | | | 15 FT Cycles | | |
| 1 | SS-1 (50-50W) SB | 0.121 | 8.2 | 0.140 | 17.9 | 16 | 0.138 | 16.7 | 15 | 0.133 | 22.5 | 10 | 0.149 | 17.6 | 24 | 0.098 | 12.9 | -19 | 0.131 | 18.5 | 9 | 0.136 | 9.0 | 13 |
| 6 | SS-1 (50-50W) NB | 0.129 | 5.8 | 0.127 | 17.0 | -1 | 0.131 | 19.0 | 1 | 0.119 | 25.6 | -8 | 0.133 | 5.0 | 3 | 0.110 | 29.1 | -15 | 0.116 | 29.3 | -10 | 0.085 | 36.9 | -34 |
| 5 | SS-1 (30-70W) | 0.156 | 18.7 | 0.157 | 11.6 | 1 | 0.162 | 16.9 | 4 | 0.152 | 7.8 | -3 | 0.158 | 10.3 | 1 | 0.134 | 15.6 | -14 | 0.111 | 20.3 | -29 | 0.119 | 17.2 | -24 |
| 2 | SS-1H (50-50W) SB | 0.152 | 14.7 | 0.150 | 13.7 | -1 | 0.144 | 15.2 | -5 | 0.158 | 18.6 | 4 | 0.147 | 5.3 | -3 | 0.109 | 23.7 | -28 | 0.108 | 7.5 | -28 | 0.109 | 9.6 | -28 |
| 9 | SS-1H (50-50W) NB | 0.172 | 27.1 | 0.124 | 9.3 | -28 | 0.122 | 14.5 | -29 | 0.128 | 2.9 | -26 | 0.122 | 9.6 | -29 | 0.113 | 14.4 | -34 | 0.119 | 15.1 | -31 | 0.117 | 14.4 | -32 |
| 4 | MS-1 (70-30W) | 0.169 | 22.4 | 0.151 | 7.1 | -11 | 0.151 | 7.5 | -10 | 0.151 | 9.7 | -11 | 0.150 | 5.3 | -11 | 0.117 | 24.7 | -31 | 0.148 | 7.6 | -12 | 0.140 | 9.3 | -17 |
| 7 | CSS-1H (50-50W) | 0.131 | 27.1 | 0.132 | 11.8 | 1 | 0.134 | 10.1 | 2 | 0.131 | 13.5 | 1 | 0.131 | 15.1 | 0 | 0.122 | 3.0 | -7 | 0.122 | 18.0 | -6 | 0.126 | 9.5 | -3 |
| 3 | TackMax | 0.159 | 25.5 | 0.145 | 18.4 | -9 | 0.164 | 8.7 | 3 | 0.147 | 18.2 | -7 | 0.125 | 20.5 | -22 | 0.106 | 9.6 | -33 | 0.139 | 2.8 | -12 | 0.116 | 18.4 | -27 |
| 10 | Cleanbond | 0.149 | 15.2 | 0.127 | 15.4 | -15 | 0.123 | 15.8 | -17 | 0.113 | 9.2 | -24 | 0.144 | 10.3 | -3 | 0.132 | 37.4 | -11 | 0.151 | 2.5 | 1 | 0.128 | 7.9 | -14 |
| 8 | Colasphalt Tack | 0.119 | 5.0 | 0.140 | 13.5 | 17 | 0.139 | 12.1 | 16 | 0.142 | 17.2 | 19 | 0.139 | 16.1 | 16 | 0.123 | 15.6 | 3 | 0.138 | 9.5 | 16 | 0.108 | 33.1 | -10 |

| | | Std Dev ($N/mm^3$) | | | | | | | |
|---|---|---|---|---|---|---|---|---|---|
| Section | Material | Baseline | Year 1 | Year 1 IWP | Year 1 OWP | Year 1 Centre | 3 FT Cycles | 9 FT Cycles | 15 FT Cycles |
| 1 | SS-1 (50-50W) SB | 0.010 | 0.025 | 0.023 | 0.030 | 0.026 | 0.013 | 0.024 | 0.012 |
| 6 | SS-1 (50-50W) NB | 0.008 | 0.022 | 0.025 | 0.031 | 0.007 | 0.032 | 0.034 | 0.031 |
| 5 | SS-1 (30-70W) | 0.029 | 0.018 | 0.027 | 0.012 | 0.016 | 0.021 | 0.023 | 0.020 |
| 2 | SS-1H (50-50W) SB | 0.022 | 0.020 | 0.022 | 0.029 | 0.008 | 0.026 | 0.008 | 0.010 |
| 9 | SS-1H (50-50W) NB | 0.047 | 0.012 | 0.018 | 0.004 | 0.012 | 0.016 | 0.018 | 0.017 |
| 4 | MS-1 (70-30W) | 0.038 | 0.011 | 0.011 | 0.015 | 0.008 | 0.029 | 0.011 | 0.013 |
| 7 | CSS-1H (50-50W) | 0.035 | 0.016 | 0.013 | 0.018 | 0.020 | 0.004 | 0.022 | 0.012 |
| 3 | TackMax | 0.040 | 0.027 | 0.014 | 0.027 | 0.026 | 0.010 | 0.004 | 0.021 |
| 10 | Cleanbond | 0.023 | 0.020 | 0.019 | 0.010 | 0.015 | 0.049 | 0.004 | 0.010 |
| 8 | Colasphalt Tack | 0.006 | 0.019 | 0.017 | 0.024 | 0.022 | 0.019 | 0.013 | 0.036 |

## Table H.5 Average Energy to Peak Stress Results for All Core Groups

| | | Average Energy to Peak (J/m$^2$) | COV | Average Energy to Peak (J/m$^2$) | COV | % Change | Average Energy to Peak (J/m$^2$) | COV | % Change | Average Energy to Peak (J/m$^2$) | COV | % Change | Average Energy to Peak (J/m$^2$) | COV | % Change | Average Energy to Peak (J/m$^2$) | COV | % Change | Average Energy to Peak (J/m$^2$) | COV | % Change | Average Energy to Peak (J/m$^2$) | COV | % Change |
|---|---|---|---|---|---|---|---|---|---|---|---|---|---|---|---|---|---|---|---|---|---|---|---|---|
| Section | Material | Baseline | | Year 1 | | | Year 1 IWP | | | Year 1 OWP | | | Year 1 Centre | | | 3 FT Cycles | | | 9 FT Cycles | | | 15 FT Cycles | | |
| 1 | SS-1 (50-50W) SB | 1108 | 26.7 | 1861 | 11.4 | 68 | 1971 | 7.5 | 78 | 1767 | 13.0 | 59 | 1845 | 13.5 | 66 | 1762 | 27.6 | 59 | 1764 | 22.1 | 59 | 1741 | 11.3 | 57 |
| 6 | SS-1 (50-50W) NB | 1521 | 11.4 | 2127 | 13.5 | 40 | 1884 | 8.5 | 24 | 2190 | 10.2 | 44 | 2306 | 13.6 | 52 | 1726 | 11.5 | 13 | 1505 | 12.5 | -1 | 1813 | 23.8 | 19 |
| 5 | SS-1 (30-70W) | 1220 | 8.3 | 2091 | 17.3 | 71 | 2289 | 5.4 | 88 | 2042 | 23.4 | 67 | 1942 | 19.9 | 59 | 1568 | 3.0 | 29 | 1862 | 17.9 | 53 | 1736 | 23.8 | 42 |
| 2 | SS-1H (50-50W) SB | 1616 | 22.8 | 2127 | 13.3 | 32 | 2407 | 10.7 | 49 | 1866 | 7.9 | 15 | 2107 | 4.5 | 30 | 1999 | 8.3 | 24 | 1748 | 3.9 | 8 | 2021 | 17.2 | 25 |
| 9 | SS-1H (50-50W) NB | 1311 | 32.3 | 1763 | 15.3 | 34 | 1792 | 11.7 | 37 | 1729 | 20.9 | 32 | 1766 | 16.7 | 35 | 1982 | 13.1 | 51 | 1862 | 14.1 | 42 | 2230 | 8.9 | 70 |
| 4 | MS-1 (70-30W) | 1370 | 15.3 | 1958 | 13.1 | 43 | 2160 | 4.7 | 58 | 1763 | 18.0 | 29 | 1947 | 3.9 | 42 | 2038 | 15.8 | 49 | 1941 | 11.5 | 42 | 1747 | 4.4 | 28 |
| 7 | CSS-1H (50-50W) | 1837 | 11.6 | 2129 | 11.2 | 16 | 2300 | 3.1 | 25 | 2050 | 14.5 | 12 | 2038 | 11.8 | 11 | 2095 | 0.8 | 14 | 1970 | 9.0 | 7 | 2095 | 6.6 | 14 |
| 3 | TackMax | 1360 | 6.7 | 1988 | 12.8 | 46 | 2200 | 4.1 | 62 | 2041 | 6.9 | 50 | 1724 | 13.5 | 27 | 1986 | 7.7 | 46 | 1993 | 11.6 | 46 | 1537 | 21.8 | 13 |
| 10 | Cleanbond | 1699 | 17.7 | 2234 | 8.7 | 32 | 2350 | 12.5 | 38 | 2198 | 6.8 | 29 | 2155 | 1.3 | 27 | 1908 | 2.7 | 12 | 1808 | 13.0 | 6 | 1977 | 9.2 | 16 |
| 8 | Colasphalt Tack | 1588 | 9.1 | 1925 | 12.9 | 21 | 1801 | 14.6 | 13 | 1992 | 10.8 | 25 | 1999 | 13.5 | 26 | 1945 | 4.3 | 23 | 1905 | 10.8 | 20 | 2073 | 7.3 | 31 |

| | | Std Dev (J/m$^2$) | | | | | | | |
|---|---|---|---|---|---|---|---|---|---|
| Section | Material | Baseline | Year 1 | Year 1 IWP | Year 1 OWP | Year 1 Centre | 3 FT Cycles | 9 FT Cycles | 15 FT Cycles |
| 1 | SS-1 (50-50W) SB | 295 | 212 | 149 | 230 | 248 | 486 | 389 | 197 |
| 6 | SS-1 (50-50W) NB | 173 | 287 | 159 | 224 | 314 | 198 | 188 | 432 |
| 5 | SS-1 (30-70W) | 101 | 361 | 124 | 478 | 387 | 47 | 333 | 413 |
| 2 | SS-1H (50-50W) SB | 368 | 283 | 258 | 146 | 95 | 165 | 68 | 349 |
| 9 | SS-1H (50-50W) NB | 424 | 269 | 211 | 361 | 296 | 260 | 263 | 198 |
| 4 | MS-1 (70-30W) | 210 | 257 | 102 | 317 | 76 | 321 | 223 | 77 |
| 7 | CSS-1H (50-50W) | 214 | 239 | 71 | 298 | 241 | 17 | 177 | 139 |
| 3 | TackMax | 92 | 255 | 90 | 142 | 232 | 153 | 232 | 334 |
| 10 | Cleanbond | 301 | 193 | 294 | 150 | 27 | 51 | 235 | 181 |
| 8 | Colasphalt Tack | 144 | 248 | 264 | 215 | 269 | 84 | 206 | 151 |